Library and Information Centre / Centre de Documentation (GSLA)
RECEIVED - REÇU LE
JUN 27 1983
Transport Canada / Transports Canada

TP 4191 E

# DEVELOPMENT OF A PREDICTION MODEL FOR DYNAMIC RESPONSE AND BOW LOADING OF SHIPS

For

Transportation Development Centre,
1000 Sherbrooke Street. West,
P.O. Box 549
Place de L'Aviation
Montreal, Quebec,
H3A 2R3.

By

Melville Shipping Ltd.
Esso Plaza, East Tower
425 First Street S.W.
Calgary, Alberta
T2P 3L8

May 1983

PROJECT TEAM

The study was carried out by Melville Shipping Ltd. and their contractor H.G. Engineering Ltd. on behalf of Transportation Development Centre under the direction of TDC Project Officer Mr. R. Nishizaki to whom the authors gratefully acknowledge his advise and assistance.

The personnel engaged in the study were viz:

| | |
|---|---|
| Mr. R. A. Dick | Melville Shipping Ltd. |
| Mr. E. W. Thompson | Melville Shipping Ltd. |
| Dr. H. Cheung | Melville Shipping Ltd. |
| Mr. D. N. Baker | Melville Shipping Ltd. |
| Mr. P. J. Wyld | Melville Shipping Ltd. |
| Dr. A. Firman | H.G. Engineering Ltd. |
| Mr. I. Tabsh | H.G. Engineering Ltd. |

The contents of this report represent the opinions and judgement of the Consultants, and do not necessarily reflect the official views or policies of Transport Canada.

## REPORT DOCUMENTATION FORM

| 1. Transport Canada Report No. | 2. TDC Project No. | 3. Recipient's Catalogue No. |
|---|---|---|
| TP 4191E | 4738 | |

**4. Title and Subtitle**

DEVELOPMENT OF A PREDICTION MODEL FOR DYNAMIC RESPONSE AND BOW LOADING OF SHIPS

**5. Report Date**
May 1983

**6. Performing Organization Report No.**
P 82-29

**7. Author(s)**
E.W. Thompson, H.C. Cheung

**8. Transport Canada File No.**
D1460-186

**9. Performing Organization Name and Address**
Melville Shipping Ltd.
Esso Plaza, East Tower, Suite 1900
425 First Street South West
Calgary, Alberta T2P 3L8

**10. DSS File No.**
17SU.T8200-2-2512

**11. DSS or Transport Canada Contract No**
1SU82-00186

**12. Sponsoring Agency Name and Address**
Transportation Development Centre (TDC)
1000 Sherbrooke Street West
Suite 2421
Montreal, Quebec H3A 2R3

**13. Type of Report and Period Covered**
Final; Sept. 82 - March 83

**14. Sponsoring Agency Code**
TDC 4738

**15. Supplementary Notes**

**16. TDC Project Officer**
R.S. Nishizaki

**17. Abstract**

This final report documents the work to develop a Canadian prediction model for dynamic response and bow loading of ships. The purpose is to construct a basic analytical tool to determine bow global loads and hull bending stresses of ships when ramming level, homogeneous ice formations.

A computerized mathematical model was developed to simulate the ship to ice interaction force using the horizontal rigid and vertical quasi-rigid motions of the ship. The output was used as the exciting force to compute the resulting deflections, moments and stresses in the ship, based on the dynamic characteristics of the ship and calculated using a finite element beam model for determining the elastic modes of vibration.

The prediction model provides results similar to those obtained from a model developed by the Technical Research Centre of Finland. It is concluded that a Canadian model has been successfully developed; however, comparison with full-scale data indicates possible underestimation of the longitudinal bending stress of the ship hull.

| 18. Key Words | 19. Distribution Statement |
|---|---|
| Ships structure, ice, icebreaking, dynamic loads, stresses, mathematical models | A limited number of copies available from the sponsoring agency |

| 20. Security Classification (of this report) | 21. Security Classification (of this page) | 22. No. of Pages | 23. Price |
|---|---|---|---|
| Unclassified | Unclassified | | Free |

# FORMULE DE DOCUMENTATION POUR RAPPORT

| 1 N° du rapport Transports Canada | 2 N° de l'étude — CDT | 3 N° de catalogue du destinataire |
|---|---|---|
| TP 4191E | 4738 | |

| 4 Titre et sous-titre | 5 Date du rapport |
|---|---|
| Development of a Prediction Model for Dynamic Response and Bow Loading of Ships | mai 1983 |
| | 6 N° du rapport de l'organisme exécutant: P 82-29 |

| 7 Auteur(s) | 8 N° de dossier Transports Canada |
|---|---|
| E.W. Thompson, H.C. Cheung | D1460-186 |

| 9 Nom et adresse de l'organisme exécutant | 10 N° de dossier — ASC |
|---|---|
| Melville Shipping Ltée<br>Esso Plaza, East Tower, Suite 1900<br>425 première avenue sud ouest<br>Calgary (Alberta) T2P 3L8 | 17SU.T8200-2-2512 |
| | 11 N° de contrat — ASC ou Transports Canada: 1SU82-00186 |

| 12 Nom et adresse de l'organisme parrain | 13 Genre de rapport et période visée |
|---|---|
| Centre de développement des transports (CDT)<br>1000 ouest, rue Sherbrooke<br>Suite 2421<br>Montréal (Québec) H3A 2R3 | Final; sept. 82 - mars 83 |
| | 14 Code de l'organisme parrain: CDT 4738 |

| 15 Remarques additionnelles | 16 Agent de projet — CDT |
|---|---|
| | R.S. Nishizaki |

17 Resume

Rapport définitif présentant le résultat des travaux visant l'élaboration, au Canada, d'un modèle mathématique capable de figurer la réponse dynamique des carènes ainsi que la charge s'exerçant sur la proue des navires chargeant une glace homogène, d'épaisseur uniforme. Par cette étude, on visait l'édification d'un modèle d'analyse permettant de calculer les charges globales s'exerçant sur la proue du navire et les efforts de flexion agissant sur la poutre-navire dans les conditions précitées.

Le modèle mathématique informatisé élaboré permet de figurer l'interaction entre la carène et la glace, connaissant les mouvements verticaux semi-rigides et horizontaux rigides du navire. Les résultats ainsi obtenus, appliqués comme forces excitatrices, permettent de calculer les forces correspondantes (fléchissements, moments et contraintes) induites dans la poutre, connaissant les caractéristiques dynamiques du navire et à l'aide de la méthode des éléments finis appliquée à une poutre modèle dont on peut ainsi déterminer les modes propres de vibration élastique.

Le modèle mathématique élaboré a donné des résultats qui se comparent à ceux du modèle réalisé par le centre de recherches appliquées de Finlande, indiquant que le modèle canadien est maintenant au point. Cependant, la comparaison des données ainsi obtenues avec celles acquises lors d'essais en vraie grandeur montre que les flexions longitudinales agissant sur la poutre-navire semblent avoir été sous-estimées.

| 18. Mots-clés | 19. Diffusion |
|---|---|
| Structures navales, glace, déglaçage, efforts dynamiques, contraintes, modèles mathématiques | Le CDT dispose d'un nombre limité d'exemplaires |

| 20. Classification de sécurité (de ce rapport) | 21. Classification de sécurité (de cette page) | 22. Nombre de pages | 23. Prix |
|---|---|---|---|
| non-classifié | non-classifiée | | Gratuit |

TABLE OF CONTENTS


| | | |
|---|---|---|
| 1.0 | INTRODUCTION | 1 |
| 2.0 | DESCRIPTION OF THE PREDICTION MODEL | 5 |
| 2.1 | General | 5 |
| 2.2 | Ship/Ice Interaction Model | 8 |
| 2.2.1 | Effective Ice Pressure | 12 |
| 2.2.2 | Contact Area | 14 |
| 2.3 | Finite Element Beam Model | 14 |
| 2.3.1 | Added Mass | 17 |
| 2.3.2 | Damping Factors | 17 |
| 3.0 | RESULTS AND DISCUSSIONS | 21 |
| 3.1 | General | 21 |
| 3.2 | Natural Frequency and Modal Shape | 23 |
| 3.3 | Bow Loading and Movement | 26 |
| 3.4 | Hull Girder Vibratory Response | 31 |
| 4.0 | CONCLUSIONS | 43 |
| 5.0 | RECOMMENDATIONS | 44 |
| 6.0 | REFERENCES | 45 |
| 7.0 | APPENDICES | A1 |
| Appendix I | "Dynamic Analysis of the M.V. ARCTIC Hull Girder In Response to Ice Impact" by H.G. Engineering Ltd. | A1 |
| Appendix II | Additional Calculation Data of the Prediction Model | B1 |

LIST OF FIGURES


| | | |
|---|---|---|
| Figure 1 | M.V. ARCTIC Outline General Arrangement | 4 |
| Figure 2 | Applied Forces and Nodal Points Distribution for the Finite Element Model | 7 |
| Figure 3 | Schematic Description of the Pridiction Model | 9 |
| Figure 4 | Ship/Ice Interaction | 11 |
| Figure 5 | Measured Effective Ice Pressure | 13 |
| Figure 6 | Estimated Ice Contact Area of M.V. ARCTIC | 15 |
| Figure 7 | Estimated Added Mass, Shape Factor and Local Correction Factor for M.V. ARCTIC | 18 |
| Figure 8 | Comparison of the Calculated Modal Shapes of the 4 Node Vertical Vibration Mode | 25 |
| Figure 9a | Calculated Bow Force for Ramming Multi-Year Ice | 27 |
| Figure 9b | Calculated Bow Force for Ramming Multi-Year Ice | 28 |
| Figure 9c | Calculated Bow Force for Ramming Multi-Year Ice | 29 |
| Figure 10 | Maximum Vertical Bow Force Versus Ramming Speed | 30 |
| Figure 11 | Penetration Distance Versus Ramming Speed | 32 |
| Figure 12a | Calculated Vertical Rigid Body and Elastic Motions of M.V. ARCTIC | 33 |
| Figure 12b | Calculated Vertical Rigid Body and Elastic Motions of M.V. ARCTIC | 34 |
| Figure 12c | Calculated Vertical Rigid Body and Elastic Motions of M.V. ARCTIC | 35 |
| Figure 12d | Calculated Vertical Rigid Body and Elastic Motions of M.V. ARCTIC | 36 |
| Figure 12e | Calculated Vertical Rigid Body and Elastic Motions of M.V. ARCTIC | 37 |
| Figure 13a | Calculated Longitudinal Bending Stress Induced by Ice Ramming | 38 |
| Figure 13b | Calculated Longitudinal Bending Stress Induced by Ice Ramming | 39 |
| Figure 13c | Calculated Longitudinal Bending Stress Induced by Ice Ramming | 40 |
| Figure 14 | Ice Induced Longitudinal Stress Versus Ramming Speed | 42 |

LIST OF TABLES


| | | |
|---|---|---|
| Table 1 | M.V. ARCTIC - Principal Particulars | 3 |
| Table 2 | Nodal Co-Ordinates and Masses Applied in the Finite Element Beam Model for the M.V. ARCTIC Dynamic Response Simulation | 16 |
| Table 3 | Damping Factors of M.V. ARCTIC | 20 |
| Table 4 | Cases of Ice Ramming Study with the Prediction Model | 22 |
| Table 5 | Comparison of Calculated and Measured Natural Frequencies (Hz) of Vertical Vibration of M.V. ARCTIC | 24 |

## 1.0 INTRODUCTION

This report describes the work carried out to develop a Canadian prediction model for dynamic response and bow loading of ships. The work was sponsored by the Transportation Development Centre (TDC), Montreal, Quebec, and contracted by the Department of Supply and Services, Hull, Quebec, (Contract No. 1SU 82-00186). The intention of the model was to construct a basic analytical tool "to determine design loads for Arctic class vessels as well as to permit an upgrading of the structural requirements of the Canadian Arctic Shipping Pollution Prevention Regulations." This work was carried out by Melville Shipping Ltd. and their subcontractor, H. G. Engineering Ltd., Don Mills, Ontario.

The overall knowledge of the amplitudes and time history of the loads on the bow of a vessel when breaking ice is required so that the bow and hull girder may be designed accordingly. For vessels of high length to breadth ratio, accurate evaluation of the longitudinal strength would be especially required.

In the past two years, extensive study of the hull girder response of M.V. ARCTIC has been carried out by full scale mesurements. A series of dedicated ice breaking tests (Ref. 1 and 2) were performed when the ship was operating in the Canadian Arctic during the months of June through November. The results from these tests have prompted the development of an analytical model to quantify the relationship between the hull girder stresses and bow loading for commercial ice capable vessels.

A mathematical model of M.V. ARCTIC has been developed by the Technical Research Centre of Finland, VTT (Valtion Teknillinen Tutkimuskeskus), managed by Melville Shipping Ltd. on behalf of the Canadian Coast Guard (Ref. 3). This model simulates the ship/ice interaction when ramming multi-year ice and is able to assess the total bow force and the corresponding dynamic response of the hull girder.

The present project was initiated by the need to develop and demonstrate a Canadian capability in the field of modeling ship/ice interaction. The Canadian model was developed in parallel with that prepared by VTT.

The Canadian model, developed using a finite element beam modelling technique, has demonstrated similar capabilities of the VTT model and permits the prediction of:

- the dynamic response of the hull girder in the form of stresses, strains and displacements under the action of arbitrary bow loads;
- the bow force from observed vertical response of the hull due to collision with infinite floes.

The mathematical model has been developed to simulate the ship/ice interaction based on an empirical effective ice pressure/contact area relationship. From the relationship the ice impact load and the dynamic response of the ship hull girder during the process of ramming large multi-year ice floes can be calculated. The ice condition chosen for the model development represents the worst condition in terms of bow loading and hull bending stress and is similar to that used by VTT.

In order to correlate with the known full-scale tests results and the predictions obtained from the Finnish model for the M.V. ARCTIC, the present model has also been exercised with the same ship input data. The M.V. ARCTIC is a 28,000 tonne deadweight ice breaking bulk carrier, designed by Camat International Consultant Ltd. In accordance with the Canadian Arctic Shipping Pollution Prevention Regulations for Ice Class 2 ships. The principal dimensions and other particulars of importance of this vessel are shown in Table 1 and an outline general arrangement is illustrated in Figure 1.

| | |
|---|---|
| Length Overall (LOA) | 209.55 m |
| Length Between Perpendiculars (LBP) | 196.59 m |
| Breadth Extreme (B) | 22.93 m |
| Depth Moulded (D) | 15.24 m |
| Draft (Full) (H) | 10.93 m |
| Displacement (Full) | 38,104 tonnes |
| Installed Power | 14,770 BHP (Metric) |
| a) Main Engine - M.A.N. 52/55A<br>14 Cylinder 450 r.p.m. | |
| b) Gearbox - Renk Single reduction,<br>vertical offset, with 3.147 reduction ratio | |
| Propeller Diameter | 5.27 m |
| a) Lips - Controllable pitch - four blades<br>- single propeller - 143 r.p.m. located in<br>Wageningen 19A nozzle with 25 mm tip clearance | |
| Bollard Pull at Full Power | 160 tonnes |
| Classification - Lloyd's [✠ 100A1, Ice Class 1A Super, LMC]<br>- Arctic Class 2 (CASPPR) | |
| Ballast Capacity | 28,329 tonnes |
| Fuel Capacity | 1,852 tonnes |

TABLE 1

M.V. ARCTIC - PRINCIPAL PARTICULARS

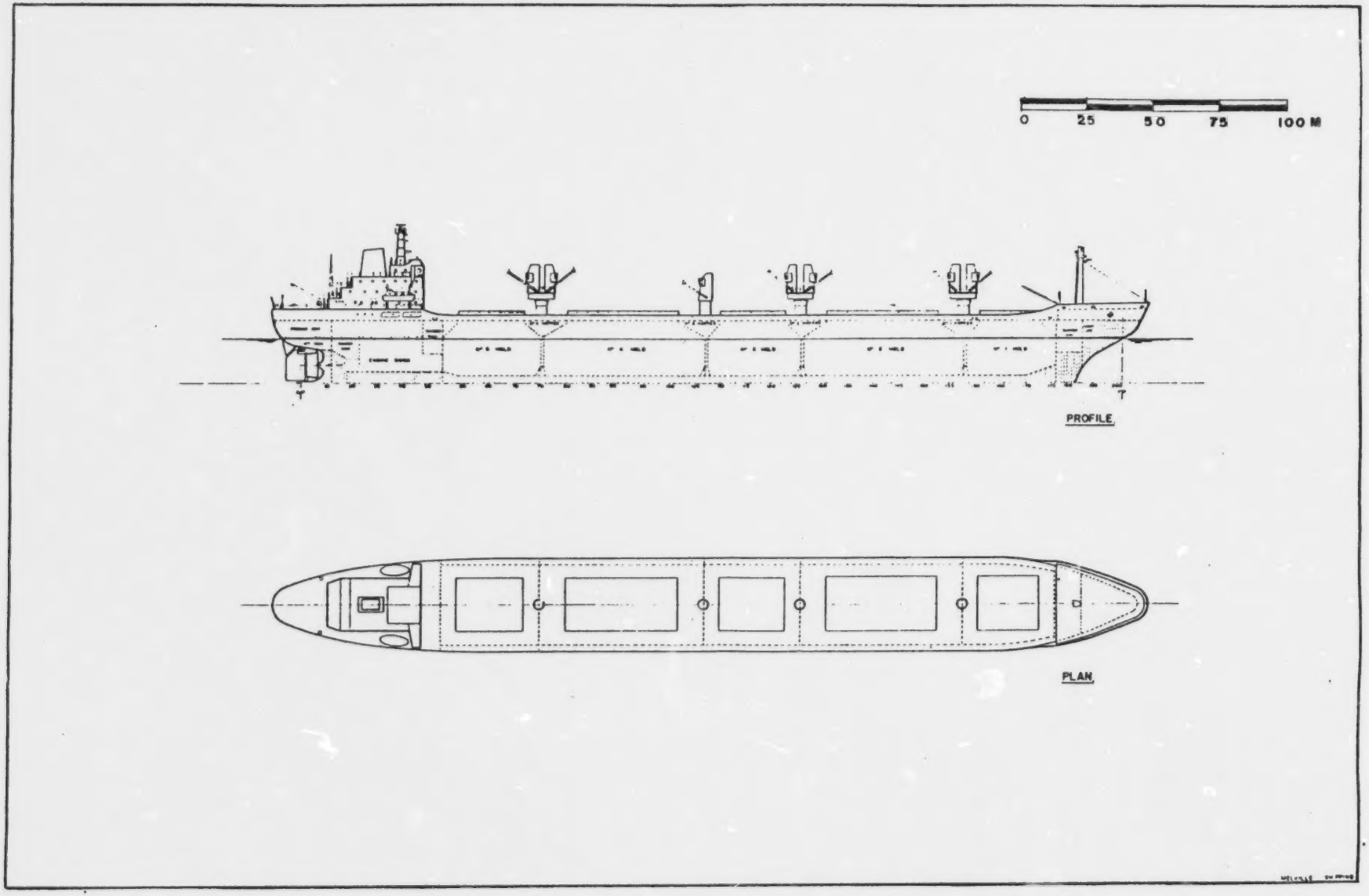


M.V. ARCTIC OUTLINE GENERAL ARRANGEMENT

FIGURE 1

## 2.0 DESCRIPTION OF THE PREDICTION MODEL

### 2.1 General

The mechanism of ice breaking by a ship can be addressed in two distinct operating modes, continuous ice breaking and ramming. The geometry of the bows of ice classed ships are specially designed to break ice in the continuous mode by bending and shearing to take advantage of the lower strength of ice in these modes of failure. The global loads on the bow are substantially lower when breaking ice continuously than when ramming. The ramming mode is used when the ice is sufficiently strong or the downward component of force at the bow is no longer sufficient to break the ice continuously by bending and shearing. When ramming, the kinetic energy of the ship is used to achieve penetration into the ice, during which time the ice crushing mode of failure is dominant. It is this interaction of the ship with the ice that is of concern for the structural integrity of Arctic class vessels, especially when the bow enters a previously formed notch.

The prediction model has been constructed for the evaluation of ship hull girder dynamic response and bow loading when ramming.

The terms static, quasi-static and dynamic are used extensively in this report. These terms are not to be interpreted as implying rates of application of load but to distinguish between still water (static), simple bending due to point support of a beam (quasi-static), and vibratory behaviour as the vessel or beam responds at its natural frequencies of vibration.

Ship/ice interaction is a complex problem of statics and dynamics and has been a crucial subject in icebreaker technology. The complexity of ship/ice interaction stems not only from the inhomogenity of ice strength and geometrical properties, but also from the effects of the ship's geometry and response to impact. These factors play an important role in the determination of the variation of ice load distribution upon the vessel.

As the ship progressively penetrates the ice, energy is dissipated by ice failure until the ship can no longer fail the ice and is brought to a stop.

The reaction of the consolidated ice, because of the shape of an ice breaking bow, produces a large upward force at the bow during forward motion. It is the reaction to this force which breaks ice by flexure or shear when in the continuous mode and causes a change of the ship's trim which in turn generates a so called "quasi-static" bending along the ship.

The stresses associated with quasi-static bending will increase as a function of bow emersion. Hence the maximum quasi-static bending stresses of the hull girder will occur during ramming when bow emersion is at a maximum.

During penetration of the ice when ramming, the ship is mostly supported by buoyancy acting as an elastic foundation to the ship hull structure. Any abrupt change of ice force will excite the hull structure and result in vibratory motions and stresses. The vibratory stresses which are excited are superimposed on the quasi-static bending stress, and characterized by the dominance of the fundamental vertical natural frequency of vibration of the hull girder. The on-set of the vibrations, however, varies significantly in different ice impact conditions, which can be attributed to the inter-relationship between the transient ice load and the resultant ship's rigid and elastic motions.

The assessment of ice impact load in the present model has been approached with the emphasis on probing the most severe vertical dynamic response of the ship hull. Calculation of the transverse and torsional response of the ship has not been considered in the present stage of program development. It should be noted that the hull is regarded as a uniform beam and while changes in cross sections (modulus) are recognised, no account is given to such stress intensifying factors as stress concentrations.

The present model considers a total bow force, symmetrical with respect to the ship centre line, applied where "crushing" contact with ice is expected. The ship structure is represented by a finite element beam model to simulate the longitudinal movement of the ship and the rigid body, quasi-static and vibratory motions of the hull girder in the vertical direction.

The model was developed with the aid of a computer. The method of ice load calculation, the structural response model and the ship data used in the calculations are briefly described in the subsections which follow. The computer programs were developed and run by H.G. Engineering Ltd. Details of the formulations used in the computerized model, and the results, are documented in the report of H.G. Engineering Ltd. attached as an Appendix.

The model which has been developed, consists of two principal parts:

- A finite-element model of the ship's hull girder
- A ship/ice interaction simulation model

The vibration characteristics of the ship in the vertical directions are generated using a general-purpose finite element program and the ship structure is represented by a series of equivalent beam sections as shown in Figure 2. The natural frequencies, modal shapes and modal moments for the quasi-rigid and elastic modes of the ship vertical motion are calculated.

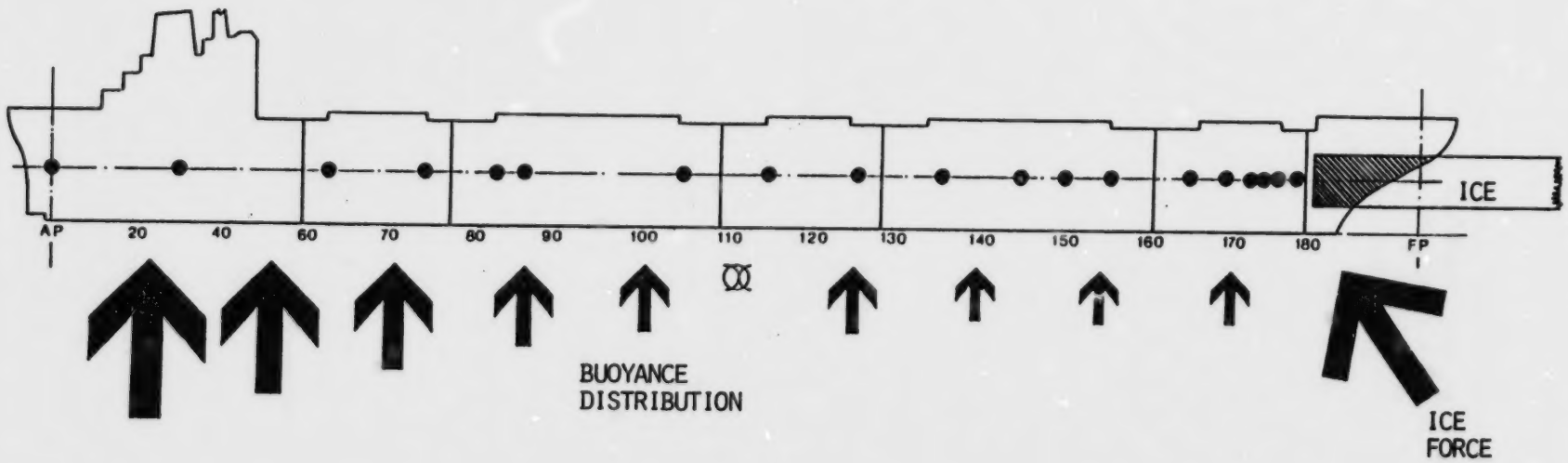


APPLIED FORCES AND NODAL POINTS DISTRIBUTION
FOR THE FINITE ELEMENT MODEL
FIGURE 2

The transient ship response is then computed by assessing the "instantaneous" ice force exerted upon the ship bow during ramming using a time incremental method. From the calculation of ice force, the rigid body and the dynamic responses of the ship are calculated. The results are then translated to predictions of hull girder bending stress at various ship sections.

The applied forces of the system, defined in the vertical plane perpendicular to the beam of the ship, include a total ice force exerted upon the ship bow and the buoyance distribution along the ship (Figure 2). The ice force is determined from an algorithm previously developed, and the buoyance is calculated from the ship hull geometry and the ship's vertical motion. Details of these calculation methods are presented in the subsections which follow.

Figure 3 presents a flow diagram of the prediction model. The model contains a total of six computer programs written for a Hewlett-Packard 9800 series computer. The functions of these programs are outlined below.

| Program | Function |
|---|---|
| FESDEC | A general finite element system for desk top computers. This program is used to calculate the natural frequencies and modal shapes of the ship. |
| RGDMDS | This calculates the modal moments at the nodes for quasi-rigid modes of motion. |
| EMODLM | This calculates the modal moments at the nodes for elastic modes of motion. |
| DRrTRN | This calculates the ship/ice interaction forces and the resulting horizontal and vertical rigid body motions of the ship. |
| DRTRAN | This program is the transient dynamics post processor of "FESDEC". It calculates the elastic response of the ship due to the excitation force determined from "DRrTRN". |
| MAX | This processes the calculation results obtained from "DRrTRN" and "DRTRAN" and determines the total responses of the ship when ramming ice. |

## 2.2 Ship/ice Interaction Model

The calculation of ice load has been developed in a similar manner to that used by VTT. The approach used in the VTT model simulates the dynamic

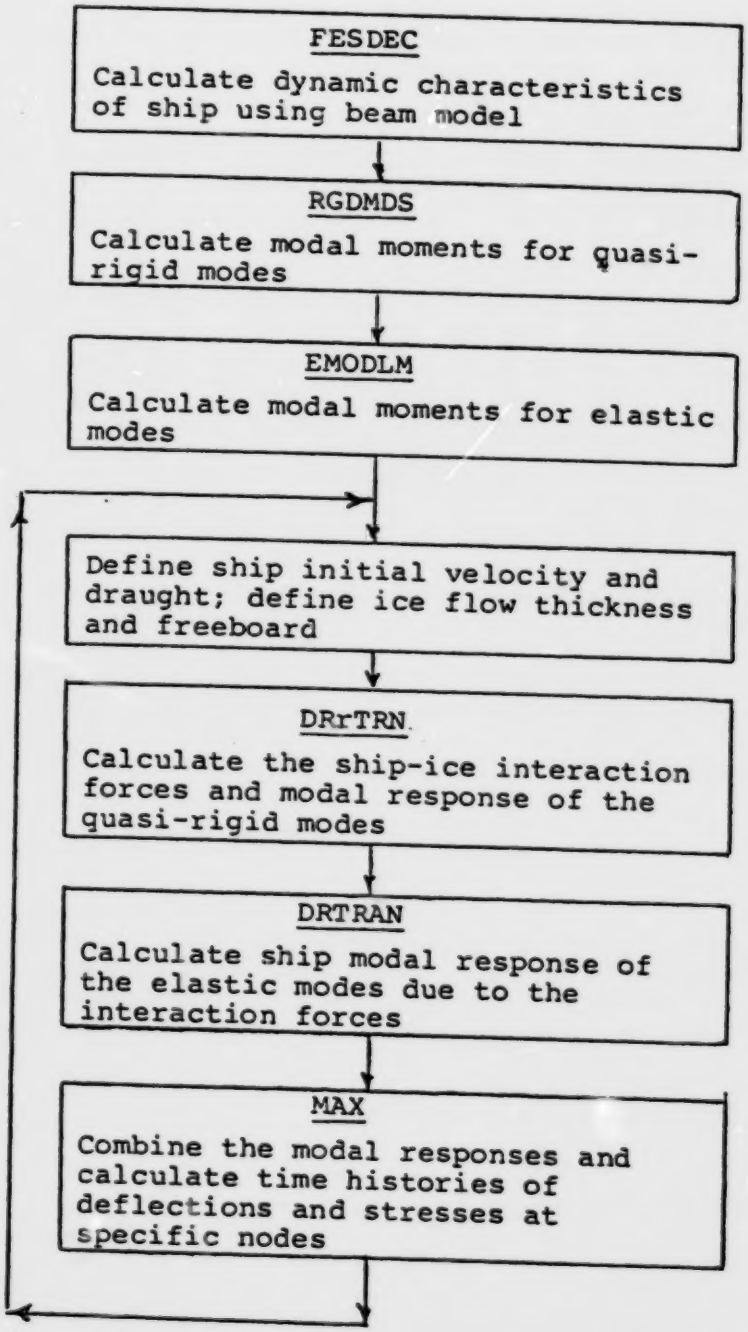
FESDEC
Calculate dynamic characteristics of ship using beam model
RGDMDS
Calculate modal moments for quasi-rigid modes
EMODLM
Calculate modal moments for elastic modes
Define ship initial velocity and draught; define ice flow thickness and freeboard
DRrTRN
Calculate the ship-ice interaction forces and modal response of the quasi-rigid modes
DRTRAN
Calculate ship modal response of the elastic modes due to the interaction forces
MAX
Combine the modal responses and calculate time histories of deflections and stresses at specific nodes

SCHEMATIC DESCRIPTION OF THE PREDICTION MODEL

FIGURE 3

ice failure phenomena by a static "effective ice pressure" versus contact area relationship in conjunction with a simulation of the vessel response. This simple modelling method is capable of estimating the trend of bow loading under different impact conditions.

The prediction model, although it adopts the VTT approach as its base, has been built with a modular structure to provide allowance for future model modifications.

The ship/ice interaction model of the present work was developed based on the following principal assumptions:

- two dimensional modelling (longitudinal and vertical);
- only the ice crushing mode of failure is considered;
- ice force is applied normal to the contact surface of the ship's bow;
- friction and hydrodynamic force for longitudinal motion is not included;
- use is made of an effective ice pressure/contact area relationship as suggested by the Canadian Coast Guard (Ref. 3);
- consolidated ice is considered stationary under the impact of the ship;
- simple ice geometry is used, uniform thickness and regular ice edge.

An illustration of the ship/ice interaction model is presented in Figure 4. In the model, the properties of the ice floe are defined by its thickness, freeboard and the crushing strength. For a given crushing contact condition, the total bow force F is evaluated by the expression,

$$\vec{F} = p\vec{A}$$

where:

p = effective ice pressure

$\vec{A}$ = contact area

The ship's motion is defined by its longitudinal transition and its vertical rigid body and elastic oscillations. These include the pitching and heaving modes, the quasi-static bending during ramming and the lower vertical vibration modes of the ship. The crushing contact area is determined from the relative positions, both vertically and longitudinally, between the ship and the ice, which are dictated by the ice force and the

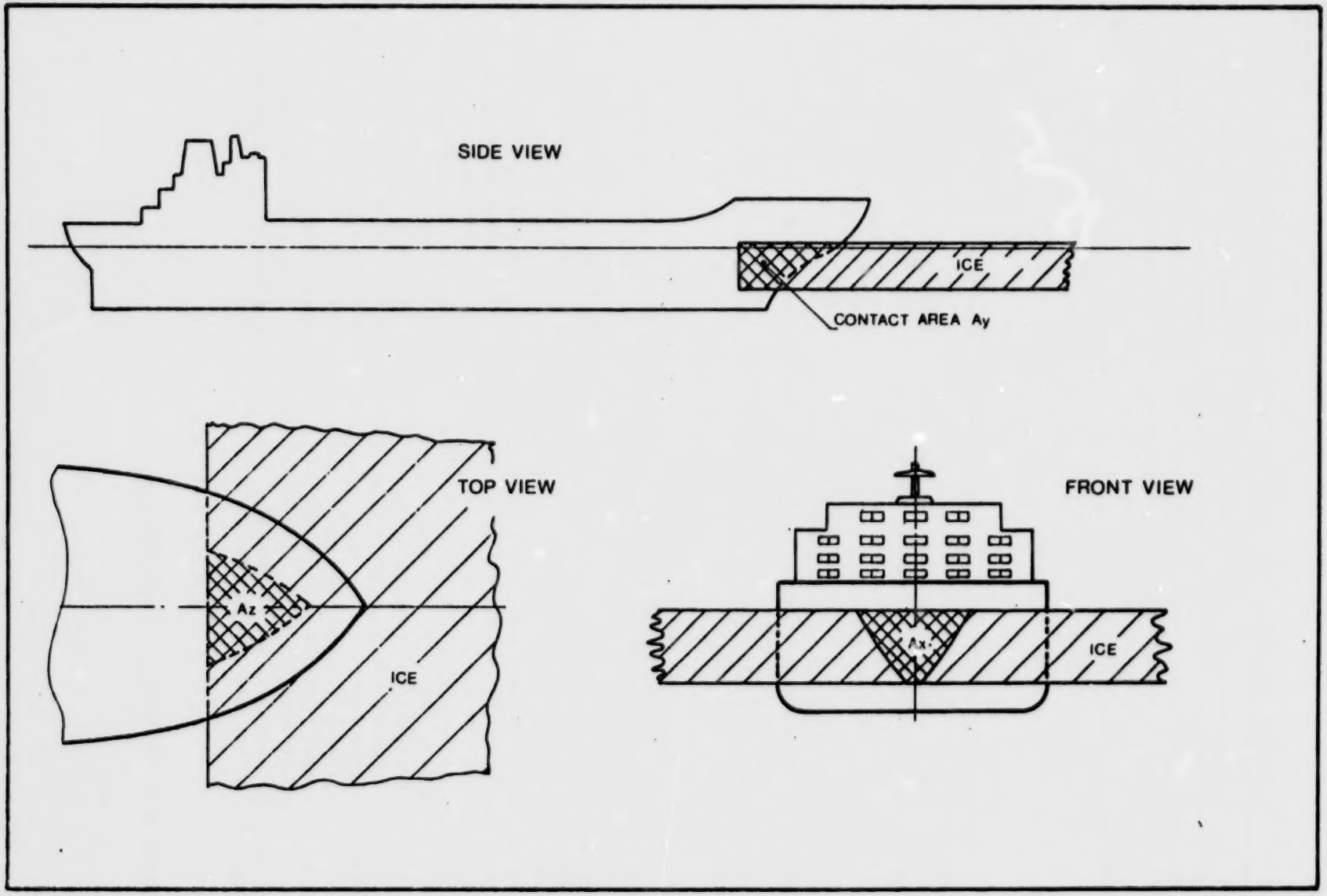


SHIP/ICE INTERACTION

FIGURE 4

ship's original momentum. The geometry of the ship bow, therefore, is required to determine the contact area for a given penetration condition. Since the ice force to be calculated and the ship/ice relative positions are inter-related, an iteration method on a time incremental basis is used for calculating the time history of bow load. As the crushing pressure should only be applied when the ship is penetrating ice, the notch in the ice floe created by the ship's bow is "memorized" by the computer program during the ramming simulation calculation.

### 2.2.1 Effective Ice Pressure

Use of the effective ice pressure concept, postulated in the VTT model, and the present ship/ice interaction model is an attempt, by means of a simple static equation, to quantify the dynamic variation of ice reaction force exerted upon the ship bow when ramming. It has been shown (Ref. 4) that the effective ice fracture strength is strongly dependent on the imperfections in the structure of the ice. The model assumes that the ice failure by crushing is uniform during impact. In practice ice failure due to ship impact is irregular in both the spatial and time domain due to the stress concentrations induced by cracks, ice dislocations and non-homogenity found in naturally occurring ice. Therefore, the average ice pressure for a large contact area is lower than the ice strength measurement from a small sample size would suggest.

Some evidence of this area/volume dependency of ice crushing pressure is indicated in the recent results of full scale ice ramming tests using ice breaking vessels as shown in Figure 5. In the figure, the measured ice pressure data of the M.V. ARCTIC was deduced from the records of the ship deceleration when ramming first-year level ice and ridge features in Admiralty Inlet, N.W.T. (Ref. 1). The deceleration was monitored by a fore-and-aft accelerometer and a doppler speed log. Ice pressure data recorded from other ships, either by means of direct pressure measurement or deduced from the ice retardation force, were reproduced from the published report, entitled "Updating the Arctic Pollution Prevention Regulations, Group I & II", (Ref. 5). In addition, the borehole jack data of ice confined compressive strength measured in-situ in various ice conditions was included for comparisons. It is shown that for small contact areas, the measured ice pressure by the Fenco borehole jack method is in the range of 20-30 MPa for multi-year ice, and 7-10 MPa for first-year. As the contact area increases, the trend of reduction of ice pressure appears to fall into a straight line approximation in the log-log plot. The line drawn in the figure was suggested by the Canadian Coast Guard and has been used by MSL and VTT in the model for multi-year ice,

$$p = 4.4\ A^{-0.5}\ \text{MPa}$$

where A is the total contact area expressed in $m^2$.

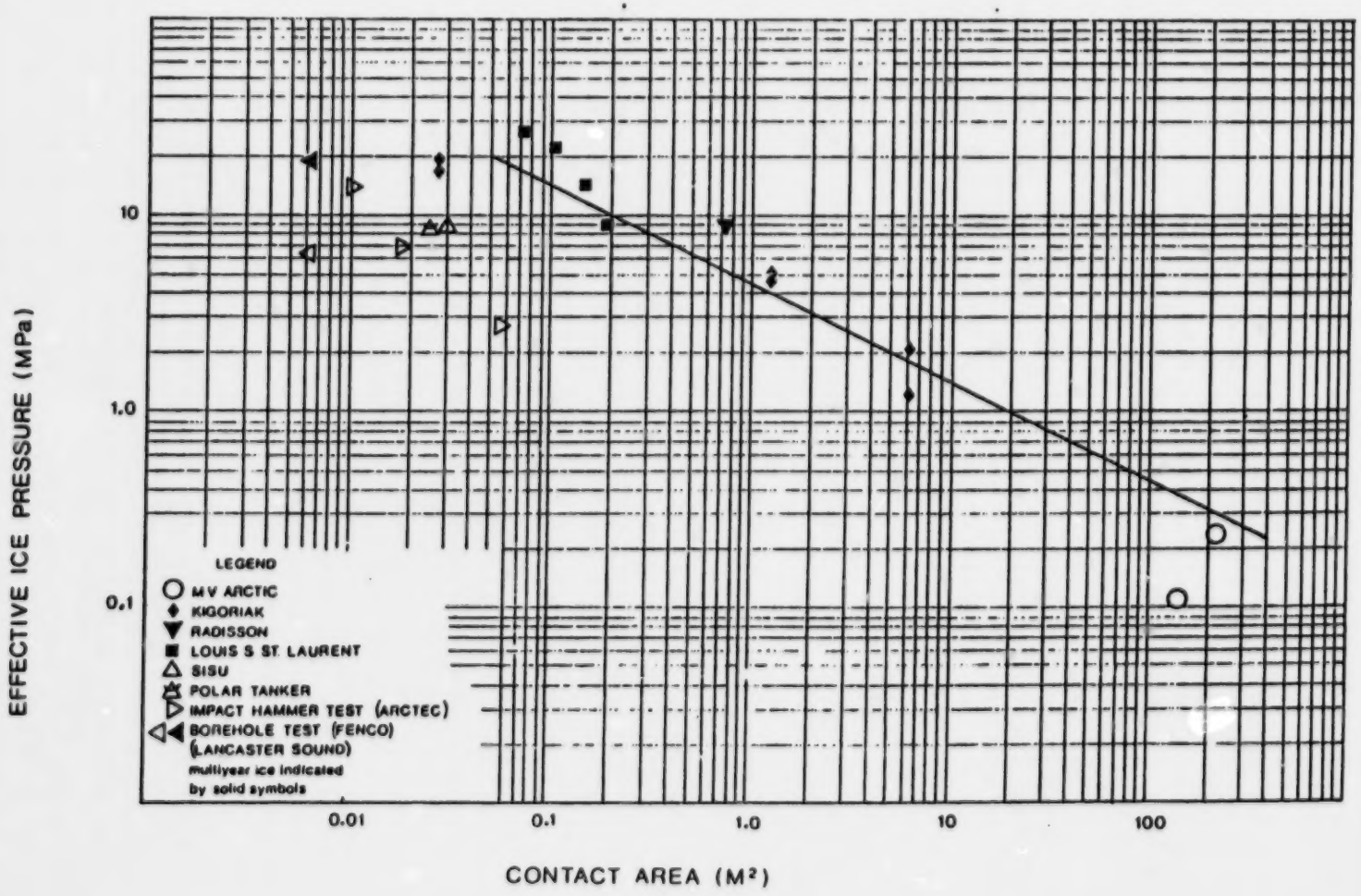


MEASURED EFFECTIVE ICE PRESSURE

FIGURE 5

### 2.2.2 Contact Area

The bow geometry of M.V. ARCTIC has been input to the computer program in the form of arrays with a resolution of about 5 m longitudinally and 1.5 m vertically. The total ice contact area and its direction are defined as a function of ship penetration distance, ice thickness and the ship draught at the fore end. Interpolation technique has been applied to approximate the curvature of the ship's bow.

Figure 6 depicts the estimated ice crushing contact area of M.V. ARCTIC for different ice thicknesses and penetration distances. The ship draught has been assumed constant at 10.8 m during the penetration in the estimates shown in the figure. By applying the effective ice pressure formula shown in the previous subsection, a total ice reaction force of approximately 65 MN is expected when ramming a 3 m thick ice floe at 20 m penetration.

In the simulation model, the calculated ice reaction force fluctuates during ramming as influenced by the vertical movements of the bow.

## 2.3 Finite Element Model

The structure of M.V. ARCTIC has been approximated by a discrete two dimensional beam model using a finite element computer program of an acronym "FESDEC" (Ref. 6). The ship was modelled using 19 nodes of concentrated mass linked by beam elements and restrained by grounded springs. The distribution of the nodes were designed to ensure sufficient accuracy in the prediction of hull girder vertical vibrations of low frequency modes. Each node was defined on the ship centre line vertical plane, and was allowed to possess three degrees of freedom of motion including rotation and transition in vertical and longitudinal directions. A total of 57 degrees of freedom were employed in the finite element model. The nodal co-ordinates and masses are presented in Table 2. A graphical display of the nodal points distribution is shown in Figure 2. The masses were lumped according to the distribution of the light ship and deadweight of the grain load condition, and the entrained water associated with the vibrational motion of the ship. Calculation of the added mass is given in Section 2.3.1.

The stiffness parameters were determined to account for the structural restraints of the ship and the buoyancy force generated by the vertical movements. The sectional Bonjean curves of M.V.ARCTIC have been analysed and linear approach was adopted for the buoyancy stiffness calculation (Appendix I). Damping factors were derived from empirical data for elastic vibrations and from theoretical prediction for heaving and pitching, and are summarized in Section 2.3.2. The bow force calculated from the ship/ice interaction model was applied to the most forward nodal point of the beam model containing the mass of the ship forward of that nodal point. Details of the computation method to generate the ship response during ramming are documented in Appendix I.

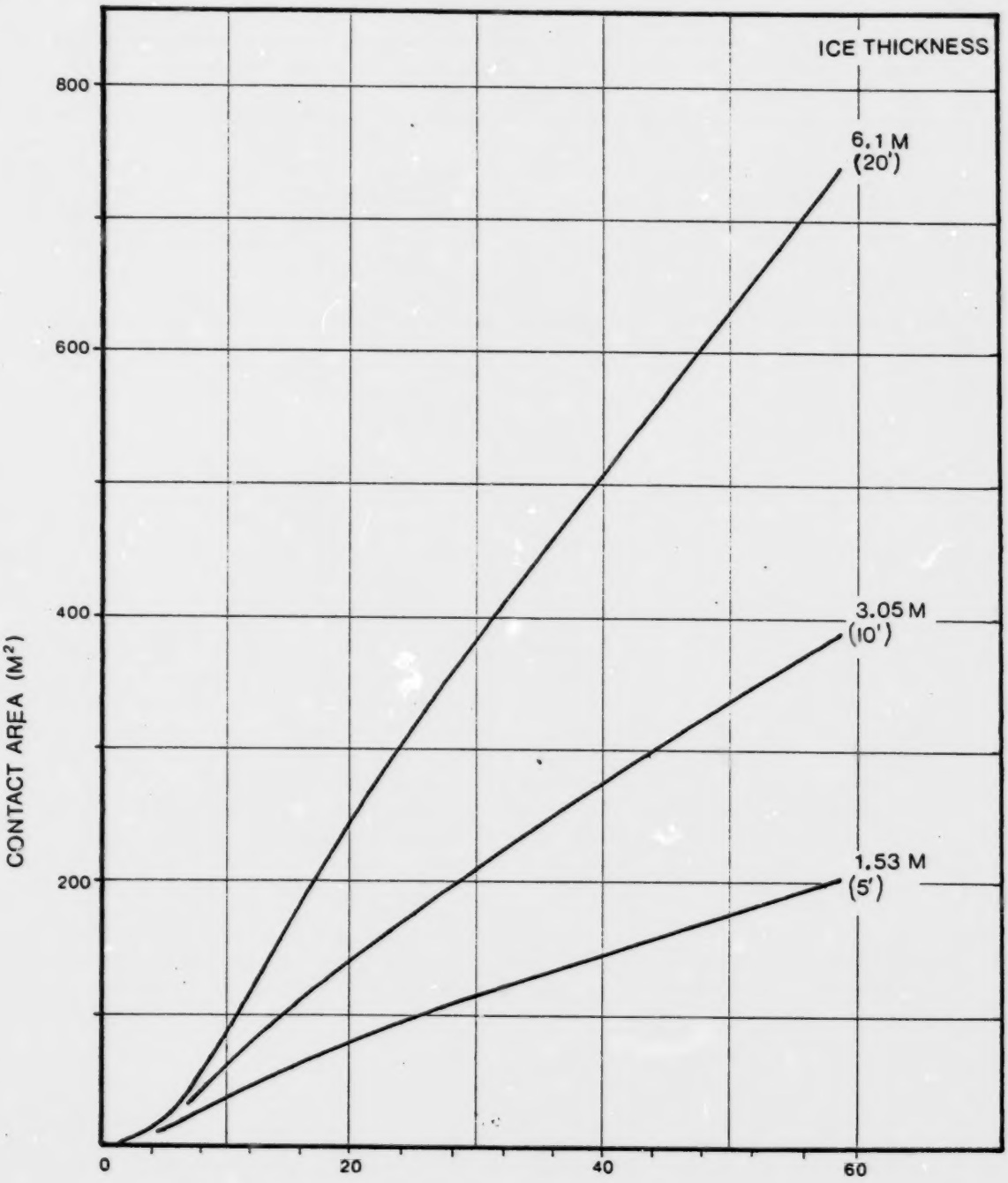


ESTIMATED ICE CONTACT AREA OF M.V. ARCTIC

FIGURE 6

| Node No | Ref. No Used In Appendix | Long. Distance From A.P.* (m) | Vertical Distance From Keel (m) | Mass (t) | Approx. Frame No. |
|---|---|---|---|---|---|
| 1 | 1 | 0 | 8.15 | 0.713 | 0 |
| 2 | 2 | 20.5 | 8.375 | 2.854 | 32 |
| 3 | 3 | 41.0 | 8.6 | 4.843 | 65 |
| 4 | 5 | 55.0 | 7.55 | 4.005 | 75 |
| 5 | 7 | 65.0 | 7.95 | 1.618 | 87 |
| 6 | 9 | 68.0 | 7.15 | 8.968 | 92 |
| 7 | 10 | 92.0 | 7.15 | 8.383 | 106 |
| 8 | 12 | 104.0 | 7.85 | 5.610 | 115 |
| 9 | 14 | 117.0 | 7.15 | 4.717 | 126 |
| 10 | 16 | 129.0 | 7.85 | 4.740 | 135 |
| 11 | 18 | 141.0 | 7.125 | 10.71 | 146 |
| 12 | 19 | 153.0 | 7.1 | 2.623 | 156 |
| 13 | 21 | 160.0 | 7.5 | 1.565 | 162 |
| 14 | 22 | 165.0 | 7.6 | 1.840 | 165 |
| 15 | 23 | 170.0 | 7.8 | 3.306 | 169 |
| 16 | 24 | 172.5 | 8.0 | 0.433 | 172 |
| 17 | 25 | 175.0 | 8.15 | 0.399 | 174 |
| 18 | 26 | 177.5 | 8.55 | 0.355 | 176 |
| 19 | 27 | 180.0 | 9.05 | 1.770 | 178 |

* A.P. - Aft Perpendicular

TABLE 2

NODAL CO-ORDINATES AND MASSES APPLIED IN THE FINITE ELEMENT BEAM MODEL FOR THE M.V. ARCTIC DYNAMIC RESPONSE SIMULATION

### 2.3.1 Added Mass

In addition to the static buoyancy force, the influence of a dynamically varying force exerted upon the submerged surface of the vessel is taken into consideration by an augmentation of the mass in the ship motion equation. The added mass used in the present model was determined by conventional method for ships in open water (Ref. 7). No correction for ice influence has been made.

The longitudinal distribution of added mass for the vertical motion of a ship in open water can be expressed by

$$M_l = \frac{\pi}{8} \rho B_l^2 C_l . k_l . J$$

where $M_l$ = added mass per unit length of section l
$\rho$ = water density
$B_l$ = beam at water line
$C_l$ = shape factor
$k_l$ = local correction factor
$J$ = three dimensional correction factor (J-Factor)

Figure 7 shows the estimated distribution of added mass along the length of M.V. ARCTIC, with the associated shape factor and local correction factor determined by the method of Anderson and Norrand (Ref. 7) and Orsero and Armand (Ref. 8), respectively. An average J-Factor of 0.77 has been used. The calculated total added mass in grain load condition is about 88% of the ship total weight. As to be discussed in Section 3.2, the calculated natural frequencies of vertical vibration are found to agree reasonably well with the measured data, therefore no refinements of the estimated added mass parameters have been made.

No added mass was used for the longitudinal motion of M.V. ARCTIC since the hydrodynamic force for this direction has not been included in the calculations.

### 2.3.2 Damping Factors

The damping force which acts in the opposite direction of the motion of the ship has been treated as linearly proportional to the corresponding velocity.

Damping in the heaving and pitching modes, induced mainly by waves due to oscillatory movements, were computed by established methods of naval architecture (Ref. 9). Strip theory was applied and sectional damping

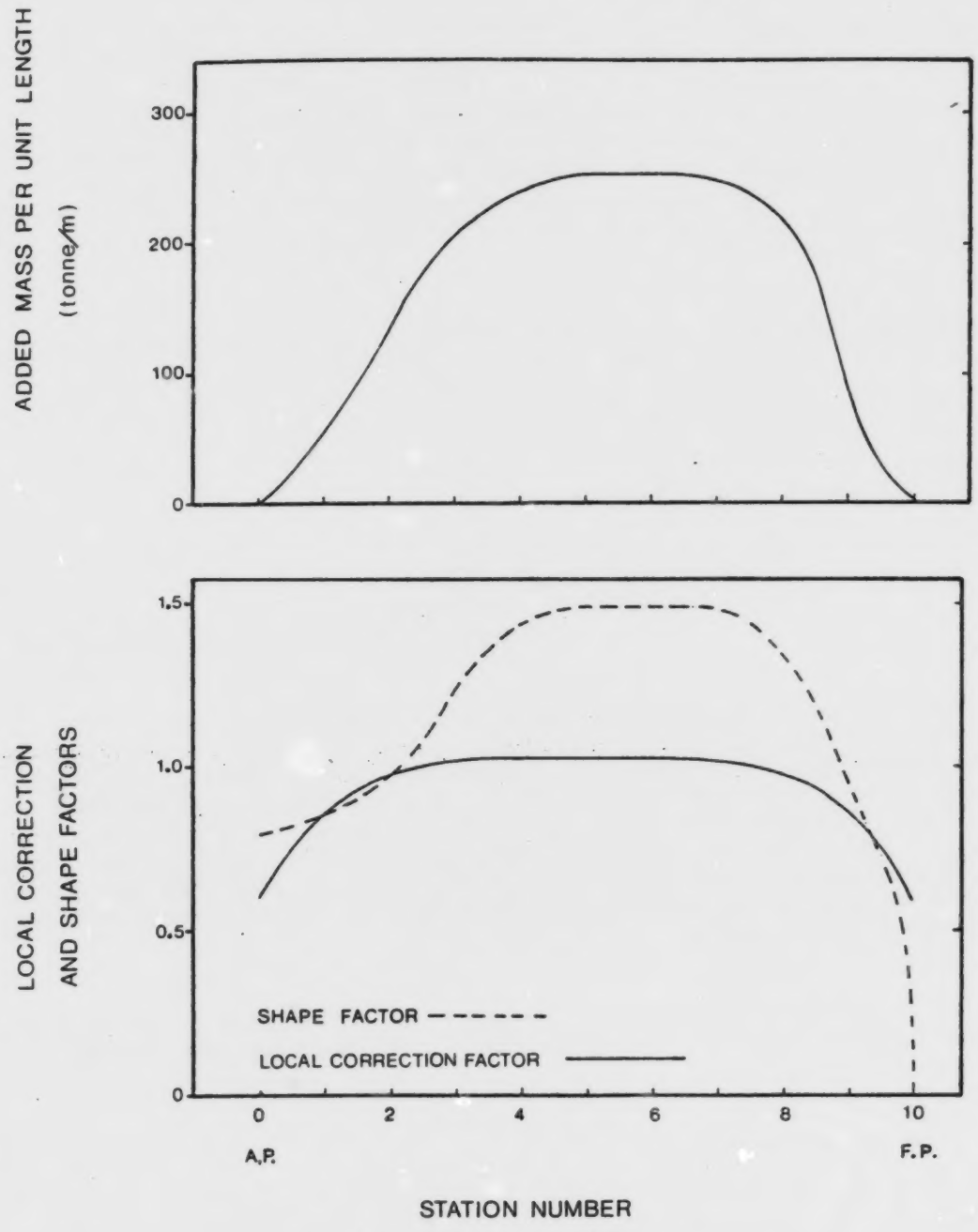


ESTIMATED ADDED MASS, SHAPE FACTOR
AND LOCAL CORRECTION FACTOR FOR M.V. ARCTIC

FIGURE 7

coefficients were determined from the vibration frequency and the hull geometry. The estimated damping coefficient for M.V. ARCTIC is about 11.7 x $10^6$ kg/sec for heaving and 3.6 x $10^{10}$ kg $m^2$/sec for pitching, for a frequency of about 0.125 Hz. The corresponding fraction of critical damping, in each case, is about 0.11.

For vertical elastic vibratory motions of the ship, damping due to structural and hydrodynamic factors are considered. The damping factors used in the model were derived from the exciter test performed by VTT on the M.V. ARCTIC, under the supervision of MSL (Ref. 10). The test was made in still water at grain load condition. It should be noted that these damping factors were obtained from the results of tests in open water with the vessel responding as a uniformally supported beam on elastic foundations. When ramming the bow of the vessel undergoes partial restraint by the ice and some differences in damping may apply.

Table 3 summarises the calculated and measured damping factors applied in the ship dynamic response calculations.

| Vibration Mode | Fraction of Critical Damping |
|---|---|
| Pitching | 0.11 |
| Heaving | 0.11 |
| 2 node vert. | 0.058 |
| 3 node vert. | 0.22 |
| 4 node vert. | 0.22 |
| 5 node vert. | 0.35 |
| 6 node vert. | 0.40 |

TABLE 3

DAMPING FACTORS OF M.V. ARCTIC

## 3.0 RESULTS AND DISCUSSIONS

### 3.1 General

Nine ramming cases have been investigated for M.V. ARCTIC using the prediction model. Table 4 summarizes the various input parameters used in the test runs. Two different ice thickness conditions were used to correlate with the results of the VTT model and the experimental data previously reported. The effect of impact speed on bow load and ship's response, for each ice conditions, was examined. The effect of damping has been investigated by exercising the model in several cases with the damping factors suppressed. The calculations and analysis described in this section were intended to test the capabilities of the computer program. A complete sensitivity analysis of the prediction model with respect to various ship and ice conditions and the modelling assumptions of ship/ice interaction has not been attempted.

The calculated results of the test are fully documented in Appendices I & II. The prediction model output has been presented in the form of:

- time history of the bow force, rigid body and flexible motion of the ship during the ramming cycle;
- time history of the longitudinal bending stress at selected sections;
- moment distribution;
- natural frequencies, modal properties and modal deflections for each ramming case.

The following full scale tests performed on M.V. ARCTIC have been used to correlate with the present model predictions:

- ramming tests performed on multi-year ice floes in Lancaster Sound, N.W.T., November 1981. The ice floes were relatively small, about 50-70 m diameter and 2-2.5 m thick. The ship was operated at deep draft ballast condition (Ref. 2).
- ramming tests performed on first-year ridged ice, in Admiralty Inlet, N.W.T., July 1981. The ice condition was land-fast, with thickness in level ice region about 1.5 m. The keel depth of ice ridges was in the range of 2-3 m. The ship was operated in deep draft ballast condition (Ref. 1).
- exciter test performed in still water, March 1981. The ship was in grain load condition (Ref. 10).

| Case No. | Ice Thickness (m) | Impact Speed (kt) | Damping Factors |
|---|---|---|---|
| 1 | 2.5 | 2 | On |
| 2 | 2.5 | 2 | Off |
| 3 | 2.5 | 4 | On |
| 4 | 2.5 | 6 | On |
| 5 | 10 | 2 | On |
| 6 | 10 | 2 | Off |
| 7 | 10 | 4 | On |
| 8 | 10 | 6 | On |
| 9 | 10 | 8 | On |

TABLE 4

CASES OF ICE RAMMING STUDY WITH THE PREDICTION MODEL

- ice breaking tests performed in Lake Melville, Labrador, February/March 1981. The ice condition was first-year, land-fast, with thickness of about 0.5-1 m for level ice, and about 2-3 m for ridged features (Ref. 12).

In the following subsections, the computed natural frequencies and modal shapes are discussed, and the calculated results for ramming 10 m thick level uniform multi-year ice at 2, 4 and 6 knot impact speeds, are presented in comparisons with those obtained from the VTT model. In addition, some calculated results for ramming 2.5 m thick level ice are discussed with the data obtained from full-scale test measurements. The ice feature is considered to be infinite, i.e., does not move on impact.

## 3.2 Natural Frequencies and Modal Shape

Table 5 displays the calculated natural frequencies of vertical vibration of M.V. ARCTIC in comparisons with those calculated by the VTT model and the results obtained by measurement during the exciter test (Ref. 10) and during the experimental voyage in Lake Melville, Labrador (Ref. 12). It should be noted that the natural frequencies of vibration will vary according to ship draft, trim and mass distribution within the vessel. The vibration data measured during the icebreaking tests in Lake Melville was analysed by FFT techniques. As can be seen in the table, the average difference between the calculated and the measured natural frequencies of vertical vibration to the 6 node mode is about 2% which is within the uncertainty of the experimental data. The discrepencies range between 1% and 8%. This can be recognized as the result of different approximation levels employed in the finite element calculations. The VTT model uses a three dimension approach for the calculation of ship response and employs more than twelve times the degrees of freedom used in the Canadian model. In spite of this, the agreement is found very good for the lower frequencies of hull girder responses which are most important in the ship/ice interaction.

Similarly, good agreement between the modal shapes calculated by the VTT model and the present work is found for the low frequency vibrations. Figure 8 illustrates the relative vertical displacement along the ship for the 4 node vertical vibration generated from the models. It should be noted that for this mode of vibration, only about 4 elements per half wave in average were represented by the present model, and discrepancies are expected to be more apparent as the number of nodes increases.

Examination of the computed modal amplitudes in various impact conditions (Appendix I) reveals that the 2 node vibrational mode is always dominant in the simulated ship elastic response. The estimated contributions from high frequency mode (greater than 5 Hz) are about four orders of magnitude lower than the 2 node vibration amplitude. This is consistent with the Fourier analysis result of the full-scale vibration data (Ref. 11).

| Vibration Mode | CALCULATED | | MEASURED | |
|---|---|---|---|---|
| | Present Work | VTT Model (Ref. 3) | Exciter Test (Ref. 3) | Ice breaking (Ref. 12) |
| Coupled (pitch & rigid body heave) Motions | 0.11<br>0.14 | | | |
| 2 node | 0.91 | 0.98 | 0.93 | 0.89 |
| 3 node | 1.85 | 1.97 | 1.98 | 1.9 |
| 4 node | 2.82 | 2.80 | 3.12 | 2.6 |
| 5 node | 4.14 | 3.84 | 3.98 | 3.8 |
| 6 node | 4.93 | 4.65 | 4.86 | 4.8 |

TABLE 5

COMPARISON OF CALCULATED AND MEASURED NATURAL FREQUENCIES (Hz) OF VERTICAL VIBRATION OF M.V. ARCTIC

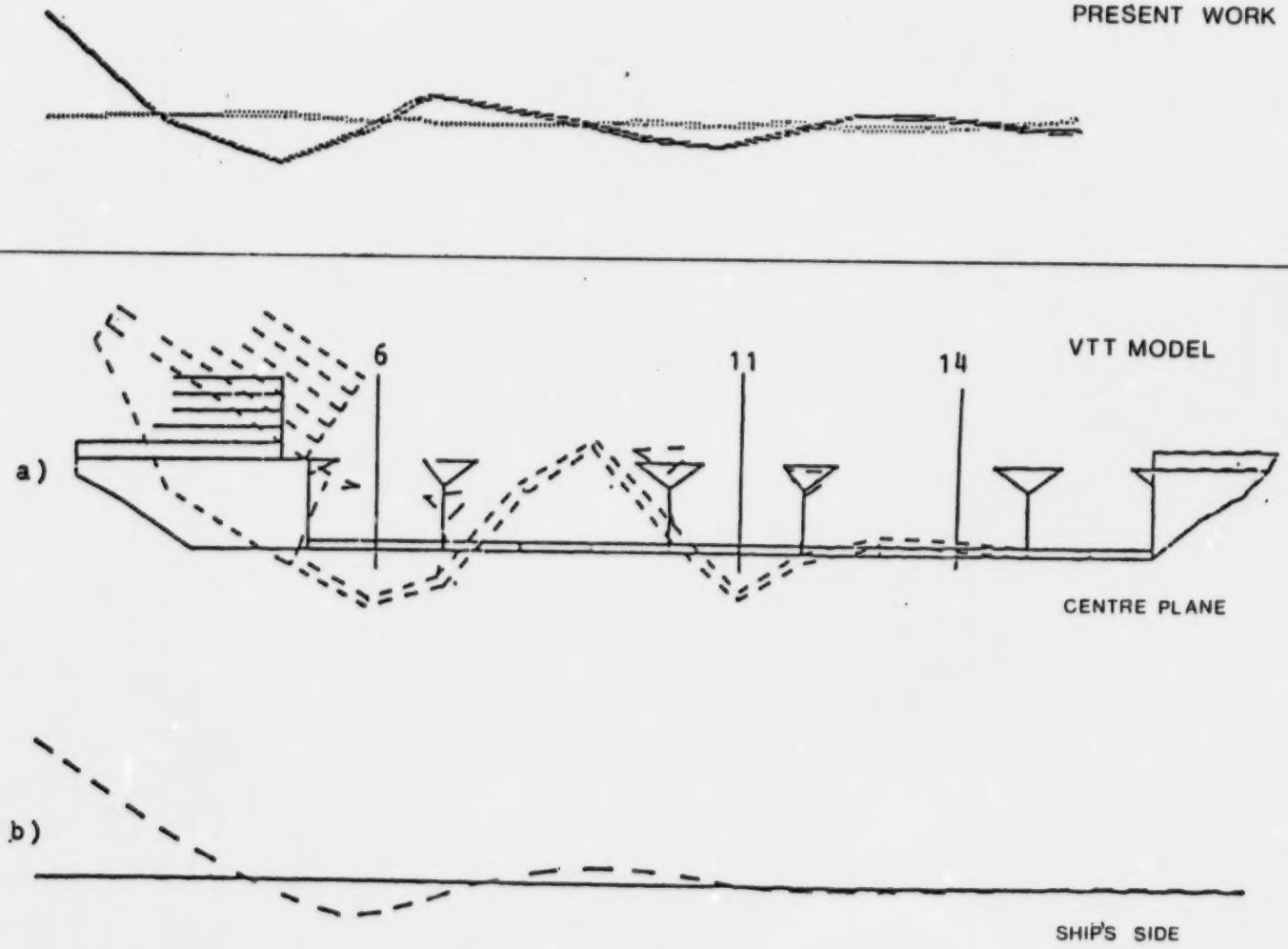


COMPARISON OF THE CALCULATED MODAL SHAPES OF THE
4 NODE VERTICAL VIBRATION MODE

FIGURE 8

## 3.3 Bow Force and Movement

The similarities between the present model and the VTT model are demonstrated in Figures 9a - 9c in which the estimated bow forces are plotted as a function of time when the ship is ramming ice of 10 m thick at a speed of 2, 4 and 6 knots, respectively. From both calculations, the predicted ship/ice interaction for this ramming condition has a total time span of 12-14 seconds from initial contact to final separation from the consolidated ice. The maximum ice reaction force exerted upon the ship bow is expected to be attained in less than 10 seconds after the initial impacts. Also, during the penetration stage, a similar "plateau" in the force diagram, reflecting the bow shape of M.V. ARCTIC, is exhibited in the calculation result of each model. In addition, both calculations result in the prediction of an oscillating behaviour in the ice reaction force when the ship is sliding back from the ice. This is the case even though the estimated oscillating force patterns as well as the magnitude of bow force, which are sensitive to the model parameters and computation approximations, are not exactly the same.

The confidence of the accuracy of the bow load evaluation is further enhanced by the agreement with the estimates based on the "White" prediction equation (Ref. 13). In his investigation of icebreaker ramming capabilities, R. M. White has developed in correlation with some full scale ship performance data, an analytical method to calculate ice loads for various hull forms of ice transitting ships. His work has led to the establishment of a simple linear expression for the vertical bow force with respect to ramming speed. The bow force to ship speed ratio is dictated by the so called "White ratio" which is related to the principal particulars of the ship's hull. The calculated bow force for M.V. ARCTIC is shown in Figure 10. Both the VTT and the present results shown in the figure were calculated for 10 m thick ice conditions to assess the highest anticipated bow force. As can be seen in this figure, the predictions from the three analytical models are within 25% over the speed range of 2 to 8 knots, and the White estimates lie consistently between the calculated values of the present and VTT model. A more distinct non-linear relationship between the maximum bow force and ship speed is shown in the present calculations, as compared to the results of VTT model.

When the ship rams consolidated ice, the ice crushing contact area and the total ice reaction force will increase. Since the reaction force is assumed to be perpendicular to the contact area of the bow, the resultant transverse component of the force becomes more significant as the distance of penetration increases. Therefore, according to the present exponential ice pressure assumption (Section 2.3), at high impact speed, a high vertical bow force may develop in the earlier stage of the penetration period and the force may subsequently reduce due to the ship's pitching and penetration motion (Appendix I, Figure 20).

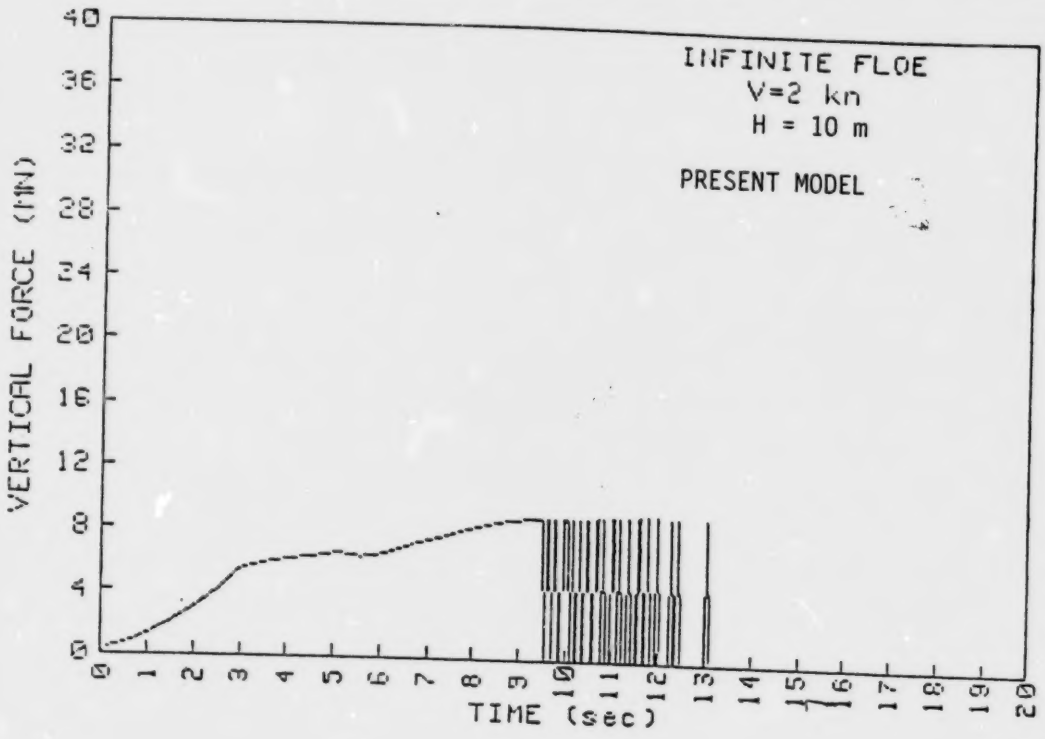


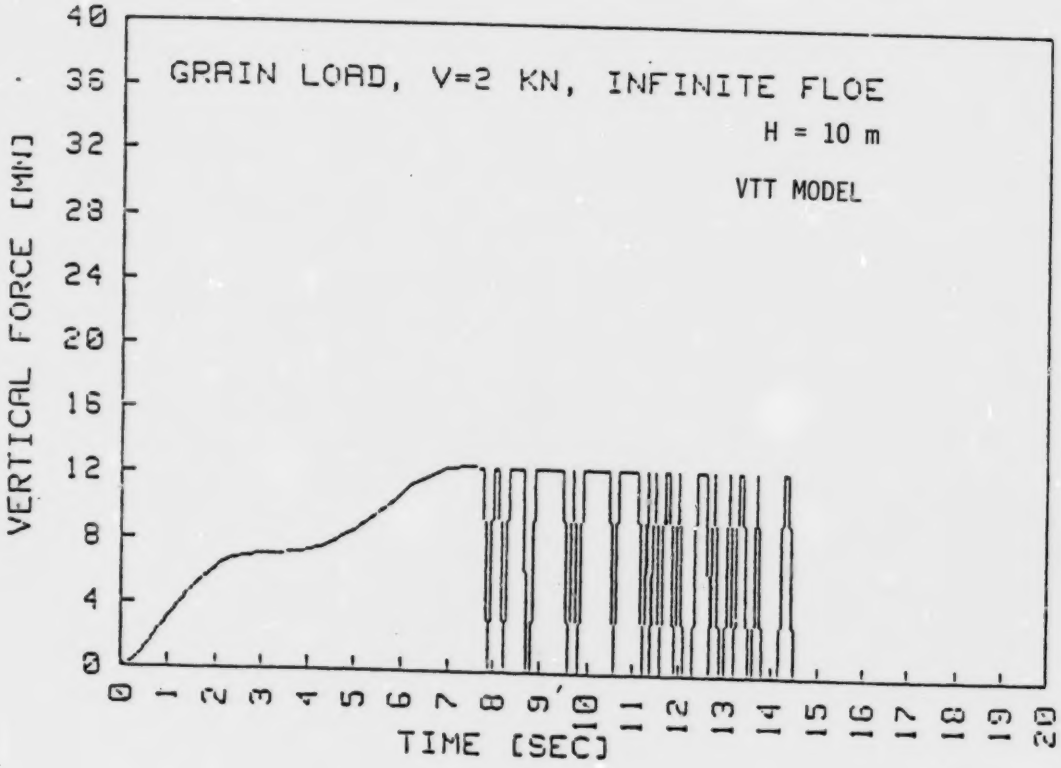


CALCULATED BOW FORCE FOR RAMMING MULTI-YEAR ICE

FIGURE 9A

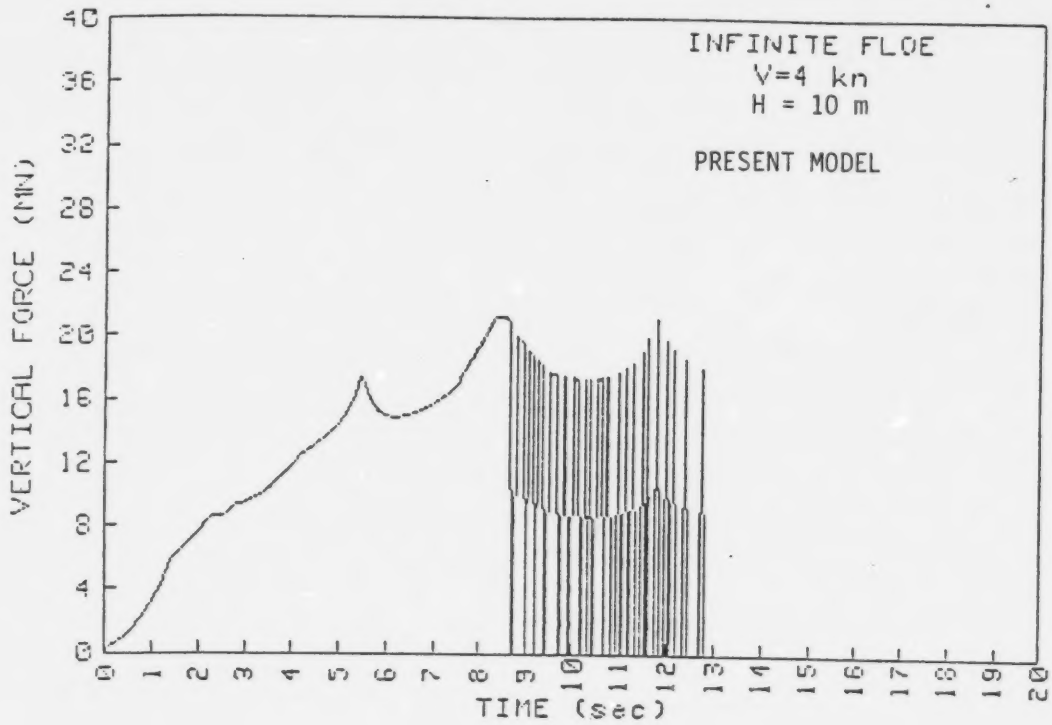


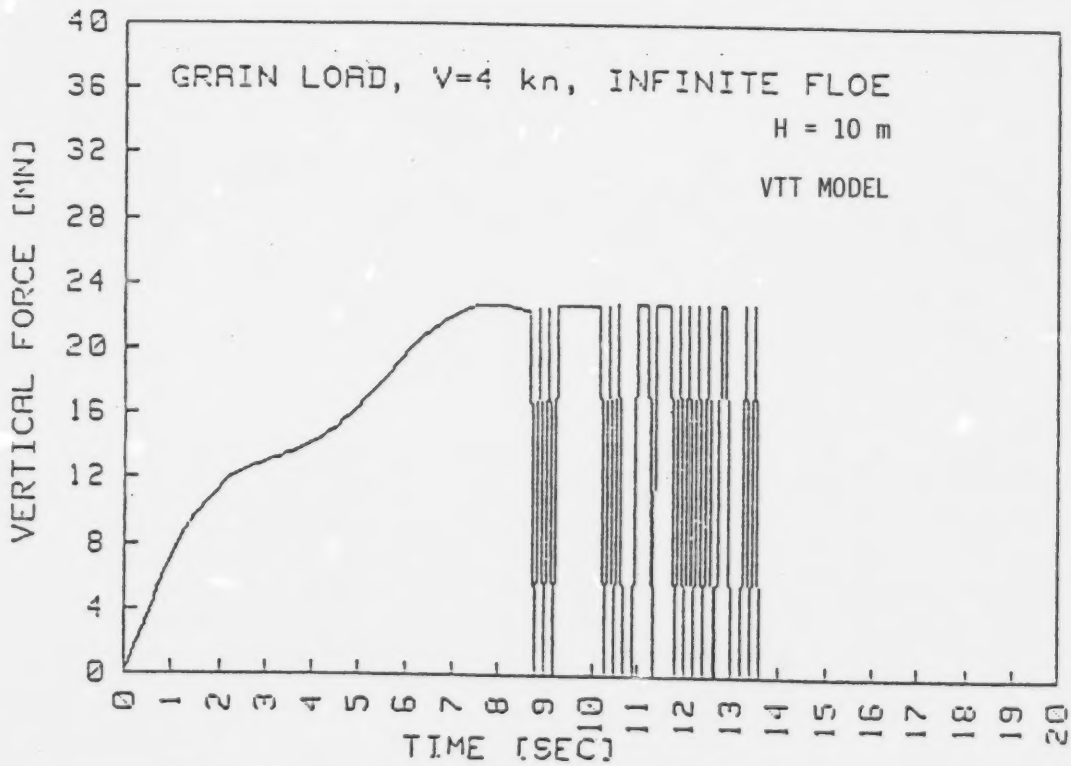


CALCULATED BOW FORCE FOR RAMMING MULTI-YEAR ICE

FIGURE 9B

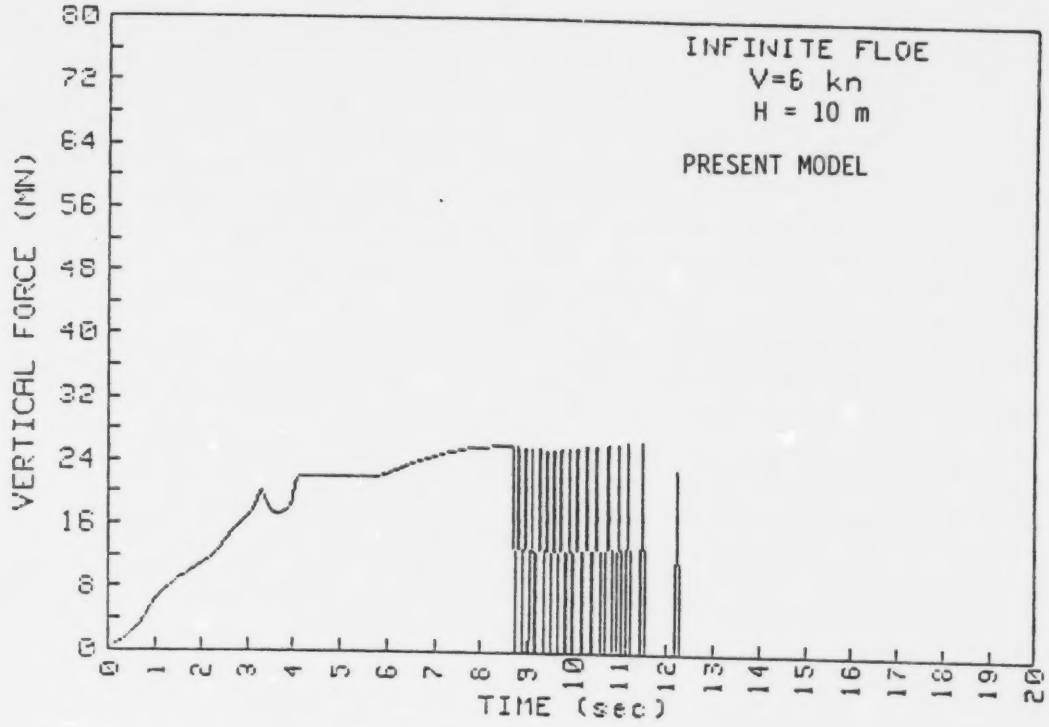


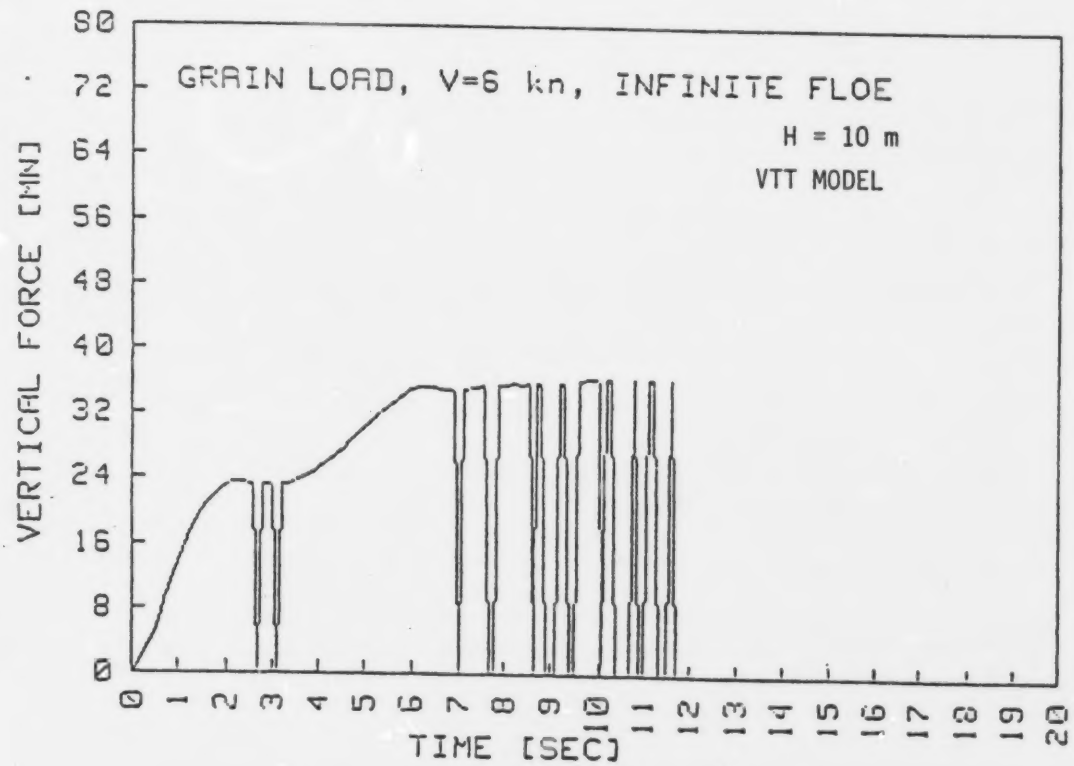


CALCULATED BOW FORCE FOR RAMMING MULTI-YEAR ICE

FIGURE 9C

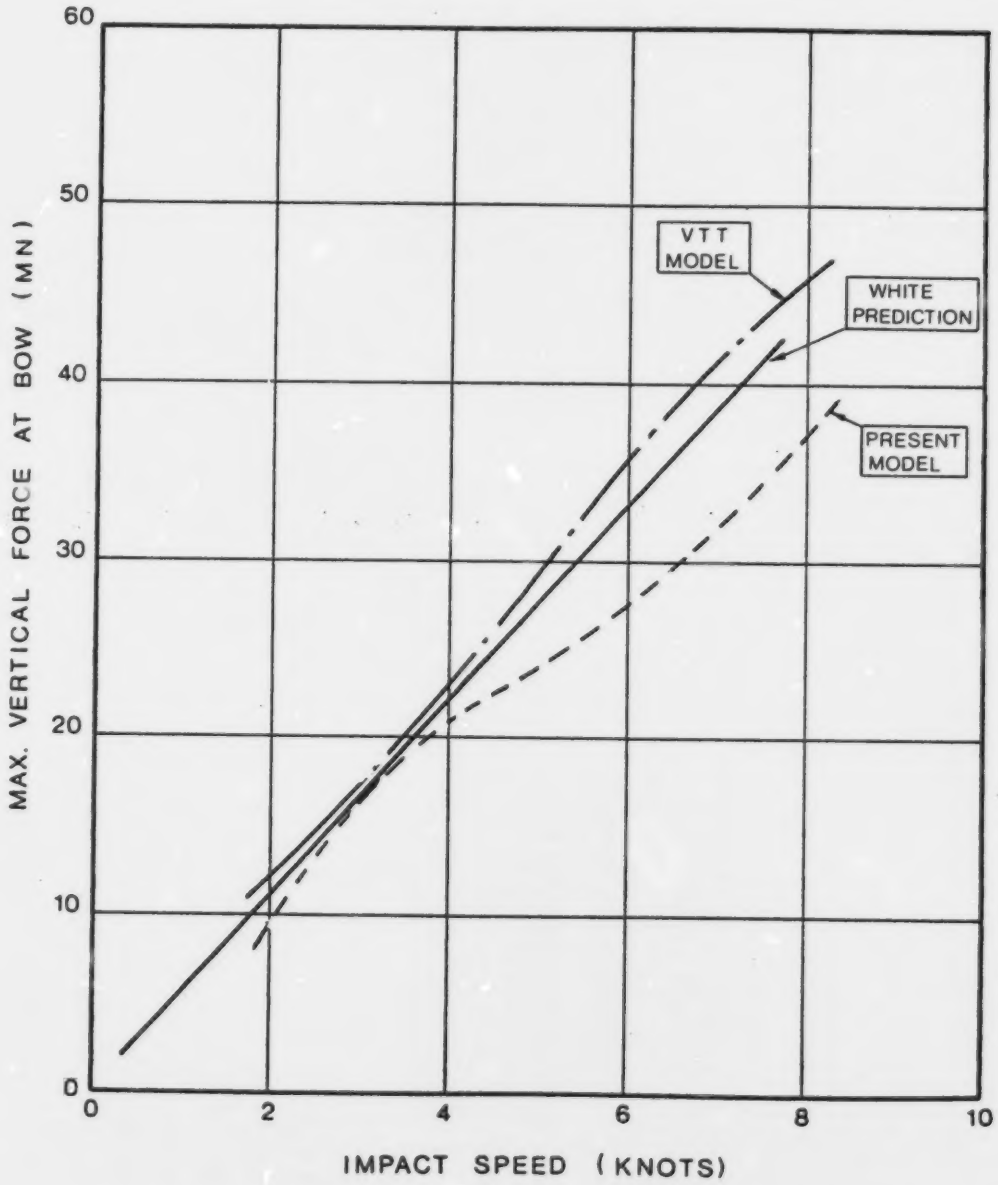


MAXIMUM VERTICAL BOW FORCE VERSUS RAMMING SPEED

FIGURE 10

Figure 11 illustrates the calculated and measured ice penetration distances of M.V. ARCTIC in various ramming conditions. The calculated maximum horizontal penetrations in ice for thickness of 25 m and 10 m differ significantly in the high impact speed range but have similar magnitudes for speed less than 3 knots. The calculations were based on the assumption of regular ice edge for each ram. In practice, ramming is required when the continuous ice breaking mode is not feasible, and a notch from the previous penetration is usually present. In this case, higher reaction forces are developed at the initial impact with the ice.

The full-scale data shown in the figure was obtained from a ridge ramming tests performed in Admiralty Inlet (Ref. 11). The average observed ice penetration distance appears to be comparable with the model prediction. The scatter of the observation data indicates that large variations and irregularities in ship/ice interaction occur in practical ramming operations due to the non-homogeneous nature of natural ice and these have not been reproduced in the theoretical model.

The calculated vertical rigid body and elastic modes of the motion are compared with the VTT calculations in Figures 12a - 12e. The calculations were made for various impact speeds (2-6 knots), ramming on level uniform ice of a thickness of 10 m. Figures 12a, b and d display the results calculated from the present model and Figures 12c and e show the results of the VTT model. Both models predict a bow emersion of about 1 - 4 m depending on the impact speed, superimposed with a maximum elastic motion amplitude in the order of 0.1 m. The calculated vertical displacement from the present model is displayed at Frame No. 178 position, about 23 m from the fore end of the ship. Recognising the difference in longitudinal positions as shown, the agreements between the bow motion estimates from the two analytical models are found acceptable. In general, the models show that the bow motion amplitude exhibits a linear relationship with ship impact speed when ramming ice, as expected.

### 3.4 Hull Girder Vibratory Response

With respect to the variation of ice retardation force, the dynamic response of each nodal point of the finite element beam model was determined through a time incremental method (Appendix I). The time history of nodal movements and the corresponding bending stress at the ship deck or keel structure were generated using the known structural properties of M.V. ARCTIC. Figures 13a - 13c display some calculated stress data for various ramming speeds. The corresponding output obtained from the VTT model are also included in the figures for comparison. The bending stresses are shown at selected sections near midship where the bending stresses are found to be the greatest. The still water bending stress of the ship has not been considered here and it should be added arithmatically to the instantaneous stresses to obtain the total stress values.

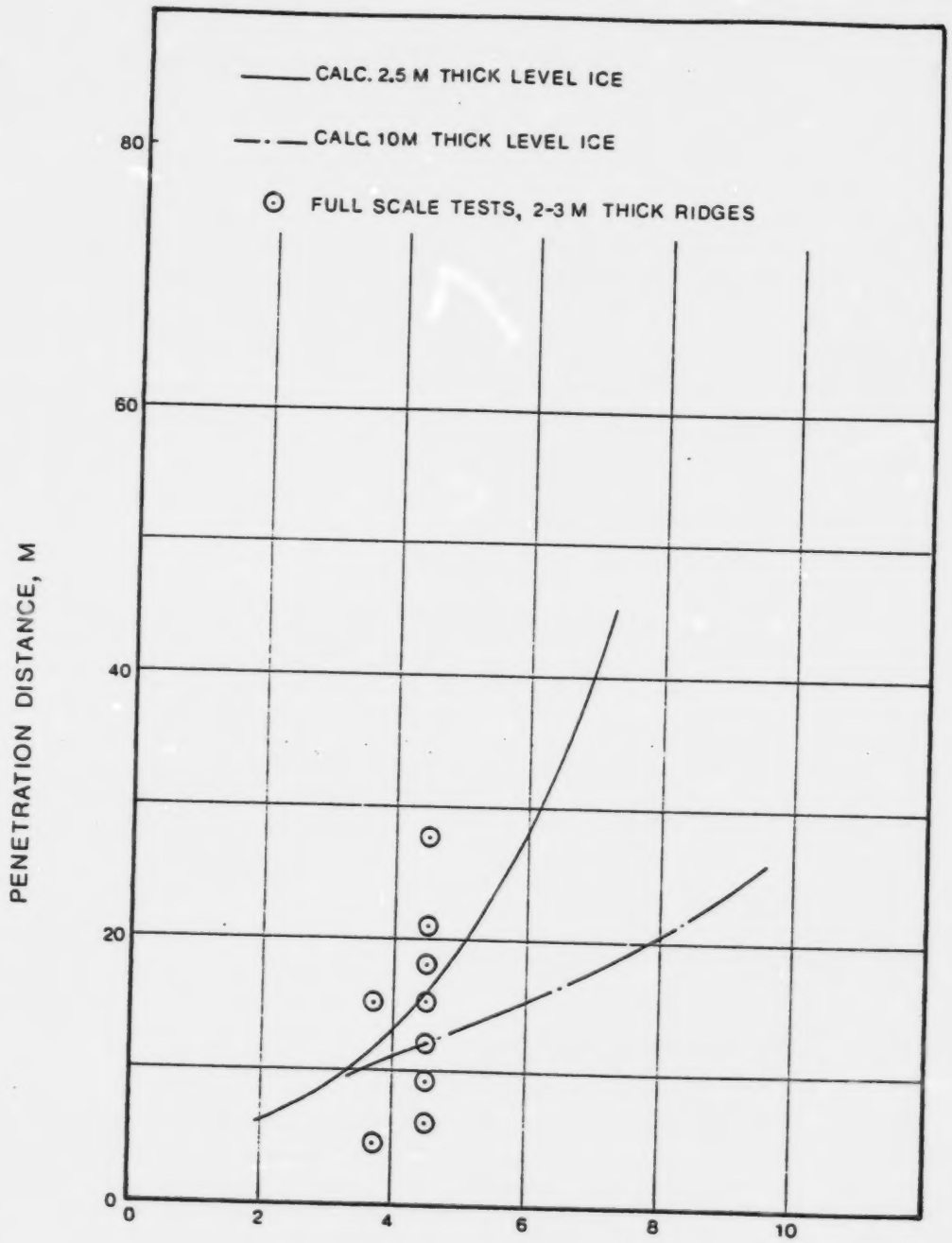


PENETRATION DISTANCE VERSUS RAMMING SPEED

FIGURE 11

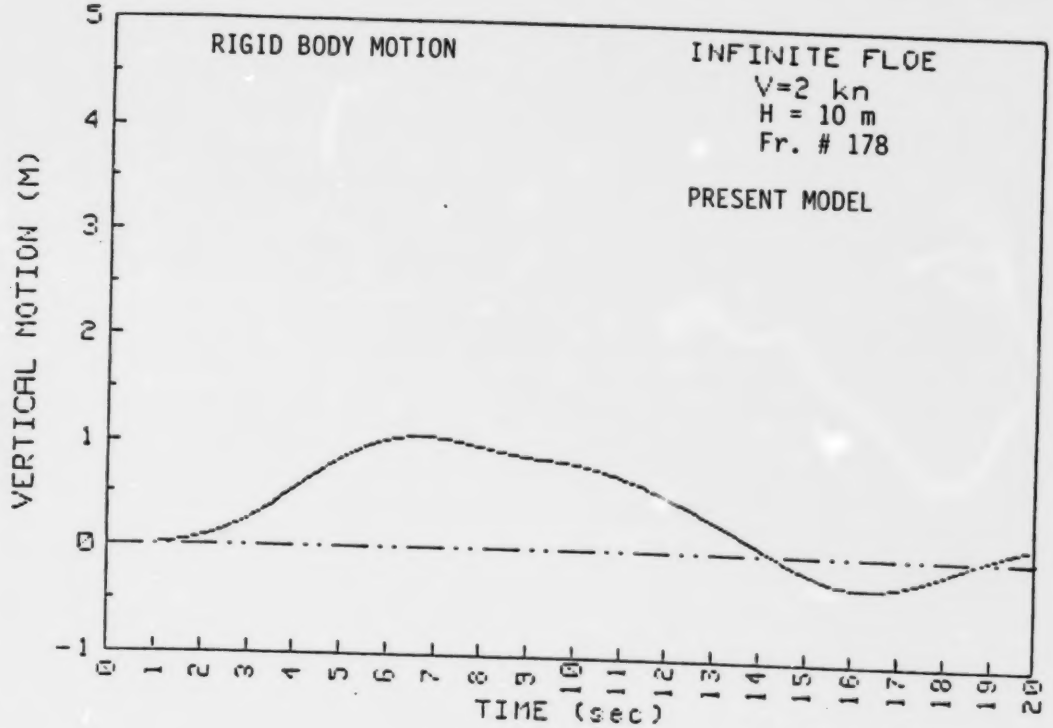


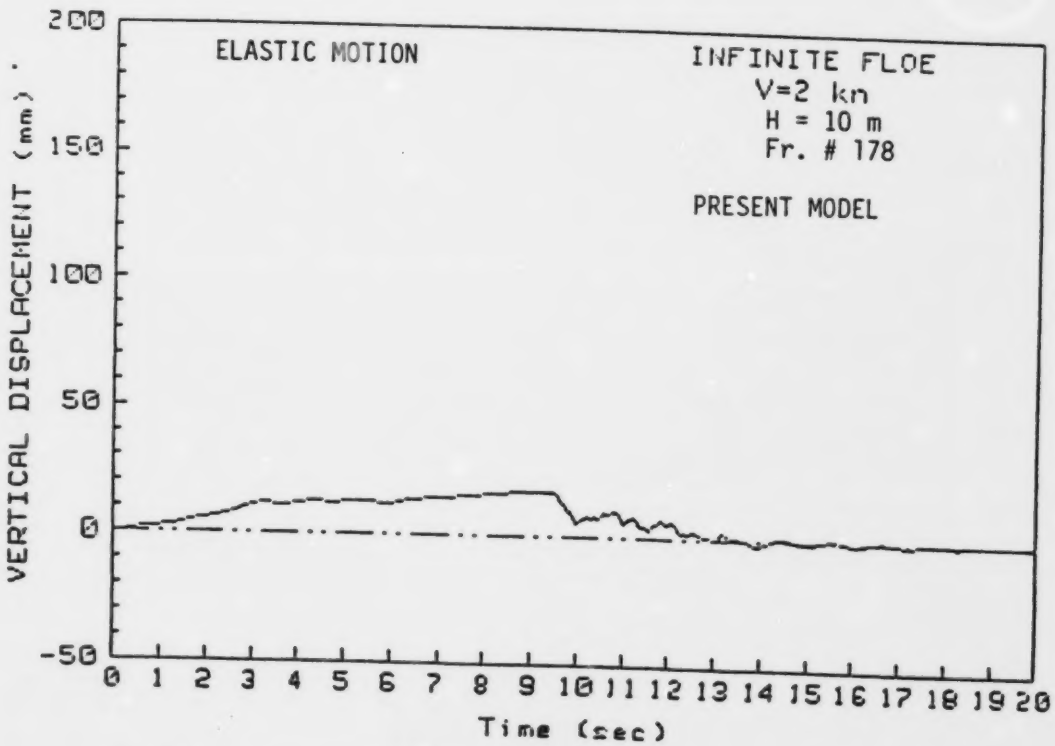


CALCULATED VERTICAL RIGID BODY AND ELASTIC MOTIONS
OF M.V. ARCTIC

FIGURE 12A

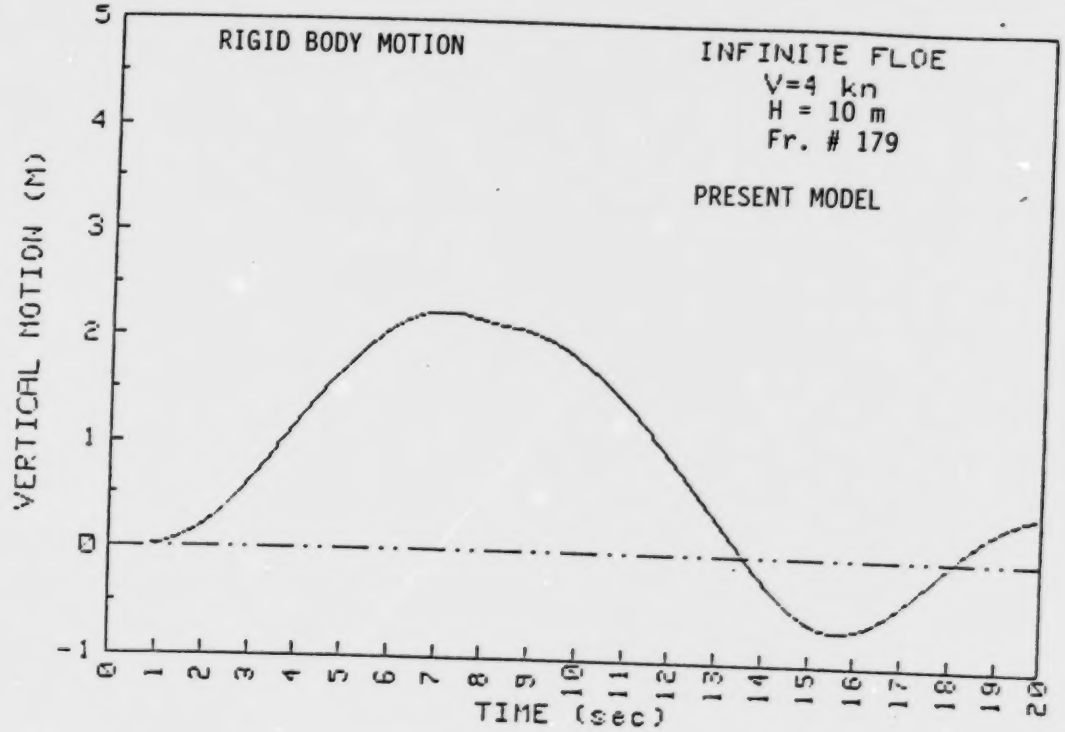


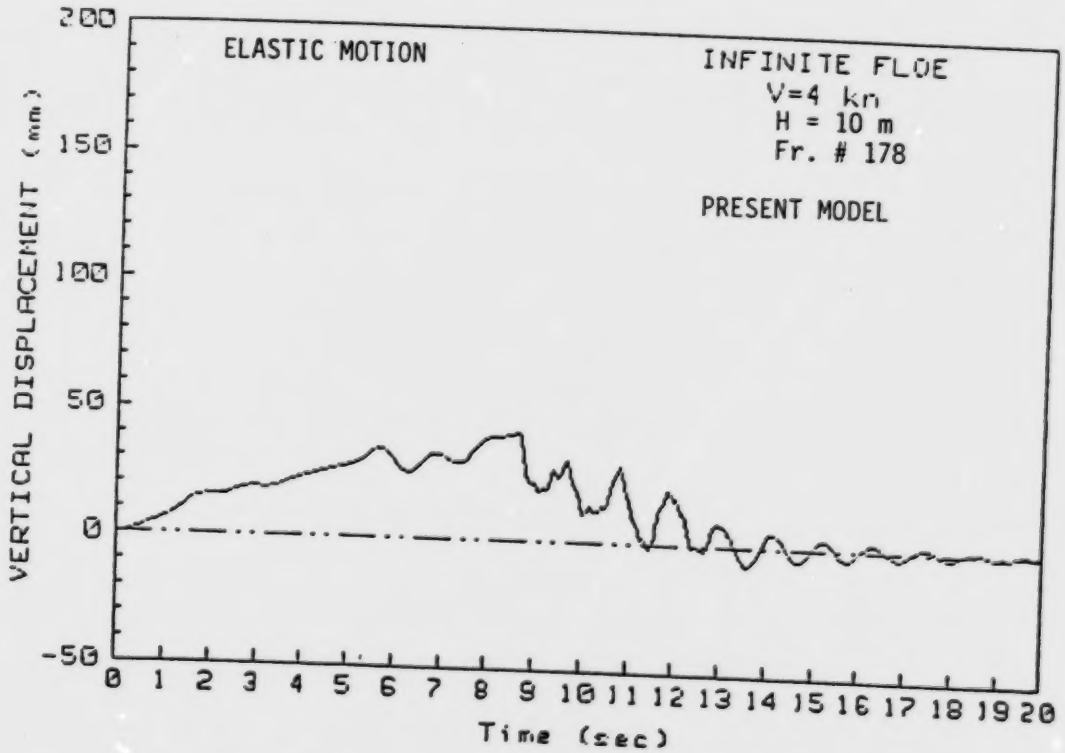


CALCULATED VERTICAL RIGID BODY AND ELASTIC MOTIONS
OF M.V. ARCTIC

FIGURE 12B

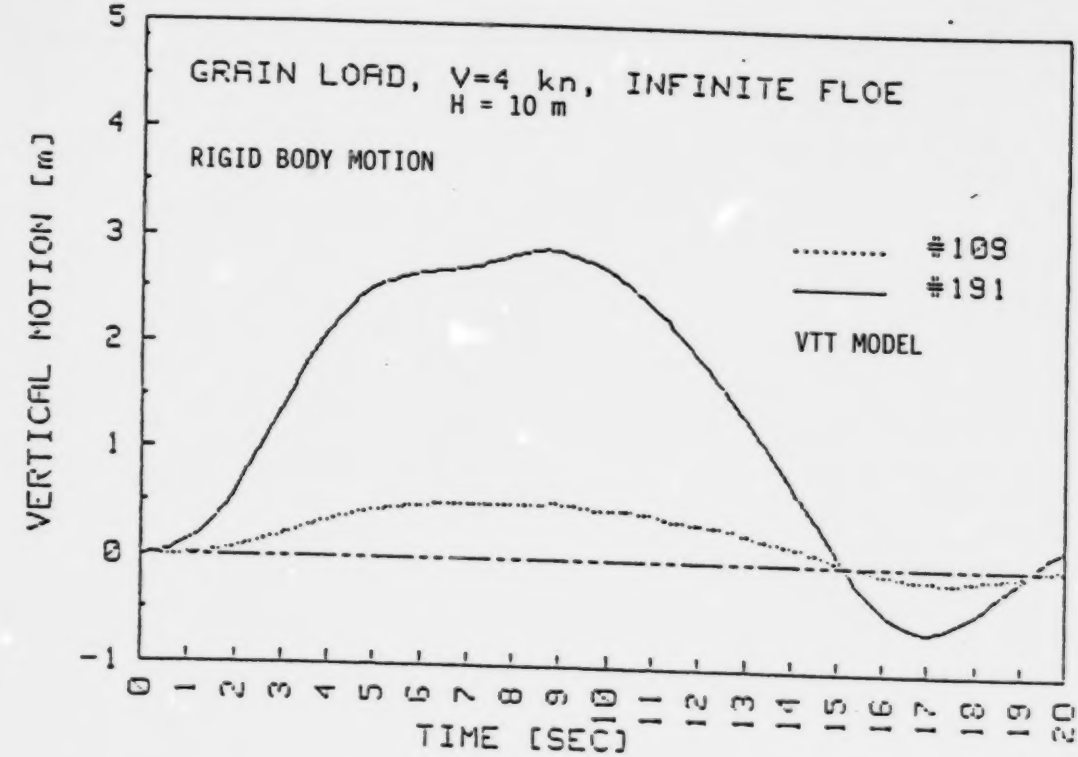


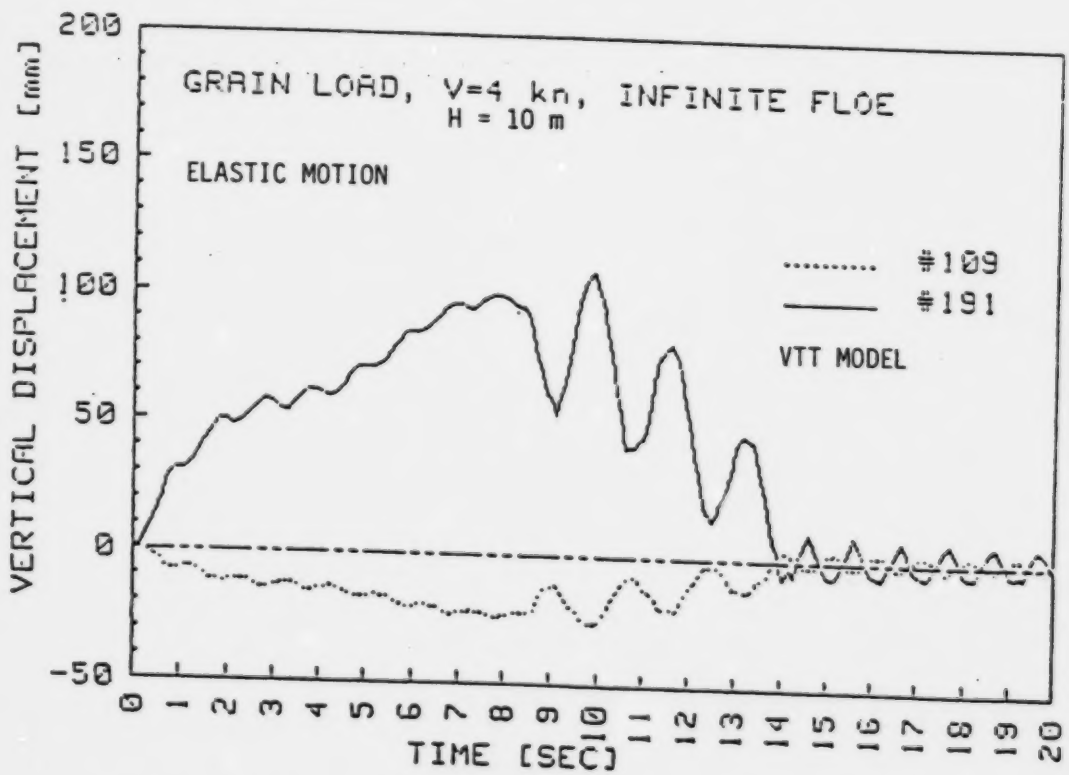


CALCULATED VERTICAL RIGID BODY AND ELASTIC MOTIONS
OF M.V. ARCTIC

FIGURE 12C

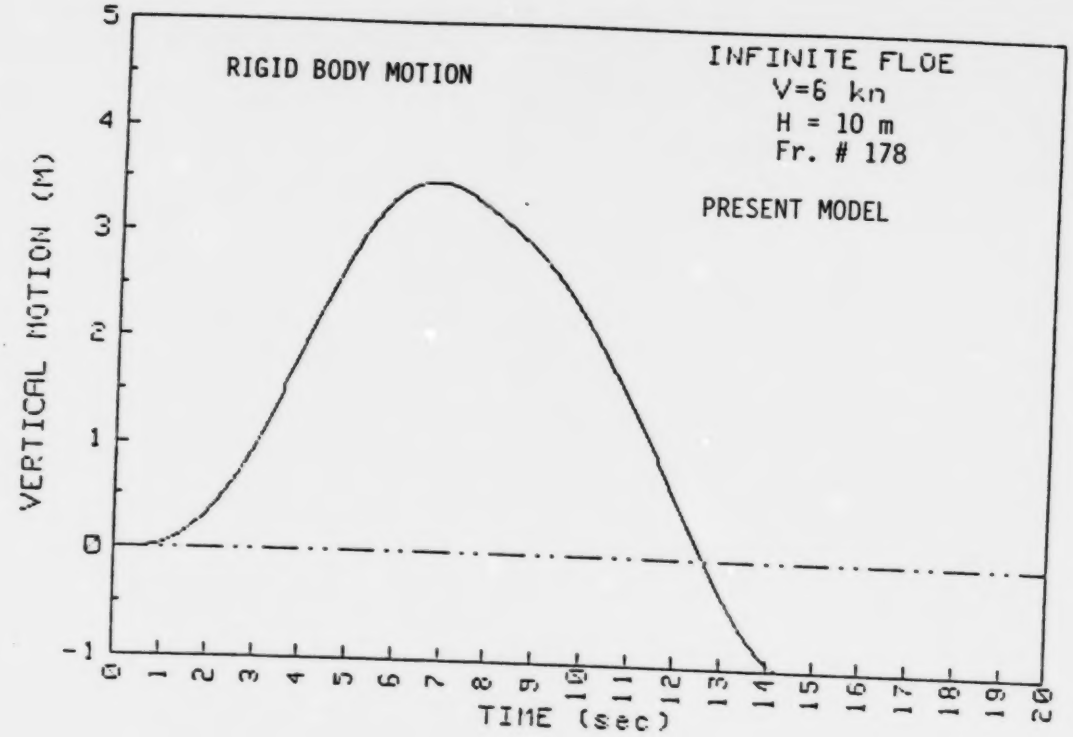


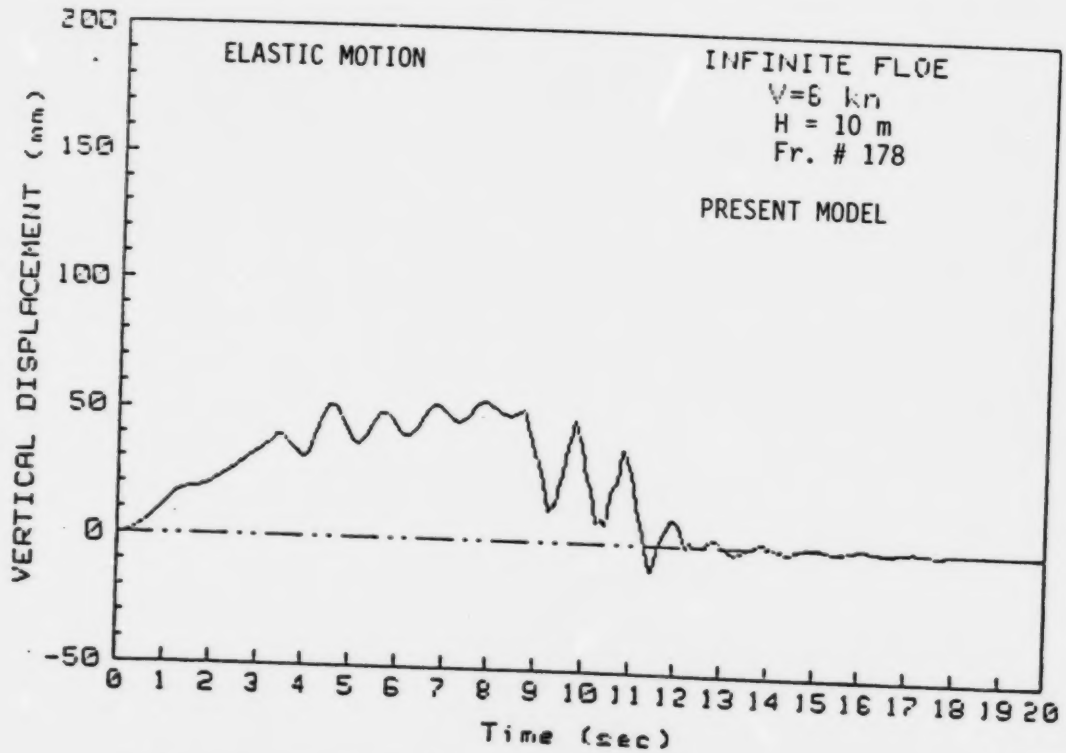


CALCULATED VERTICAL RIGID BODY AND ELASTIC MOTIONS
OF M.V. ARCTIC

FIGURE 12D

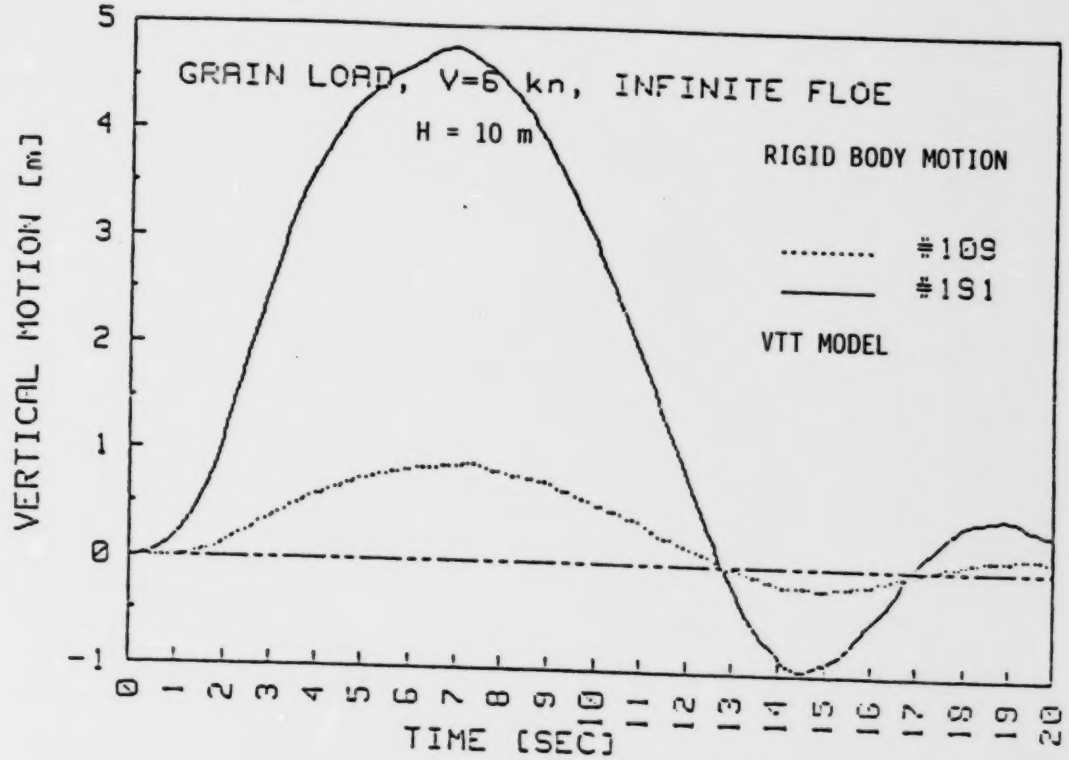


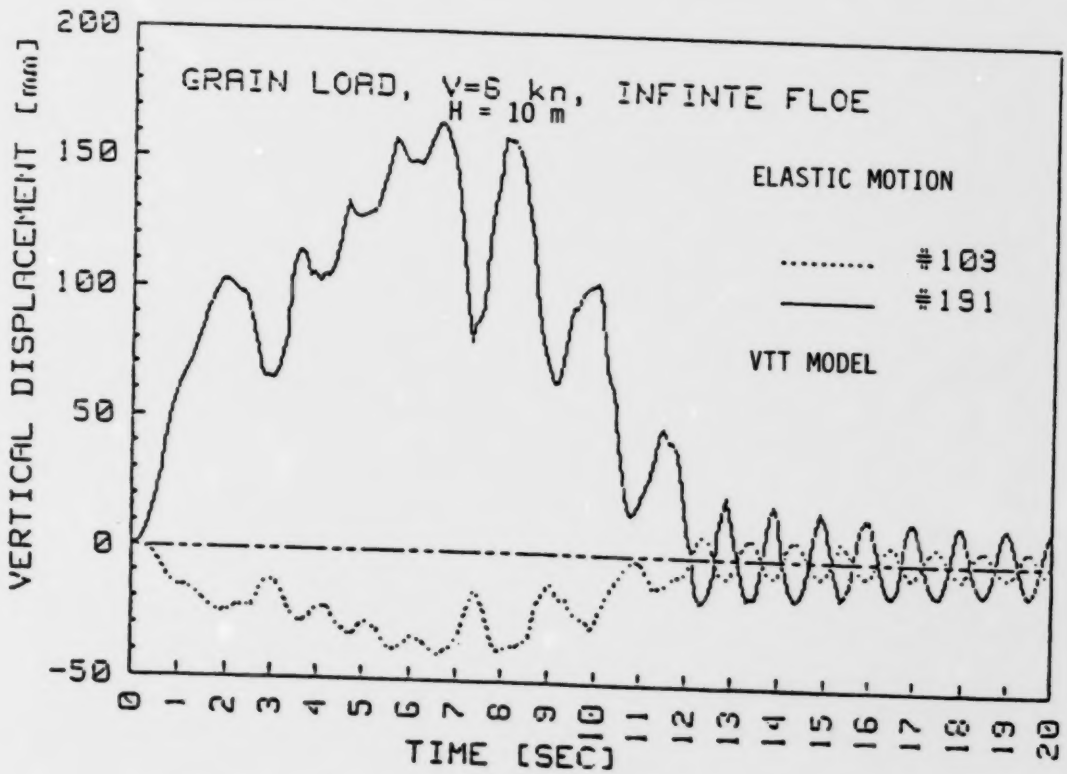


CALCULATED VERTICAL RIGID BODY AND ELASTIC MOTIONS
OF M.V. ARCTIC

FIGURE 12E

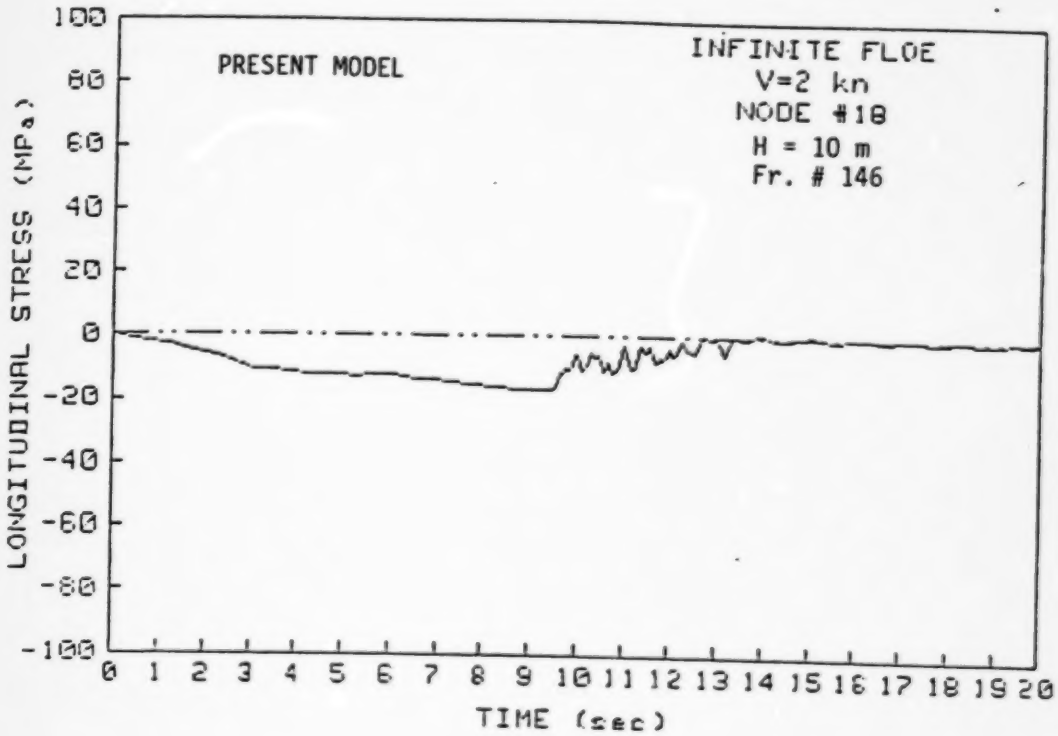


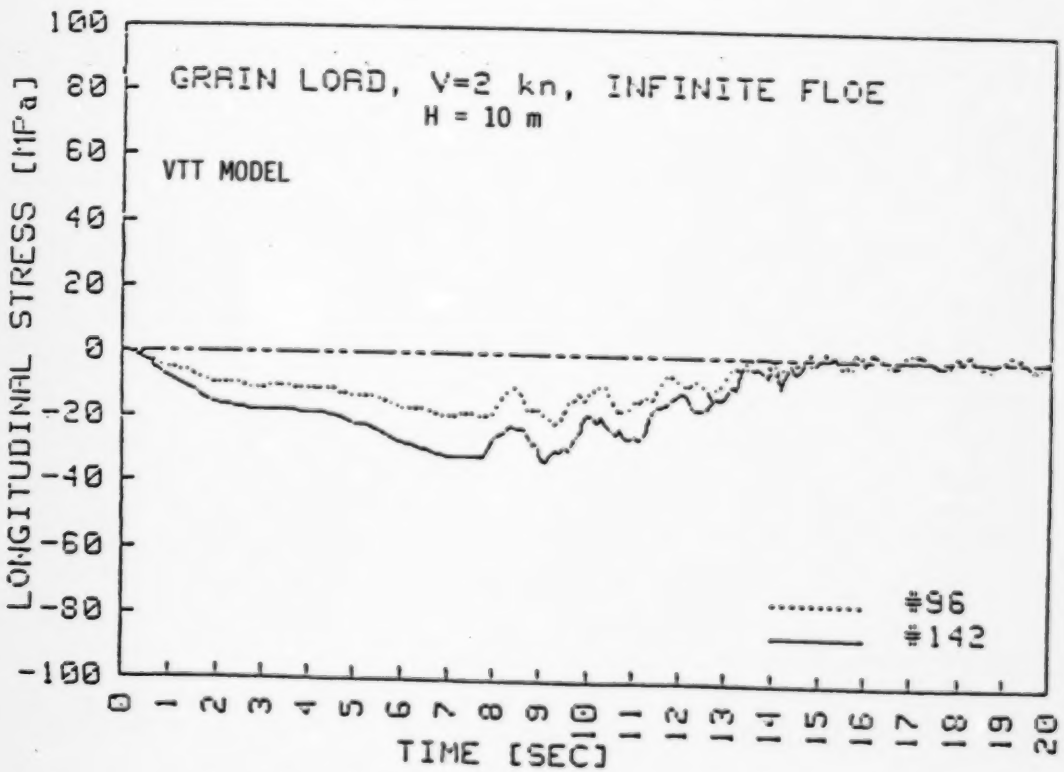


CALCULATED LONGITUDINAL BENDING STRESS
INDUCED BY ICE RAMMING

FIGURE 13A

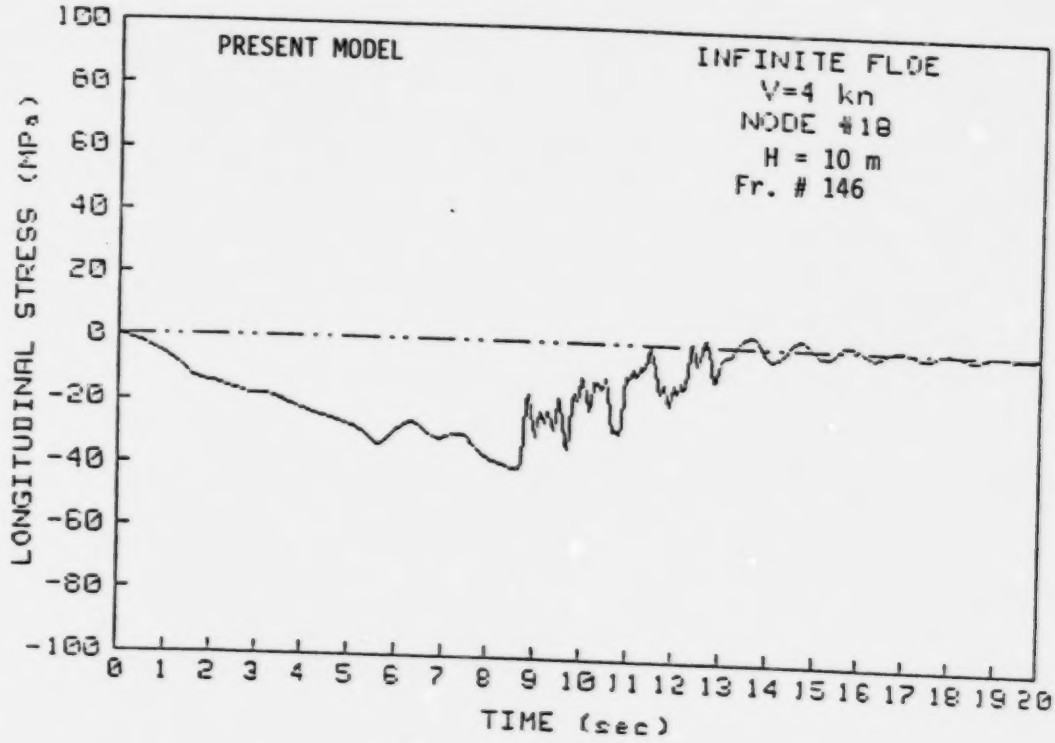


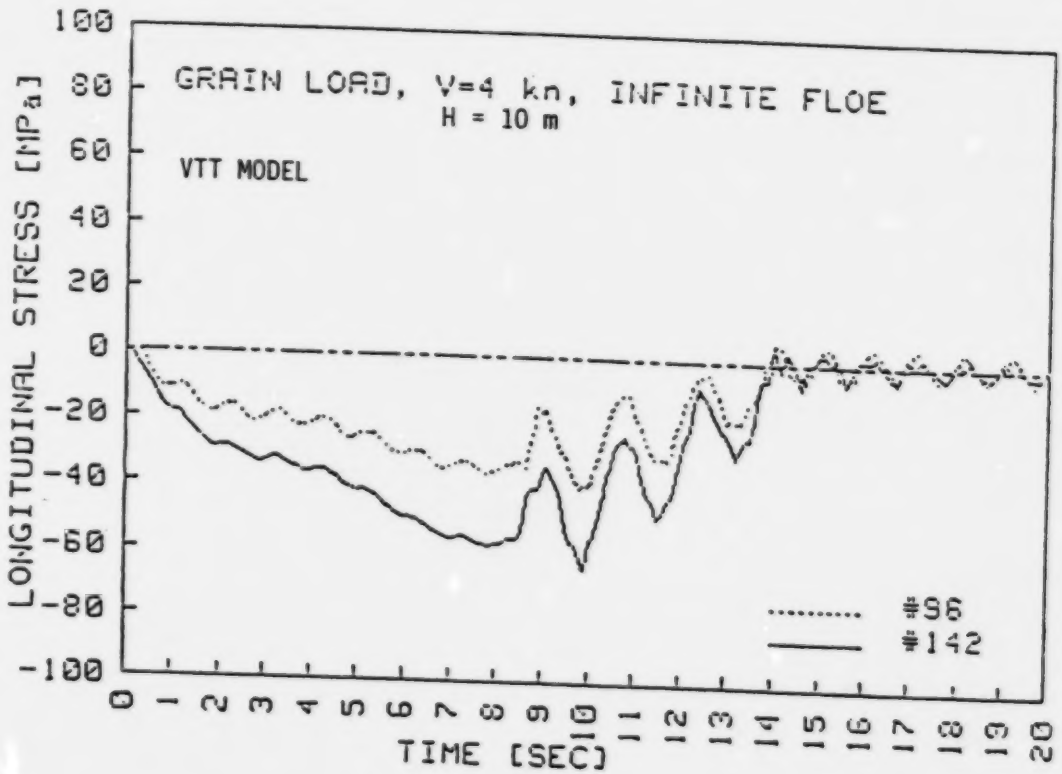


CALCULATED LONGITUDINAL BENDING STRESS
INDUCED BY ICE RAMMING

FIGURE 13B

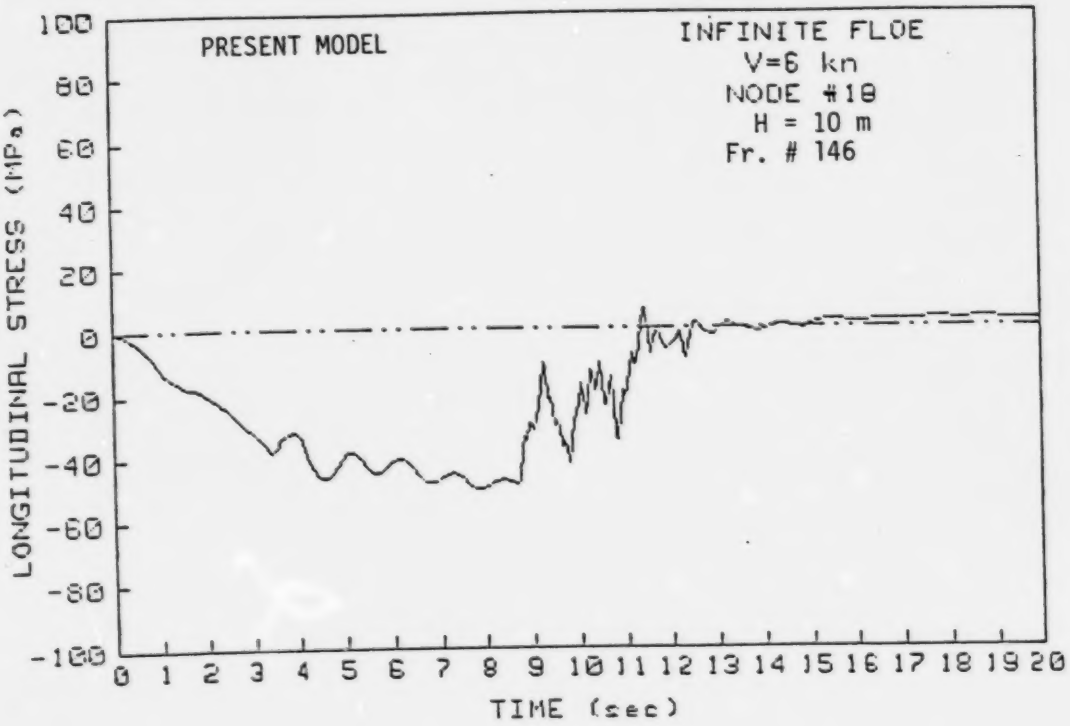


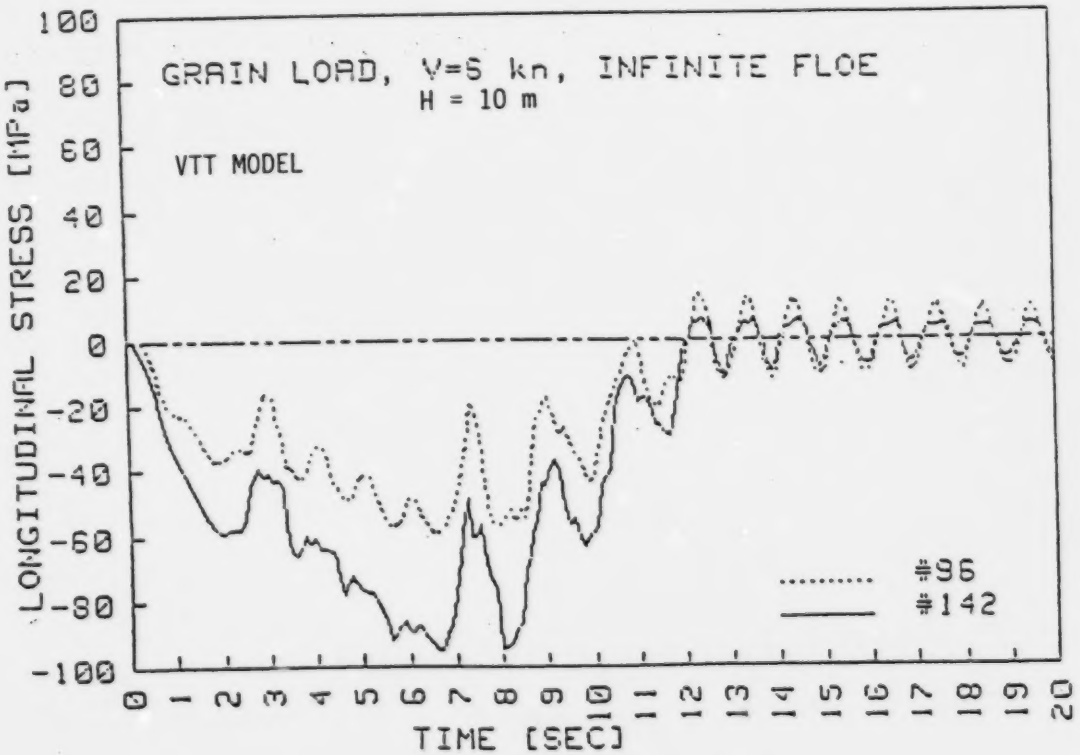


CALCULATED LONGITUDINAL BENDING STRESS
INDUCED BY ICE RAMMING

FIGURE 13C

The time history of the bending stresses exhibits the same two components of hull girder response as identified in the full-scale test, i.e., the quasi-static and vibratory components. As expected, the calculated ship response in hull bending stress when ramming increases with the speed of impact (Figure 13a - 13c). The characteristics of the quasi-static component is found to reproduce reasonably well the measurement data obtained from the full-scale tests (Ref. 1, 2). The quasi-static bending stress, which is induced by bow emersion, increases gradually during ice impact and reduces as the ship slides back into the water.

Both the VTT and present model indicate that the vibratory component of the hull bending stress, when the ship is ramming ice, is larger during the sliding phase. However, this is not supported by the full-scale test records. The major excitation of the ship hull, as observed from ramming experiments, occurs at the initial impact, thereafter minor excitation can occur but in general, the amplitude of the vibrations decreases progressively. The magnitude of excitation is related to the rate of change of ice force exerted on the ship.

The absence of large excitation during the impact and penetration phase in the results of both models suggests that a refinement of the ship/ice interaction may be required. In addition, the "on-off" characteristics of the ice force calculated from both models (Figures 9a-9c) during the sliding phase may not be realistic as no evidence of the resulting ship response has beeh found from the available full-scale ramming data. From inspection of the model output data of bow force, a relationship between rate of change of force and the resulting vibratory excitation of the hull girder can be seen.

After the ship is completely separated from the consolidated ice, an expected free, damped vibration behaviour is predicted from both models with a dominance of the 2 node vertical vibration frequency.

The general trends of stress variation resulted from the present calculations are quite similar to those of the VTT model. However, the estimated stress levels from the present model appear to be lower. The discrepancies are mainly due to the differences in the calculation of ice load and nodal movements in the finite element model.

The predicted maximum stresses induced by ramming have been checked against the strain gauge data recorded during the multi-year ice ramming tests (Ref. 2). Figure 14 shows the comparison of the calculated and measured ice induced longitudinal stress at Frame 145 on the main deck of M.V. ARCTIC. As shown in the figure, a possible underestimation of the longitudinal stress by the prediction model is indicated, although the dependency of impact speed is reproduced quite well. It is suggested that more experimental data is needed for justification, since similar discrepancy was noticed in the VTT model results (Ref. 3).

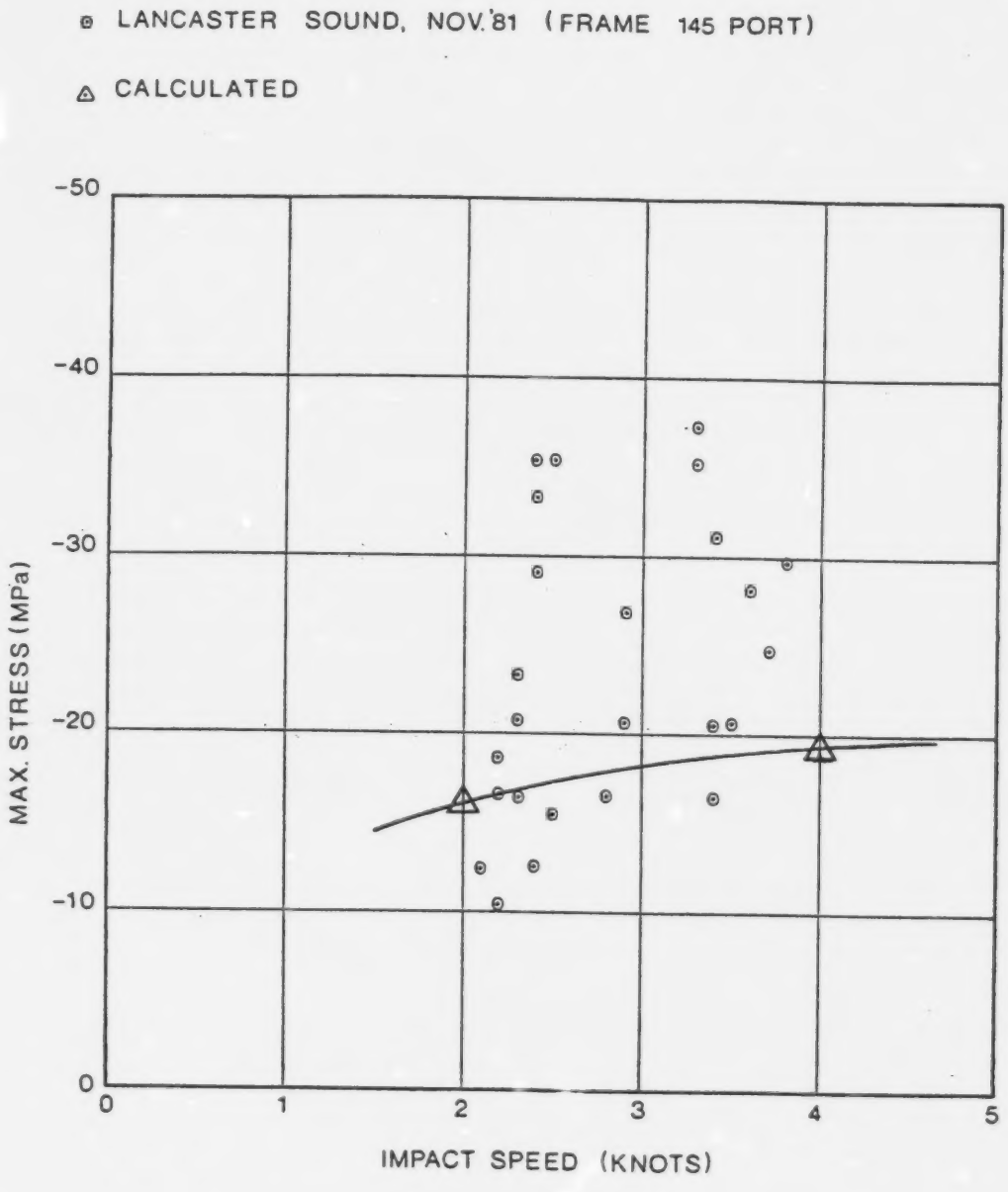


ICE INDUCED LONGITUDINAL STRESS VERSUS RAMMING SPEED

FIGURE 14

## 4.0 CONCLUSIONS

Conclusions regarding the development of the Canadian prediction model for ship dynamic response and ice force calculation in ramming operations are summarized below:

1. The prediction model has been successfully developed in parallel with a similar mathematical model constructed by the Technical Research Centre of Finland, (VTT). The present model was developed in Canada by Melville Shipping Ltd. and H. G. Engineering Ltd.

2. The present model utilizes a two dimensional idealization of the ship structure and is validated by good agreement with the VTT model in the prediction of the natural frequencies of vibration and modal shapes.

3. Analysis of the results of the present model and the VTT model indicated that small discrepencies occurred in the predicted time history of bow force, motions and longitudinal bending stresses during the ramming cycle. These discrepancies are considered acceptable due to the different model assumptions and analytical approaches used in the calculations.

4. The results which have been calculated by both models have been compared with full-scale data which has been recorded during various dedicated tests. Direct comparisons between the computed data and the full-scale data are difficult to make due to different ice strengths and differences between finite floes (full-scale data). The general interpolated trend does indicate that both models underestimate the amplitudes of both the quasi-static stresses and the vibratory stresses. It is believed that the reason for the lack of good correlation between the computed and measured results lies with the inadequacy of the ship/ice interaction model (DRrTRN) (see Figure 3), and this model should be further refined.

5. The calculation results are wholly dependent on the veracity of the ship/ice interaction model. Both the Finnish and Canadian models use a static, empirical ice pressure versus contact area relation in the calculation of bow load during ramming. Further investigation on the validity of this model for ship dynamic response calculation is required.

6. For the M.V. ARCTIC the White prediction equation for bow force appears to give similar results to the mathematical models and it is difficult to justify the use of more sophisticated techniques for the calculation of the force. From information supplied by VTT of their modelling assumptions it is not possible to determine the reason for the differences between the models of the amplitude of the vibratory stresses.

## 5.0 RECOMMENDATIONS

As discussed in previous sections, the ship/ice interaction model is the most important component of the prediction model for evaluation of ship dynamic response and bow loading when ramming ice. The ice model used by both Melville and VTT in their work is recognized as a simplification of the actual ice breaking process. While this approach is seen to give acceptable results of maximum bow loading and vertical quasi-static stresses in the hull girder, the dynamic stresses predicted by the two models are not in agreement with the full-scale measurements and refinement of the ship/ice interaction model should be undertaken.

In addition to improvements to the model, the model should be extended to other modes of ship/ice interaction such as the torsional and transverse response of the hull girder when ramming ice. It was believed that the vertical response of the hull to ice impacts is the most significant although there is now full-scale evidence to suggest that either the torsional or transverse stresses induced in the hull when ramming under certain circumstances may be more severe.

The model has been developed for the predictions of bow loads and hull girder response when ramming infinite floes. Little full-scale data exists from which the model may be calibrated and it is recommended that if the data becomes available it should be used for calibration purposes. While the ramming of infinite floes may give rise to the most severe global loads and stresses of the bow and hull girder, consideration should be given to expanding and modifying the model to simulate oblique collisions at high speed with a variety of ice features. This may be considered by some to be the more significant hazard to vessels operating in ice infested waters.

1. "Measurement of Hull Girder Bending Strain & Vibrations on the M.V. ARCTIC in Admiralty Inlet, July 1981", Melville Shipping Ltd., 1982.

2. "Measurement of Hull Girder Bending Strain & Vibration During Ramming of Multi-Year Ice Floes, Lancaster Sound, November 1981", Melville Shipping Ltd., 1982.

3. "Continuation of Stress Analysis, Mathematical Model of the Hull Girder Structure of the M.V. ARCTIC", Melville Shipping Ltd., 1982.

4. "The Influence of Imperfections on the Strength of Ice", H. H. G. Jellinek, Proceedings of Physical Society, LXXI, 5, pp.797-814.

5. "Updating the Arctic Shipping Pollution Prevention Regulations, Group I & II", Arctec Canada Ltd., 1982.

6. "Finite Element System for Desktop Computers (FESDEC) User's Manual", H.G. Engineering Ltd.

7. "A Method for the Calculation of Vertical Vibration with Several Nodes and Some Other Aspects of Ship Vibration", G. Anderson and K. Narrand, Transactions of RINA, Vol III, pp.367-383.

8. "A Numerical Determination of the Entrained Water in Ship Vibration", P. Orsero and J.L. Armand, International Journal for Numerical Methods in Engineering, Vol. 13, 1979.

9. "Dynamics of Marine Vehicles", R. Bhattacharyya, John Wiley and Sons, 1978.

10. "M.V. ARCTIC Dynamic Exciter Tests", Melville Shipping Ltd., 1982.

11. "M.V. ARCTIC Data Collection and Instrumentation", Fenco Consultants Ltd. and Melville Shipping Ltd., April 1982.

12. "M.V. ARCTIC Experimental Voyage to Lake Melville, Labrador in February/March 1981", Melville Shiping Ltd, October 1981.

13. "Prediction of Icebreaker Capability", R. M. White, Transaction RINA, pp.225-251, 1969.

14. "Handbook of Shock and Vibration", Harris and Crede, McGraw-Hill Handbooks, 1961.

APPENDIX I

"DYNAMIC ANALYSIS OF THE M.V. ARCTIC HULL GIRDER
IN RESPONSE TO ICE IMPACT"

BY H. G. ENGINEERING LTD.

# Dynamic Analysis of the M.V. Arctic Hull Girder in Response to Ice Impact

by

Dr. A. Firmin

Mr. I. Tabsh

H.G. ENGINEERING LTD.

Prepared for: Melville Shipping Ltd.
December 1982
Report #16501

## Table of Contents

SUMMARY

1.0 INTRODUCTION

2.0 FINITE ELEMENT MODEL OF THE HULL GIRDER

- 2.1 The Hull Girder
- 2.2 Distribution of Mass
- 2.3 Buoyancy Effects

3.0 THE DYNAMIC SOLUTION OF THE HULL GIRDER MODEL

- 3.1 The Dynamic Model
- 3.2 Quasi-Rigid Body Motion
- 3.3 The Elastic Modes of the Hull Girder
- 3.4 Modal Damping

4.0 SHIP ICE RESPONSE MODEL

5.0 RESULTS

6.0 CONCLUSIONS

REFERENCES

APPENDICES

- A Finite Element Input Data and Output Results
- B Distribution of Mass to Nodal Points
- C Distribution of Stiffness due to Buoyancy Effects
- D Solution of the Uncoupled Equations of Motion
- E Calculation of Quasi-Rigid Body Motion and Moments
- F Validation of FESDEC Transient Dynamics Program
- G Response of Idealized Version of Vertical Force

# DYNAMIC ANALYSIS OF THE M.V. ARCTIC HULL GIRDER IN RESPONSE TO ICE IMPACT


## SUMMARY

The dynamic response of the M.V. Arctic hull girder to impacting a thin finite floe of ice was computed for various initial velocities of the ship. Dynamic characteristics of the ship were calculated using a finite element beam model for determining the elastic modes of vibration. A model was developed to evaluate the ship/ice interaction force using the horizontal rigid and vertical quasi-rigid motions of the ship. These forces were used to excite the elastic modes of vibration and compute the resulting deflections/moments/stresses in the ship.

## 1.0 INTRODUCTION

The dynamic response of the hull girder of the M.V. Arctic has previously been studied experimentally (1) and theoretically (2). An independent study has been conducted by H.G. Engineering, in which a computer model simulating the interaction of the ship with ice has been developed and run for a number of hull speeds and ice thicknesses. A simple structural model based upon the finite element approach has been built to predict the natural modes of the ship. The transient response of the resulting modes has been determined using the same ice model as reported in reference 2. The program to evaluate this response has been independently developed and may not follow exactly the same steps as were taken in the previous work. The results presented are however of the same form being the bow force and ship response as a function of time.

A lumped mass-beam idealization was used to represent the hull girder and the associated masses of the mechanical equipment and cargo. The computed modes compared well with those measured and reported in reference 1. The bow forces were calculated from a knowledge of the ice model, the rigid body forward motion of the ship and the quasi-static pitching and heaving of the ship. The resulting vertical bow forces were used to excite the response of the elastic modes. At each time step the displacements, bending moments and stresses were calculated and plotted.

## 1.0 INTRODUCTION (cont'd)

The ice-interaction model assumed an infinite floe of varying thickness. In order to compare the theoretical model developed here with the ice ramming tests conducted aboard the M.V. Arctic an extension must be made to include the dynamics of a finite ice floe.

## 2.0 FINITE ELEMENT MODEL OF THE HULL GIRDER

### 2.1 The Hull Girder

Although the hull of the M.V. Arctic is a three dimensional assemblage of plates, frames and stiffeners, the relatively slender hull lends itself to being represented as a series of equivalent beam sections. The approximation inherent in such an assumption is that plane sections remain plane and the bending stress distribution varies linearly through the depth of the section. It was considered that in this case such assumptions would be sufficient to accurately predict the first few modes of vibration of the hull girder.

The essential structural properties required to prepare the stiffness model for bending in the vertical plane are the second moment of area about the neutral axis and the position of the neutral axis from the keel datum. These values are given in figures 1 and 2. The section moduli which are required for the calculation of the resulting stresses are shown in figures 3 and 4. For axial compression modes of the hull, the area of the hull plates and stiffeners carrying end load must also be included, and this is shown in figure 5 as a function of the position along the hull.

The nodes of the finite element model were chosen primarily to coincide with the structural discontinuities as illustrated. However further subdivisions were included to add accuracy where the section properties were rapidly changing.

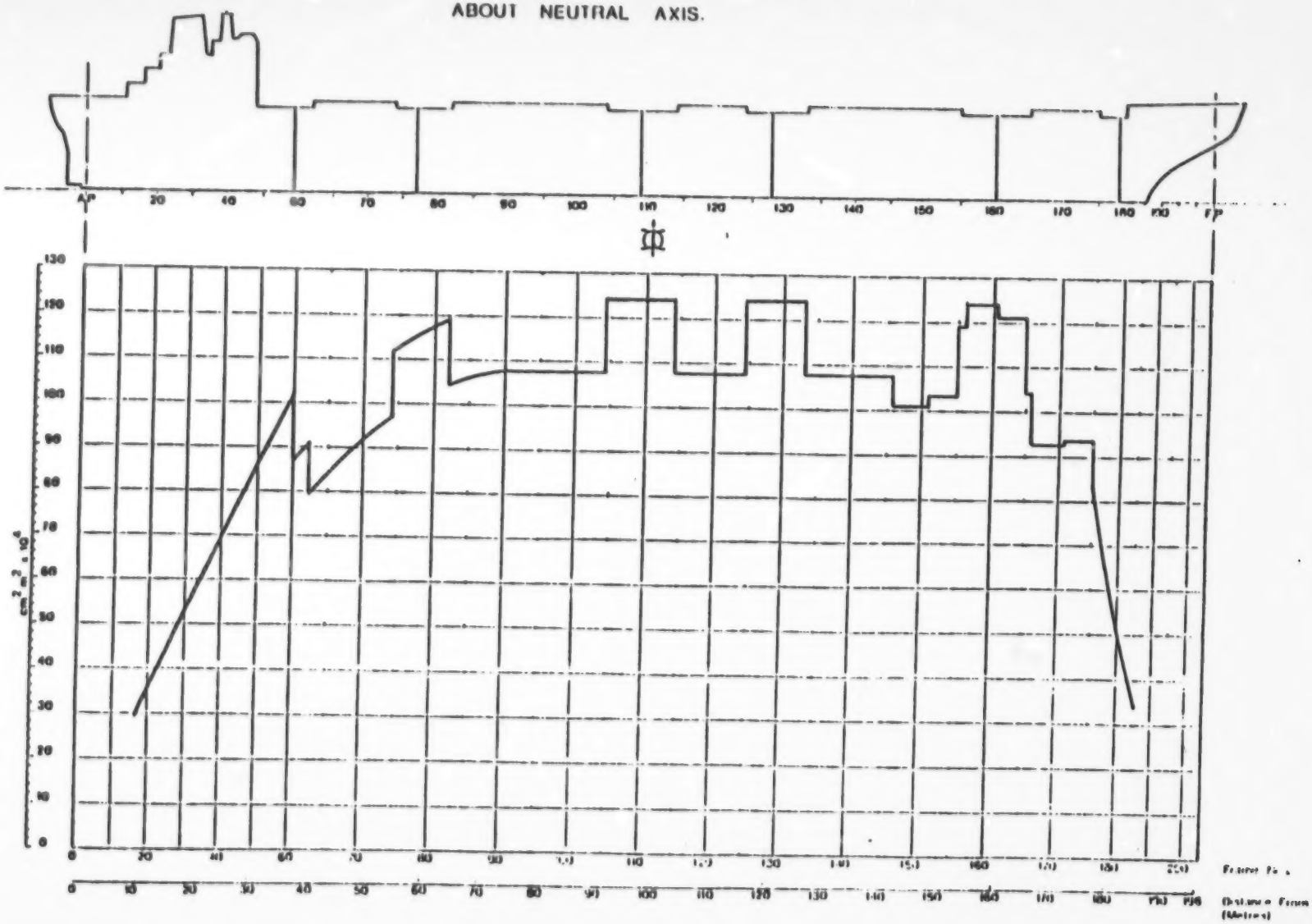


Figure 1

LONGITUDINAL DISTRIBUTION OF NEUTRAL AXIS

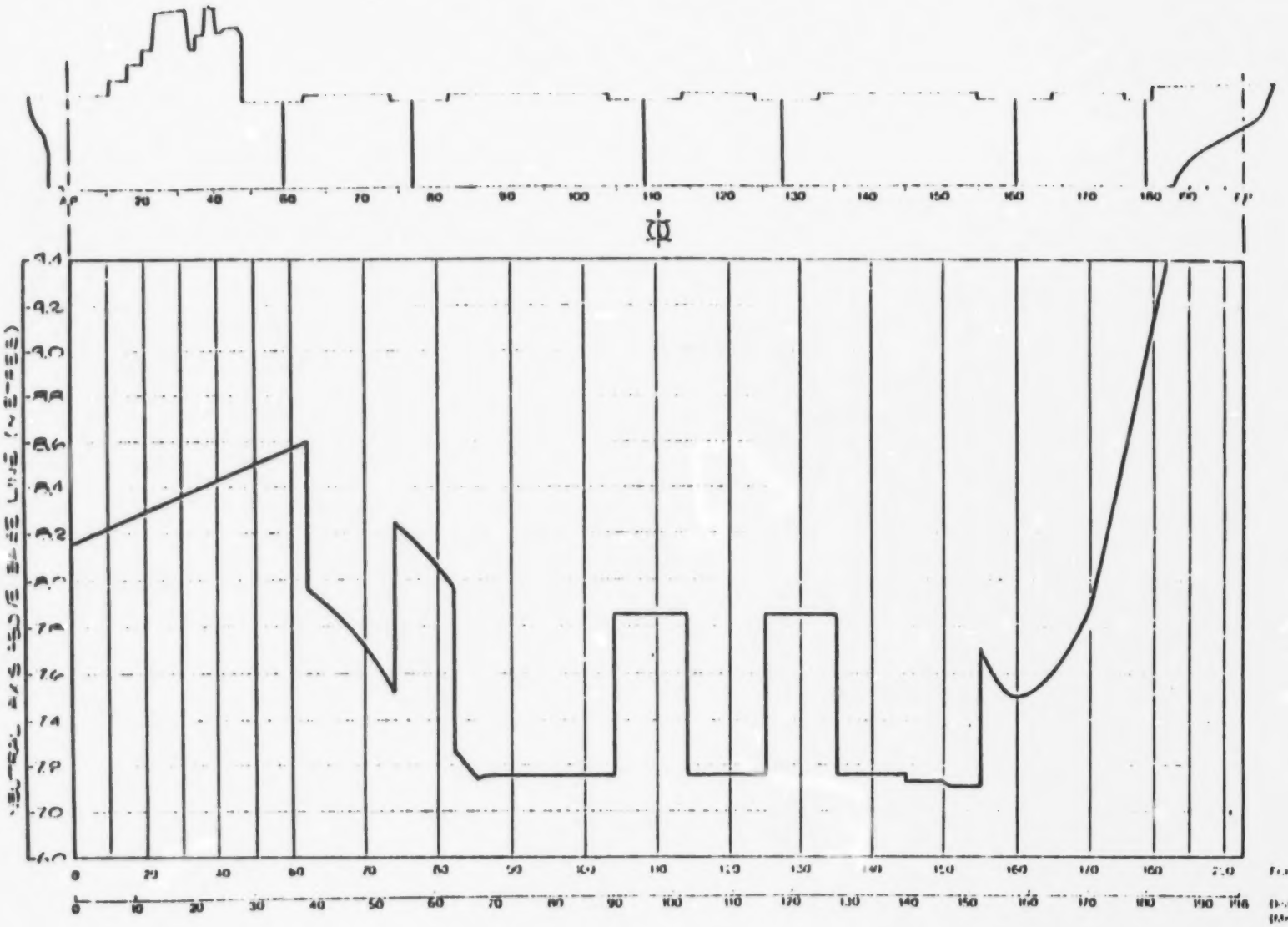

Figure 2

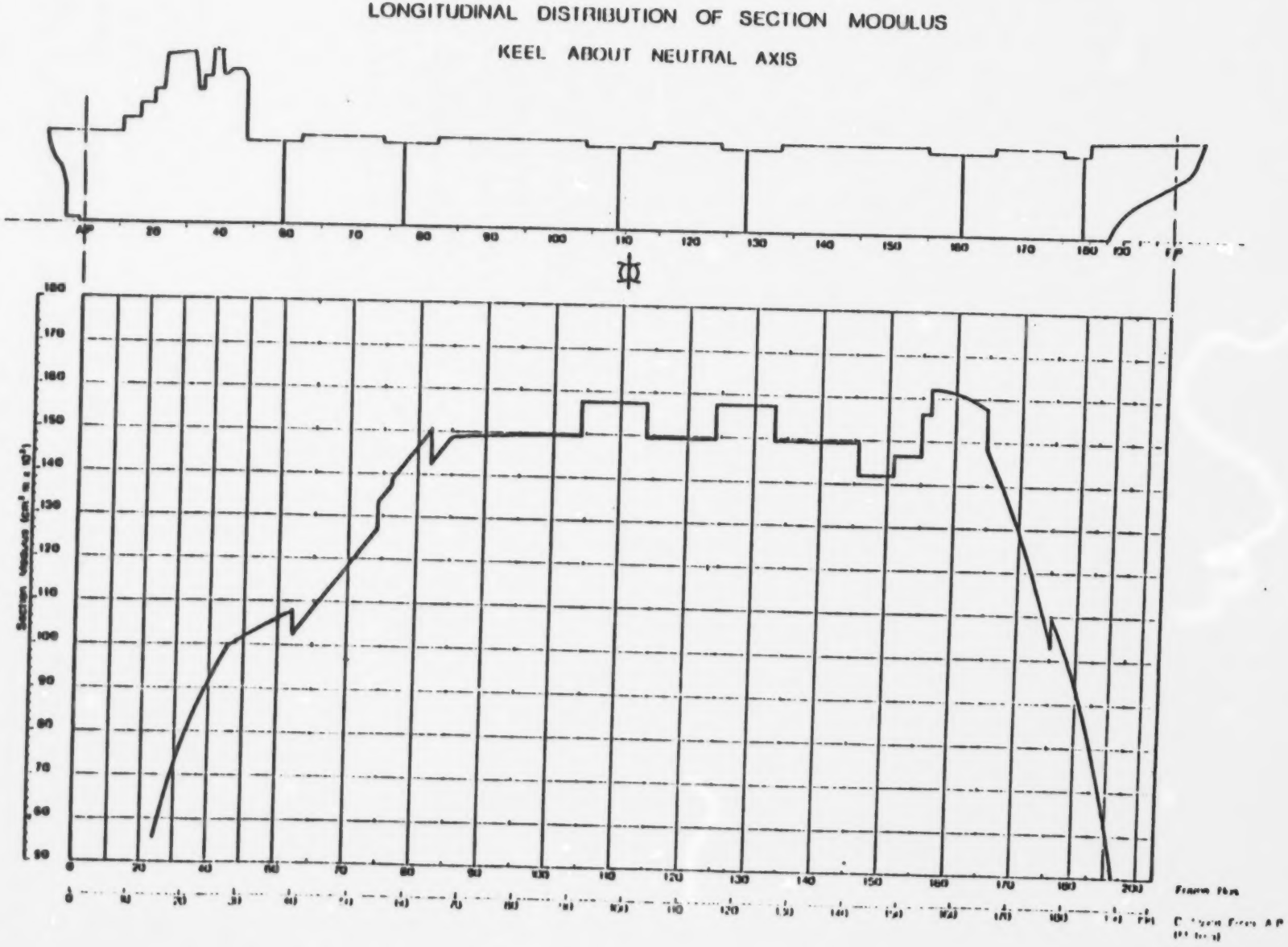
LONGITUDINAL DISTRIBUTION OF SECTION MODULUS
KEEL ABOUT NEUTRAL AXIS

Figure 3

LONGITUDINAL DISTRIBUTION OF SECTION MODULUS

DECK ABOUT NEUTRAL AXIS

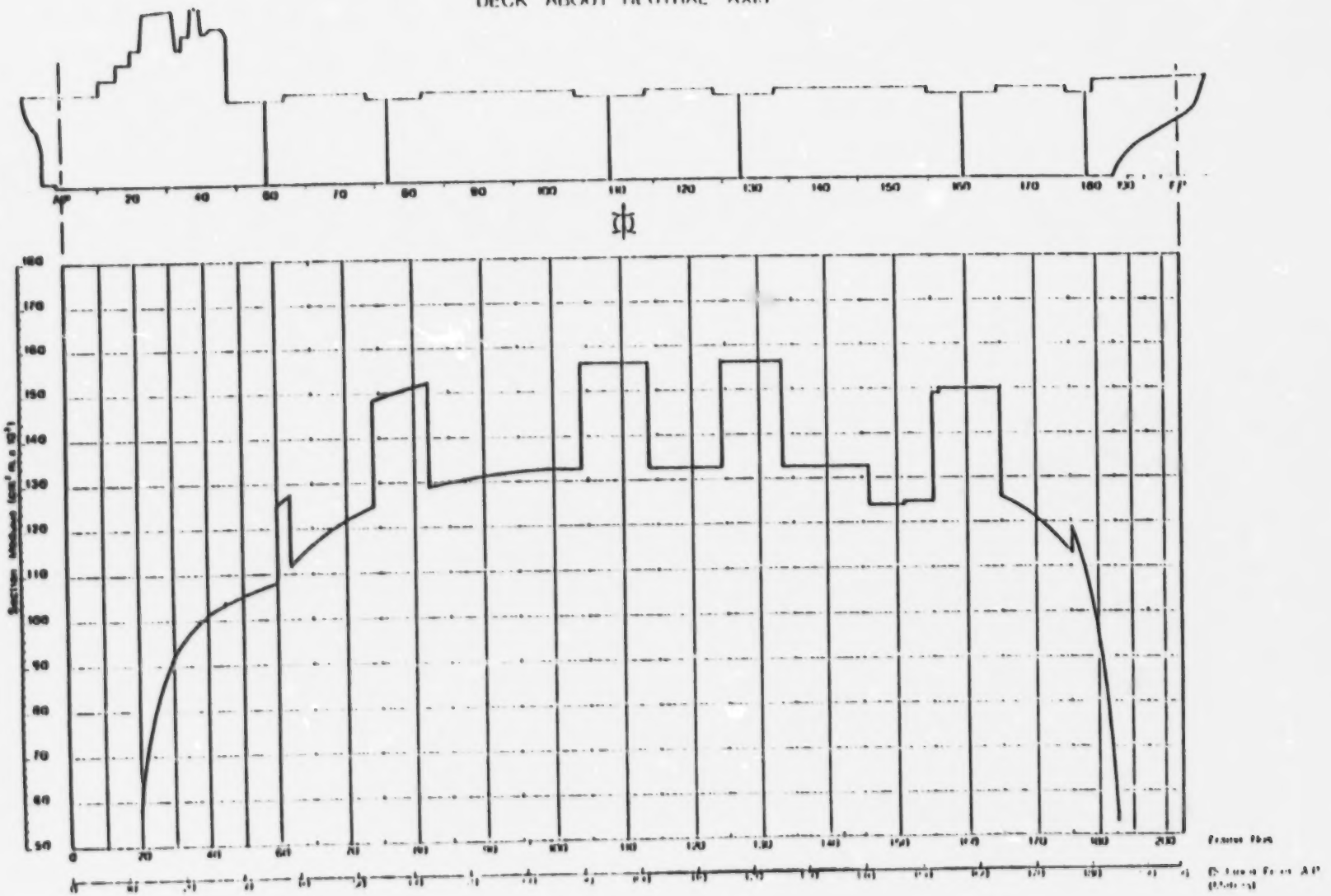

Figure 4

Figure 5

## 2.1 The Hull Girder (cont'd)

Figure 6 shows the position of the nodal points relative to the hull. In all, 19 nodes were used along the hull. The stiffness of the hull is characterized by 'beam' finite elements having three degrees of freedom (dof) at each node; two translations parallel and perpendicular to the keel and a rotation about the normal to these axes. The formulation of the stiffness equations and their solution follow the standard displacement method as described, for example, in reference 3. The effective area for transverse shear was taken to be half the cross-sectional area mentioned above which is approximately correct for the hollow closed tube of near rectangular proportions that is typical of the ship's cross-section. Standard material properties for mild steel were assumed to apply i.e. Young's modulus = $2 \times 10^{11}$ $N/M^2$ and Poisson's ratio = 0.3. All dimensions are given in metres. A full listing of the Finite Element model data as prepared for the FESDEC (4) program is given in Appendix A.

## 2.2 The Distribution of Mass

In addition to the hull stiffness, the buoyancy of the water and the distributed and discrete masses of the ship must be considered. As this data is not necessarily available at the same sections chosen for the nodal points an interpolation procedure was developed to determine the required

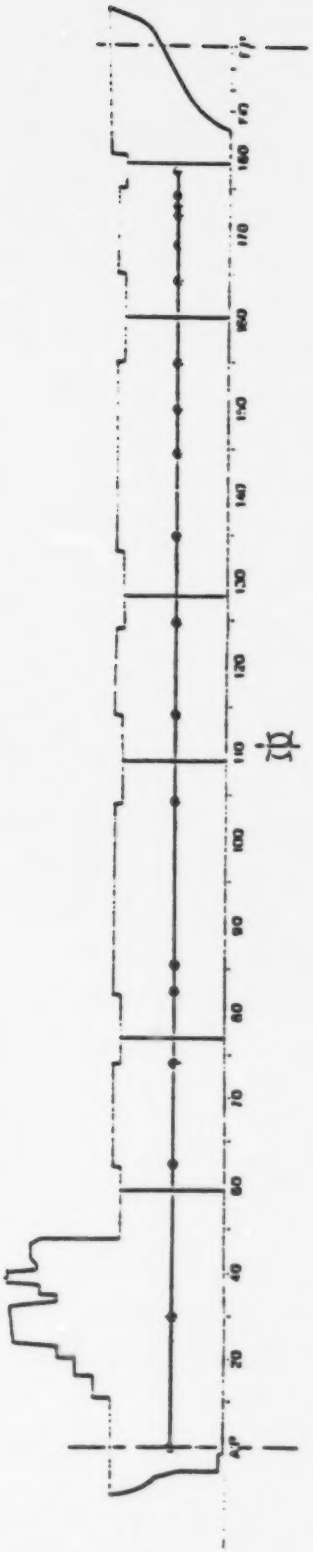

Figure 6. DISTRIBUTION OF NODAL POINTS FOR THE FINITE ELEMENT MODEL

## 2.2 The Distribution of Mass (cont'd)

lumped values. Programs were written to automate this process for each of the sets of data considered. The results of the interpolation of the mass data and the original mass values and their locations are given in Appendix B. The added mass effects of the fluid were provided by Melville Shipping. A linearized representation, given in Appendix B, was used to calculate the lumped values. A total mass of 69,460,000 kgs was distributed along the length of the hull. The ship was assumed to be in the grain load condition.

## 2.3 Buoyancy Effects

The effects of buoyancy can be effectively represented in the stiffness model by foundation springs whose stiffness is calculated from the slope of the Bonjean curve at the waterline assumed for the grain loading condition. The stiffness can be generated from the integral expression

$$K_i = \int_{x_1}^{x_2} \rho g \frac{dA}{dl}\, dx$$

where $\rho$ = density of water = 1000 kg/M$^3$

$g$ = acceleration due to gravity = 9.81 M/sec$^2$

$\frac{dA}{dl}$ = slope of the Bonjean curve at the 11.0 m draught

$x_1$, $x_2$ = length of hull considered.

## 2.3 Buoyancy Effects (cont'd)

The Bonjean curves have been plotted in Appendix C. As can be seen, the slope of these curves remains linear over a considerable range of draught for all but the bow and stern sections. Thus even for relatively large pitching and heaving motion the restoring buoyancy forces remain linear. This means that in this respect the linear dynamic model of the ship's motion as a rigid body is an accurate representation. This additional data for the Finite Element model is given in Appendix A.

## 3.0 THE DYNAMIC SOLUTION OF THE HULL GIRDER MODEL

### 3.1 The Dynamic Model

The equations of motion for the lumped parametric representation of the hull girder can be written as follows:

$$M\ddot{u} + C\dot{u} + Ku = F(t) \qquad \text{.....(3.1)}$$

where

- $u, \dot{u}, \ddot{u}$ are the displacement, velocity and acceleration vectors, respectively
- $M$ is the lumped mass matrix
- $C$ is the damping matrix
- $K$ is the stiffness matrix
- $F(t)$ is the time varying force vector.

If it is assumed that the motions and relative deflections are small then equation (3.1) can be taken as linear. This assumption permits the motion to be represented as a series of uncoupled normal modes with natural frequencies $\omega_i$.

Hence

$$u = \sum \phi_i q_i \qquad \text{.....(3.2)}$$

where $\phi_i$ is a mode shape vector for the $i^{th}$ mode and $q_i$ is the generalized coordinate amplitude of the mode.

3.1 The Dynamic Model (cont'd)

Because the modes are orthogonal the equations of motion can be uncoupled into a set of equations

$$\ddot{q}_i + 2\zeta_i\omega_i\dot{q}_i + \omega^2{}_i q_i = Q_i \qquad \ldots\ldots\ldots(3.3)$$

where $\zeta_i$ is the model damping coefficient
and $Q_i$ is the generalized force for the $i^{th}$ mode.

In general the response of a structure can be determined by considering a few of its lowest modes. In particular the response of the M.V. Arctic is expected to be dominated by its first two bending modes.

The frequencies and mode shapes of the equations of motion are determined through the solution of the eigenvalue problem

$$(K - \omega^2 M)q = 0 \qquad \ldots\ldots\ldots(3.4)$$

where there are as many eigenvalues (frequencies) in the solution as there are dynamic degrees of freedom.

If the excitation force is known as a function of time, the response can be calculated for each mode in an incremental manner and the total solution from a summation of the modal contributions.

3.1 The Dynamic Model (cont'd)

After the modal amplitudes are calculated the physical displacements can be recovered from equation (3.2). Finally the bending moments can be calculated for each Finite Element from the deflections. The mathematical detail behind the transient computation is given in Appendix D.

3.2 The Quasi-Rigid Body Motion

As the ship impacts the ice a vertical upthrust is imparted to the bow which causes the ship to heave and pitch. This quasi rigid body motion can be calculated as part of the modal solution to the Finite Element model or by considering a rigid hull girder with translational masses and buoyancy springs distributed along its length. The latter was used as a check against the dynamic solution, the first two modes of which are the coupled form of the pitch and heave modes. The calculation for the quasi rigid body modes, based upon the lumped mass model, is given in Appendix E. By taking moments of the buoyancy and inertia forces the quasi-static bending moments can be calculated at any point along the hull. The horizontal rigid body and quasi-rigid body characteristics, as calculated by the method of Appendix E, for the lumped data used in the Finite Element model are shown in Figure 7.

M.V.ARCTIC - Natural Frequencies and Mode Shapes
JOB.NAME MV1

MODEL CHARACTERISTICS

| MODE | FREQUENCY (HZ) | (R/S) | EQUIVALENT MASS | EQUIVALENT LOAD |
|---|---|---|---|---|
| 1 | 0.000 | 0.000 | 6.946E+07 | -1.000E+00 |
| 2 | 0.108 | 0.679 | 2.384E+07 | 1.000E+00 |
| 3 | 0.134 | 0.843 | 1.088E+07 | -3.818E-01 |

| NODE | X-COOR | STIFFNESS | MASS | MODE 1 | MODE 2 | MODE 3 |
|---|---|---|---|---|---|---|
| 1 | 0.00 | 9.150E+05 | 7.128E+05 | 1.0000 | -0.1745 | 1.0000 |
| 2 | 20.50 | 3.190E+06 | 2.854E+06 | 1.0000 | -0.0407 | 0.8420 |
| 3 | 41.00 | 3.565E+06 | 4.843E+06 | 1.0000 | 0.0930 | 0.0853 |
| 5 | 55.00 | 2.594E+06 | 4.005E+06 | 1.0000 | 0.1844 | 0.5778 |
| 7 | 65.00 | 1.411E+06 | 1.618E+06 | 1.0000 | 0.2496 | 0.5010 |
| 9 | 68.00 | 2.966E+06 | 3.968E+06 | 1.0000 | 0.2692 | 0.4760 |
| 10 | 92.00 | 3.974E+06 | 6.383E+06 | 1.0000 | 0.4258 | 0.2938 |
| 12 | 104.00 | 2.761E+06 | 5.610E+06 | 1.0000 | 0.5041 | 0.2016 |
| 14 | 117.00 | 2.761E+06 | 4.717E+06 | 1.0000 | 0.5889 | 0.1015 |
| 16 | 129.00 | 2.650E+06 | 4.740E+06 | 1.0000 | 0.6672 | 0.0097 |
| 18 | 141.00 | 2.650E+06 | 1.071E+07 | 1.0000 | 0.7455 | -0.0824 |
| 19 | 153.00 | 2.098E+06 | 2.623E+06 | 1.0000 | 0.8238 | -0.1745 |
| 21 | 160.00 | 1.315E+06 | 1.565E+06 | 1.0000 | 0.8695 | -0.2282 |
| 22 | 165.00 | 1.074E+06 | 1.840E+06 | 1.0000 | 0.9021 | -0.2660 |
| 23 | 170.00 | 7.702E+05 | 3.306E+06 | 1.0000 | 0.9347 | -0.3050 |
| 24 | 172.50 | 4.922E+05 | 4.426E+05 | 1.0000 | 0.9511 | -0.3242 |
| 25 | 175.00 | 4.726E+05 | 3.989E+05 | 1.0000 | 0.9674 | -0.3434 |
| 26 | 177.50 | 4.467E+05 | 3.551E+05 | 1.0000 | 0.9837 | -0.3626 |
| 27 | 180.00 | 2.103E+05 | 1.770E+06 | 1.0000 | 1.0000 | -0.3818 |

MODAL FORCE / MOMENT FOR RIGID MODES

| MODE | MODE 1 | MODE 2 | MODE 3 |
|---|---|---|---|
| 1 | 0.000E+00 | 0.000E+00 | 0.000E+00 |
| 2 | -7.128E+05 | -2.098E+06 | 8.370E+06 |
| 3 | -3.567E+06 | -5.761E+06 | 3.080E+07 |
| 5 | -6.410E+06 | -6.527E+06 | 5.739E+07 |
| 7 | -1.241E+07 | -5.695E+06 | 7.063E+07 |
| 9 | -1.403E+07 | -4.947E+06 | 7.500E+07 |
| 10 | -2.300E+07 | -6.504E+06 | 7.083E+07 |
| 12 | -3.136E+07 | -6.722E+06 | 6.175E+07 |
| 14 | -3.699E+07 | -5.812E+06 | 4.870E+07 |
| 16 | -4.171E+07 | -6.264E+05 | 3.592E+07 |
| 18 | -4.645E+07 | 7.888E+06 | 2.306E+07 |
| 19 | -5.716E+07 | -3.864E+06 | 1.511E+07 |
| 21 | -5.979E+07 | -5.592E+06 | 1.019E+07 |
| 22 | -6.135E+07 | -4.247E+06 | 6.439E+06 |
| 23 | -6.319E+07 | -1.685E+06 | 3.003E+06 |
| 24 | -6.650E+07 | -2.451E+06 | 2.486E+06 |
| 25 | -6.694E+07 | -2.332E+06 | 1.824E+06 |
| 26 | -6.734E+07 | -1.514E+06 | 1.000E+06 |
| 27 | -6.769E+07 | 0.000E+00 | 0.000E+00 |

**Figure 7 RIGID AND QUASI-RIGID BODY CHARACTERISTICS**

## 3.3 The Elastic Modes of the Hull Girder

A complete set of mode shapes and frequencies as produced by the FESDEC program are given in Appendix A. A summary of the frequencies of the bending modes are compared to those measured in reference 1. The additional modes not mentioned involve mainly axial motion and were not excited in the tests.

COMPARISON OF FREQUENCIES (Hz)

| | HGE # is | Measured Frequencies | HGE Model |
|---|---|---|---|
| Quasi rigid body modes | 1 | - | 0.11 |
| | 2 | - | 0.14 |
| 2-node | 3 | 0.93 | 0.91 |
| 3-node | 5 | 1.98 | 1.85 |
| 4-node | 6 | 3.12 | 2.82 |
| 5-node | 8 | 3.98 | 4.14 |
| 6-node | 11 | 4.86 | 4.93 |

## 3.4 Modal Damping

The damping values for the elastic modes were taken from the measurements given on page 15 of reference 1 and are summarized below.

| Mode No. (HGE) | Frequency Hz | Generalized Damping g | Modal Damping % crit |
|---|---|---|---|
| 3 | 0.93 | 0.02 | 5.84 |
| 5 | 1.98 | 0.036 | 22.39 |
| 6 | 3.12 | 0.022 | 21.56 |
| 8 | 3.98 | 0.028 | 35.01 |
| 11 | 4.86 | 0.026 | 39.70 |

For the quasi-rigid modes 11% was used.

## 4.0 SHIP/ICE RESPONSE MODEL

The prediction of the ship/ice interaction force is a complex process. Based on various research studies and empirical data, it is suggested that the contact pressure can be calculated using the relationship

$$p = CA^{e} \qquad \text{.....(4.1)}$$

where $p$ = contact pressure (MPa)

$A$ = surface area of the ship in contact with ice ($m^2$)

C and e are empirical factors with values 4.4 and -0.5 respectively. The horizontal and vertical force components are

$$\left.\begin{aligned} F_x &= pA_x \\ F_z &= pA_z \end{aligned}\right\} \text{.....(4.2)}$$

where $A_x$ and $A_z$ are the projections of the contact area A on the vertical and horizontal planes respectively.

The contact area A in EQ (4.1) is dependent on the degree of the ship's penetration into the ice. This displacement however is a function of the initial velocity of the ship before impacting the ice and the ship/ice interaction forces.

4.0 SHIP/ICE RESPONSE MODEL (cont'd)

In other words

$$\left.\begin{aligned} & A = f\,(x,z) \\ & x = g_1\,(V_{ox},\ F_x);\ z = g_2\,(V_{oz},\ F_z) \\ \text{or}\quad & A = h\,(V_{ox},\ V_{oz},\ F_x,\ F_z) \end{aligned}\right\} \qquad \text{.....(4.3)}$$

where f, $g_1$, $g_2$ and h define functional relationships between the different variables.

It is clear from EQ (4.3) that no closed form solution can be found. A model was designed to evaluate the contact forces using an iterative approach in the time domain. Basically, the model consists of the following steps:

1. Define the initial conditions. These include
   * speed of the ship
   * draught
   * ice floe thickness and free board
   * dynamic characteristics of the ship for the two quasi-rigid vertical modes identified in the previous section.

2. Set the force at the end of the current time step to be equal to that at the beginning as determined from the previous time step ( assume all forces are zero in the first time step).

3. Evaluate the horizontal (x) and vertical (z) deflections of the ship at the end of the time step using the modal solution technique described in the previous section. Note that for the vertical motion only the quasi-rigid modes (first two) are used.

## 4.0 SHIP/ICE RESPONSE MODEL (cont'd)

4. Evaluate D, the total horizontal penetration of the ship into the ice (D is a function of x, z and the profile of the ship, see figure 8). If D> = DMAX then continue at step (6). DMAX is the maximum value of D updated at the end of each time step.

5. If D < DMAX then the ship is no longer impacting the ice. Set the force at the end of the time step to zero. Evaluate x and z based on this new force value and proceed to step (6).

6. Using the (x, z) deflections, evaluate the horizontal (Fx) and vertical (Fz) forces using EQ (4.1) and EQ (4.2). Note that A, Ax, Az are given in table form for different (x, z) values. Linear interpolation is used for intermediate values.

7. Compare the force evaluated in step (6) to that assumed in the current iteration. Compute the ratio

$$R = \left[ (Fx^2 + Fz^2)_{OLD} / (Fx^2 + Fz^2)_{NEW} \right]^{\frac{1}{2}}$$

8. If R is outside a specified range (1 $\pm$ TOL) then set forces at the end of the time step equal to those evaluated in step (6). Iterate starting with step (3).

## 4.0 SHIP/ICE RESPONSE MODEL (cont'd)

9. If R is within the specified range then update DMAX = MAXIMUM (D, DMAX) and proceed to the next time step starting from step (2).

During this process the horizontal and vertical forces are stored to be used later for exciting the elastic modes of the ship. Also, the displacements and velocities evaluated during every time step constitute the horizontal rigid body motion and the vertical motions of the two quasi-rigid modes.

The response of the elastic modes to the contact force is computed using the FESDEC Transient Response Post Processor. Six modes were excited and the resulting modal displacement and velocity were stored. Damping values for each mode were calculated from the experimental data provided (see Section 3.4).*

Finally, the total deflections, moments, and stresses at various nodal points were computed by combining the different modal solutions. Modal deflections were multiplied by the appropriate modal deflection/moment at the required section and summed up for all modes considered.

* Appendix F presents a validation of the FESDEC Transient Response solution. Also, the input data for one of the cases analyzed in this report is presented in Figure 9.

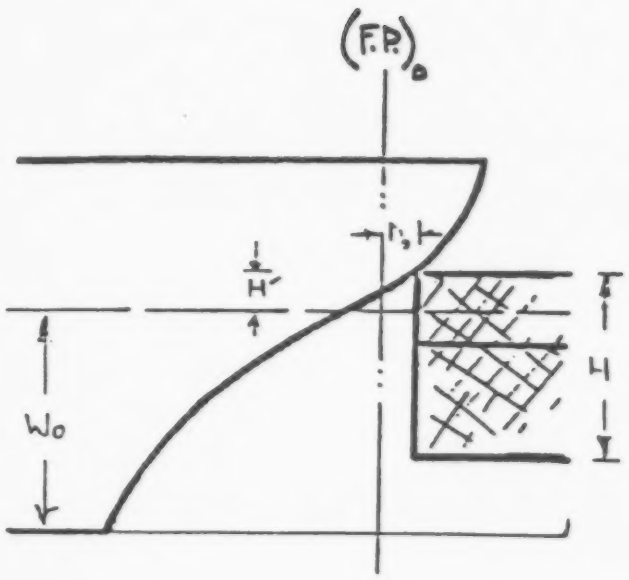


BEFORE IMPACT

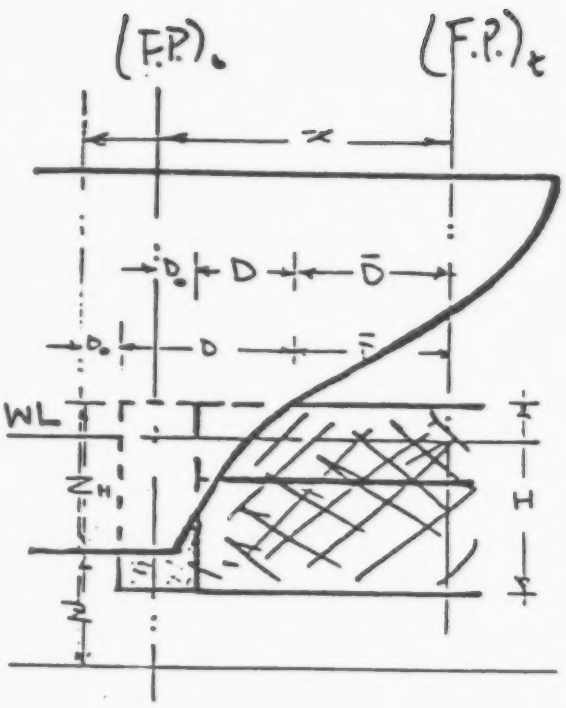


AFTER IMPACT

$P(z)$ = Distance from F.P. to ship at height z.

$Z_p(x)$ = Height of point at distance x from F.P.

$A^o(x,z)$ = Area of hull from F.P. to x and below height z.

$A^o{}_x(x,z)$ = Projection of A(x,z) on a vertical plane.

$A^o{}_z(x,z)$ = Projection of A (x,z) on a horizontal plane.

$D_o = P(W_o + H')$

$z_H = W_o + H' - z$

$\bar{D} = P(z_H)$

$D = x + D_o - \bar{D}$

D < DMAX: Ship off ice

$F_x = F_z = 0$

D> =DMAX: Ship on ice

$z_n$ = MAXIMUM $(z_H - H,\ z_p(x+D_o), \phi)$

$A = A^o(x+D_o, z_H) - A^o(x+D_o, z_n)$

$A_x = A^o{}_x(x+D_o, z_H) - A^o{}_x(x+D_o, z_n)$

$A_z = A^o{}_z(x+D_o, z_H) - A^o{}_z(x+D_o, z_n)$

$p = CA^e$

$F_x = pA_x$

$F_z = pA_z$

Figure 8 CALCULATION OF SHIP/ICE ITERACTION FORCE

## 5.0 RESULTS

The different models described earlier were used to determine the time variation of the horizontal and vertical components of the interaction force and the resulting response of the ship. Four different cases were run. In all cases, a thin infinite floe of ice 2.5m thick with 0.25m free board was assumed. The ship draught in the equilibrium position was 10.8 meters. No added mass was used in considering the horizontal motion. The initial velocities for cases 1 to 3 were 2, 4, and 6 knots respectively. Case 4 assumed a 2 knots initial velocity with no damping present, all other runs include the damping factors reported in Section 3.4. No attempt was made to vary the ice model parameters (C and e). Figure 9 shows the input data for the FESDEC Transient Response Program (DRTRAN) for case 1. All other cases have the same input except for the amplitude of the force excitation. These values are calculated using the ship/ice interaction model described in Section 4.0.

Figures 10 to 25 present the results for the four cases considered. For cases 1, 2 and 3 the following responses are shown:

Set 1: Time history plots of the horizontal and vertical components of the ship/ice interaction force and the corresponding rigid and quasi-rigid motions of the ship.

M.V.ARCTIC - Natural Frequencies and Mode Shapes
JOBNAME MV1

| MODE # | MODE TYPE | FREQUENCY (Hz) | FREQUENCY RAD/SEC | EQUIVALENT MASS | DAMPING (%) |
|---|---|---|---|---|---|
| 1 | FLST | 1.0805E-01 | 6.7838E-01 | 2.3807E+07 | 11.00 |
| 2 | FLST | 1.3400E-01 | 6.4194E-01 | 1.1136E+07 | 11.00 |
| 3 | FLST | 9.1072E-01 | 5.7222E+00 | 6.1391E+06 | 5.84 |
| 5 | FLST | 1.8529E+00 | 1.1642E+01 | 5.2993E+06 | 22.39 |
| 6 | FLST | 2.8206E+00 | 1.7723E+01 | 7.3518E+06 | 21.56 |
| 8 | FLST | 4.1339E+00 | 2.5974E+01 | 3.1484E+06 | 35.01 |
| 9 | FLST | 4.9256E+00 | 3.0974E+01 | 1.8504E+07 | 39.70 |
| 11 | FLST | 6.6859E+00 | 4.2009E+01 | 9.6934E+06 | 49.57 |

RESPONSE TIME DOMAIN

START TIME : 0.00

END TIME : 24.95
INCREMENT : 0.05

INITIAL CONDITIONS

INITIAL DISPLACEMENTS

| -NODE- | ----DX---- | ----DY---- | ----DZ---- | ----RX---- | ----RY---- | ----RZ---- |
|---|---|---|---|---|---|---|
| ALL | 0.000E+00 | 0.000E+00 | 0.000E+00 | 0.000E+00 | 0.000E+00 | 0.000E+00 |

INITIAL VELOCITIES

| -NODE- | ----VX---- | ----VY---- | ----VZ---- | ----WX---- | ----WY---- | ----WZ---- |
|---|---|---|---|---|---|---|
| ALL | 0.000E+00 | 0.000E+00 | 0.000E+00 | 0.000E+00 | 0.000E+00 | 0.000E+00 |

FORCE/AMPLITUDE EXCITATION DATA

| TIME | AMPLITUDE CASE 1 | CASE 2 |
|---|---|---|
| 0.00 | 0.000E+00 | 0.000E+00 |
| 0.05 | 8.481E+04 | 1.061E+05 |
| 0.10 | 1.752E+05 | 2.192E+05 |
| 0.15 | 2.547E+05 | [illegible]+00 |
| 0.20 | [illegible]+00 | 0.000E+00 |
| [illegible] | 5.467E+06 | 8.936E+06 |
| 12.80 | 0.000E+00 | 0.000E+00 |

FORCE VECTOR #1 : AMPLITUDE CASE 2 - SCALE FACTOR 1.000E+00

| -NODE- | ----FX---- | ----FY---- | ----FZ---- | ----MX---- | ----MY---- | ----MZ---- |
|---|---|---|---|---|---|---|
| 27 | 0.000E+00 | 1.000E+00 | 0.000E+00 | 0.000E+00 | 0.000E+00 | 0.000E+00 |

**Figure 9 INPUT DATA FOR THE FESDEC TRANSIENT DYNAMICS PROGRAM**

5.0 RESULTS (cont'd)

Set 2: A list of the maximum values of the following parameters

Modal deflections of selected modes
Quasi-rigid moments
Elastic moments
Total moments

at the nodes are given and the times at which they occur. (See Figure 6 for the position of the corresponding frame numbers).

Set 3: Time history plot of the elastic deflection of the bow.

Set 4: Time history plot of the maximum stress in the ship. The minimum section modulus at each node was used to compute the stress.

Set 5: Moment diagram of the total moment is shown at the time that corresponds to the maximum stress described in Set 4.

Positions of the zero response and the end time of the interaction force are shown by dotted lines on the time history plots for sets 4 and 5.

Only result set 1 is given for loadcase 4. This is for reasons explained later.

Figures 10 to 14 present the responses for case 1. The force increases smoothly to a maximum value and then oscillates from near that maximum down to zero. The oscillations can best be explained by considering each component of motion separately. As the ship moves backwards in the span of a time step, it creates a separation between the bow and the bow print in the ice.

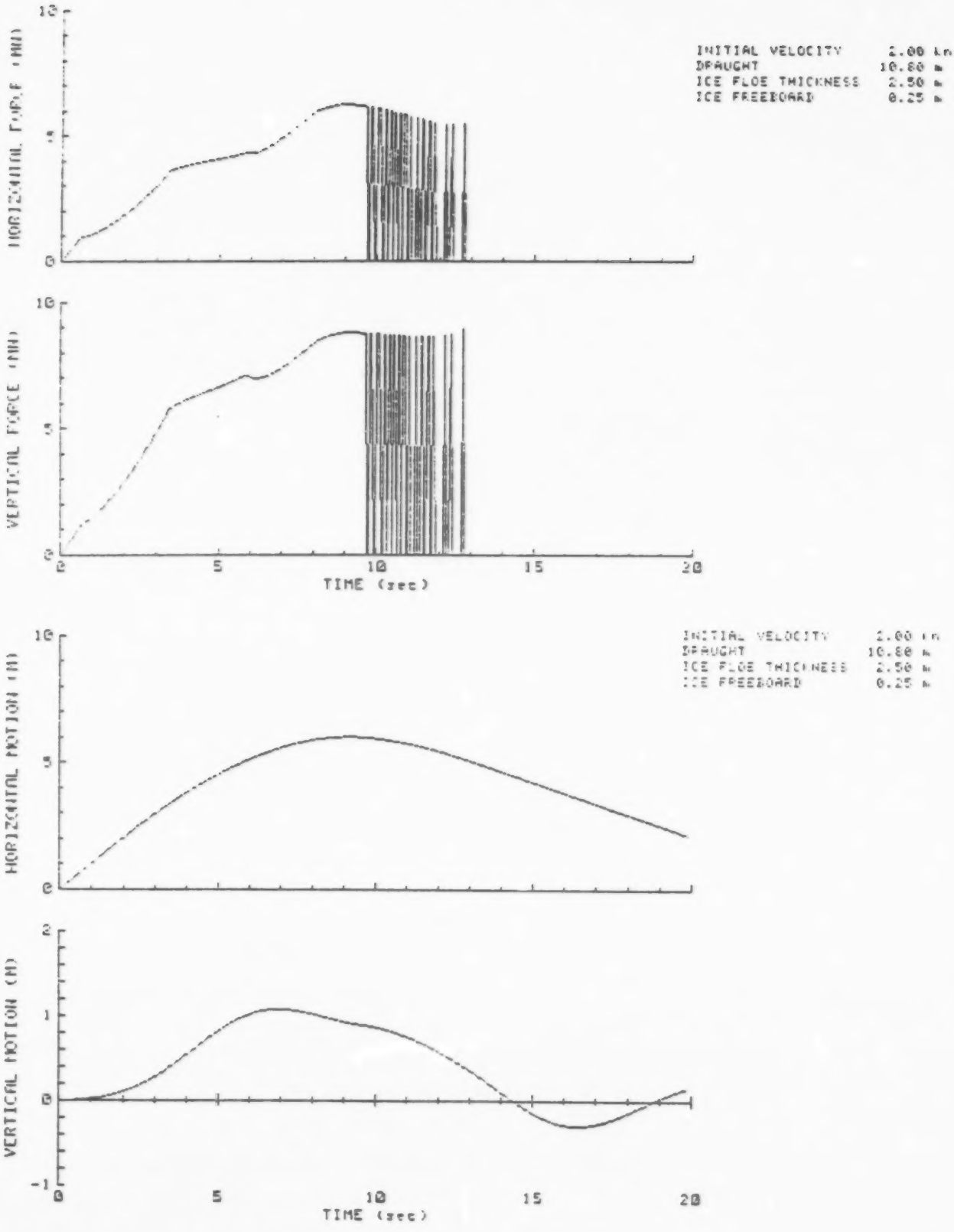


Figure 10 HORIZONTAL AND VERTICAL FORCE AND MOTION - Case 1

| VARIABLE | MAX. VALUE | TIME |
|---|---|---|
| NORMAL DEFLECTION : RIGID MODE #1 | 6.011E+00 | 9.20 |
| NORMAL DEFLECTION : RIGID MODE #2 | 9.099E-01 | 7.10 |
| NORMAL DEFLECTION : RIGID MODE #3 | -4.552E-01 | 6.15 |
| NORMAL DEFLECTION : ELASTIC MODE #1 | 9.127E-01 | 7.10 |
| NORMAL DEFLECTION : ELASTIC MODE #2 | -4.570E-01 | 6.20 |
| NORMAL DEFLECTION : ELASTIC MODE #3 | 2.552E-02 | 11.90 |
| NORMAL DEFLECTION : ELASTIC MODE #5 | -5.950E-03 | 9.15 |
| NORMAL DEFLECTION : ELASTIC MODE #6 | 1.813E-03 | 10.15 |
| NORMAL DEFLECTION : ELASTIC MODE #8 | -6.755E-04 | 10.10 |
| NORMAL DEFLECTION : ELASTIC MODE #9 | 3.562E-04 | 10.10 |
| NORMAL DEFLECTION : ELASTIC MODE #11 | 5.768E-04 | 10.05 |
| NODE #1 : RIGID MOMENT | 0.000E+00 | 0.00 |
| NODE #1 : ELASTIC MOMENT | 0.000E+00 | 0.00 |
| NODE #1 : TOTAL MOMENT | 0.000E+00 | 0.00 |
| NODE #2 : RIGID MOMENT | -5.639E+06 | 6.45 |
| NODE #2 : ELASTIC MOMENT | 1.620E+07 | 12.40 |
| NODE #2 : TOTAL MOMENT | 1.325E+07 | 12.40 |
| NODE #3 : RIGID MOMENT | -2.175E+07 | 6.35 |
| NODE #3 : ELASTIC MOMENT | -4.844E+07 | 11.85 |
| NODE #3 : TOTAL MOMENT | -6.071E+07 | 11.85 |
| NODE #5 : RIGID MOMENT | -3.177E+07 | 6.30 |
| NODE #5 : ELASTIC MOMENT | -8.928E+07 | 11.85 |
| NODE #5 : TOTAL MOMENT | -1.104E+08 | 11.85 |
| NODE #7 : RIGID MOMENT | -3.707E+07 | 6.30 |
| NODE #7 : ELASTIC MOMENT | -1.181E+08 | 11.90 |
| NODE #7 : TOTAL MOMENT | -1.425E+08 | 11.90 |
| NODE #9 : RIGID MOMENT | -3.840E+07 | 6.25 |
| NODE #9 : ELASTIC MOMENT | -1.293E+08 | 11.90 |
| NODE #9 : TOTAL MOMENT | -1.547E+08 | 11.90 |
| NODE #10 : RIGID MOMENT | -3.786E+07 | 6.30 |
| NODE #10 : ELASTIC MOMENT | -1.806E+08 | 11.90 |
| NODE #10 : TOTAL MOMENT | -2.114E+08 | 11.90 |
| NODE #12 : RIGID MOMENT | -3.392E+07 | 6.30 |
| NODE #12 : ELASTIC MOMENT | -1.947E+08 | 11.85 |
| NODE #12 : TOTAL MOMENT | -2.220E+08 | 10.15 |
| NODE #14 : RIGID MOMENT | -2.720E+07 | 6.30 |
| NODE #14 : ELASTIC MOMENT | -1.966E+08 | 10.70 |
| NODE #14 : TOTAL MOMENT | -2.206E+08 | 10.70 |
| NODE #16 : RIGID MOMENT | -1.706E+07 | 6.20 |
| NODE #16 : ELASTIC MOMENT | -1.986E+08 | 9.35 |
| NODE #16 : TOTAL MOMENT | -2.119E+08 | 9.40 |

Figure 11 MAXIMUM RESPONSE VALUES (ship velocity - 2 knots)

| | | | |
|---|---|---|---|
| NODE #18 : | RIGID MOMENT | -4.147E+06 | 5.30 |
| NODE #18 : | ELASTIC MOMENT | -2.059E+08 | 9.35 |
| NODE #18 : | TOTAL MOMENT | -2.080E+08 | 9.40 |
| NODE #19 : | RIGID MOMENT | -1.025E+07 | 6.45 |
| NODE #19 : | ELASTIC MOMENT | -1.626E+08 | 9.35 |
| NODE #19 : | TOTAL MOMENT | -1.711E+08 | 9.35 |
| NODE #21 : | RIGID MOMENT | -9.568E+06 | 6.60 |
| NODE #21 : | ELASTIC MOMENT | -1.199E+08 | 9.35 |
| NODE #21 : | TOTAL MOMENT | -1.278E+08 | 9.35 |
| NODE #22 : | RIGID MOMENT | -6.667E+06 | 6.65 |
| NODE #22 : | ELASTIC MOMENT | -8.441E+07 | 9.35 |
| NODE #22 : | TOTAL MOMENT | -8.993E+07 | 9.35 |
| NODE #23 : | RIGID MOMENT | -3.033E+06 | 6.65 |
| NODE #23 : | ELASTIC MOMENT | -4.753E+07 | 9.35 |
| NODE #23 : | TOTAL MOMENT | -5.003E+07 | 9.30 |
| NODE #24 : | RIGID MOMENT | -3.312E+06 | 6.75 |
| NODE #24 : | ELASTIC MOMENT | -3.379E+07 | 9.35 |
| NODE #24 : | TOTAL MOMENT | -3.655E+07 | 9.30 |
| NODE #25 : | RIGID MOMENT | -2.912E+06 | 6.80 |
| NODE #25 : | ELASTIC MOMENT | -2.116E+07 | 9.35 |
| NODE #25 : | TOTAL MOMENT | -2.360E+07 | 9.25 |
| NODE #26 : | RIGID MOMENT | -1.810E+06 | 6.85 |
| NODE #26 : | ELASTIC MOMENT | -9.803E+06 | 9.35 |
| NODE #26 : | TOTAL MOMENT | -1.132E+07 | 9.20 |
| NODE #27 : | RIGID MOMENT | 0.000E+00 | 0.00 |
| NODE #27 : | ELASTIC MOMENT | 0.000E+00 | 0.00 |
| NODE #27 : | TOTAL MOMENT | 0.000E+00 | 0.00 |

Figure 11 (cont'd)

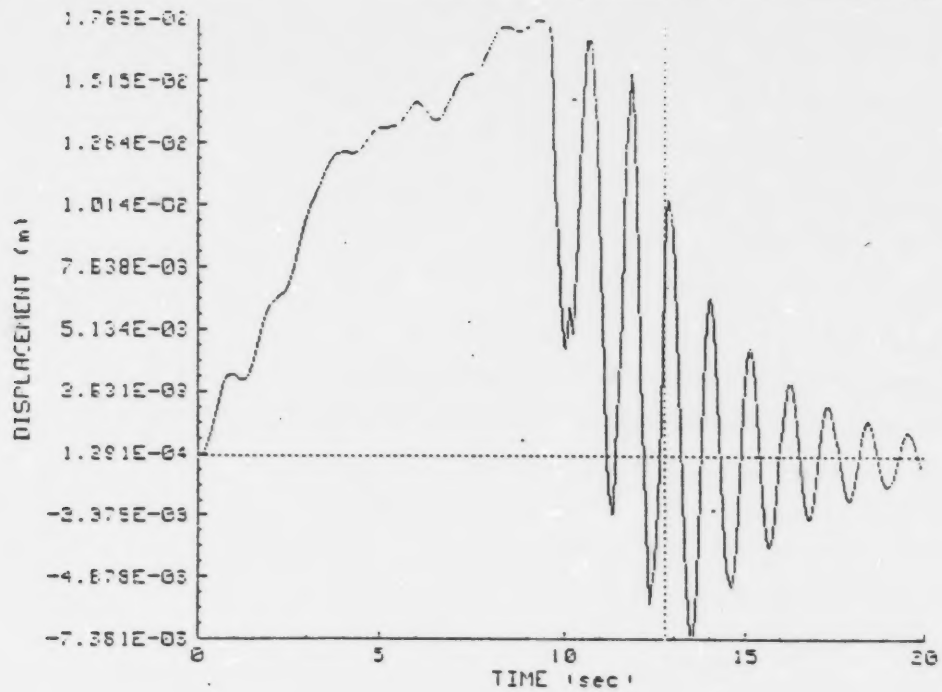


TOTAL VERTICAL ELASTIC DISPLACEMENT AT NODE #27

Figure 12

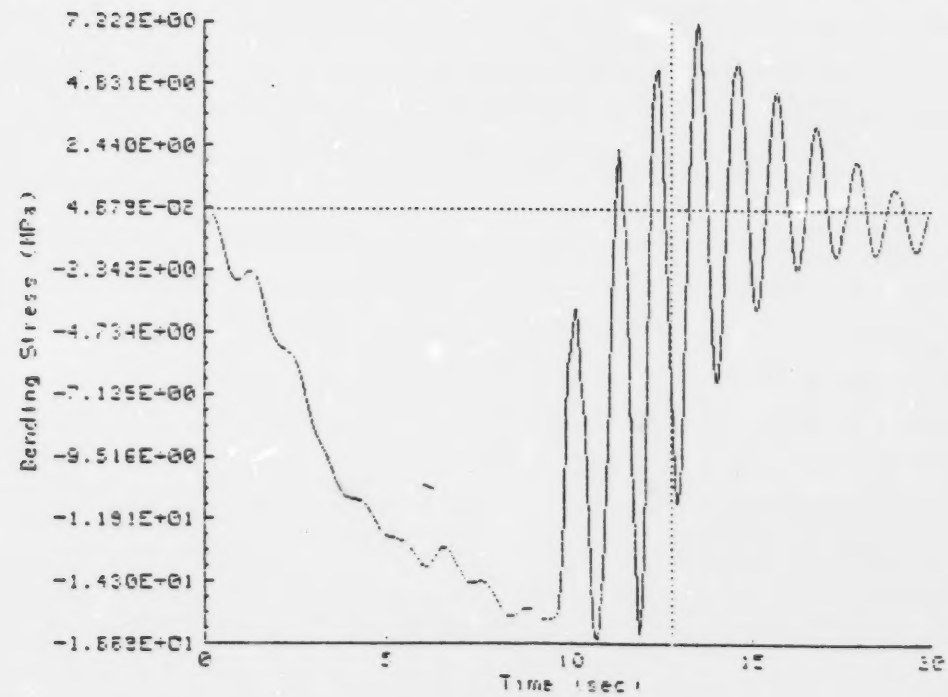


Time History of Total Stresses at Node #12

Figure 13

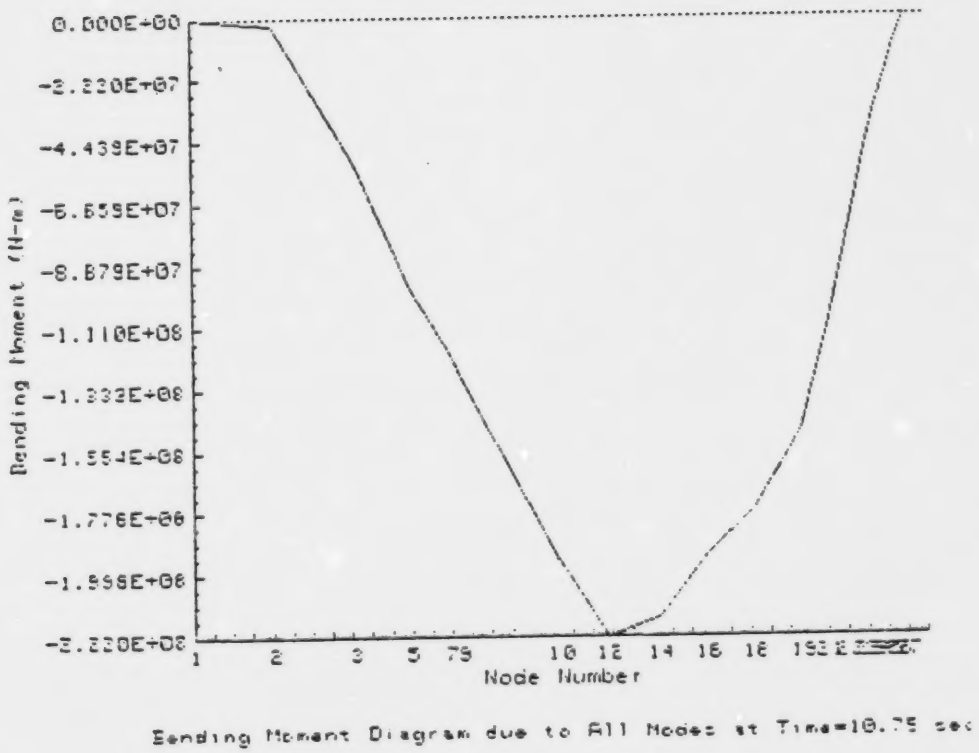


Bending Moment Diagram due to All Modes at Time=10.75 sec

Figure 14

5.0 RESULTS (cont'd)

If the vertical downward motion is greater than the separation, then the ship is still impacting ice and the force is non zero. However, if the vertical motion is less than the separation, then the force must be zero. Hence the oscillation is a function of both the horizontal backward motion and the profile of the ship which define the separation, and the vertical motion of the ship which is decelerated by the contact force. In the real situation, the time step is infinitesimal and the effects of these force oscillations would not be felt. The vertical motion is smooth as shown in Figure 10.

Another observation is the "kinks" in the smooth gradual buildup of the force. These are a result of the combined response of the quasi-rigid heave and pitching modes of the ship. This can also be seen in the plot of the vertical motion.

The elastic deflection is shown in Figure 12. The ship oscillates about the quasi-static deflection resulting from the slow increase in the force. As expected, the dynamic component is a small fraction of the total displacement. The behaviour is quite different for the period of oscillating force. Appendix G described the response of a single degree of freedom system to an idealized version of the force diagram in Figure 10. The results indicate that the response of the system is sensitive to the distribution of the force pulses.

5.0 RESULTS (cont'd)

Such a distribution may dampen or amplify the response depending on the frequency of the oscillating force relative to the natural frequencies of the ship. The response after the pulsating force is a damped free vibration with an initial velocity. The response is as would be expected.

Figure 13 shows the time history of the total stress. The behaviour is very similar to that of the elastic deflection since it is about six times the quasi-rigid response. Note that in the free vibration stage the stress oscillates about the quasi-rigid value as opposed to the zero stress equilibrium position.

Results for cases 2 and 3 are similar to those of case 1. Note that the force increases at a higher rate with the increase in velocity. Consequently, the dynamic excitation of the quasi-rigid modes becomes more pronounced with the increase in initial velocity. Also, the damping of the vertical modes leads to a decrease in the vertical force due to a smaller vertical motion while the horizontal force remains relatively constant. Results for cases 2 and 3 are shown in Figures 15 to 19 and 20 to 24 respectively.

Finally, figure 25 shows the force and response for case 4. Recall that this is the same as case 1 except that the quasi-rigid modes are undamped. The force variations are very similar. The vertical motion is fractionally lower. It is expected that the stresses and moments would show very little variation. For higher velocities where the dynamic components are more important, the damping effect may be more dominant.

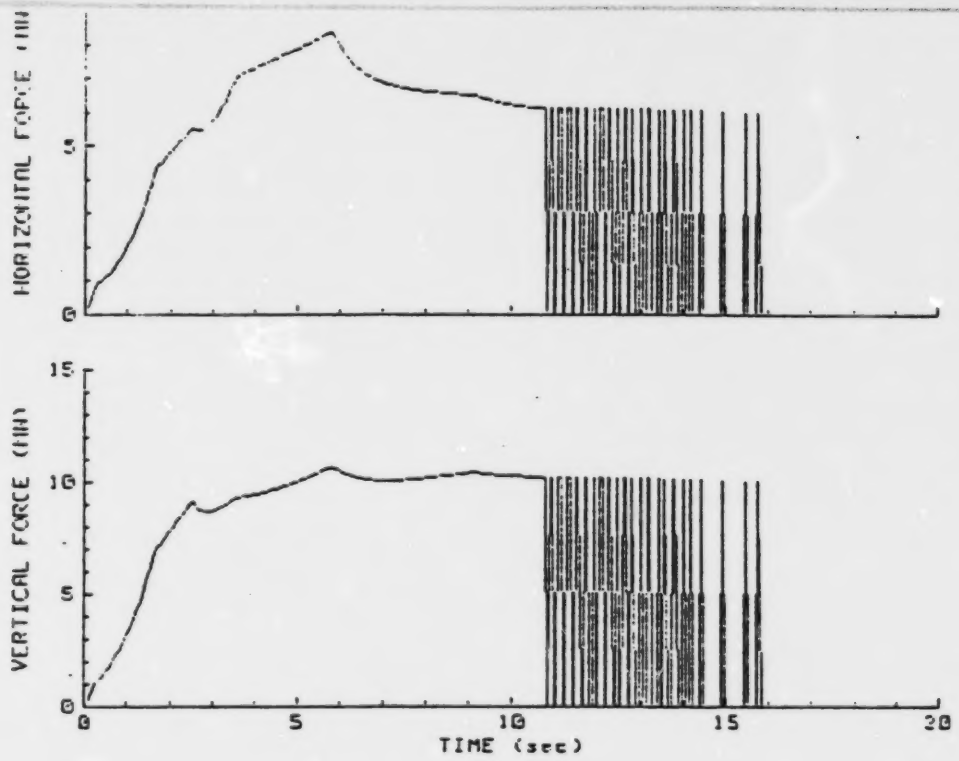


INITIAL VELOCITY 4.00 kn
DRAUGHT 10.00 m
ICE FLOE THICKNESS 2.50 m
ICE FREEBOARD 0.25 m

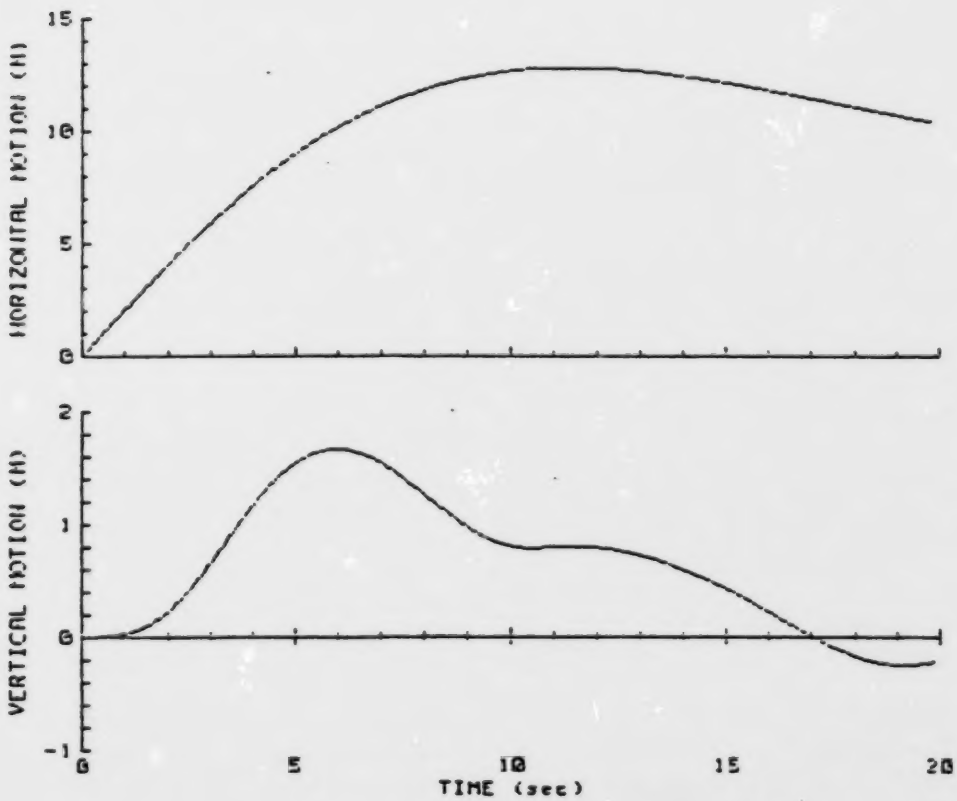


Figure 15 HORIZONTAL AND VERTICAL FORCE AND MOTION - Case 2

| VARIABLE | MAX. VALUE | TIME |
|---|---|---|
| NORMAL DEFLECTION : RIGID MODE #1 | 1.277E+01 | 11.45 |
| NORMAL DEFLECTION : RIGID MODE #2 | 1.402E+00 | 6.20 |
| NORMAL DEFLECTION : RIGID MODE #3 | -7.246E-01 | 5.15 |
| NORMAL DEFLECTION : ELASTIC MODE #1 | 1.405E+00 | 6.20 |
| NORMAL DEFLECTION : ELASTIC MODE #2 | -7.262E-01 | 5.15 |
| NORMAL DEFLECTION : ELASTIC MODE #3 | 3.027E-02 | 6.10 |
| NORMAL DEFLECTION : ELASTIC MODE #5 | -7.221E-03 | 5.90 |
| NORMAL DEFLECTION : ELASTIC MODE #6 | 2.129E-03 | 5.90 |
| NORMAL DEFLECTION : ELASTIC MODE #8 | -6.775E-04 | 13.85 |
| NORMAL DEFLECTION : ELASTIC MODE #9 | 3.393E-04 | 13.80 |
| NORMAL DEFLECTION : ELASTIC MODE #11 | 6.756E-04 | 11.35 |
| NODE #1 : RIGID MOMENT | 0.000E+00 | 0.00 |
| NODE #1 : ELASTIC MOMENT | 0.000E+00 | 0.00 |
| NODE #1 : TOTAL MOMENT | 0.000E+00 | 0.00 |
| NODE #2 : RIGID MOMENT | -8.825E+06 | 5.40 |
| NODE #2 : ELASTIC MOMENT | 1.399E+07 | 11.35 |
| NODE #2 : TOTAL MOMENT | -1.297E+07 | 11.85 |
| NODE #3 : RIGID MOMENT | -3.419E+07 | 5.35 |
| NODE #3 : ELASTIC MOMENT | -3.341E+07 | 6.15 |
| NODE #3 : TOTAL MOMENT | -6.607E+07 | 5.10 |
| NODE #5 : RIGID MOMENT | -5.008E+07 | 5.30 |
| NODE #5 : ELASTIC MOMENT | -7.261E+07 | 6.15 |
| NODE #5 : TOTAL MOMENT | -1.196E+08 | 6.10 |
| NODE #7 : RIGID MOMENT | -5.857E+07 | 5.25 |
| NODE #7 : ELASTIC MOMENT | -9.257E+07 | 6.15 |
| NODE #7 : TOTAL MOMENT | -1.472E+08 | 6.10 |
| NODE #9 : RIGID MOMENT | -6.075E+07 | 5.25 |
| NODE #9 : ELASTIC MOMENT | -1.024E+08 | 6.15 |
| NODE #9 : TOTAL MOMENT | -1.569E+08 | 6.10 |
| NODE #10 : RIGID MOMENT | -5.976E+07 | 5.25 |
| NODE #10 : ELASTIC MOMENT | -1.648E+08 | 6.10 |
| NODE #10 : TOTAL MOMENT | -2.408E+08 | 6.10 |
| NODE #12 : RIGID MOMENT | -5.349E+07 | 5.30 |
| NODE #12 : ELASTIC MOMENT | -2.287E+08 | 6.10 |
| NODE #12 : TOTAL MOMENT | -2.791E+08 | 6.10 |
| NODE #14 : RIGID MOMENT | -4.286E+07 | 5.30 |
| NODE #14 : ELASTIC MOMENT | -2.430E+08 | 6.10 |
| NODE #14 : TOTAL MOMENT | -2.636E+08 | 6.05 |
| NODE #16 : RIGID MOMENT | -2.709E+07 | 5.20 |
| NODE #16 : ELASTIC MOMENT | -2.447E+08 | 6.05 |
| NODE #16 : TOTAL MOMENT | -2.699E+08 | 6.05 |

**Figure 16 MAXIMUM RESPONSE VALUES (ship velocity = 4 knots)**

| | | |
|---|---|---|
| NODE #18 : RIGID MOMENT | -7.627E+06 | 11.55 |
| NODE #18 : ELASTIC MOMENT | -2.516E+08 | 6.00 |
| NODE #18 : TOTAL MOMENT | -2.561E+08 | 6.00 |
| NODE #19 : RIGID MOMENT | -1.603E+07 | 5.4[illegible] |
| NODE #19 : ELASTIC MOMENT | -1.981E+08 | 6.00 |
| NODE #19 : TOTAL MOMENT | -2.[illegible]E+08 | 6.[illegible] |
| NODE #21 : RIGID MOMENT | -1.485E+07 | 5.60 |
| NODE #21 : ELASTIC MOMENT | -1.456E+08 | 5.95 |
| NODE #21 : TOTAL MOMENT | -1.603E+08 | 5.95 |
| NODE #22 : RIGID MOMENT | -1.037E+07 | 5.65 |
| NODE #22 : ELASTIC MOMENT | -1.024E+08 | 5.95 |
| NODE #22 : TOTAL MOMENT | -1.127E+08 | 5.95 |
| NODE #23 : RIGID MOMENT | -4.703E+06 | 5.65 |
| NODE #23 : ELASTIC MOMENT | -5.759E+07 | 5.90 |
| NODE #23 : TOTAL MOMENT | -6.227E+07 | 5.90 |
| NODE #24 : RIGID MOMENT | -5.119E+06 | 5.60 |
| NODE #24 : ELASTIC MOMENT | -4.095E+07 | 5.90 |
| NODE #24 : TOTAL MOMENT | -4.606E+07 | 5.90 |
| NODE #25 : RIGID MOMENT | -4.496E+06 | 5.85 |
| NODE #25 : ELASTIC MOMENT | -2.564E+07 | 5.90 |
| NODE #25 : TOTAL MOMENT | -3.014E+07 | 5.90 |
| NODE #26 : RIGID MOMENT | -2.793E+06 | 5.90 |
| NODE #26 : ELASTIC MOMENT | -1.188E+07 | 5.90 |
| NODE #26 : TOTAL MOMENT | -1.467E+07 | 5.90 |
| NODE #27 : RIGID MOMENT | 0.000E+00 | 0.00 |
| NODE #27 : ELASTIC MOMENT | 0.000E+00 | 0.00 |
| NODE #27 : TOTAL MOMENT | 0.000E+00 | 0.00 |

Figure 16 (cont'd)

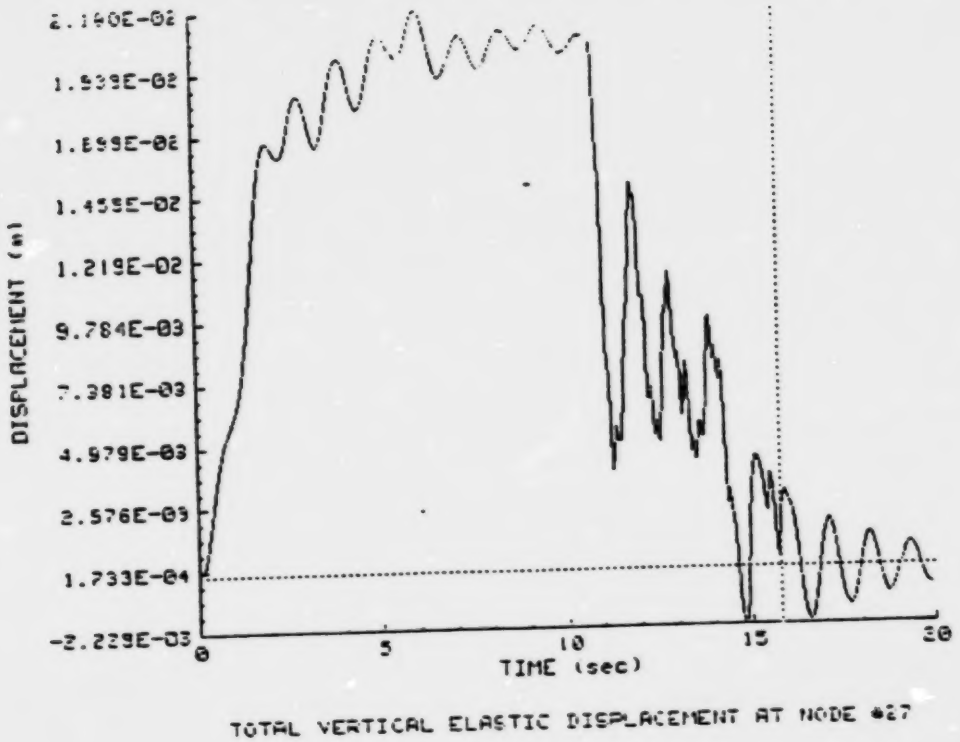


TOTAL VERTICAL ELASTIC DISPLACEMENT AT NODE #27

Figure 17

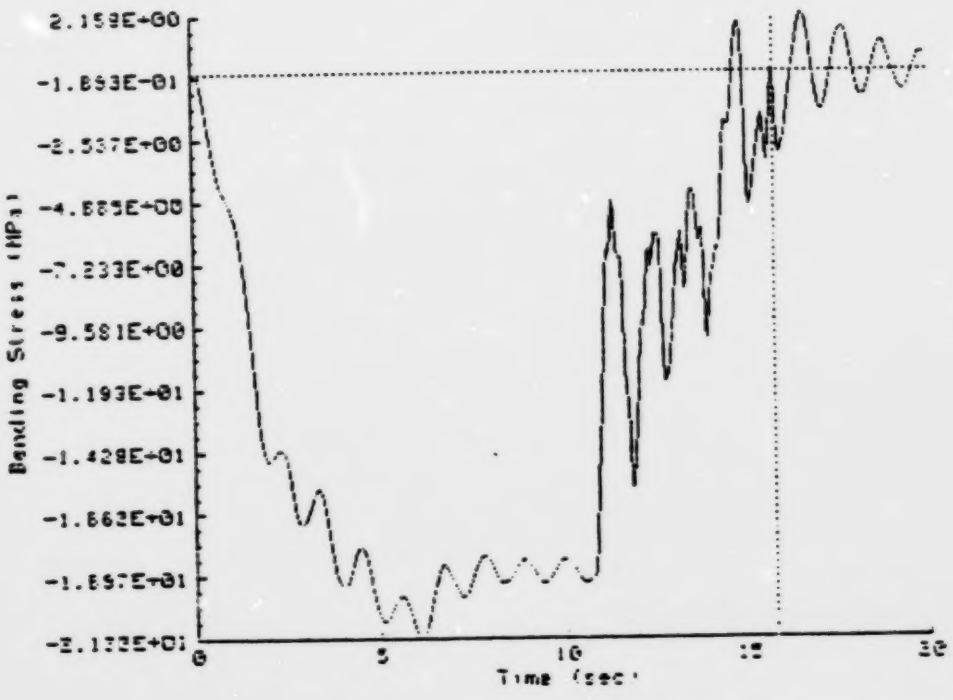


Time History of Total Stresses at Node #14

Figure 18

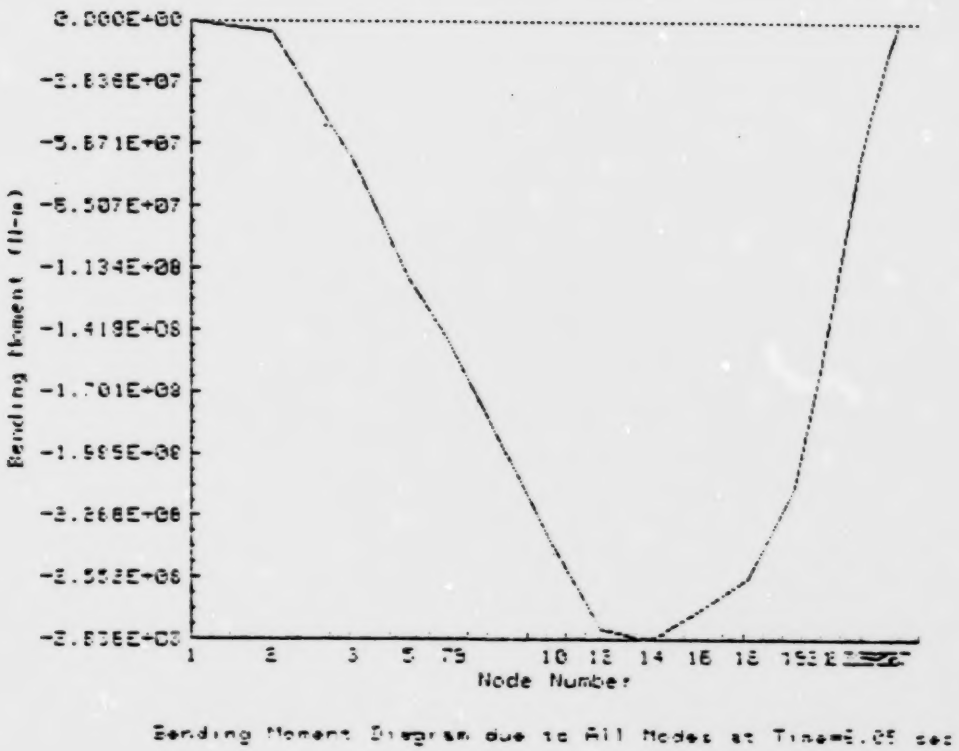


Bending Moment Diagram due to All Modes at Time=1.05 sec

Figure 19

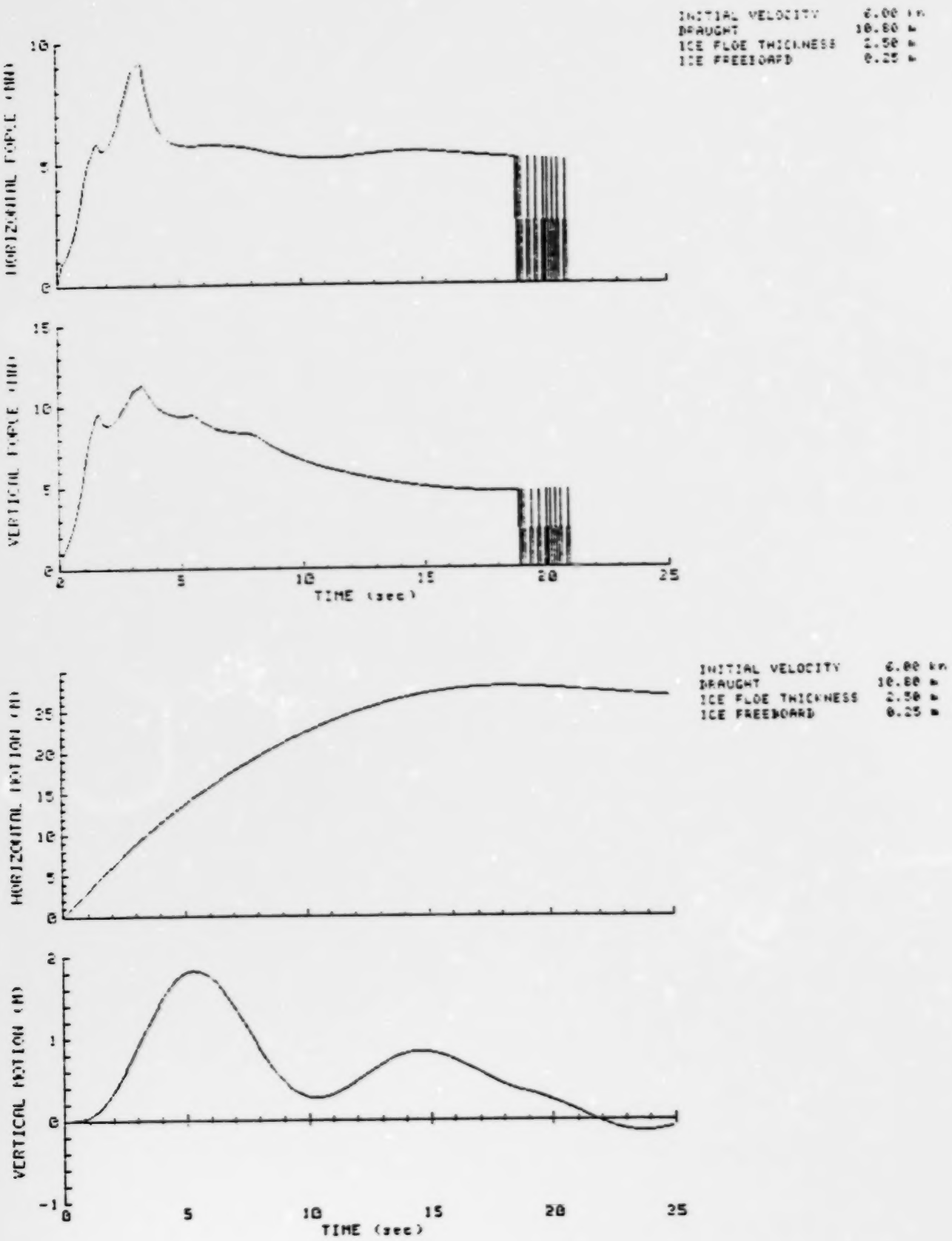


Figure 20 HORIZONTAL AND VERTICAL FORCE AND MOTION - Case 3

| VARIABLE | MAX.VALUE | TIME |
|---|---|---|
| NORMAL DEFLECTION : RIGID MODE #1 | 2.803E+01 | 18.20 |
| NORMAL DEFLECTION : RIGID MODE #2 | 1.526E+00 | 5.50 |
| NORMAL DEFLECTION : RIGID MODE #3 | -8.237E-01 | 4.70 |
| NORMAL DEFLECTION : ELASTIC MODE #1 | 1.528E+00 | 5.50 |
| NORMAL DEFLECTION : ELASTIC MODE #2 | -8.249E-01 | 4.70 |
| NORMAL DEFLECTION : ELASTIC MODE #3 | 3.119E-02 | 2.90 |
| NORMAL DEFLECTION : ELASTIC MODE #5 | -7.615E-03 | 3.50 |
| NORMAL DEFLECTION : ELASTIC MODE #6 | 2.256E-03 | 3.50 |
| NORMAL DEFLECTION : ELASTIC MODE #8 | -6.746E-04 | 3.45 |
| NORMAL DEFLECTION : ELASTIC MODE #9 | 3.550E-04 | 3.45 |
| NORMAL DEFLECTION : ELASTIC MODE #11 | 6.592E-04 | 3.45 |
| NODE #1 : RIGID MOMENT | 0.000E+00 | 0.00 |
| NODE #1 : ELASTIC MOMENT | 0.000E+00 | 0.00 |
| NODE #1 : TOTAL MOMENT | 0.000E+00 | 0.00 |
| NODE #2 : RIGID MOMENT | -9.928E+06 | 4.90 |
| NODE #2 : ELASTIC MOMENT | 5.579E+06 | 2.30 |
| NODE #2 : TOTAL MOMENT | -6.924E+06 | 4.90 |
| NODE #3 : RIGID MOMENT | -3.859E+07 | 4.85 |
| NODE #3 : ELASTIC MOMENT | -3.571E+07 | 2.85 |
| NODE #3 : TOTAL MOMENT | -6.882E+07 | 4.90 |
| NODE #5 : RIGID MOMENT | -5.663E+07 | 4.80 |
| NODE #5 : ELASTIC MOMENT | -7.670E+07 | 2.85 |
| NODE #5 : TOTAL MOMENT | -1.241E+08 | 3.85 |
| NODE #7 : RIGID MOMENT | -6.633E+07 | 4.75 |
| NODE #7 : ELASTIC MOMENT | -9.792E+07 | 2.85 |
| NODE #7 : TOTAL MOMENT | -1.533E+08 | 3.85 |
| NODE #9 : RIGID MOMENT | -6.885E+07 | 4.75 |
| NODE #9 : ELASTIC MOMENT | -1.082E+08 | 2.85 |
| NODE #9 : TOTAL MOMENT | -1.656E+08 | 3.85 |
| NODE #10 : RIGID MOMENT | -6.765E+07 | 4.80 |
| NODE #10 : ELASTIC MOMENT | -1.919E+08 | 2.90 |
| NODE #10 : TOTAL MOMENT | -2.469E+08 | 3.80 |
| NODE #12 : RIGID MOMENT | -6.050E+07 | 4.80 |
| NODE #12 : ELASTIC MOMENT | -2.354E+08 | 2.90 |
| NODE #12 : TOTAL MOMENT | -2.844E+08 | 3.75 |
| NODE #14 : RIGID MOMENT | -4.845E+07 | 4.80 |
| NODE #14 : ELASTIC MOMENT | -2.486E+08 | 2.90 |
| NODE #14 : TOTAL MOMENT | -2.881E+08 | 3.75 |
| NODE #16 : RIGID MOMENT | -3.076E+07 | 4.70 |
| NODE #16 : ELASTIC MOMENT | -2.495E+08 | 3.65 |
| NODE #16 : TOTAL MOMENT | -2.754E+08 | 3.70 |

**Figure 21 MAXIMUM RESPONSE VALUES (ship velocity = 6 knots)**

| | | | |
|---|---|---|---|
| NODE #18 : | RIGID MOMENT | -8.329E+06 | 4.15 |
| NODE #18 : | ELASTIC MOMENT | -2.582E+08 | 3.60 |
| NODE #18 : | TOTAL MOMENT | -2.660E+08 | 3.60 |
| NODE #19 : | RIGID MOMENT | -1.804E+07 | 4.90 |
| NODE #19 : | ELASTIC MOMENT | -2.046E+08 | 3.50 |
| NODE #19 | TOTAL MOMENT | -2.184E+08 | 3.55 |
| NODE #21 : | RIGID MOMENT | -1.658E+07 | 5.05 |
| NODE #21 : | ELASTIC MOMENT | -1.511E+08 | 3.50 |
| NODE #21 : | TOTAL MOMENT | -1.631E+08 | 3.50 |
| NODE #22 : | RIGID MOMENT | -1.154E+07 | 5.05 |
| NODE #22 : | ELASTIC MOMENT | -1.066E+08 | 3.50 |
| NODE #22 : | TOTAL MOMENT | -1.148E+08 | 3.50 |
| NODE #23 : | RIGID MOMENT | -5.240E+06 | 5.05 |
| NODE #23 : | ELASTIC MOMENT | -6.014E+07 | 3.50 |
| NODE #23 : | TOTAL MOMENT | -6.389E+07 | 3.50 |
| NODE #24 : | RIGID MOMENT | -5.674E+06 | 5.15 |
| NODE #24 : | ELASTIC MOMENT | -4.277E+07 | 3.50 |
| NODE #24 : | TOTAL MOMENT | -4.672E+07 | 3.50 |
| NODE #25 : | RIGID MOMENT | -4.968E+06 | 5.20 |
| NODE #25 : | ELASTIC MOMENT | -2.679E+07 | 3.50 |
| NODE #25 : | TOTAL MOMENT | -3.019E+07 | 3.50 |
| NODE #26 : | RIGID MOMENT | -3.080E+06 | 5.25 |
| NODE #26 : | ELASTIC MOMENT | -1.241E+07 | 3.50 |
| NODE #26 : | TOTAL MOMENT | -1.450E+07 | 3.50 |
| NODE #27 : | RIGID MOMENT | 0.000E+00 | 0.00 |
| NODE #27 : | ELASTIC MOMENT | 0.000E+00 | 0.00 |
| NODE #27 : | TOTAL MOMENT | 0.000E+00 | 0.00 |

**Figure 21 (Cont'd)**

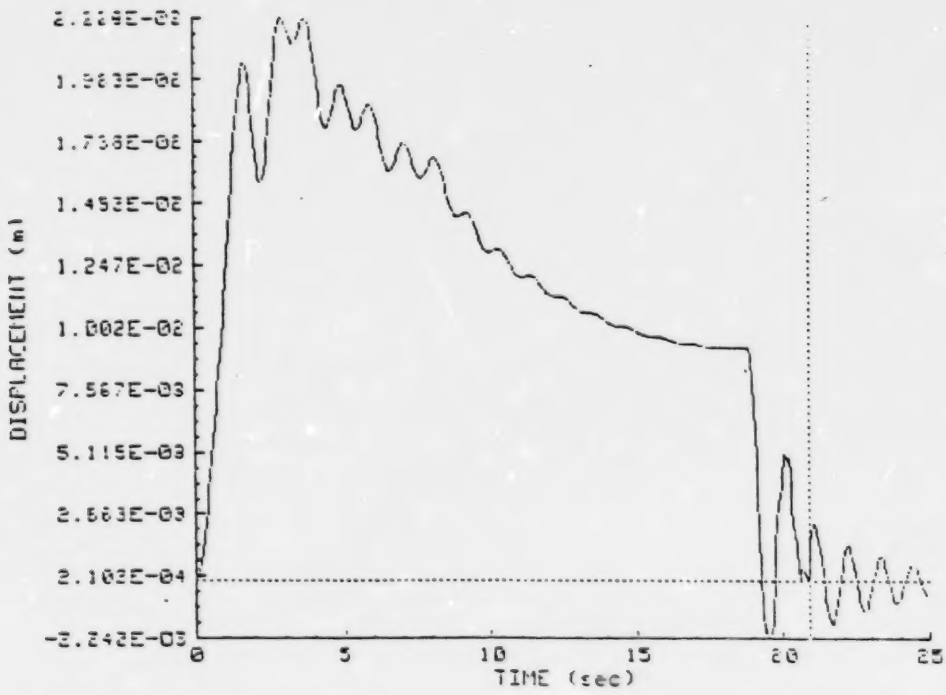


TOTAL VERTICAL ELASTIC DISPLACEMENT AT NODE #27

Figure 22

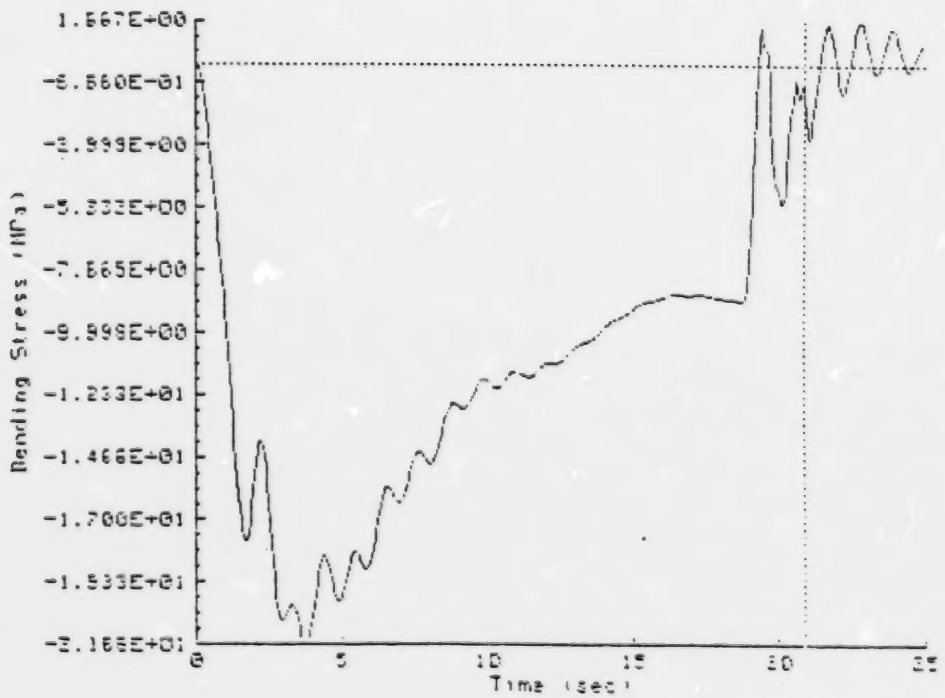


Time History of Total Stresses at Node #12

Figure 23

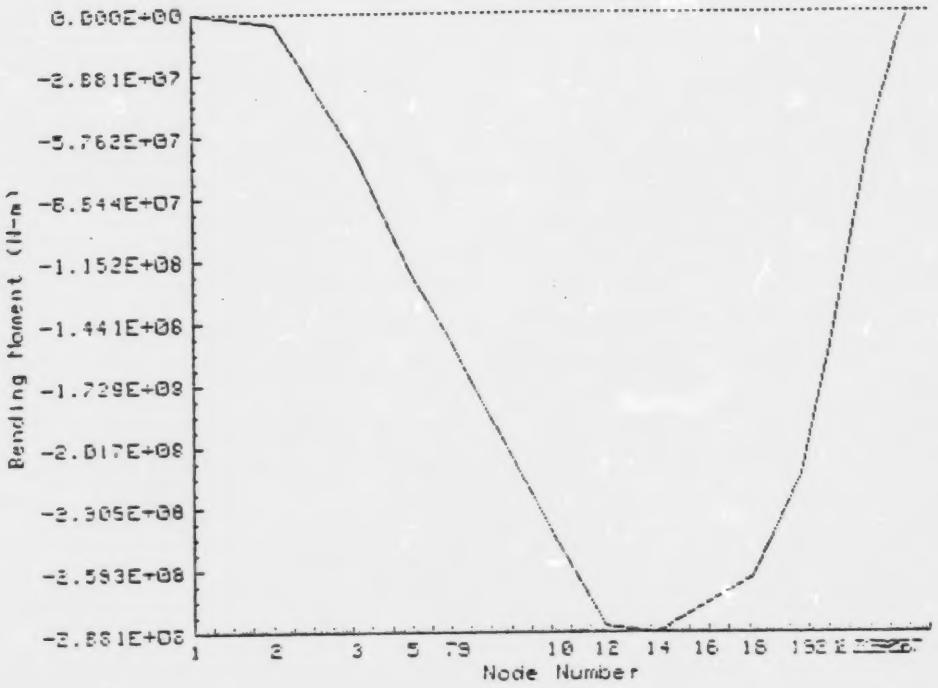


Bending Moment Diagram due to All Modes at Time=3.75 sec

Figure 24

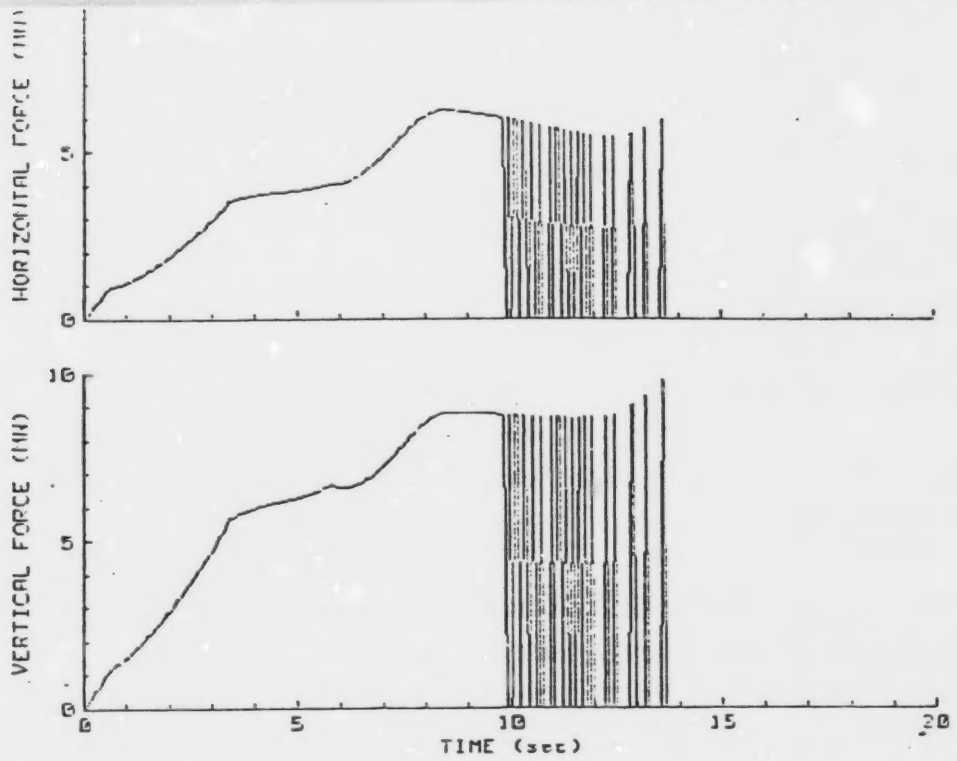


INITIAL VELOCITY 2.00 kn
DRAUGHT 10.00 m
ICE FLOE THICKNESS 2.50 m
ICE FREEBOARD 0.25 m

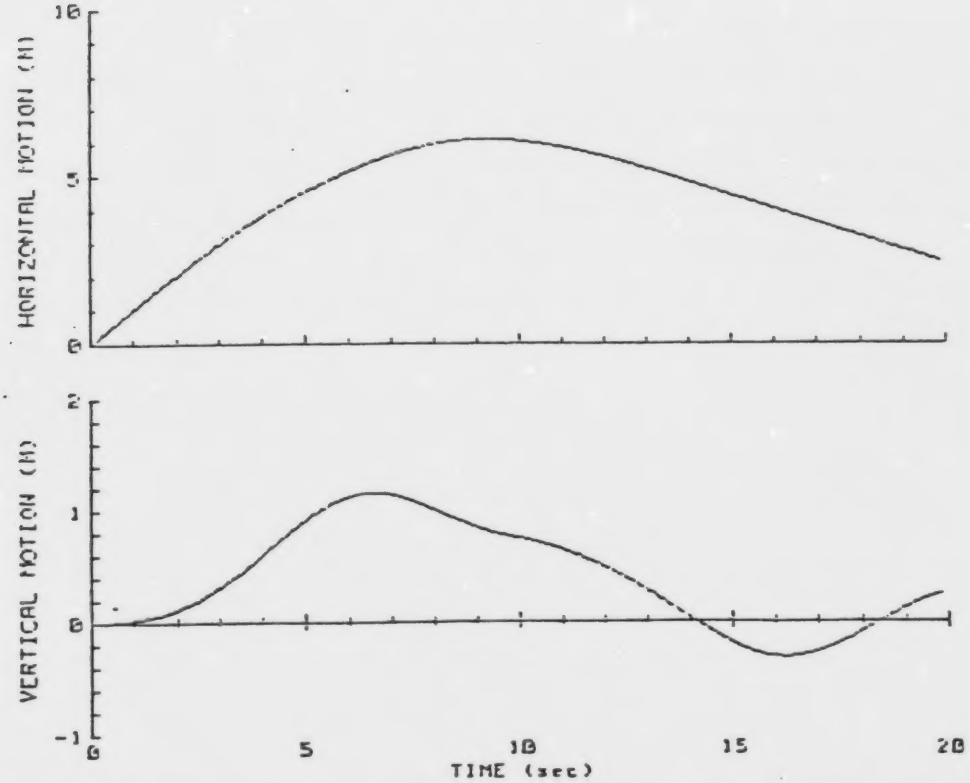


Figure 25 HORIZONTAL AND VERTICAL FORCE AND MOTION WITH NO DAMPING FOR VERTICAL MODES

## 6.0 CONCLUSIONS

A dynamic model of the hull girder of the M.V. Arctic has been built using a lumped mass/ beam finite element model. The resulting mode shapes and frequencies agree well with the first half dozen measured modes.

An ice-interaction model has been developed as part of a transient dynamic program to compute the response of the ship to ice impact. A variety of hull speeds and ice thicknesses have been used to demonstrate the way in which the nature of the response changes with these parameters. Bow forces, deflections and peak bending stresses have been reported as a function of time.

The model reported here is limited to an infinite floe area as no account of the dynamics of the ice motion have been included. Further a single ice-pressure/area model has been used to represent the force on the bow and this inadequately represents the discontinuous nature of the failure of the ice. This may be important as a fluctuation in the bow force, as the ship rides up on the ice, may cause elastic modes of the hull girder to be excited.

REFERENCES

1. Exciter test of the bulk carrier M.V. Arctic.
Technical Research Centre of Finland (TRCF)
Report LAI-335A/82.

2. Mathematical model of the M.V. Arctic ramming multi-year ice floes.
TRCF Report LAI-335B/82.

3. The Theory of Matrix Structural Analysis,
J.S. Przemieniecki, McGraw-Hill.

4. Finite Element System for Desktop Computers (FESDEC)
User's Manual, H.G. Engineering.

# APPENDIX A

## Finite Element Beam Model
## Input Data and Output Results

This appendix includes the following listings:

1. Input data
2. Natural frequencies and equivalent masses
3. Modal deflections for the first 8 vertical modes
4. Modal moments at the nodal points for the first 8 vertical modes.

Also, plots of first 8 vertical modes are enclosed.

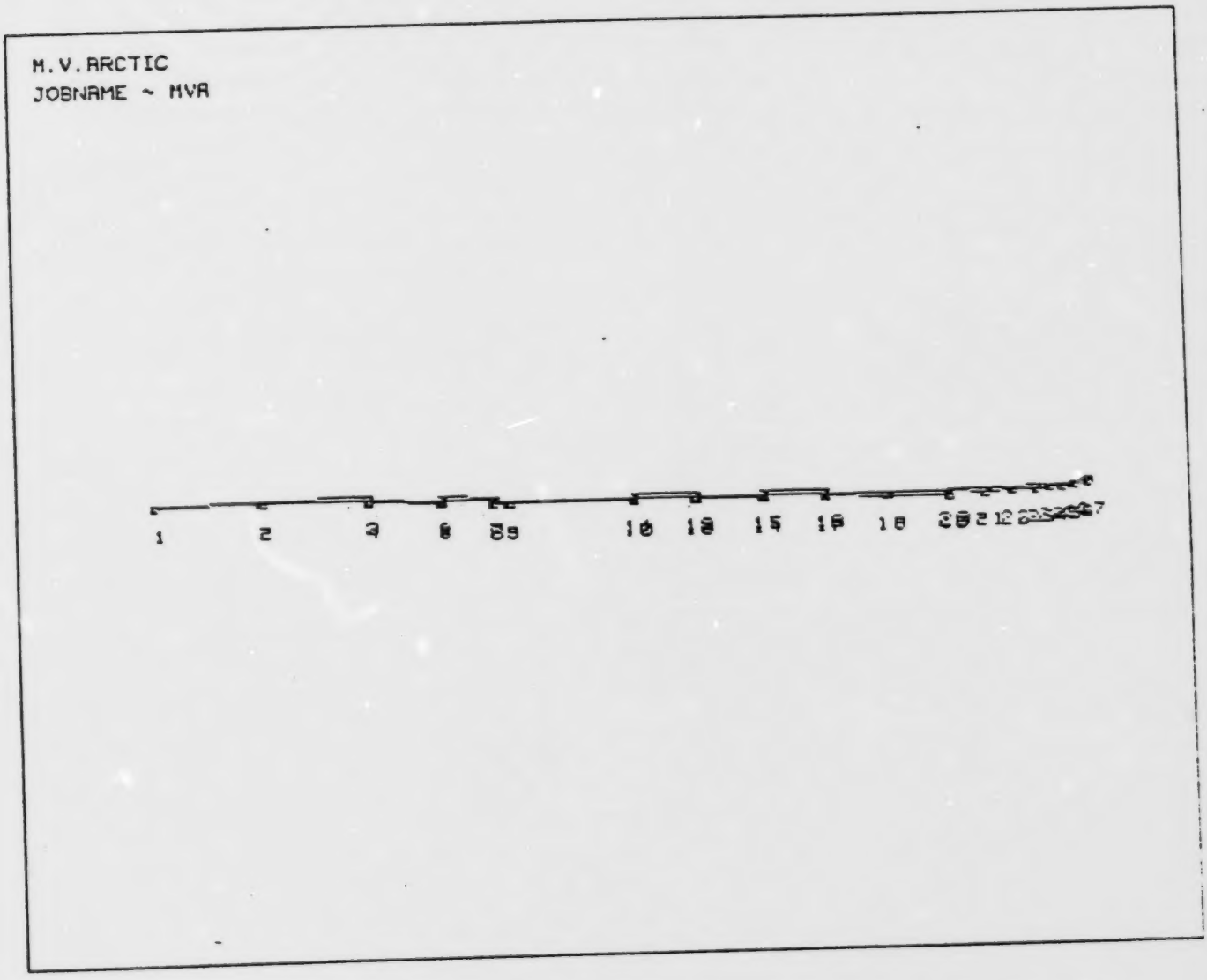


Figure A1 F.E. MODEL OF HULL GIRDER

JOBNAME - MV1

JOB TITLE - M.V.ARCTIC - Natural Frequencies and Mode Shapes

NODAL COORDINATES

| NODE | X | Y |
|---|---|---|
| 1 | 0.0000 | 8.1500 |
| 2 | 20.5000 | 8.3750 |
| 3 | 41.0000 | 8.6000 |
| 4 | 41.0000 | 7.9500 |
| 5 | 55.0000 | 7.5500 |
| 6 | 55.0000 | 8.2500 |
| 7 | 65.0000 | 7.9500 |
| 8 | 65.0000 | 7.2500 |
| 9 | 68.0000 | 7.1500 |
| 10 | 92.0000 | 7.1500 |
| 11 | 92.0000 | 7.8500 |
| 12 | 104.0000 | 7.8500 |
| 13 | 104.0000 | 7.1500 |
| 14 | 117.0000 | 7.1500 |
| 15 | 117.0000 | 7.8500 |
| 16 | 129.0000 | 7.8500 |
| 17 | 129.0000 | 7.1500 |
| 18 | 141.0000 | 7.1250 |
| 19 | 153.0000 | 7.1000 |
| 20 | 153.0000 | 7.6100 |
| 21 | 160.0000 | 7.5000 |
| 22 | 165.0000 | 7.6000 |
| 23 | 170.0000 | 7.8000 |
| 24 | 172.5000 | 8.0000 |
| 25 | 175.0000 | 8.1500 |
| 26 | 177.5000 | 8.5500 |
| 27 | 180.0000 | 9.0500 |

---

ELEMENT DATA - GROUP 1 TYPE - PLBM

| EL.NO | N1 | E1 | N2 | E2 | MAT | SECT |
|---|---|---|---|---|---|---|
| 1 | 1 | | 2 | | STEL | A |
| 2 | 2 | | 3 | | STEL | B |
| 3 | 3 | | 5 | | STEL | C |
| 4 | 5 | | 7 | | STEL | D |
| 5 | 7 | | 9 | | STEL | E |
| 6 | 9 | | 10 | | STEL | F |
| 7 | 10 | | 12 | | STEL | G |
| 8 | 12 | | 14 | | STEL | H |

| | | | | |
|---|---|---|---|---|
| 9 | 14 | 16 | STEL | I |
| 10 | 16 | 18 | STEL | J |
| 11 | 18 | 19 | STEL | K |
| 12 | 19 | 21 | STEL | L |
| 13 | 21 | 22 | STEL | M |
| 14 | 22 | 23 | STEL | N |
| 15 | 23 | 24 | STEL | O |
| 16 | 24 | 25 | STEL | P |
| 17 | 25 | 26 | STEL | Q |
| 18 | 26 | 27 | STEL | R |

---

ELEMENT DATA - GROUP 2 TYPE - SPRG

| EL.NO | N1 | GEOM |
|---|---|---|
| 1 | 1 | a |
| 2 | 2 | b |
| 3 | 3 | c |
| 4 | 5 | d |
| 5 | 7 | e |
| 6 | 9 | f |
| 7 | 10 | g |
| 8 | 12 | h |
| 9 | 14 | i |
| 10 | 16 | j |
| 11 | 18 | k |
| 12 | 19 | l |
| 13 | 21 | m |
| 14 | 22 | n |
| 15 | 23 | o |
| 16 | 24 | p |
| 17 | 25 | q |
| 18 | 26 | r |
| 19 | 27 | s |

---

MATERIAL PROPERTIES DATA

| IDENT | E | v | rho | alpha | k |
|---|---|---|---|---|---|
| STEL | 2.0000E+11 | .300 | 0.0000E+00 | 0.0000E+00 | 0.0000E+00 |

---

GEOMETRIC PROPERTIES DATA

| ELEM | IDENT | Area | Izz | sf |
|---|---|---|---|---|
| PLBM | A | 8.500E-01 | 3.000E+01 | 5.000E-01 |
| PLBM | B | 1.490E+00 | 6.000E+01 | 5.000E-01 |
| PLBM | C | 1.360E+00 | 8.800E+01 | 5.000E-01 |
| PLBM | D | 1.560E+00 | 1.160E+02 | 5.000E-01 |
| PLBM | E | 1.480E+00 | 1.060E+02 | 5.000E-01 |
| PLBM | F | 1.520E+00 | 1.080E+02 | 5.000E-01 |
| PLBM | G | 1.620E+00 | 1.240E+02 | 5.000E-01 |
| PLBM | H | 1.520E+00 | 1.080E+02 | 5.000E-01 |
| PLBM | I | 1.620E+00 | 1.240E+02 | 5.000E-01 |
| PLBM | J | 1.520E+00 | 1.080E+02 | 5.000E-01 |
| PLBM | K | 1.500E+00 | 1.020E+02 | 5.000E-01 |
| PLBM | L | 1.650E+00 | 1.230E+02 | 5.000E-01 |
| PLBM | M | 1.760E+00 | 1.220E+02 | 5.000E-01 |
| PLBM | N | 1.600E+00 | 9.400E+01 | 5.000E-01 |
| PLBM | O | 1.520E+00 | 9.400E+01 | 5.000E-01 |
| PLBM | P | 1.500E+00 | 9.400E+01 | 5.000E-01 |
| PLBM | Q | 1.550E+00 | 9.400E+01 | 5.000E-01 |
| PLBM | R | 1.500E+00 | 6.600E+01 | 5.000E-01 |

| ELEM | IDENT | Kx | Ky | Tz |
|---|---|---|---|---|
| SPRG | a | 0.000E+00 | 9.150E+05 | 0.000E+00 |
| SPRG | b | 0.000E+00 | 3.190E+06 | 0.000E+00 |
| SPRG | c | 0.000E+00 | 3.565E+06 | 0.000E+00 |
| SPRG | d | 0.000E+00 | 2.594E+06 | 0.000E+00 |
| SPRG | e | 0.000E+00 | 1.411E+06 | 0.000E+00 |
| SPRG | f | 0.000E+00 | 2.966E+06 | 0.000E+00 |
| SPRG | g | 0.000E+00 | 3.974E+06 | 0.000E+00 |
| SPRG | h | 0.000E+00 | 2.761E+06 | 0.000E+00 |
| SPRG | i | 0.000E+00 | 2.761E+06 | 0.000E+00 |
| SPRG | j | 0.000E+00 | 2.650E+06 | 0.000E+00 |
| SPRG | k | 0.000E+00 | 2.650E+06 | 0.000E+00 |
| SPRG | l | 0.000E+00 | 2.098E+06 | 0.000E+00 |
| SPRG | m | 0.000E+00 | 1.315E+06 | 0.000E+00 |
| SPRG | n | 0.000E+00 | 1.074E+06 | 0.000E+00 |
| SPRG | o | 0.000E+00 | 7.762E+05 | 0.000E+00 |
| SPRG | p | 0.000E+00 | 4.922E+05 | 0.000E+00 |
| SPRG | q | 0.000E+00 | 4.728E+05 | 0.000E+00 |
| SPRG | r | 0.000E+00 | 4.467E+05 | 0.000E+00 |
| SPRG | s | 0.000E+00 | 2.103E+05 | 0.000E+00 |

---

NODAL SUPPRESSIONS DATA

| NODE | FREEDOM LIST |
|---|---|
| 1 | X |

---

NODAL MASS DATA

| node | Mx | My | Iz |
|---|---|---|---|
| 1 | 7.128E+05 | 7.128E+05 | 0.000E+00 |
| 2 | 2.854E+06 | 2.854E+06 | 0.000E+00 |
| 3 | 4.843E+06 | 4.843E+06 | 0.000E+00 |
| 5 | 4.005E+06 | 4.005E+06 | 0.000E+00 |
| 7 | 1.618E+06 | 1.618E+06 | 0.000E+00 |
| 9 | 8.968E+06 | 8.968E+06 | 0.000E+00 |
| 10 | 8.383E+06 | 8.383E+06 | 0.000E+00 |
| 12 | 5.610E+06 | 5.610E+06 | 0.000E+00 |
| 14 | 4.717E+06 | 4.717E+06 | 0.000E+00 |
| 16 | 4.740E+06 | 4.740E+06 | 0.000E+00 |
| 18 | 1.071E+07 | 1.071E+07 | 0.000E+00 |
| 19 | 2.623E+06 | 2.623E+06 | 0.000E+00 |
| 21 | 1.565E+06 | 1.565E+06 | 0.000E+00 |
| 22 | 1.840E+06 | 1.840E+06 | 0.000E+00 |
| 23 | 3.306E+06 | 3.306E+06 | 0.000E+00 |
| 24 | 4.426E+05 | 4.426E+05 | 0.000E+00 |
| 25 | 3.989E+05 | 3.989E+05 | 0.000E+00 |
| 26 | 3.551E+05 | 3.551E+05 | 0.000E+00 |
| 27 | 1.770E+06 | 1.770E+06 | 0.000E+00 |

SUMMED MASSES

6.946E+07 6.946E+07

NUMBER OF REQUIRED FREQUENCIES = 12

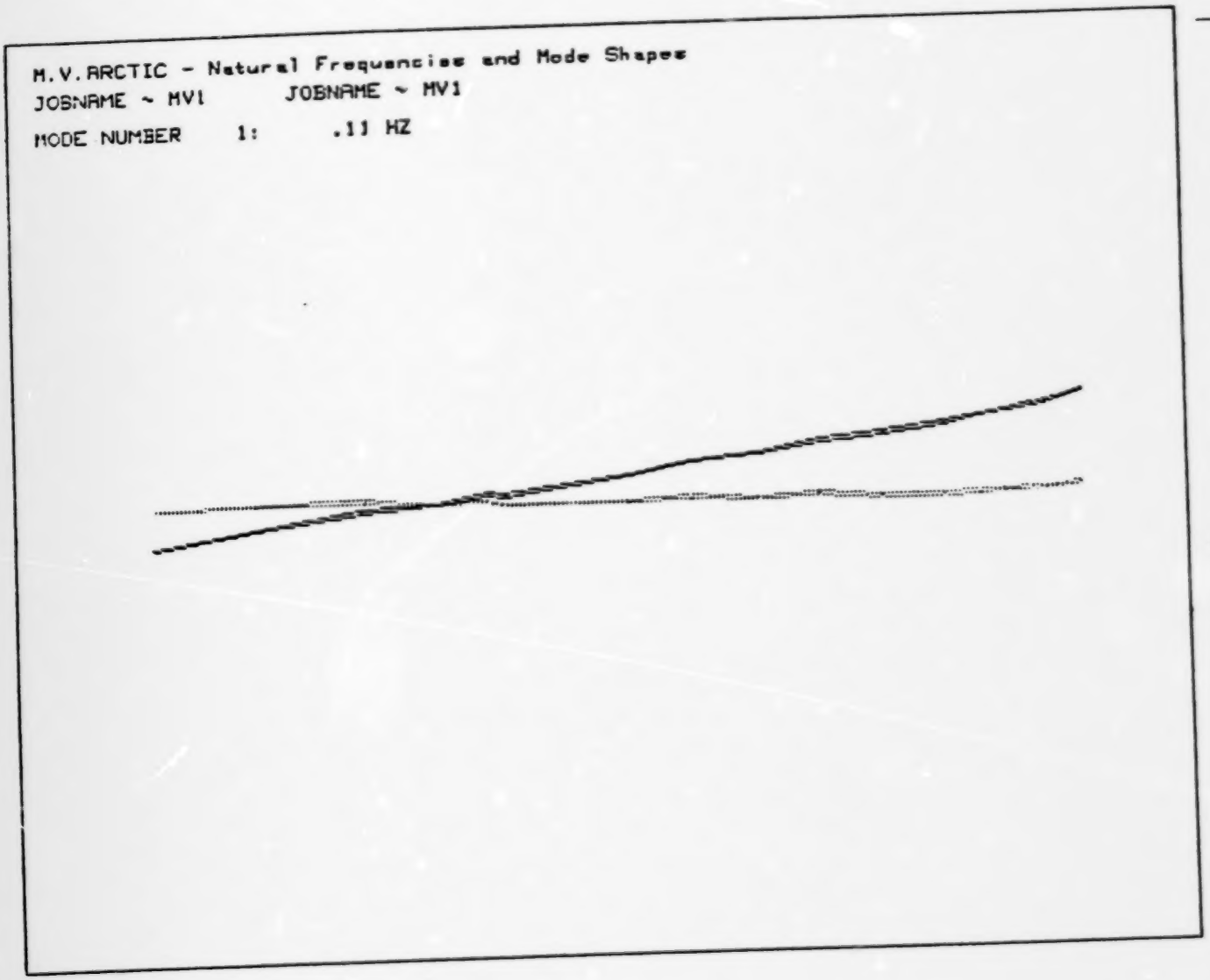


Figure A2 1ST QUASI-RIGID BODY MODE

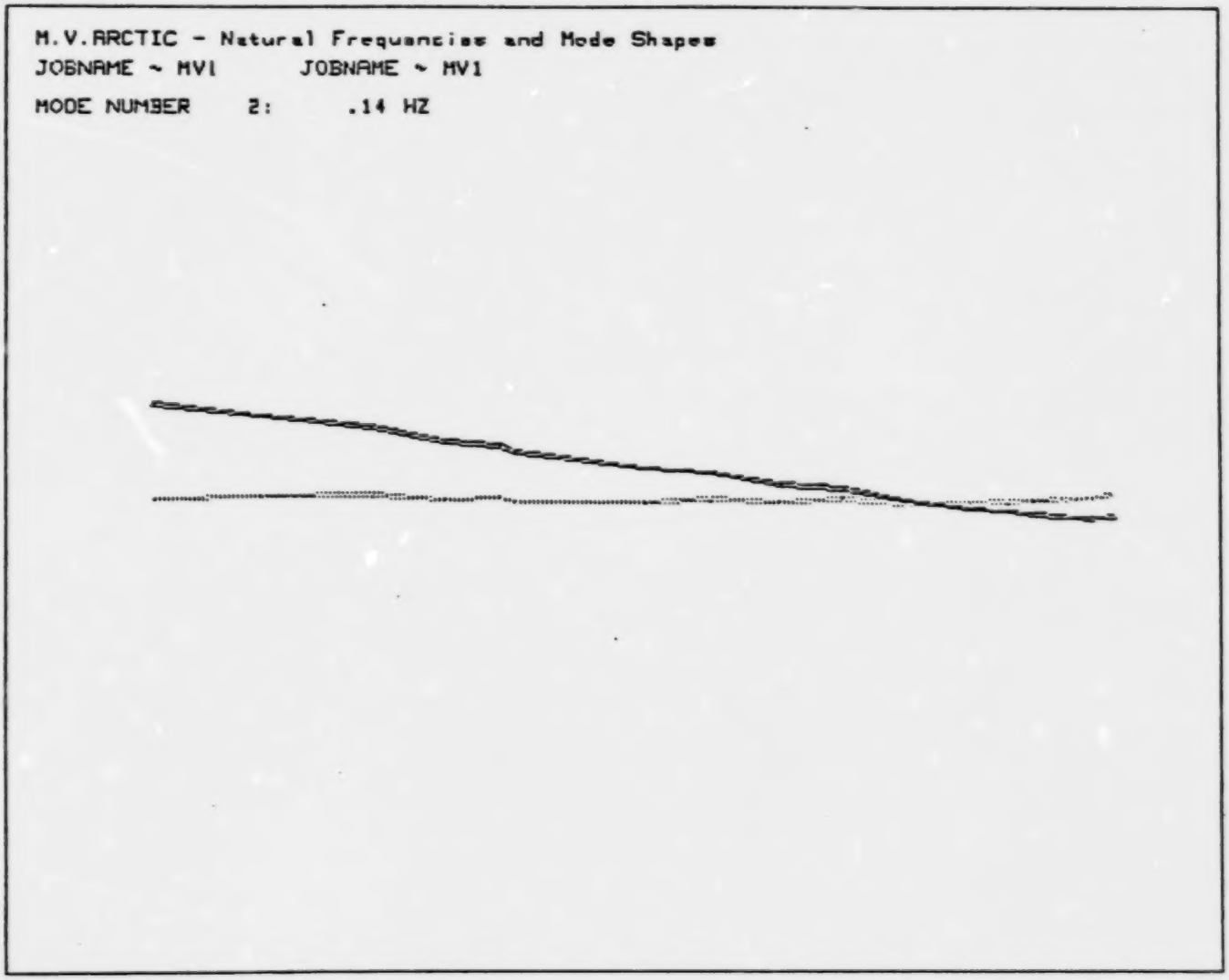


Figure A3 2ND QUASI-RIGID BODY MODE

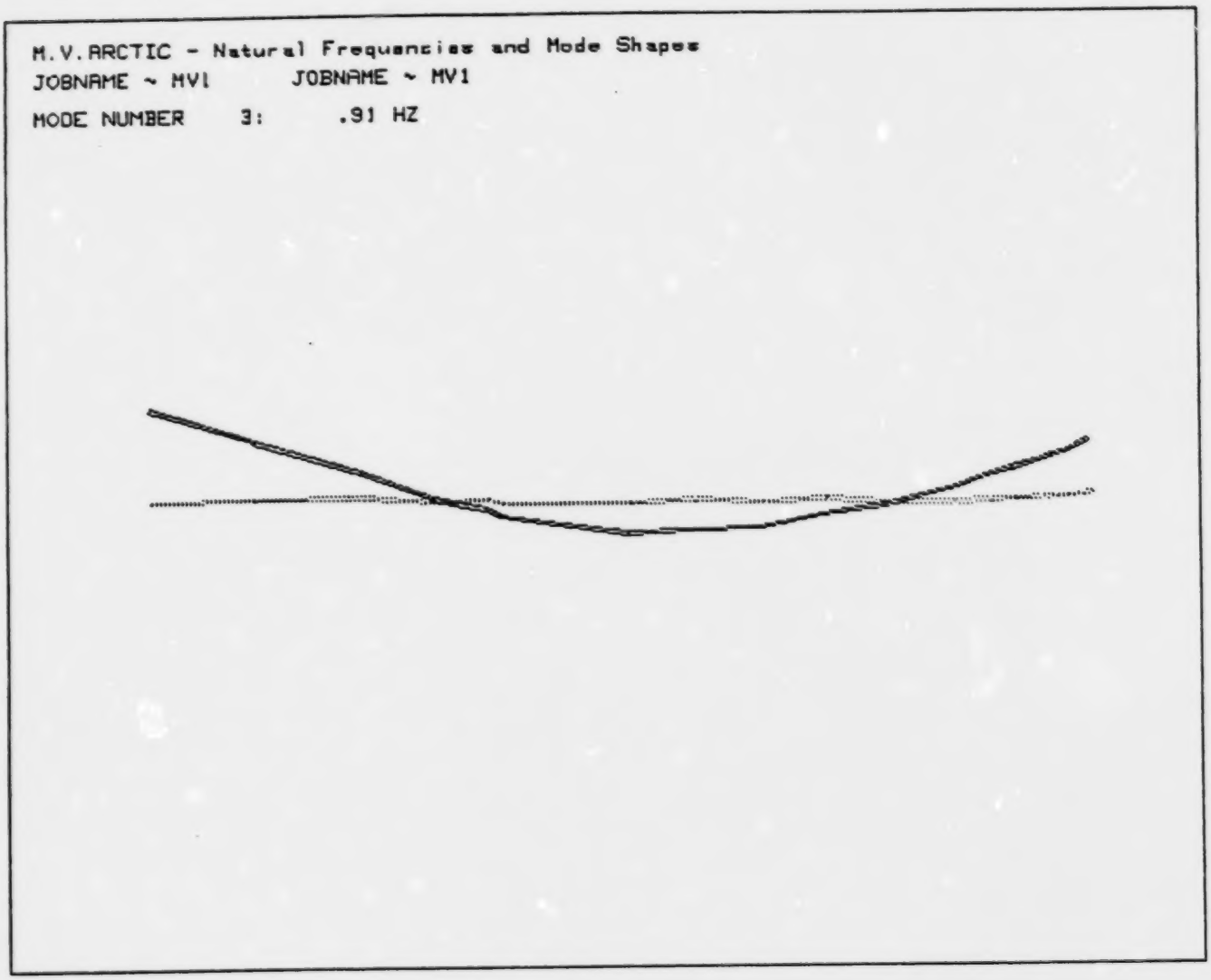


Figure A4 1ST HULL BENDING MODE

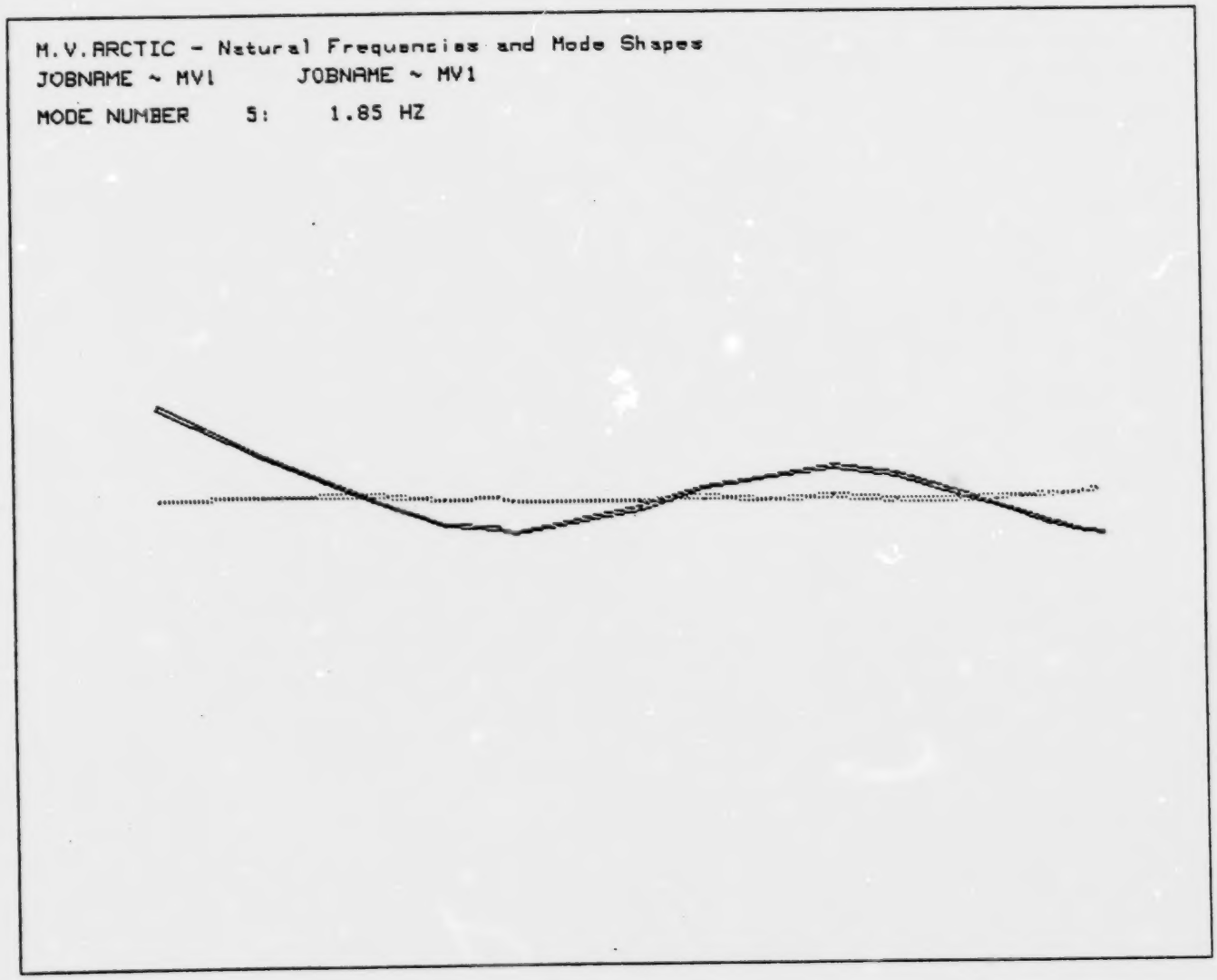


Figure A5 2ND HULL BENDING MODE

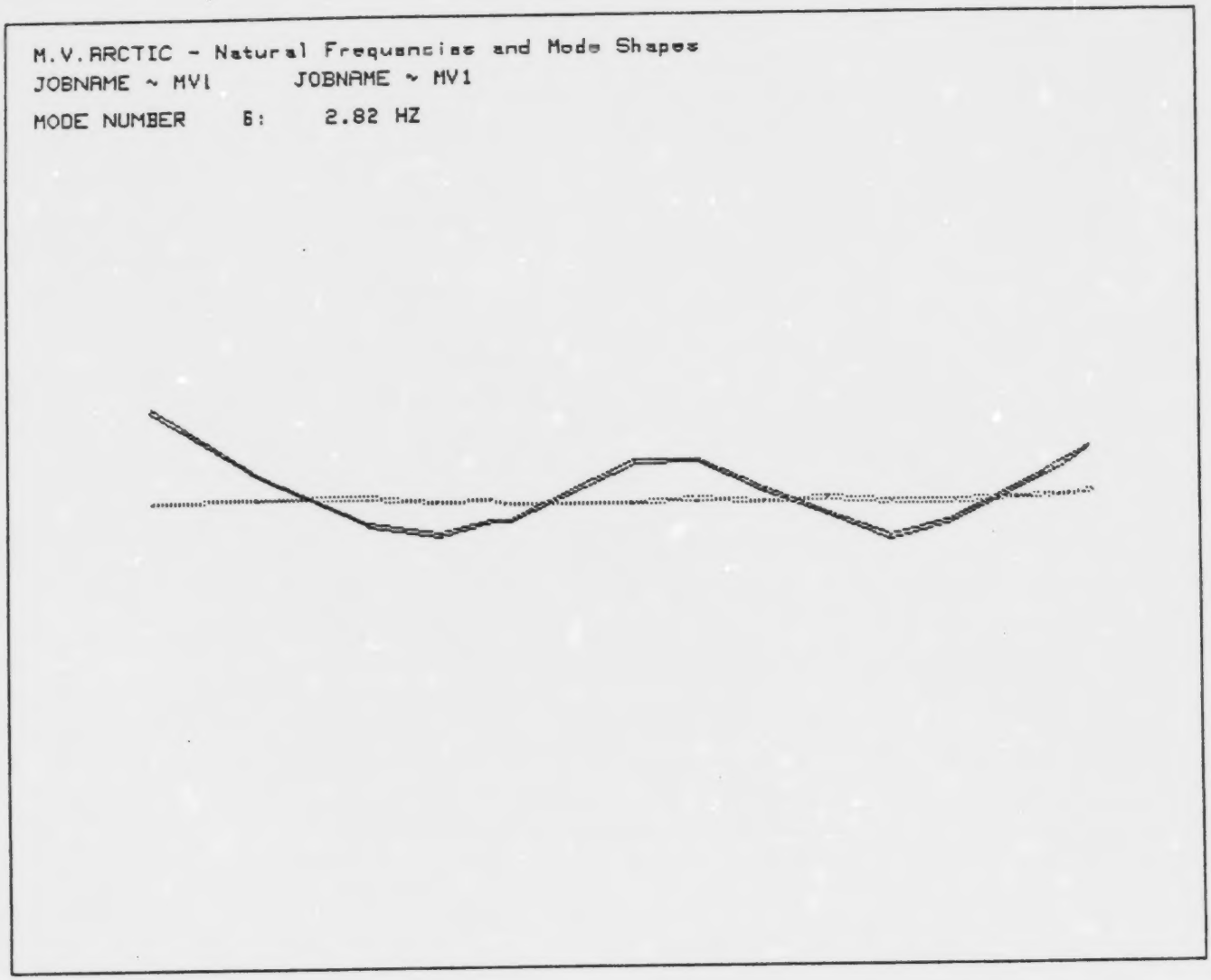


Figure A6 3RD HULL BENDING MODE

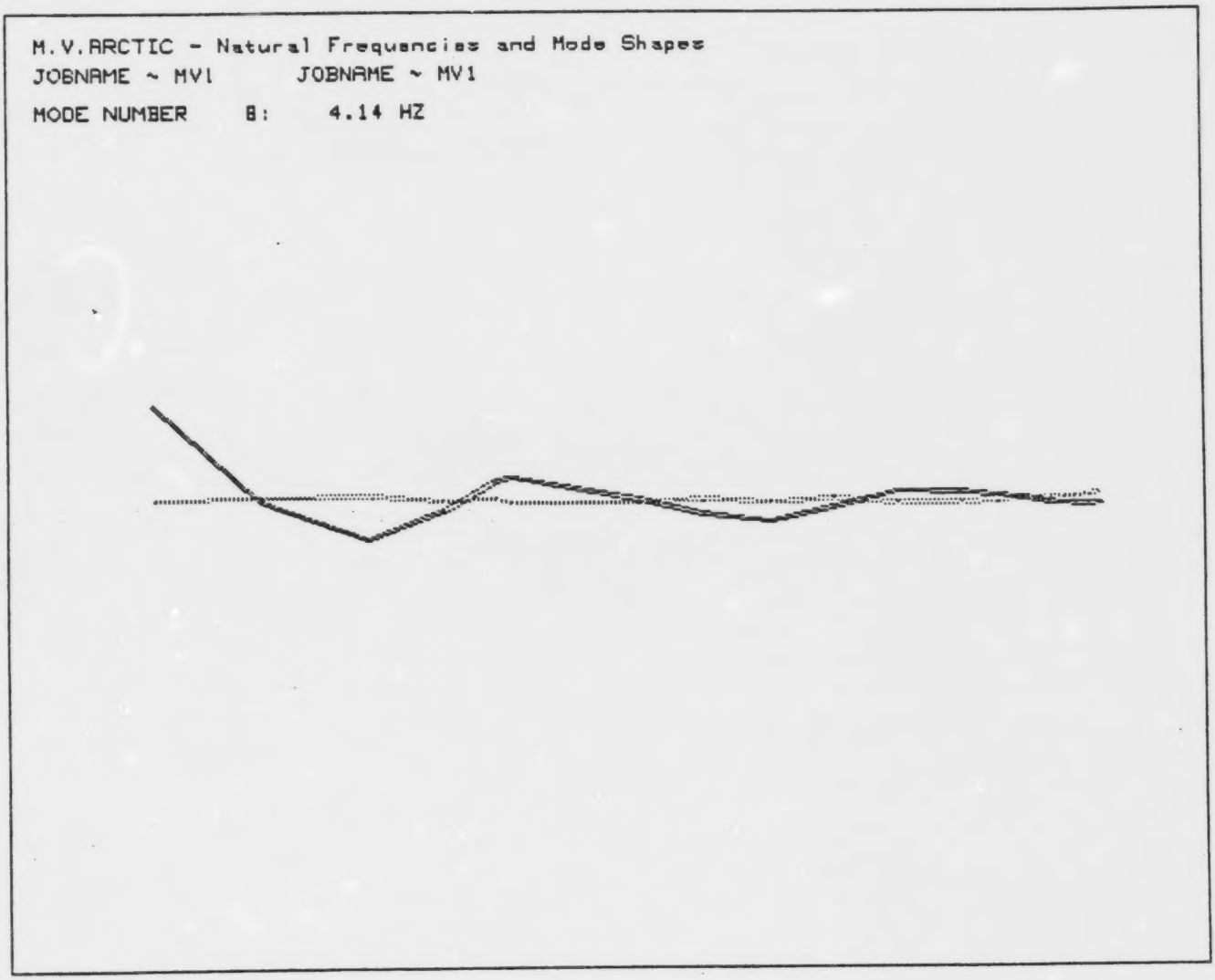


Figure A7 4TH HULL BENDING MODE

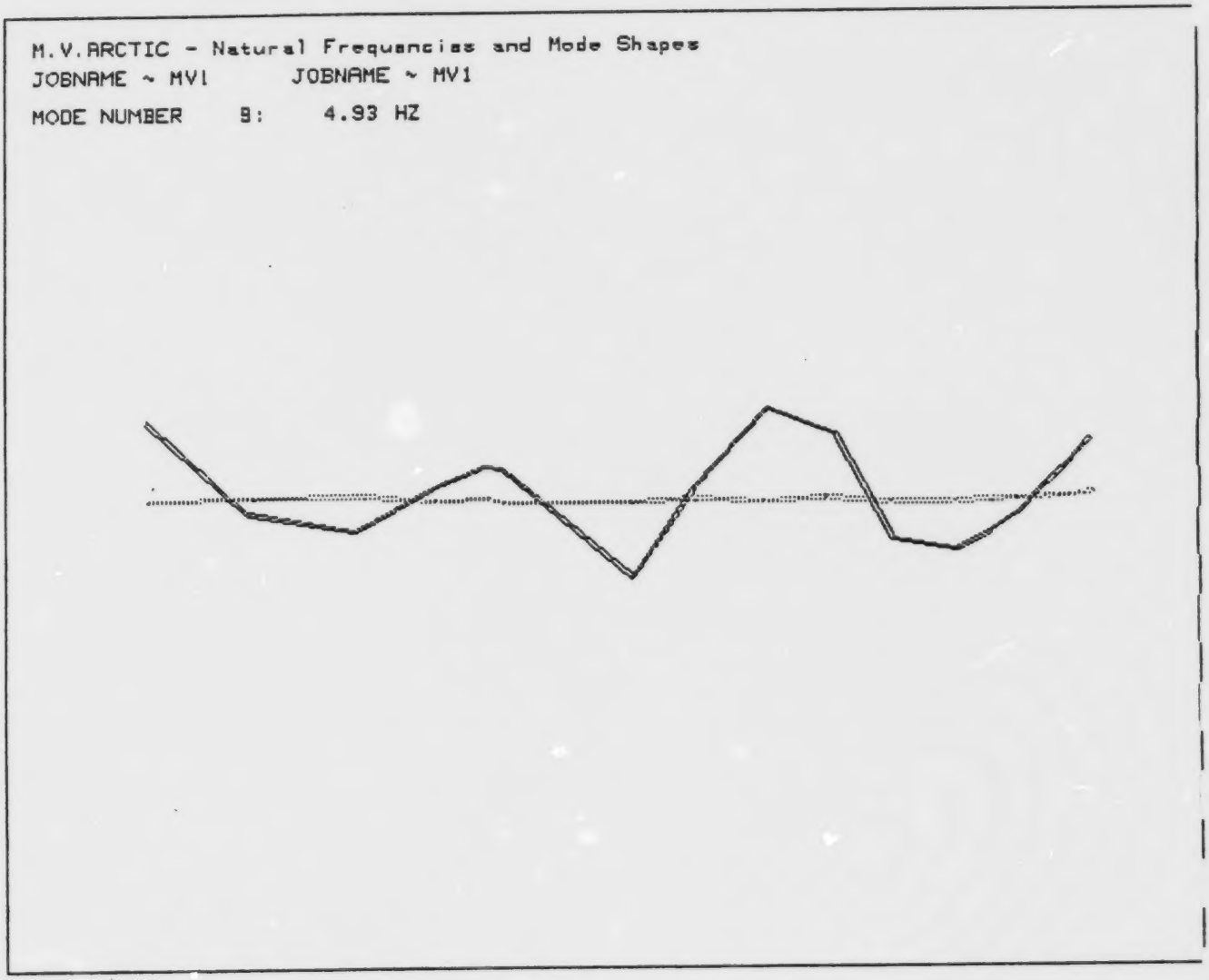


Figure A8 5TH HULL BENDING MODE

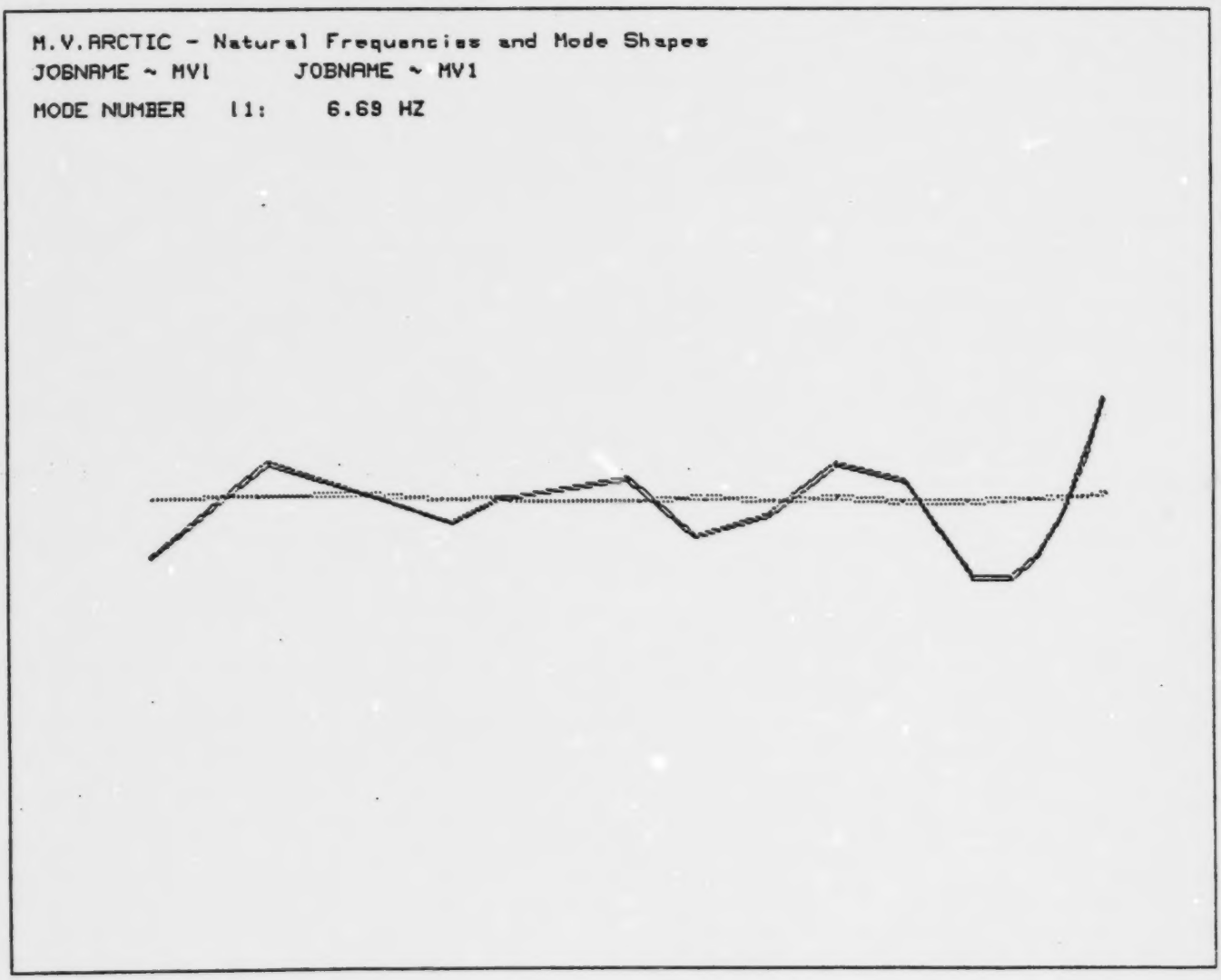


Figure A9 6TH HULL BENDING MODE

NUMBER OF ITERATIONS = 4

CALCULATED EIGENVALUES (Hz)

| | | | | | |
|---|---|---|---|---|---|
| .106 | .134 | .911 | 1.032 | 1.853 | 2.821 |
| 3.386 | 4.134 | 4.930 | 5.938 | 6.686 | 6.801 |
| 7.307 | 8.017 | 8.294 | 9.287 | 9.767 | 11.041 |
| 12.467 | 16.489 | | | | |

EQUIVALENT MASSES:

| | | | | | |
|---|---|---|---|---|---|
| 2.381E+07 | 1.114E+07 | 6.139E+06 | 4.638E+07 | 5.299E+06 | 7.352E+06 |
| 3.624E+07 | 3.148E+06 | 1.850E+07 | 2.996E+07 | 9.693E+06 | 2.629E+06 |

NODAL DISPLACEMENTS

MODE NO. 1 - M.V.ARCTIC - Natural Frequencies and Mode Shapes

NATURAL FREQUENCY = .679 rads/sec
.108 Hz (cps)

| node | x | y | z | rx | ry | rz |
|---|---|---|---|---|---|---|
| 1 | suppressed | -1.742E-01 | ---- | ---- | ---- | 6.502E-03 |
| reactions | 1.227E+05 | ---- | ---- | ---- | ---- | ---- |
| 2 | -1.448E-03 | -4.098E-02 | ---- | ---- | ---- | 6.506E-03 |
| 3 | -2.903E-03 | 9.239E-02 | ---- | ---- | ---- | 6.513E-03 |
| 5 | 3.944E-03 | 1.836E-01 | ---- | ---- | ---- | 6.518E-03 |
| 7 | 1.340E-03 | 2.488E-01 | ---- | ---- | ---- | 6.520E-03 |
| 9 | 6.561E-03 | 2.684E-01 | ---- | ---- | ---- | 6.521E-03 |
| 10 | 6.568E-03 | 4.249E-01 | ---- | ---- | ---- | 6.527E-03 |
| 12 | 2.001E-03 | 5.033E-01 | ---- | ---- | ---- | 6.531E-03 |
| 14 | 6.577E-03 | 5.882E-01 | ---- | ---- | ---- | 6.534E-03 |
| 16 | 2.000E-03 | 6.667E-01 | ---- | ---- | ---- | 6.536E-03 |
| 18 | 6.748E-03 | 7.453E-01 | ---- | ---- | ---- | 6.534E-03 |
| 19 | 6.911E-03 | 8.235E-01 | ---- | ---- | ---- | 6.533E-03 |
| 21 | 4.299E-03 | 8.692E-01 | ---- | ---- | ---- | 6.534E-03 |
| 22 | 3.645E-03 | 9.019E-01 | ---- | ---- | ---- | 6.535E-03 |
| 23 | 2.337E-03 | 9.346E-01 | ---- | ---- | ---- | 6.536E-03 |
| 24 | 1.030E-03 | 9.509E-01 | ---- | ---- | ---- | 6.536E-03 |
| 25 | 4.970E-05 | 9.673E-01 | ---- | ---- | ---- | 6.537E-03 |
| 26 | -2.567E-03 | 9.836E-01 | ---- | ---- | ---- | 6.537E-03 |
| 27 | -5.840E-03 | 1.000E+00 | ---- | ---- | ---- | 6.537E-03 |

RESIDUAL DYNAMIC REACTIONS

| Fx | Fy | Fz | Mx | My | Mz |
|---|---|---|---|---|---|
| -8.376E-02 | -1.625E+07 | 0.000E+00 | 0.000E+00 | 0.000E+00 | 0.000E+00 |

MODE NO. 2 ~ M.V.ARCTIC - Natural Frequencies and Mode Shapes

NATURAL FREQUENCY = .842 rads/sec
.134 Hz (cps)

| node | x | y | z | rx | ry | rz |
|---|---|---|---|---|---|---|
| 1 | suppressed | 1.000E+00 | ---- | ---- | ---- | -7.540E-03 |
| reactions | -2.209E+05 | ---- | ---- | ---- | ---- | ---- |
| 2 | 1.669E-03 | 8.456E-01 | ---- | ---- | ---- | -7.554E-03 |
| 3 | 3.352E-03 | 6.909E-01 | ---- | ---- | ---- | -7.593E-03 |
| 5 | -4.628E-03 | 5.848E-01 | ---- | ---- | ---- | -7.631E-03 |
| 7 | -1.584E-03 | 5.085E-01 | ---- | ---- | ---- | -7.659E-03 |
| 9 | -7.702E-03 | 4.856E-01 | ---- | ---- | ---- | -7.669E-03 |
| 10 | -7.716E-03 | 3.005E-01 | ---- | ---- | ---- | -7.751E-03 |
| 12 | -2.276E-03 | 2.071E-01 | ---- | ---- | ---- | -7.784E-03 |
| 14 | -7.752E-03 | 1.055E-01 | ---- | ---- | ---- | -7.817E-03 |
| 16 | -2.266E-03 | 1.137E-02 | ---- | ---- | ---- | -7.838E-03 |
| 18 | -7.969E-03 | -8.302E-02 | ---- | ---- | ---- | -7.855E-03 |
| 19 | -8.167E-03 | -1.775E-01 | ---- | ---- | ---- | -7.866E-03 |
| 21 | -5.016E-03 | -2.326E-01 | ---- | ---- | ---- | -7.870E-03 |
| 22 | -4.228E-03 | -2.720E-01 | ---- | ---- | ---- | -7.871E-03 |
| 23 | -2.652E-03 | -3.115E-01 | ---- | ---- | ---- | -7.873E-03 |
| 24 | -1.077E-03 | -3.312E-01 | ---- | ---- | ---- | -7.873E-03 |
| 25 | 1.049E-04 | -3.509E-01 | ---- | ---- | ---- | -7.873E-03 |
| 26 | 3.256E-03 | -3.706E-01 | ---- | ---- | ---- | -7.874E-03 |
| 27 | 7.196E-03 | -3.903E-01 | ---- | ---- | ---- | -7.874E-03 |

RESIDUAL DYNAMIC REACTIONS

| Fx | Fy | Fz | Mx | My | Mz |
|---|---|---|---|---|---|
| 5.692E-02 | -9.830E+06 | 0.000E+00 | 0.000E+00 | 0.000E+00 | 0.000E+00 |

MODE NO. 3 ~ M.V.ARCTIC - Natural Frequencies and Mode Shapes

NATURAL FREQUENCY = 5.722 rads/sec
.911 Hz (cps)

| node | x | y | z | rx | ry | rz |
|---|---|---|---|---|---|---|
| 1 | suppressed | 1.000E+00 | ---- | ---- | ---- | -1.769E-02 |
| reactions | -1.050E+08 | ---- | ---- | ---- | ---- | ---- |
| 2 | -8.616E-03 | 6.290E-01 | ---- | ---- | ---- | -1.694E-02 |
| 3 | -1.191E-02 | 2.706E-01 | ---- | ---- | ---- | -1.483E-02 |
| 5 | -3.374E-02 | 4.363E-02 | ---- | ---- | ---- | -1.249E-02 |
| 7 | -3.159E-02 | -9.269E-02 | ---- | ---- | ---- | -1.057E-02 |
| 9 | -4.236E-02 | -1.306E-01 | ---- | ---- | ---- | -9.793E-03 |
| 10 | -4.698E-02 | -3.177E-01 | ---- | ---- | ---- | -2.550E-03 |
| 12 | -5.113E-02 | -3.255E-01 | ---- | ---- | ---- | 1.081E-03 |
| 14 | -5.090E-02 | -2.702E-01 | ---- | ---- | ---- | 5.349E-03 |
| 16 | -5.863E-02 | -1.677E-01 | ---- | ---- | ---- | 8.294E-03 |
| 18 | -5.211E-02 | -2.597E-02 | ---- | ---- | ---- | 1.091E-02 |
| 19 | -5.279E-02 | 1.453E-01 | ---- | ---- | ---- | 1.275E-02 |
| 21 | -5.909E-02 | 2.504E-01 | ---- | ---- | ---- | 1.329E-02 |
| 22 | -6.082E-02 | 3.258E-01 | ---- | ---- | ---- | 1.352E-02 |
| 23 | -6.402E-02 | 4.014E-01 | ---- | ---- | ---- | 1.370E-02 |
| 24 | -6.696E-02 | 4.379E-01 | ---- | ---- | ---- | 1.374E-02 |

| | | | | | | |
|---|---|---|---|---|---|---|
| 25 | -6.917E-0 | 4.741E-01 | ---- | ---- | ---- | 1.377E-02 |
| 26 | -7.493E-02 | 5.102E-01 | ---- | ---- | ---- | 1.379E-02 |
| 27 | -8.210E-02 | 5.460E-01 | ---- | ---- | ---- | 1.380E-02 |

RESIDUAL DYNAMIC REACTIONS

| Fx | Fy | Fz | Mx | My | Mz |
|---|---|---|---|---|---|
| -7.450E-01 | -2.139E+06 | 0.000E+00 | 0.000E+00 | 0.000E+00 | 0.000E+00 |

MODE NO. 5 ~ M.V.ARCTIC - Natural Frequencies and Mode Shapes

NATURAL FREQUENCY = 11.642 rads/sec
1.853 Hz (cps)

| node | x | y | z | rx | ry | rz |
|---|---|---|---|---|---|---|
| 1 | suppressed | 1.000E+00 | ---- | ---- | ---- | -2.565E-02 |
| reactions | 2.077E+07 | ---- | ---- | ---- | ---- | ---- |
| 2 | 8.557E-03 | 4.371E-01 | ---- | ---- | ---- | -2.229E-02 |
| 3 | 1.488E-02 | -4.816E-02 | ---- | ---- | ---- | -1.431E-02 |
| 5 | 4.966E-05 | -2.632E-01 | ---- | ---- | ---- | -7.144E-03 |
| 7 | 2.696E-03 | -3.261E-01 | ---- | ---- | ---- | -2.373E-03 |
| 9 | 1.363E-03 | -3.316E-01 | ---- | ---- | ---- | -6.839E-04 |
| 10 | 1.790E-03 | -7.739E-02 | ---- | ---- | ---- | 7.048E-03 |
| 12 | -7.363E-03 | 9.915E-02 | ---- | ---- | ---- | 6.822E-03 |
| 14 | 5.680E-04 | 2.563E-01 | ---- | ---- | ---- | 3.286E-03 |
| 16 | -1.926E-03 | 3.131E-01 | ---- | ---- | ---- | -1.482E-03 |
| 18 | -4.574E-03 | 2.641E-01 | ---- | ---- | ---- | -7.843E-03 |
| 19 | -4.308E-03 | 6.106E-02 | ---- | ---- | ---- | -1.345E-02 |
| 21 | 3.723E-03 | -8.068E-02 | ---- | ---- | ---- | -1.519E-02 |
| 22 | 5.954E-03 | -1.850E-01 | ---- | ---- | ---- | -1.599E-02 |
| 23 | 1.028E-02 | -2.918E-01 | ---- | ---- | ---- | -1.660E-02 |
| 24 | 1.420E-02 | -3.412E-01 | ---- | ---- | ---- | -1.676E-02 |
| 25 | 1.714E-02 | -3.901E-01 | ---- | ---- | ---- | -1.688E-02 |
| 26 | 2.473E-02 | -4.382E-01 | ---- | ---- | ---- | -1.694E-02 |
| 27 | 3.409E-02 | -4.856E-01 | ---- | ---- | ---- | -1.697E-02 |

RESIDUAL DYNAMIC REACTIONS

| Fx | Fy | Fz | Mx | My | Mz |
|---|---|---|---|---|---|
| 1.815E+02 | -1.161E+06 | 0.000E+00 | 0.000E+00 | 0.000E+00 | 0.000E+00 |

MODE NO. 6 ~ M.V.ARCTIC - Natural Frequencies and Mode Shapes

NATURAL FREQUENCY = 17.723 rads/sec
2.821 Hz (cps)

| node | x | y | z | rx | ry | rz |
|---|---|---|---|---|---|---|
| 1 | suppressed | 1.000E+00 | ---- | ---- | ---- | -3.252E-02 |
| reactions | 8.142E+07 | ---- | ---- | ---- | ---- | ---- |
| 2 | 1.779E-02 | 2.467E-01 | ---- | ---- | ---- | -2.468E-02 |
| 3 | 2.779E-02 | -2.845E-01 | ---- | ---- | ---- | -9.062E-03 |
| 5 | 2.507E-02 | -3.374E-01 | ---- | ---- | ---- | 1.916E-03 |
| 7 | 2.074E-02 | -2.227E-01 | ---- | ---- | ---- | 6.992E-03 |
| 9 | 3.238E-02 | -1.728E-01 | ---- | ---- | ---- | 8.300E-03 |

| | | | | | | |
|---|---|---|---|---|---|---|
| 10 | 2.369E-02 | 4.423E-01 | ---- | ---- | ---- | 3.872E-03 |
| 12 | 1.650E-02 | 4.159E-01 | ---- | ---- | ---- | -3.528E-03 |
| 14 | -3.613E-03 | 1.305E-01 | ---- | ---- | ---- | -8.715E-03 |
| 16 | 4.475E-03 | -1.751E-01 | ---- | ---- | ---- | -6.973E-03 |
| 18 | -1.434E-02 | -3.837E-01 | ---- | ---- | ---- | 1.350E-03 |
| 19 | -2.033E-02 | -2.053E-01 | ---- | ---- | ---- | 1.140E-02 |
| 21 | -3.193E-02 | -4.130E-02 | ---- | ---- | ---- | 1.481E-02 |
| 22 | -3.608E-02 | 8.626E-02 | ---- | ---- | ---- | 1.645E-02 |
| 23 | -4.277E-02 | 2.221E-01 | ---- | ---- | ---- | 1.773E-02 |
| 24 | -4.792E-02 | 2.835E-01 | ---- | ---- | ---- | 1.810E-02 |
| 25 | -5.183E-02 | 3.441E-01 | ---- | ---- | ---- | 1.835E-02 |
| 26 | -6.124E-02 | 4.029E-01 | ---- | ---- | ---- | 1.849E-02 |
| 27 | -7.266E-02 | 4.605E-01 | ---- | ---- | ---- | 1.856E-02 |

RESIDUAL DYNAMIC REACTIONS

| Fx | Fy | Fz | Mx | My | Mz |
|---|---|---|---|---|---|
| 9.683E+02 | -1.129E+06 | 0.000E+00 | 0.000E+00 | 0.000E+00 | 0.000E+00 |

MODE NO. 8 ~ M.V.ARCTIC - Natural Frequencies and Mode Shapes

NATURAL FREQUENCY = 25.974 rads/sec
4.134 Hz (cps)

| node | x | y | z | rx | ry | rz |
|---|---|---|---|---|---|---|
| 1 | suppressed | 1.000E+00 | ---- | ---- | ---- | -4.133E-02 |
| reactions | -1.705E+08 | ---- | ---- | ---- | ---- | ---- |
| 2 | -9.859E-03 | -3.286E-02 | ---- | ---- | ---- | -2.459E-02 |
| 3 | -1.586E-02 | -4.642E-01 | ---- | ---- | ---- | -5.706E-04 |
| 5 | 1.553E-03 | -1.066E-01 | ---- | ---- | ---- | 7.947E-03 |
| 7 | -1.230E-02 | 2.009E-01 | ---- | ---- | ---- | 6.263E-03 |
| 9 | 3.588E-03 | 2.762E-01 | ---- | ---- | ---- | 4.423E-03 |
| 10 | -5.258E-03 | 3.888E-02 | ---- | ---- | ---- | -4.725E-03 |
| 12 | 1.381E-03 | -1.543E-01 | ---- | ---- | ---- | -3.694E-03 |
| 14 | -4.863E-03 | -2.066E-01 | ---- | ---- | ---- | 7.539E-04 |
| 16 | -1.385E-02 | -7.932E-02 | ---- | ---- | ---- | 3.272E-03 |
| 18 | -5.105E-03 | 1.142E-01 | ---- | ---- | ---- | 1.856E-03 |
| 19 | -4.774E-03 | 1.006E-01 | ---- | ---- | ---- | -2.157E-03 |
| 21 | -2.012E-03 | 5.380E-02 | ---- | ---- | ---- | -3.775E-03 |
| 22 | -9.635E-04 | 1.129E-02 | ---- | ---- | ---- | -4.622E-03 |
| 23 | 1.164E-03 | -3.844E-02 | ---- | ---- | ---- | -5.326E-03 |
| 24 | 3.008E-03 | -6.139E-02 | ---- | ---- | ---- | -5.541E-03 |
| 25 | 4.418E-03 | -8.412E-02 | ---- | ---- | ---- | -5.686E-03 |
| 26 | 7.806E-03 | -1.059E-01 | ---- | ---- | ---- | -5.769E-03 |
| 27 | 1.189E-02 | -1.270E-01 | ---- | ---- | ---- | -5.806E-03 |

RESIDUAL DYNAMIC REACTIONS

| Fx | Fy | Fz | Mx | My | Mz |
|---|---|---|---|---|---|
| 2.449E+04 | 6.473E+05 | 0.000E+00 | 0.000E+00 | 0.000E+00 | 0.000E+00 |

MODE NO. 9 ~ M.V.ARCTIC - Natural Frequencies and Mode Shapes

NATURAL FREQUENCY = 30.973 rads/sec
4.930 Hz (cps)

| node | x | y | z | rx | ry | rz |
|---|---|---|---|---|---|---|
| 1 | suppressed | 8.401E-01 | ---- | ---- | ---- | -3.840E-02 |
| reactions | -5.033E+08 | ---- | ---- | ---- | ---- | ---- |
| 2 | -5.039E-02 | -1.680E-01 | ---- | ---- | ---- | -1.859E-02 |
| 3 | -7.347E-02 | -3.697E-01 | ---- | ---- | ---- | 3.337E-03 |
| 5 | -4.271E-02 | 1.407E-01 | ---- | ---- | ---- | 5.497E-03 |
| 7 | -4.510E-02 | 3.458E-01 | ---- | ---- | ---- | -4.437E-04 |
| 9 | -3.803E-02 | 3.696E-01 | ---- | ---- | ---- | -3.362E-03 |
| 10 | 4.425E-03 | -7.945E-01 | ---- | ---- | ---- | 8.904E-03 |
| 12 | -2.156E-02 | 1.076E-01 | ---- | ---- | ---- | 1.891E-02 |
| 14 | 4.568E-02 | 1.000E+00 | ---- | ---- | ---- | 5.476E-03 |
| 16 | 7.603E-02 | 6.899E-01 | ---- | ---- | ---- | -1.132E-02 |
| 18 | 2.365E-02 | -3.964E-01 | ---- | ---- | ---- | -1.094E-02 |
| 19 | 1.631E-02 | -5.136E-01 | ---- | ---- | ---- | 6.867E-03 |
| 21 | 2.726E-03 | -3.387E-01 | ---- | ---- | ---- | 1.536E-02 |
| 22 | -3.662E-03 | -1.479E-01 | ---- | ---- | ---- | 2.014E-02 |
| 23 | -1.602E-02 | 9.725E-02 | ---- | ---- | ---- | 2.433E-02 |
| 24 | -2.606E-02 | 2.167E-01 | ---- | ---- | ---- | 2.567E-02 |
| 25 | -3.386E-02 | 3.355E-01 | ---- | ---- | ---- | 2.657E-02 |
| 26 | -5.177E-02 | 4.492E-01 | ---- | ---- | ---- | 2.709E-02 |
| 27 | -7.311E-02 | 5.587E-01 | ---- | ---- | ---- | 2.732E-02 |

RESIDUAL DYNAMIC REACTIONS

| Fx | Fy | Fz | Mx | My | Mz |
|---|---|---|---|---|---|
| 5.461E+05 | -5.205E+05 | 0.000E+00 | 0.000E+00 | 0.000E+00 | 0.000E+00 |

MODE NO. 11 ~ M.V.ARCTIC - Natural Frequencies and Mode Shapes

NATURAL FREQUENCY = 42.009 rads/sec
6.686 Hz (cps)

| node | x | y | z | rx | ry | rz |
|---|---|---|---|---|---|---|
| 1 | suppressed | -6.404E-01 | ---- | ---- | ---- | 3.339E-02 |
| reactions | 9.609E+08 | ---- | ---- | ---- | ---- | ---- |
| 2 | 1.060E-01 | 3.533E-01 | ---- | ---- | ---- | 5.559E-03 |
| 3 | 1.386E-01 | -5.056E-02 | ---- | ---- | ---- | -5.136E-03 |
| 5 | 8.705E-02 | -2.427E-01 | ---- | ---- | ---- | 1.211E-03 |
| 7 | 3.502E-02 | -1.055E-02 | ---- | ---- | ---- | 3.803E-03 |
| 9 | 3.139E-02 | 4.662E-02 | ---- | ---- | ---- | 3.606E-03 |
| 10 | -1.241E-01 | 2.405E-01 | ---- | ---- | ---- | -5.447E-03 |
| 12 | -9.725E-02 | -4.225E-01 | ---- | ---- | ---- | -3.136E-03 |
| 14 | -4.932E-02 | -1.413E-01 | ---- | ---- | ---- | 6.446E-03 |
| 16 | -2.762E-02 | 3.601E-01 | ---- | ---- | ---- | 4.198E-03 |
| 18 | 2.352E-02 | 2.217E-01 | ---- | ---- | ---- | -3.516E-03 |
| 19 | 6.290E-02 | -8.125E-01 | ---- | ---- | ---- | 8.067E-03 |
| 21 | 7.849E-02 | -8.372E-01 | ---- | ---- | ---- | 2.333E-02 |
| 22 | 8.156E-02 | -6.086E-01 | ---- | ---- | ---- | 3.461E-02 |
| 23 | 6.911E-02 | -1.522E-01 | ---- | ---- | ---- | 4.644E-02 |
| 24 | 4.705E-02 | 1.404E-01 | ---- | ---- | ---- | 5.066E-02 |
| 25 | 2.943E-02 | 4.395E-01 | ---- | ---- | ---- | 5.356E-02 |
| 26 | -1.342E-02 | 7.256E-01 | ---- | ---- | ---- | 5.524E-02 |
| 27 | -6.473E-02 | 1.000E+00 | ---- | ---- | ---- | 5.600E-02 |

RESIDUAL DYNAMIC REACTIONS

| Fx | Fy | Fz | Mx | My | Mz |
|---|---|---|---|---|---|
| 2.502E+06 | 1.968E+06 | 0.000E+00 | 0.000E+00 | 0.000E+00 | 0.000E+00 |

[illegible] - [illegible]
[illegible]

NODAL MOMENT FOR PLASTIC NODES

NODE NUMBERS SELECTED
1 2 3 5 6 8 9 11

NODE 1
0.000E+00 0.000E+00 0.000E+00 0.000E+00 0.000E+00 0.000E+00
0.000E+00 0.000E+00

NODE 2
-2.774E+00 1.439E+09 -4.301E+08 -1.100E+09 -4.809E+09 -9.001E+09
-1.705E+10 1.029E+10

NODE 3
-9.033E+00 3.714E+07 -2.036E+09 -7.369E+09 -1.309E+10 -1.831E+10
-1.951E+10 -3.765E+09

NODE 5
-4.500E+00 5.119E+07 -3.640E+09 -1.061E+10 -1.383E+10 -9.045E+09
[illegible] -1.214E-10

NODE 6
[illegible]

NODE 8
[illegible]

NODE 9
[illegible]

NODE 11
[illegible]

NODE 14
[illegible]

NODE 15
[illegible]

NODE 16
[illegible]

NODE 19
-3.000E+00 1.533E+07 -2.315E+09 7.429E+09 -1.428E+10 0.000E+00
-3.220E+10 -4.550E+10

[illegible] 27

-5.[illegible]E+00 1.[illegible]E+[illegible] -1.[illegible]E+[illegible] [illegible] -5.[illegible]E+05 -[illegible]

-2.[illegible]E+10 -5.[illegible]E+10

[illegible] 22

-4.[illegible]E+[illegible] 5.51[illegible]E+00 -[illegible].[illegible]E+00 [illegible] -[illegible].[illegible]E+05 [illegible]

-1.[illegible]E+10 -5.[illegible]E+10

[illegible] 23

-1.[illegible]E+00 [illegible].[illegible]E+00 -4.104E+00 1.468E+05 -[illegible].[illegible]E+05 [illegible]

-1.[illegible]E+10 -[illegible].[illegible]E+10

[illegible] 24

-2.[illegible]E+00 2.[illegible]E+00 -2.[illegible]E+00 [illegible] -2.[illegible]E+05 [illegible]

-[illegible].[illegible]E+05 -[illegible].[illegible]E+10

[illegible] 25

-2.[illegible]E+00 1.[illegible]E+00 -1.[illegible]E+00 [illegible] -1.[illegible]E+05 [illegible]

-[illegible].[illegible]E+05 -1.[illegible]E+10

[illegible] 26

-1.[illegible]E+00 1.[illegible]E+00 -[illegible].[illegible]E+[illegible] [illegible] -[illegible].[illegible]E+[illegible] [illegible]

-2.[illegible]E+[illegible] -[illegible].[illegible]E+[illegible]

[illegible] 27

[illegible] [illegible] [illegible] [illegible] [illegible] [illegible]

[illegible] [illegible]

## APPENDIX B

### Distribution of Mass to the Nodal Points

A program was written to lump the different masses at the nodal points. The masses distributed consisted of:

* Structural mass
* Deck equipment mass
* Non-structural added mass
* Fluid added mass

For each specified mass, whether concentrated or distributed, the program identified all the spans to which it contributes. The equivalent nodal masses were then weighted based on the location of the mass within the span. The different weightings were as follows:

* For a concentrated mass M

$$M(N1) = M \frac{r - x_1}{x_2 - x_1}$$

$$M(N2) = M \frac{x_2 - r}{x_2 - x_1}$$

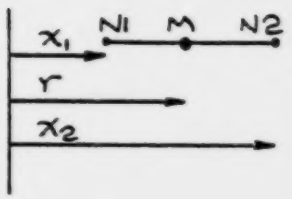


* For a distributed mass

$$M(N1) = \frac{M_1}{x_2 - x_1}\left[r_2 x_2 - \frac{r_1 + r_2}{2}(r_2 + x_2) + \frac{1}{3}(r_2^2 + r_1 r_2 + r_1^2)\right]$$

$$- \frac{M_2}{x_2 - x_1}\left[r_1 x_2 - \frac{r_1 + r_2}{2}(r_1 + x_2) + \frac{1}{3}(r_1^2 + r_1 r_2 + r_2^2)\right]$$

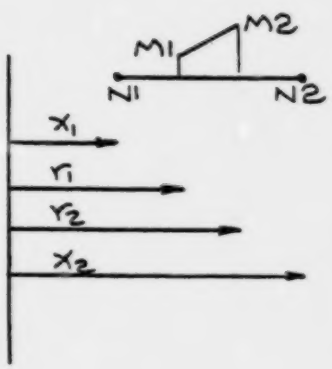

$$M(N2) = \frac{-M_1}{x_2 - x_1}\left[r_2 x_1 - \frac{r_1 + r_2}{2}(r_2 + x_1) + \frac{1}{3}(r_1^2 + r_1 r_2 + r_2^2)\right]$$

$$+ \frac{M_2}{x_2 - x_1}\left[r_1 x_1 - \frac{r_1 + r_2}{2}(r_1 + x_1) + \frac{1}{3}(r_1^2 + r_1 r_2 + r_2^2\right]$$

Plots of the weight distribution on the ship and the distribution of the added mass follow. In addition, the output from the program is also enclosed.

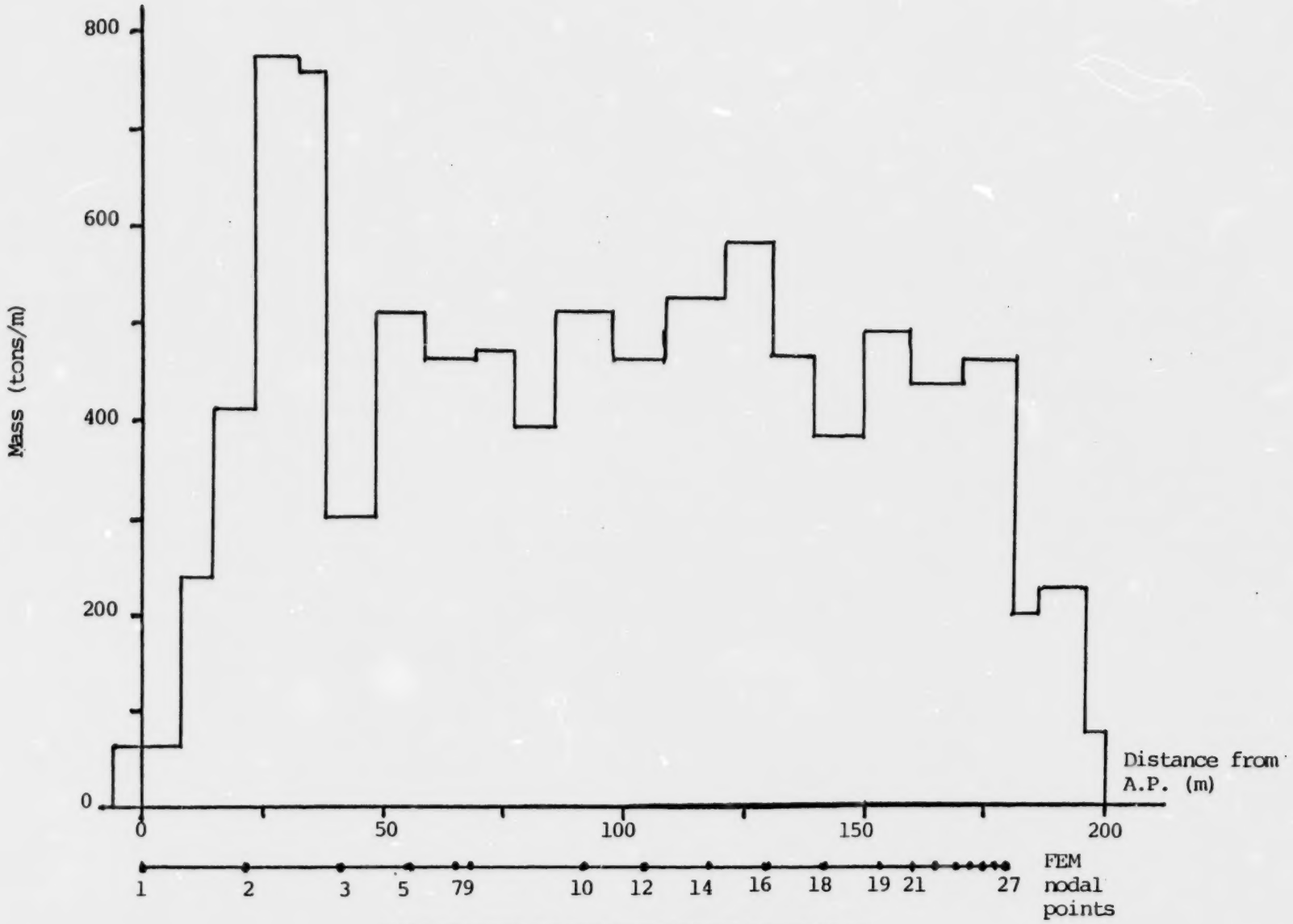


DISTRIBUTION OF NON-STRUCTURAL ADDED MASS

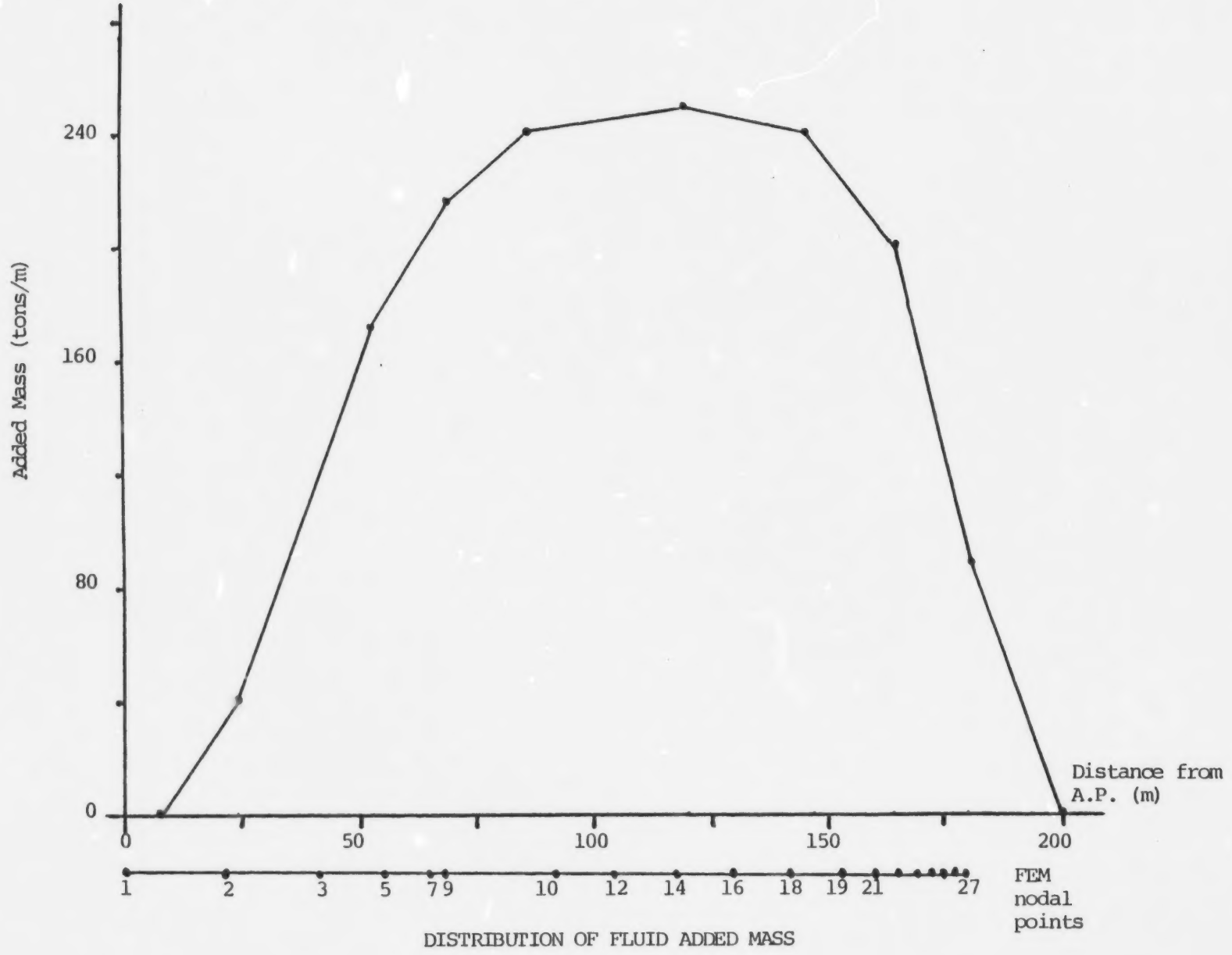


DISTRIBUTION OF FLUID ADDED MASS

********** DISCRETE MASSES **********

| MASS | COORDINATE | N1 | W1 | N2 | W2 |
|---|---|---|---|---|---|
| 51 | 35.970 | 2 | 12.514 | 3 | 38.486 |
| 55 | 57.300 | 4 | 42.350 | 5 | 12.650 |
| 56 | 75.590 | 6 | 38.290 | 7 | 17.710 |
| 56 | 96.320 | 7 | 35.840 | 8 | 20.160 |
| 56 | 119.480 | 9 | 44.427 | 10 | 11.573 |
| 56 | 137.770 | 10 | 15.073 | 11 | 40.927 |
| 55 | 158.500 | 12 | 11.786 | 13 | 43.214 |

WARNING : MASS OUTSIDE MODEL LIMITS - MASS IGNORED = 51 @ X=180.44

| | | | | | |
|---|---|---|---|---|---|
| 3200 | 168.955 | 14 | 668.800 | 15 | 2531.200 |
| 8410 | 139.315 | 10 | 1180.904 | 11 | 7229.096 |
| 2886 | 108.345 | 8 | 1921.410 | 9 | 964.590 |
| 8474 | 77.155 | 6 | 5241.522 | 7 | 3232.478 |
| 3130 | 46.995 | 3 | 1789.689 | 4 | 1340.311 |
| 69 | 34.055 | 2 | 23.376 | 3 | 45.624 |
| 90 | 27.515 | 2 | 59.202 | 3 | 30.798 |
| 35 | 29.275 | 2 | 20.018 | 3 | 14.982 |
| 54 | 25.645 | 2 | 40.447 | 3 | 13.553 |
| 121 | 33.955 | 2 | 41.583 | 3 | 79.417 |
| 8 | 23.165 | 2 | 6.960 | 3 | 1.040 |
| 10 | 21.945 | 2 | 9.295 | 3 | .705 |
| 20 | 168.245 | 14 | 7.020 | 15 | 12.980 |
| 20 | 148.055 | 11 | 8.242 | 12 | 11.758 |
| 20 | 128.245 | 9 | 1.258 | 10 | 18.742 |
| 20 | 107.515 | 8 | 14.592 | 9 | 5.408 |
| 20 | 85.985 | 6 | 5.013 | 7 | 14.988 |
| 20 | 66.165 | 5 | 12.233 | 6 | 7.767 |
| 20 | 47.185 | 3 | 11.164 | 4 | 8.836 |
| 16 | 22.255 | 2 | 14.630 | 3 | 1.370 |
| 15 | 25.605 | 2 | 11.265 | 3 | 3.735 |
| 59 | 24.445 | 2 | 47.646 | 3 | 11.354 |
| 51 | 6.095 | 1 | 35.837 | 2 | 15.163 |
| 150 | 19.295 | 1 | 8.817 | 2 | 141.183 |

WARNING : MASS OUTSIDE MODEL LIMITS - MASS IGNORED = 100 @ X=188.30

---

********** UNIFORMLY DISTRIBUTED MASSES **********

| MASS | X1 | X2 | N1 | W1 | N2 | W2 |
|---|---|---|---|---|---|---|

WARNING : R1 < CMIN - SET R1=CMIN - MASS IGNORED = 62.00
R1 : -6.810 - R2 : 0.000

WARNING : NEW LIMITS MAKE R1=R1

| | | | | | | |
|---|---|---|---|---|---|---|
| 235 | 0.000 | 7.320 | 1 | 193.044 | 2 | 41.956 |
| 411 | 7.320 | 13.410 | 1 | 203.194 | 2 | 207.806 |
| 775 | 13.410 | 22.560 | 1 | 103.846 | 2 | 496.673 |
| 775 | 13.410 | 22.560 | 2 | 165.714 | 3 | 8.767 |

| | | | | | | |
|---|---|---|---|---|---|---|
| 759 | 22.560 | 31.090 | 2 | 524.821 | 3 | 234.179 |
| 297 | 31.090 | 36.580 | 2 | 103.805 | 3 | 193.195 |
| 508 | 36.580 | 47.550 | 2 | 22.066 | 3 | 182.616 |
| 508 | 36.580 | 47.550 | 3 | 232.363 | 4 | 70.955 |
| 462 | 47.550 | 57.300 | 3 | 93.927 | 4 | 259.088 |
| 462 | 47.550 | 57.300 | 4 | 96.451 | 5 | 12.533 |
| 470 | 57.300 | 67.060 | 4 | 142.758 | 5 | 228.041 |
| 470 | 57.300 | 67.060 | 5 | 65.142 | 6 | 34.059 |
| 392 | 67.060 | 75.590 | 5 | 6.768 | 6 | 36.430 |
| 392 | 67.060 | 75.590 | 6 | 293.648 | 7 | 55.154 |
| 513 | 75.590 | 84.120 | 6 | 259.599 | 7 | 253.401 |
| 462 | 84.120 | 96.320 | 6 | 48.988 | 7 | 249.418 |
| 462 | 84.120 | 96.320 | 7 | 134.147 | 8 | 29.447 |
| 523 | 96.320 | 107.290 | 7 | 117.167 | 8 | 248.980 |
| 523 | 96.320 | 107.290 | 8 | 137.004 | 9 | 19.848 |
| 582 | 107.290 | 119.480 | 8 | 173.135 | 9 | 290.460 |
| 582 | 107.290 | 119.480 | 9 | 106.170 | 10 | 12.235 |
| 463 | 119.480 | 129.240 | 9 | 179.141 | 10 | 272.474 |
| 463 | 119.480 | 129.240 | 10 | 11.271 | 11 | .114 |
| 382 | 129.240 | 137.770 | 10 | 238.591 | 11 | 143.409 |
| 487 | 137.770 | 148.740 | 10 | 19.298 | 11 | 124.094 |
| 487 | 137.770 | 148.740 | 11 | 232.794 | 12 | 110.814 |
| 434 | 148.740 | 158.500 | 11 | 33.624 | 12 | 155.806 |
| 434 | 148.740 | 158.500 | 12 | 148.489 | 13 | 96.081 |
| 458 | 158.500 | 169.470 | 12 | 6.710 | 13 | 55.915 |
| 458 | 158.500 | 169.470 | 13 | 104.376 | 14 | 104.376 |
| 458 | 158.500 | 169.470 | 14 | 103.203 | 15 | 83.421 |

WARNING : R2 > CMAX - SET R2=CMAX - MASS IGNORED = 16.08
R1 : 169.470 - R2 : 180.440

| | | | | | | |
|---|---|---|---|---|---|---|
| 401 | 169.470 | 180.000 | 14 | 1.027 | 15 | 18.347 |
| 401 | 169.470 | 180.000 | 15 | 45.693 | 16 | 45.693 |
| 401 | 169.470 | 180.000 | 16 | 45.693 | 17 | 45.693 |
| 401 | 169.470 | 180.000 | 17 | 45.693 | 18 | 45.693 |
| 401 | 169.470 | 180.000 | 18 | 45.693 | 19 | 45.693 |

WARNING : MASS OUTSIDE MODEL LIMITS - MASS IGNORED
197 180.440 186.540

WARNING : MASS OUTSIDE MODEL LIMITS - MASS IGNORED
227 186.540 196.600

WARNING : MASS OUTSIDE MODEL LIMITS - MASS IGNORED
74 196.600 200.250

---

********** GENERAL DISTRIBUTED MASSES **********

| M1 | M2 | X1 | X2 | N1 | W1 | N2 | W2 |
|---|---|---|---|---|---|---|---|
| 7 | 40 | 0.000 | 24.000 | 1 | 168.057 | 2 | 264.365 |
| 7 | 40 | 0.000 | 24.000 | 2 | 120.106 | 3 | 11.472 |
| 40 | 172 | 24.000 | 53.000 | 2 | 463.761 | 3 | 873.963 |
| 40 | 172 | 24.000 | 53.000 | 3 | 945.340 | 4 | 790.936 |
| 172 | 216 | 53.000 | 70.000 | 3 | 24.818 | 4 | 324.359 |
| 172 | 216 | 53.000 | 70.000 | 4 | 929.020 | 5 | 972.157 |
| 172 | 216 | 53.000 | 70.000 | 5 | 308.471 | 6 | 312.353 |
| 172 | 216 | 53.000 | 70.000 | 6 | 408.967 | 7 | 17.856 |

| | | | | | | | |
|---|---|---|---|---|---|---|---|
| 216 | 240 | 70.000 | 87.000 | 6 | 2156.167 | 7 | 1719.833 |
| 240 | 250 | 87.000 | 120.000 | 6 | 125.263 | 7 | 1078.525 |
| 240 | 250 | 87.000 | 120.000 | 7 | 1456.364 | 8 | 1463.636 |
| 240 | 250 | 87.000 | 120.000 | 8 | 1602.020 | 9 | 1610.556 |
| 240 | 250 | 87.000 | 120.000 | 9 | 655.000 | 10 | 93.636 |
| 250 | 240 | 120.000 | 147.000 | 9 | 840.000 | 10 | 1395.000 |
| 250 | 240 | 120.000 | 147.000 | 10 | 1471.111 | 11 | 1462.222 |
| 250 | 240 | 120.000 | 147.000 | 11 | 1085.556 | 12 | 361.111 |
| 240 | 200 | 147.000 | 164.000 | 11 | 352.941 | 12 | 1044.706 |
| 240 | 200 | 147.000 | 164.000 | 12 | 771.373 | 13 | 752.157 |
| 240 | 200 | 147.000 | 164.000 | 13 | 493.804 | 14 | 325.020 |
| 200 | 88 | 164.000 | 180.000 | 13 | 19.767 | 14 | 176.733 |
| 200 | 88 | 164.000 | 180.000 | 14 | 453.333 | 15 | 424.167 |
| 200 | 88 | 164.000 | 180.000 | 15 | 190.208 | 16 | 182.917 |
| 200 | 88 | 164.000 | 180.000 | 16 | 168.333 | 17 | 161.042 |
| 200 | 88 | 164.000 | 180.000 | 17 | 146.458 | 18 | 139.167 |
| 200 | 88 | 164.000 | 180.000 | 18 | 124.583 | 19 | 117.292 |

WARNING : R2 > CMAX ~ SET R2=CMAX ~ MASS IGNORED = 880.00
R1 : 180.000 ~ R2 : 200.000

WARNING : NEW LIMITS MAKE R1=R2

---

TOTAL MASS ENTERED IS 69464.00
TOTAL MASS DISTRIBUTED IS 67856.92
TOTAL MASS IGNORED IS 1607.08

NODAL MASSES :

| NODE | COORDINATE | MASS |
|---|---|---|
| 1 | 0.00 | 712.80 |
| 2 | 20.50 | 2854.36 |
| 3 | 41.00 | 4842.56 |
| 4 | 55.00 | 4005.06 |
| 5 | 65.00 | 1618.00 |
| 6 | 68.00 | 8968.07 |
| 7 | 92.00 | 8382.88 |
| 8 | 104.00 | 5610.39 |
| 9 | 117.00 | 4716.86 |
| 10 | 129.00 | 4739.91 |
| 11 | 141.00 | 10713.02 |
| 12 | 153.00 | 2622.55 |
| 13 | 160.00 | 1565.31 |
| 14 | 165.00 | 1839.51 |
| 15 | 170.00 | 3306.02 |
| 16 | 172.50 | 442.64 |
| 17 | 175.00 | 398.89 |
| 18 | 177.50 | 355.14 |
| 19 | 180.00 | 162.98 |

---

## APPENDIX C

### Spring Stiffnesses due to the Buoyancy Forces

The displacement of the ship from its equilibrium position is resisted by the change in buoyancy forces due to that displacement. This behaviour can be modeled by supporting the ship on a series of grounded springs. The spring stiffness can be generated using the relationship

$$K_i = \int_{x_1}^{x_2} \rho g \frac{dA}{dI} \, dx$$

where
- $\rho$ = density of water = 1000 kg/m$^3$
- $g$ = gravity acceleration = 9.81 m/sec
- $\frac{dA}{dI}$ = rate of change of cross-sectional area with draught
- $x_1$, $x_2$ = span which contributes to the node i under consideration.

A plot of the variation of $\frac{dA}{dI}$ along the length of the ship is shown. The slopes were calculated from the bonjean curves at the various stations. The 11m draught line was used to evaluate the slope for each station. A linear distribution between stations was assumed.

Finally, the distributed stiffness was lumped to the appropriate nodal points using the same technique and weighting factors described in Appendix B. The output from the program and the various bonjean curves follow.

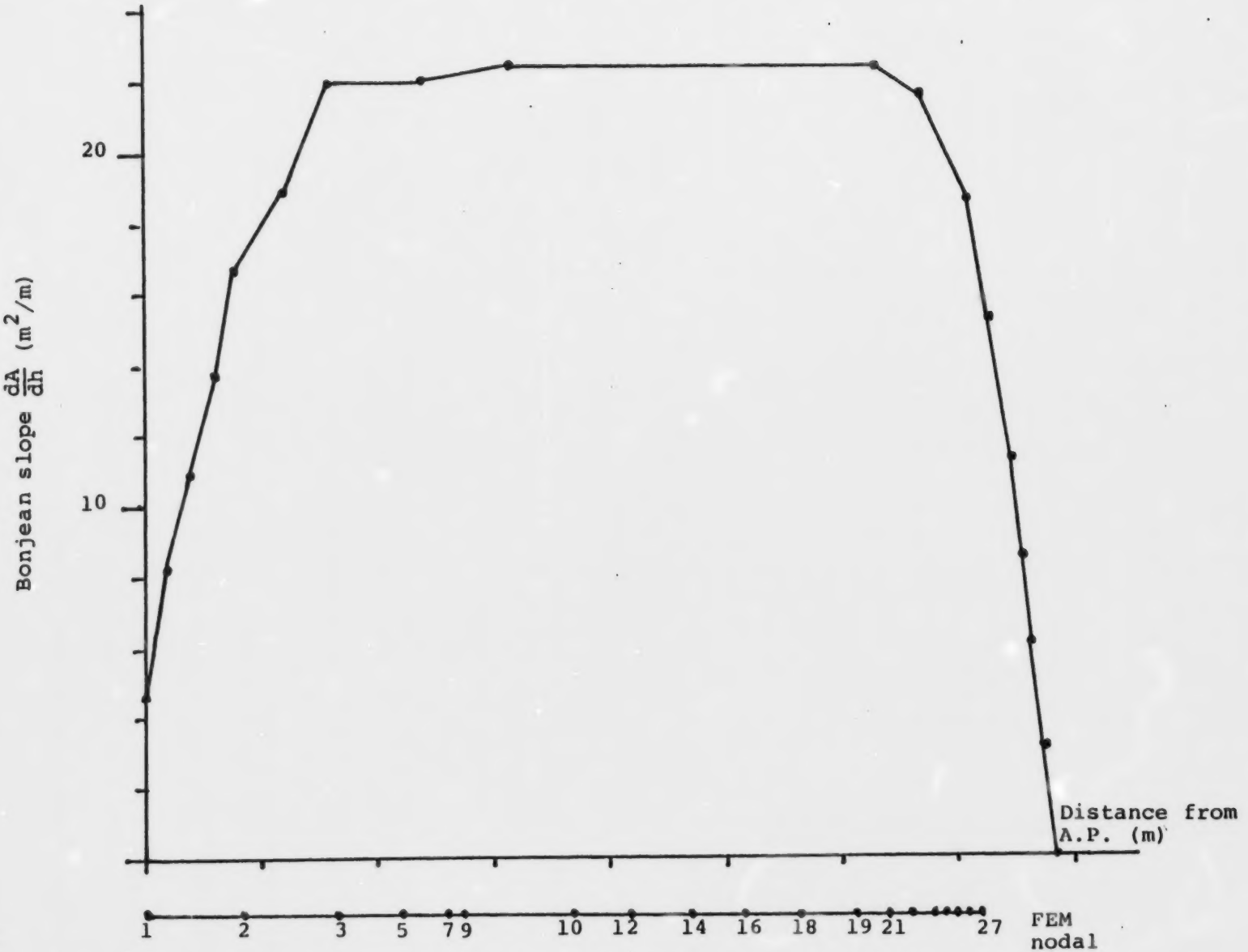


Longitudinal variation of bonjean slope at the 11m draught.

| | | | | | | | |
|---|---|---|---|---|---|---|---|
| 5 | 8 | 0.000 | 4.915 | 1 | 27.452 | 2 | 4.137 |
| 8 | 11 | 4.915 | 9.829 | 1 | 29.782 | 2 | 17.134 |
| 11 | 14 | 9.829 | 14.744 | 1 | 23.987 | 2 | 36.588 |
| 14 | 17 | 14.744 | 19.659 | 1 | 11.762 | 2 | 63.140 |
| 17 | 19 | 19.659 | 29.488 | 1 | .289 | 2 | 13.848 |
| 17 | 19 | 19.659 | 29.488 | 2 | 125.219 | 3 | 36.027 |
| 19 | 22 | 29.488 | 39.318 | 2 | 63.617 | 3 | 137.765 |
| 22 | 22 | 39.318 | 58.977 | 2 | 1.518 | 3 | 35.489 |
| 22 | 22 | 39.318 | 58.977 | 3 | 154.097 | 4 | 154.169 |
| 22 | 22 | 39.318 | 58.977 | 4 | 70.218 | 5 | 17.430 |
| 22 | 23 | 58.977 | 78.636 | 4 | 40.070 | 5 | 93.131 |
| 22 | 23 | 58.977 | 78.636 | 5 | 33.317 | 6 | 33.353 |
| 22 | 23 | 58.977 | 78.636 | 6 | 185.250 | 7 | 52.862 |
| 23 | 23 | 78.636 | 157.272 | 6 | 83.773 | 7 | 217.118 |
| 23 | 23 | 78.636 | 157.272 | 7 | 135.090 | 8 | 135.090 |
| 23 | 23 | 78.636 | 157.272 | 8 | 146.348 | 9 | 146.348 |
| 23 | 23 | 78.636 | 157.272 | 9 | 135.090 | 10 | 135.090 |
| 23 | 23 | 78.636 | 157.272 | 10 | 135.090 | 11 | 135.090 |
| 23 | 23 | 78.636 | 157.272 | 11 | 135.090 | 12 | 135.090 |
| 23 | 23 | 78.636 | 157.272 | 12 | 66.834 | 13 | 29.350 |
| 23 | 22 | 157.272 | 167.101 | 12 | 11.932 | 13 | 49.206 |
| 23 | 22 | 157.272 | 167.101 | 13 | 55.451 | 14 | 55.134 |
| 23 | 22 | 157.272 | 167.101 | 14 | 36.269 | 15 | 9.632 |
| 22 | 19 | 167.101 | 176.931 | 14 | 18.038 | 15 | 43.743 |
| 22 | 19 | 167.101 | 176.931 | 15 | 25.742 | 16 | 25.414 |
| 22 | 19 | 167.101 | 176.931 | 16 | 24.759 | 17 | 24.432 |
| 22 | 19 | 167.101 | 176.931 | 17 | 22.571 | 18 | 14.079 |

WARNING : R2 > CMAX ~ SET R2=CMAX ~ MASS IGNORED = 29.45
R1 : 176.931 ~ R2 : 181.846

| | | | | | | | |
|---|---|---|---|---|---|---|---|
| 19 | 17 | 176.931 | 180.000 | 17 | 1.201 | 18 | 9.315 |
| 19 | 17 | 176.931 | 180.000 | 18 | 22.148 | 19 | 21.437 |

WARNING : R2 > CMAX ~ SET R2=CMAX ~ MASS IGNORED = 94.25
R1 : 180.000 ~ R2 : 186.760

WARNING : NEW LIMITS MAKE R1=R2

WARNING : R2 > CMAX ~ SET R2=CMAX ~ MASS IGNORED = 115.88
R1 : 180.000 ~ R2 : 189.218

WARNING : NEW LIMITS MAKE R1=R2

WARNING : R2 > CMAX ~ SET R2=CMAX ~ MASS IGNORED = 132.74
R1 : 180.000 ~ R2 : 191.675

WARNING : NEW LIMITS MAKE R1=R2

WARNING : R2 > CMAX ~ SET R2=CMAX ~ MASS IGNORED = 139.51
R1 : 180.000 ~ R2 : 194.133

WARNING : NEW LIMITS MAKE R1=R2

WARNING : R2 > CMAX ~ SET R2=CMAX ~ MASS IGNORED = 137.54
R1 : 180.000 ~ R2 : 196.590

WARNING : NEW LIMITS MAKE R1=R2

TOTAL STIFFNESS ENTERED IS 4352.02
TOTAL STIFFNESS DISTRIBUTED IS 3702.64
TOTAL STIFFNESS IGNORED IS 649.37

NODAL STIFFNESSES :

| NODE | COORDINATE | STIFFNESS |
|---|---|---|
| 1 | 0.00 | 93.27 |
| 2 | 20.50 | 325.20 |
| 3 | 41.00 | 363.38 |
| 4 | 55.00 | 264.46 |
| 5 | 65.00 | 143.88 |
| 6 | 68.00 | 302.38 |
| 7 | 92.00 | 405.07 |
| 8 | 104.00 | 281.44 |
| 9 | 117.00 | 281.44 |
| 10 | 129.00 | 270.18 |
| 11 | 141.00 | 270.18 |
| 12 | 153.00 | 213.86 |
| 13 | 160.00 | 134.01 |
| 14 | 165.00 | 109.44 |
| 15 | 170.00 | 79.12 |
| 16 | 172.50 | 50.17 |
| 17 | 175.00 | 48.20 |
| 18 | 177.50 | 45.54 |
| 19 | 180.00 | 21.44 |

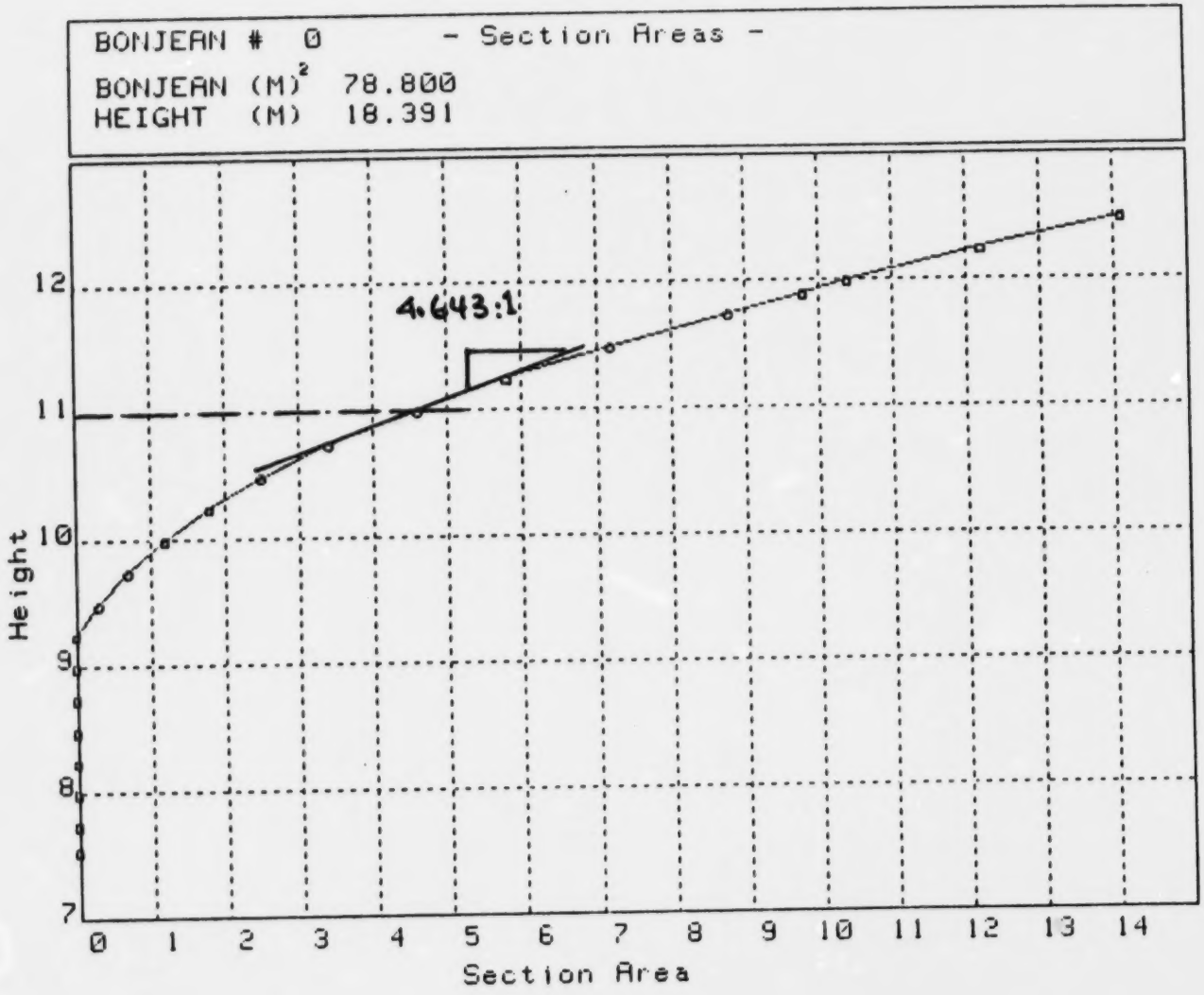
BONJEAN # 0 - Section Areas -
BONJEAN (M)² 78.800
HEIGHT (M) 18.391
4.643:1
Height
12
11
10
9
8
7
0 1 2 3 4 5 6 7 8 9 10 11 12 13 14
Section Area

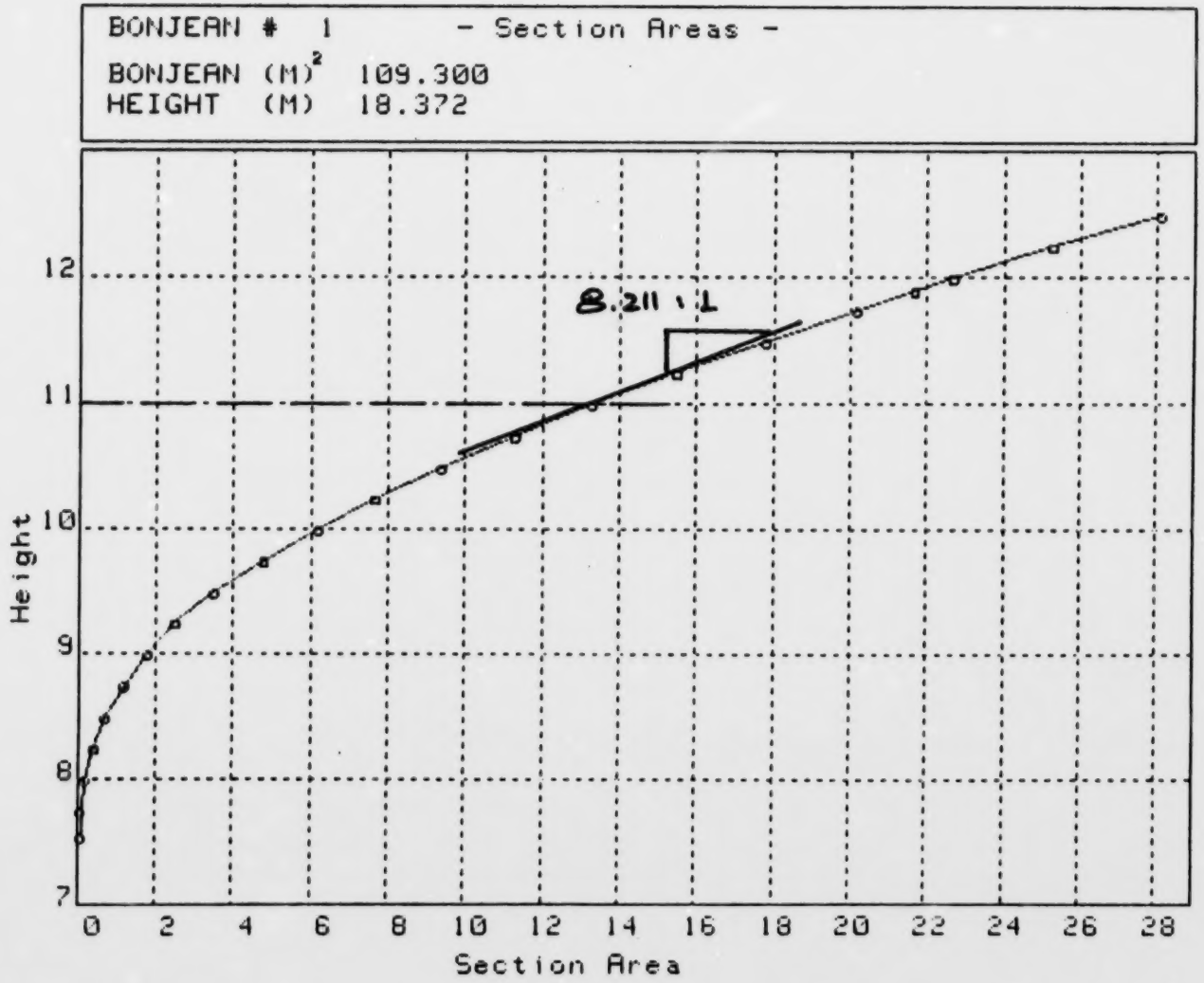
BONJEAN # 1 - Section Areas -
BONJEAN (M)² 109.300
HEIGHT (M) 18.372
8.211 : 1
Height
Section Area
7
8
9
10
11
12
0
2
4
6
8
10
12
14
16
18
20
22
24
26
28

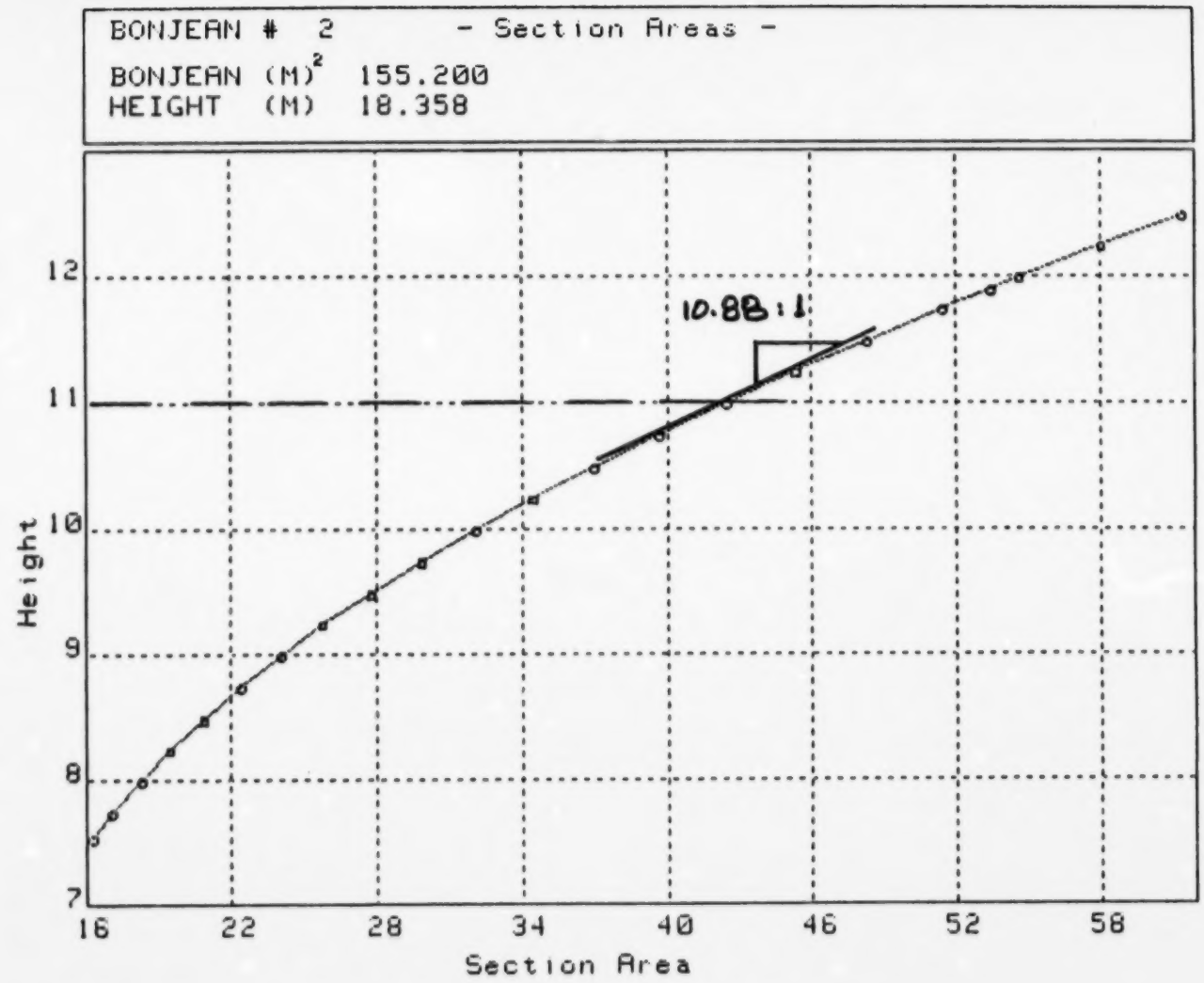
BONJEAN # 2 - Section Areas -
BONJEAN (M)² 155.200
HEIGHT (M) 18.358
10.88:1
Height
Section Area
7
8
9
10
11
12
16
22
28
34
40
46
52
58

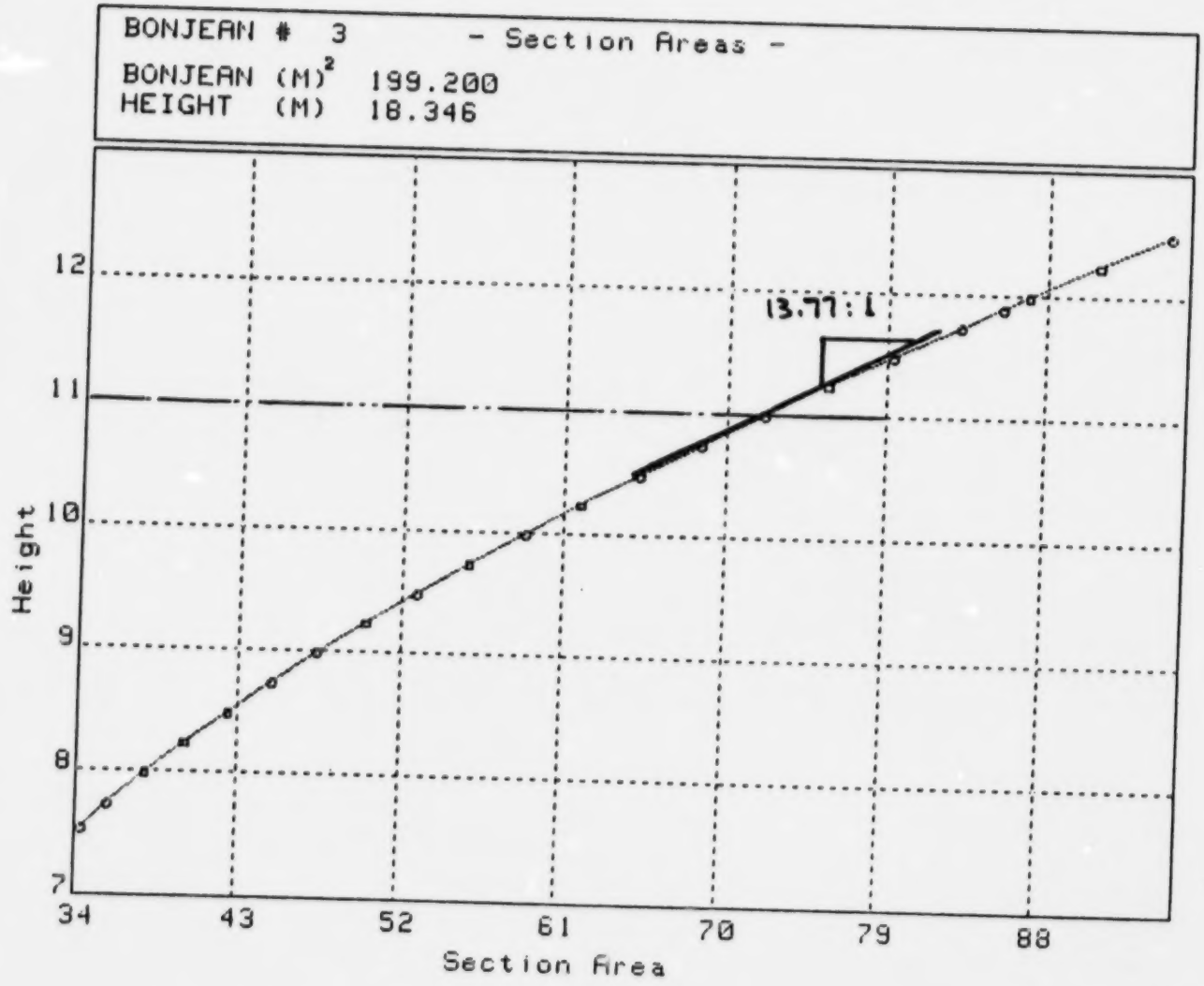
BONJEAN # 3 - Section Areas -
BONJEAN (M)$^2$ 199.200
HEIGHT (M) 18.346
13.77:1
Height
12
11
10
9
8
7
34
43
52
61
70
79
88
Section Area

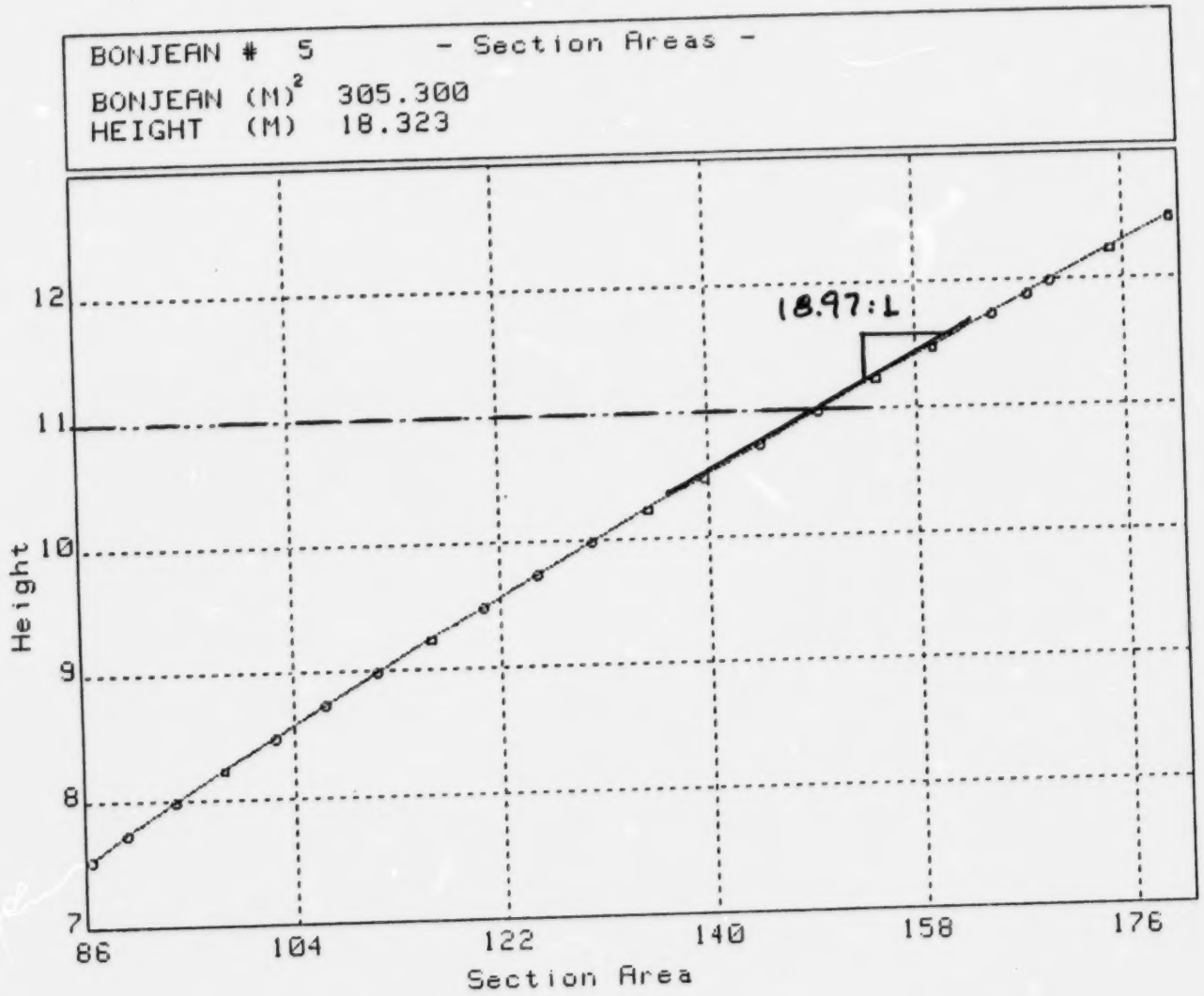
BONJEAN # 5 - Section Areas -
BONJEAN (M)$^2$ 305.300
HEIGHT (M) 18.323
18.97:1
12
11
10
9
8
7
Height
86
104
122
140
158
176
Section Area

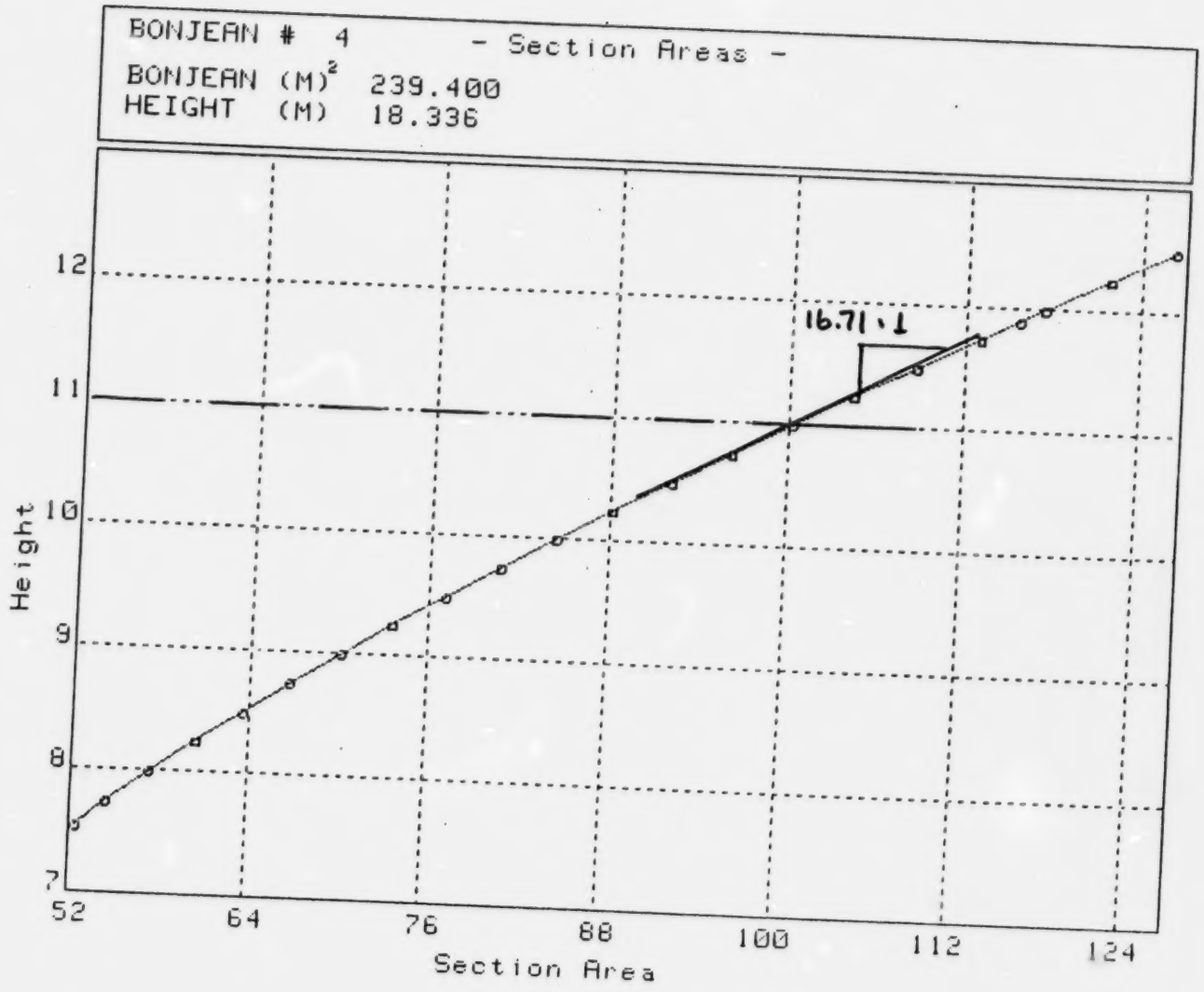
BONJEAN # 4
- Section Areas -
BONJEAN (M)² 239.400
HEIGHT (M) 18.336
16.71:1
Height
12
11
10
9
8
7
52
64
76
88
100
112
124
Section Area

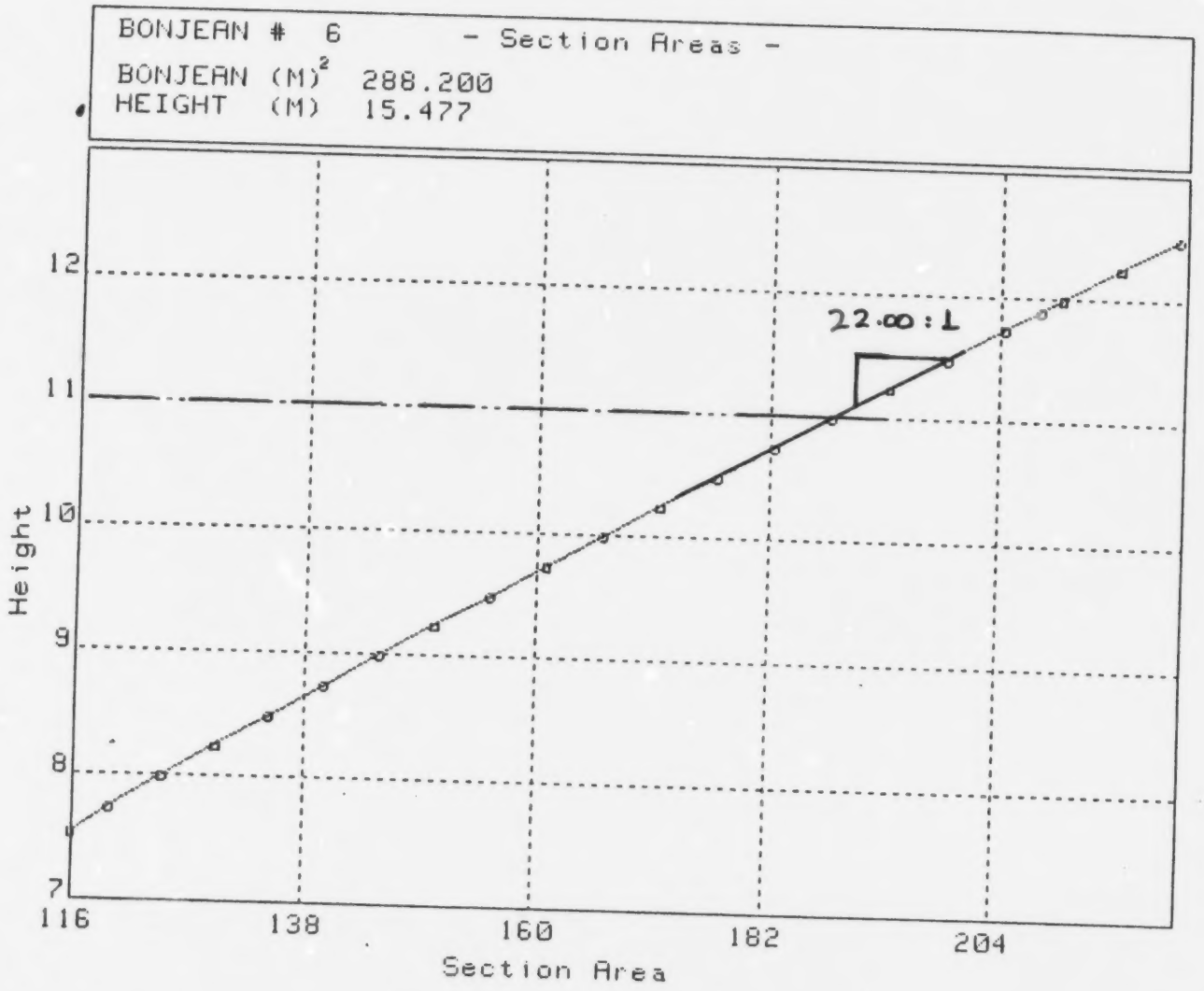
BONJEAN # 6
- Section Areas -
BONJEAN (M)$^2$ 288.200
HEIGHT (M) 15.477
22.00 : 1
12
11
10
9
8
7
Height
116
138
160
182
204
Section Area

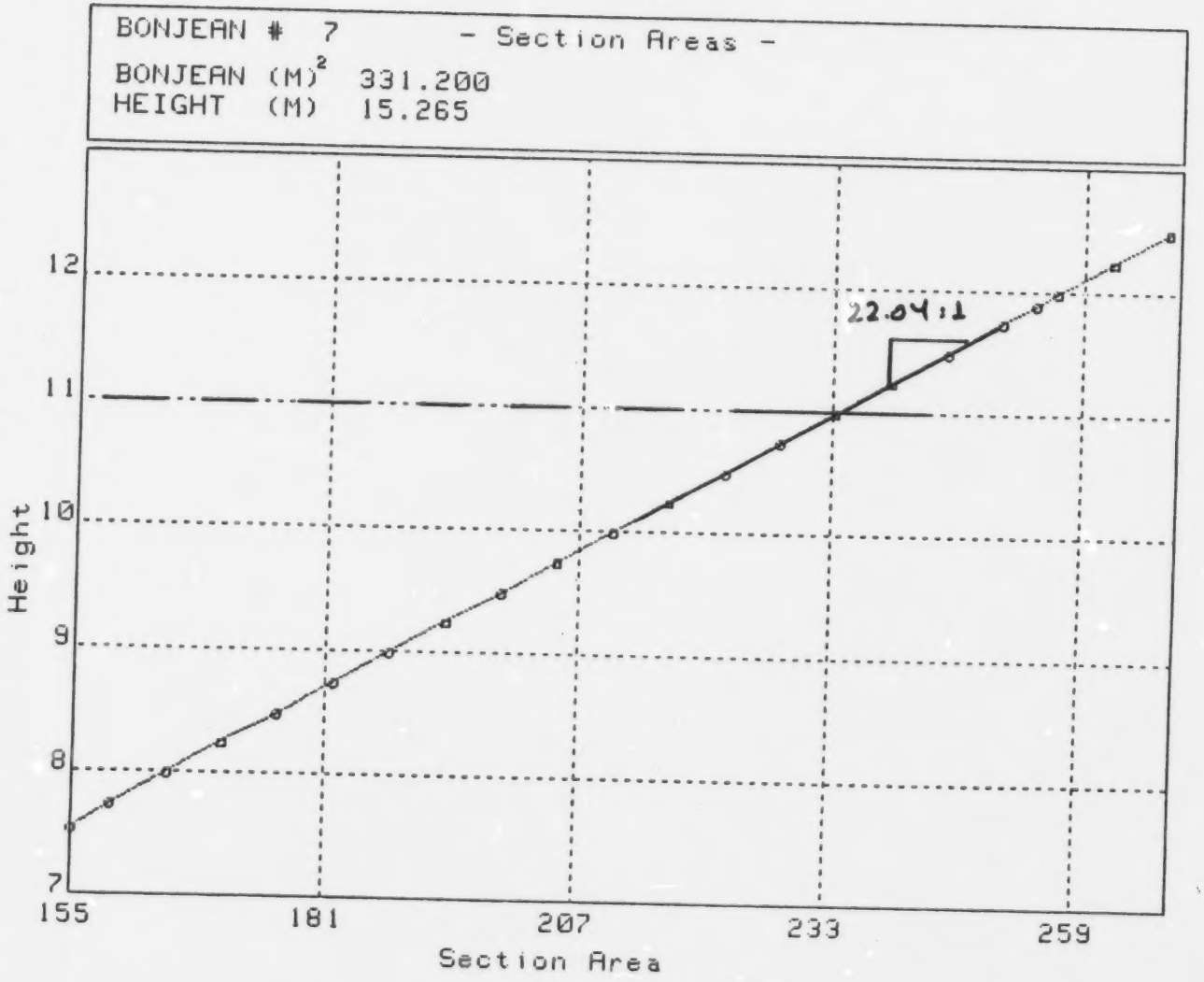
BONJEAN # 7 - Section Areas -
BONJEAN (M)$^2$ 331.200
HEIGHT (M) 15.265
22.04:1
Height
12
11
10
9
8
7
155
181
207
233
259
Section Area

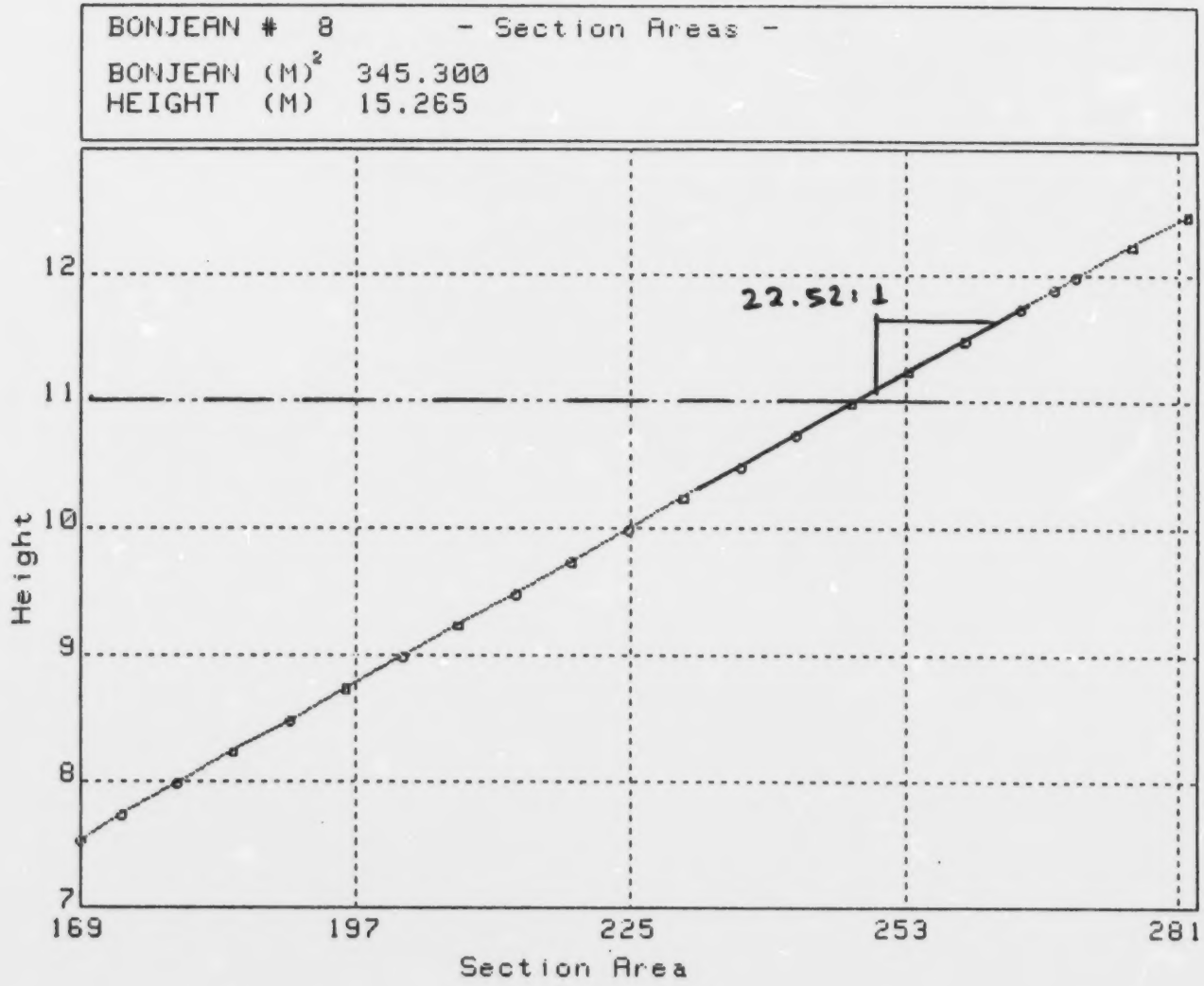
BONJEAN # 8 - Section Areas -
BONJEAN (M)² 345.300
HEIGHT (M) 15.265
22.52:1
12
11
10
9
8
7
Height
169
197
225
253
281
Section Area

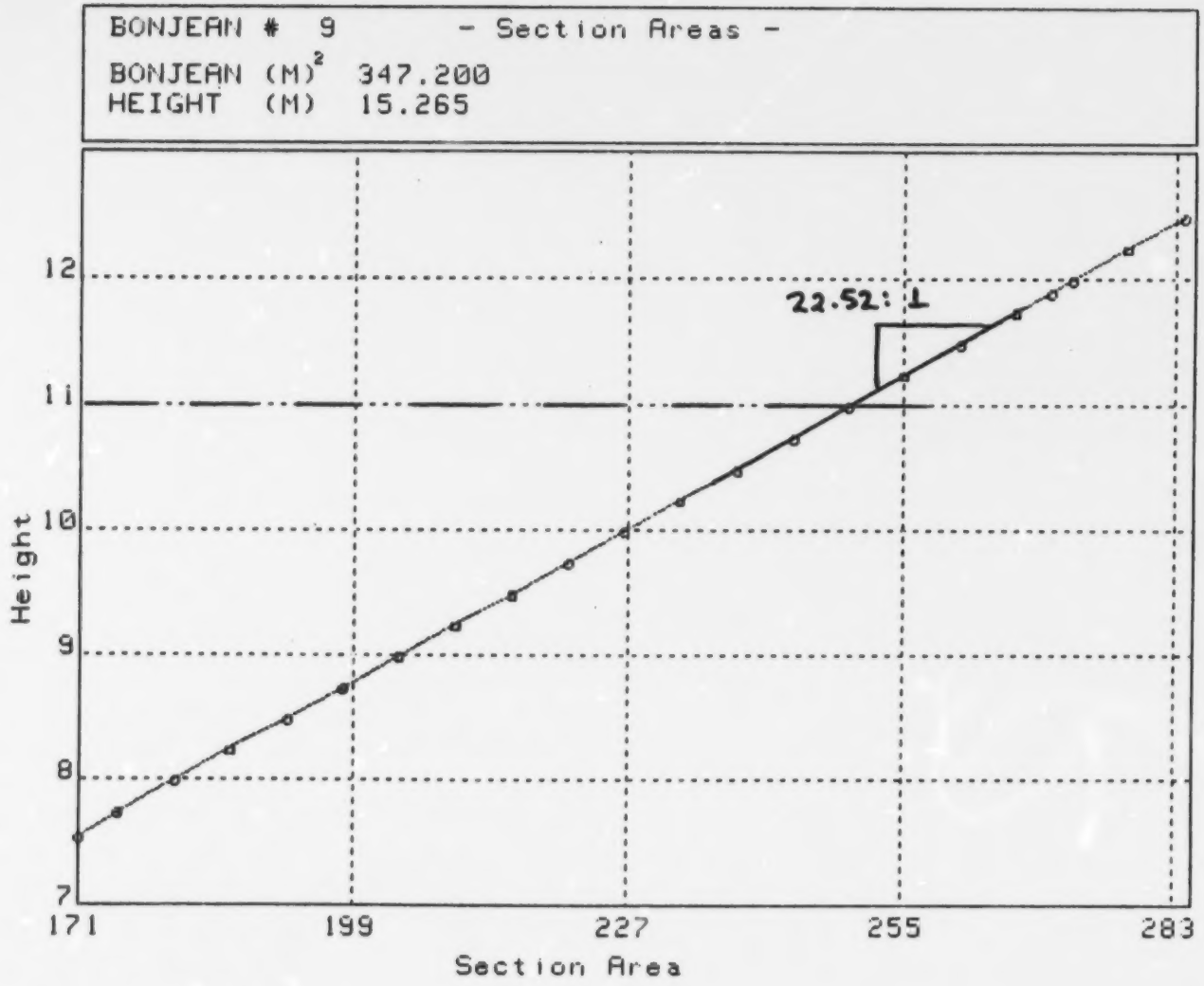
BONJEAN # 9 - Section Areas -
BONJEAN (M)² 347.200
HEIGHT (M) 15.265
22.52:1
Height
12
11
10
9
8
7
171
199
227
255
283
Section Area

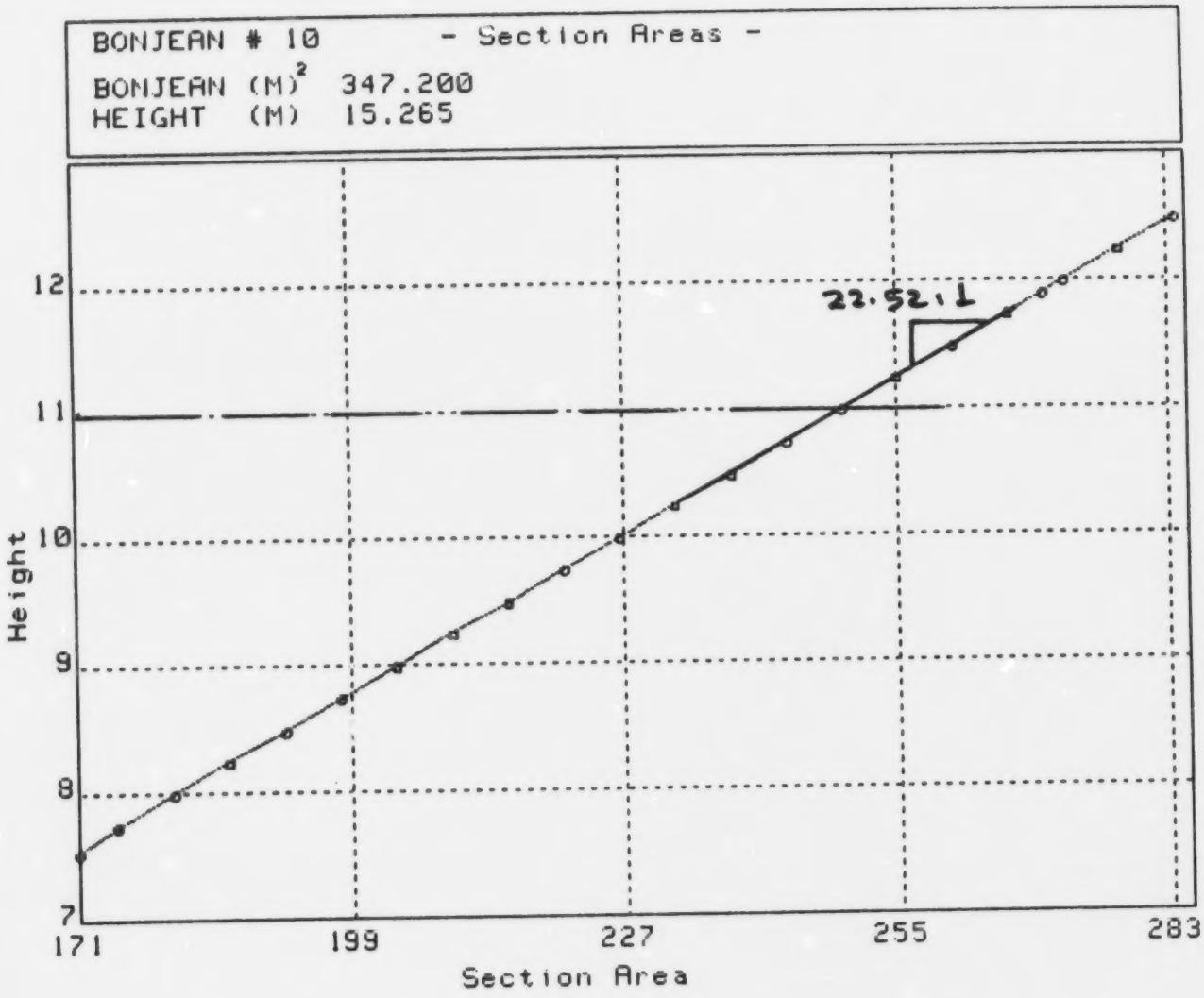
BONJEAN # 10 - Section Areas -
BONJEAN (M)² 347.200
HEIGHT (M) 15.265
22.52:1
12
11
10
9
8
7
Height
171
199
227
255
283
Section Area

A-90

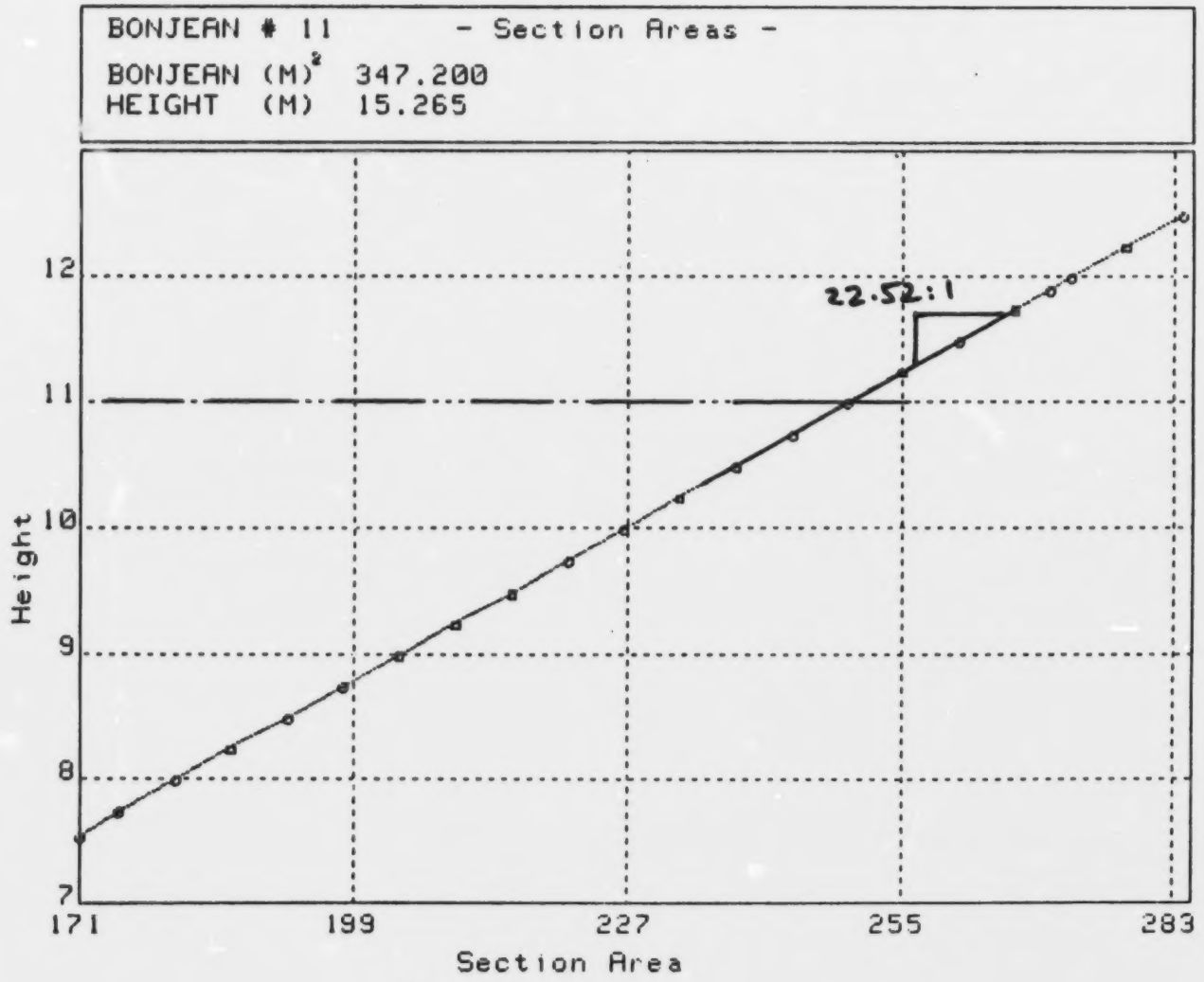
BONJEAN # 11 - Section Areas -
BONJEAN (M)² 347.200
HEIGHT (M) 15.265
22.52:1
12
11
10
9
8
7
Height
171
199
227
255
283
Section Area

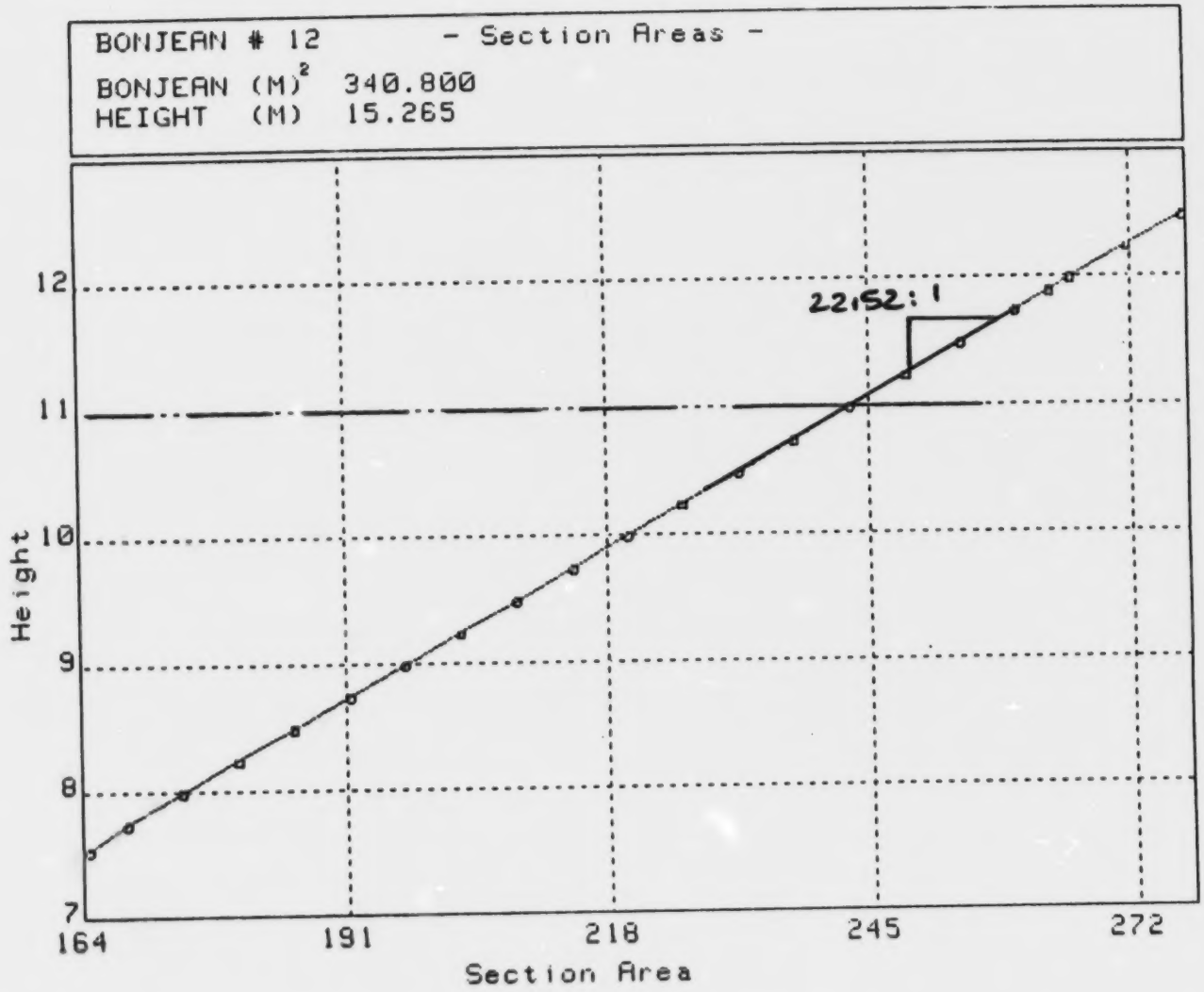
BONJEAN # 12 - Section Areas -
BONJEAN (M)² 340.800
HEIGHT (M) 15.265
22.52:1
12
11
10
9
8
7
Height
164
191
218
245
272
Section Area

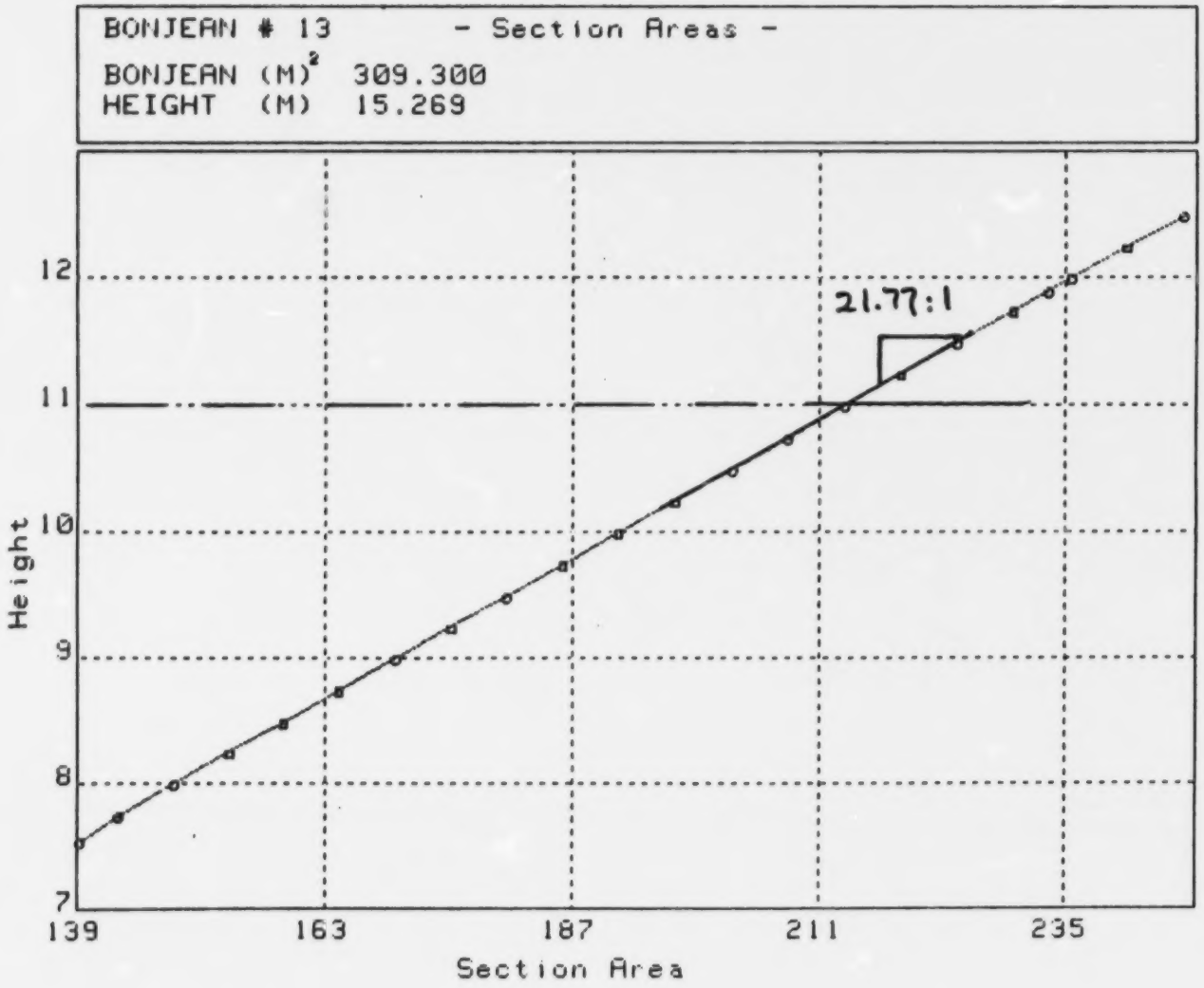
BONJEAN # 13 - Section Areas -
BONJEAN (M)² 309.300
HEIGHT (M) 15.269
21.77:1
Height
12
11
10
9
8
7
139
163
187
211
235
Section Area

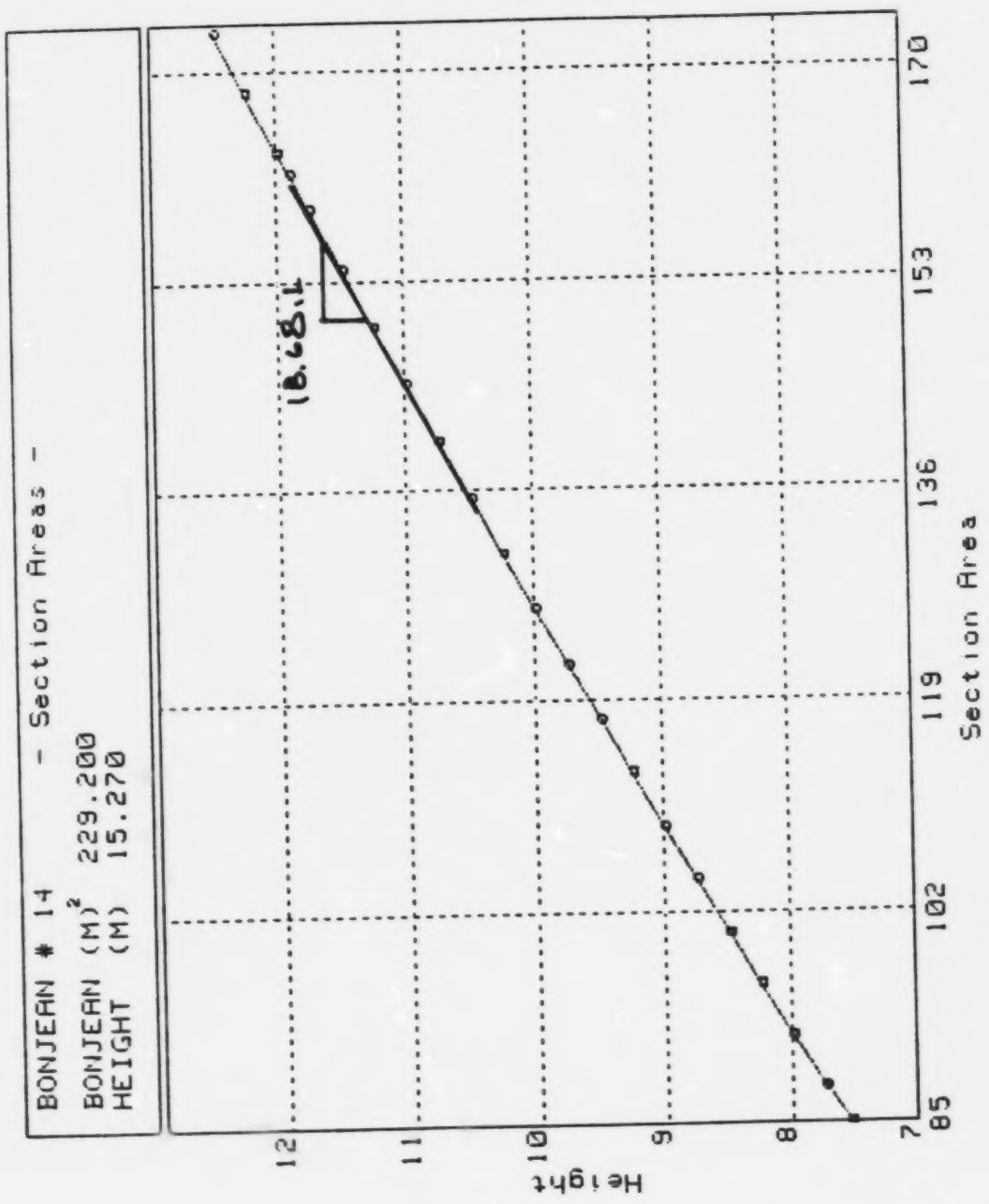
BONJEAN # 14 - Section Areas -
BONJEAN (M)² 229.200
HEIGHT (M) 15.270
18.68.1
Height
Section Area
12
11
10
9
8
7
85
102
119
136
153
170

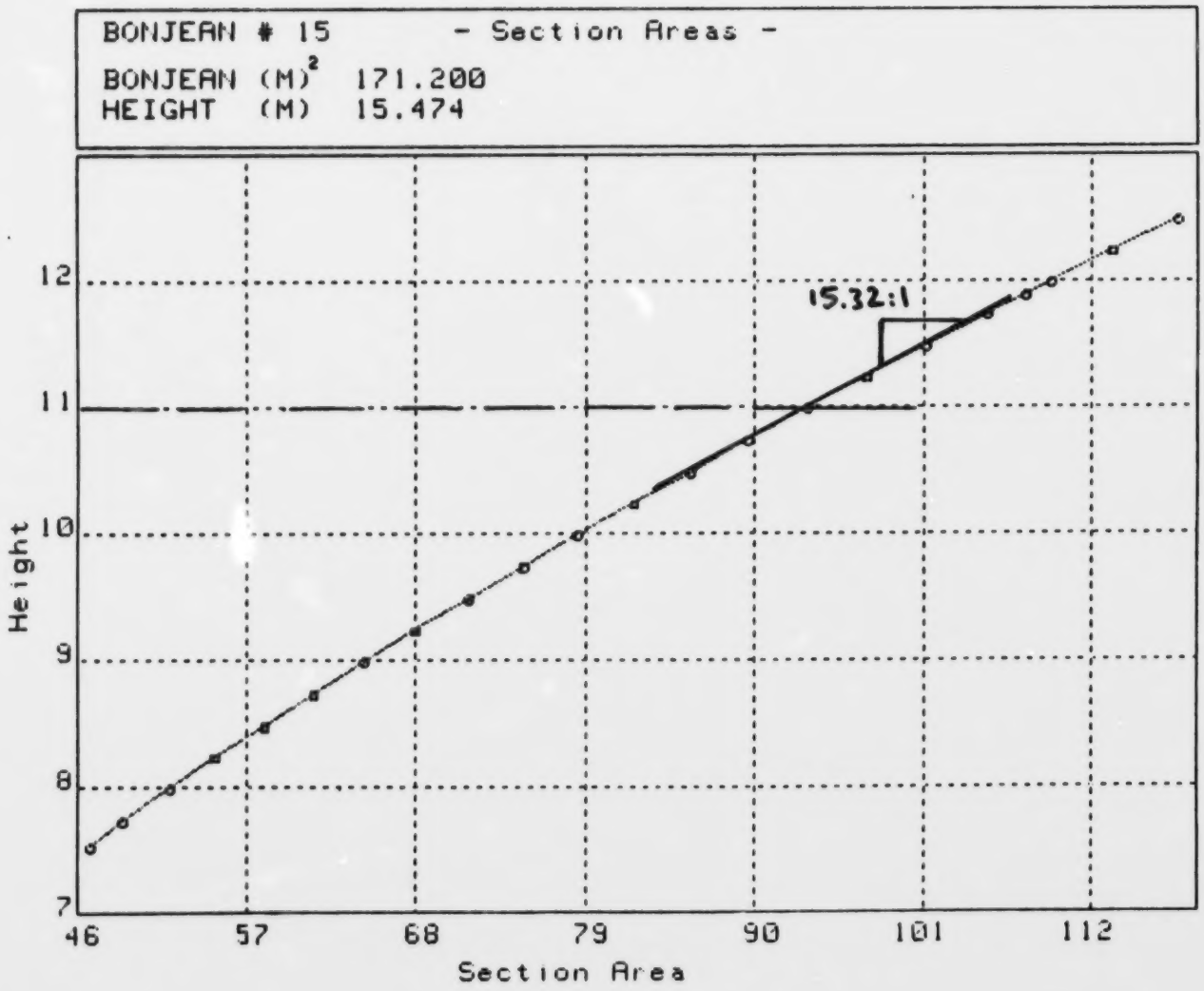
BONJEAN # 15 - Section Areas -
BONJEAN (M)² 171.200
HEIGHT (M) 15.474
15.32:1
12
11
10
9
8
7
Height
46
57
68
79
90
101
112
Section Area

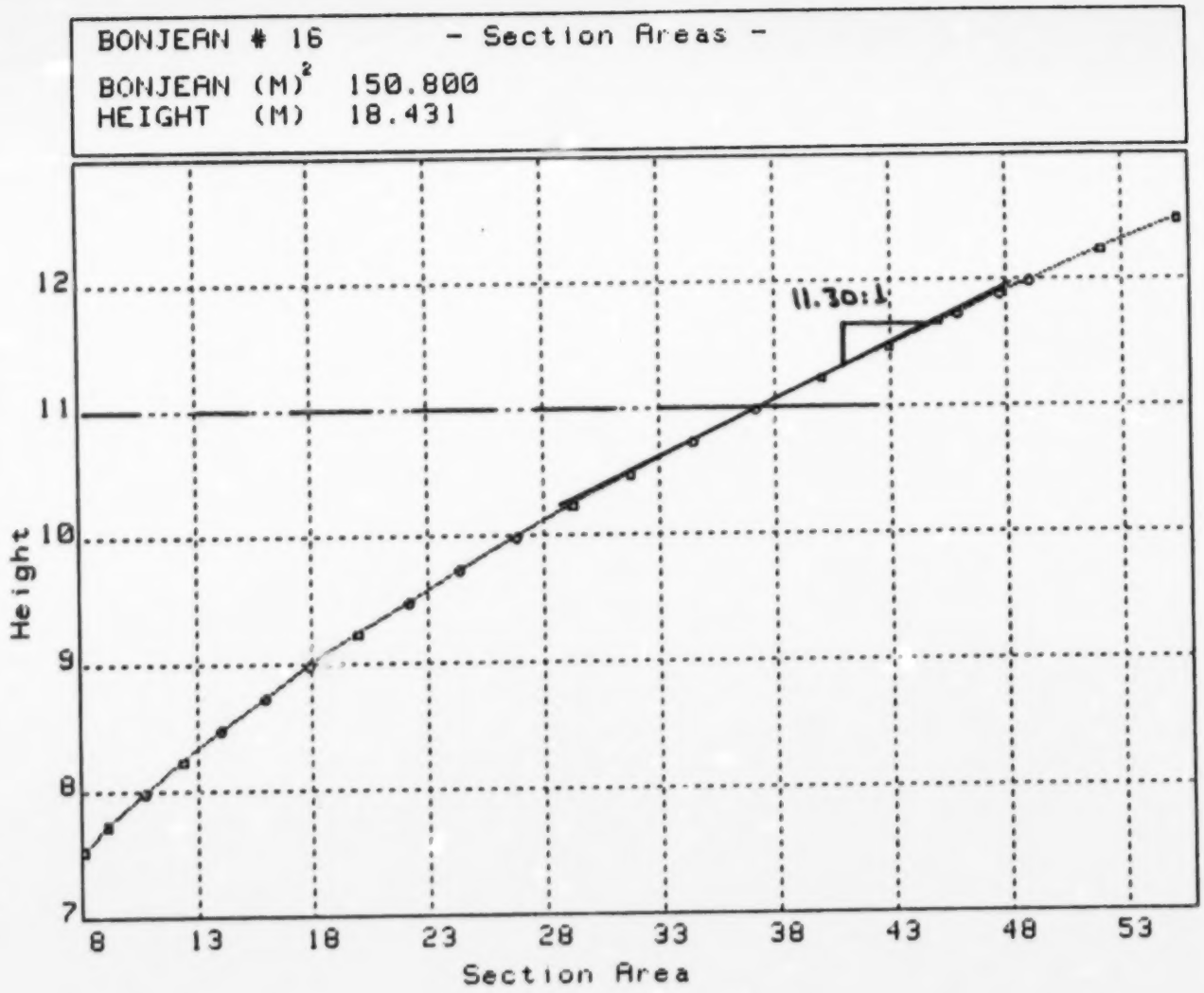
BONJEAN # 16 - Section Areas -
BONJEAN (M)$^2$ 150.800
HEIGHT (M) 18.431
11.30:1
Height
Section Area
7
8
9
10
11
12
8
13
18
23
28
33
38
43
48
53

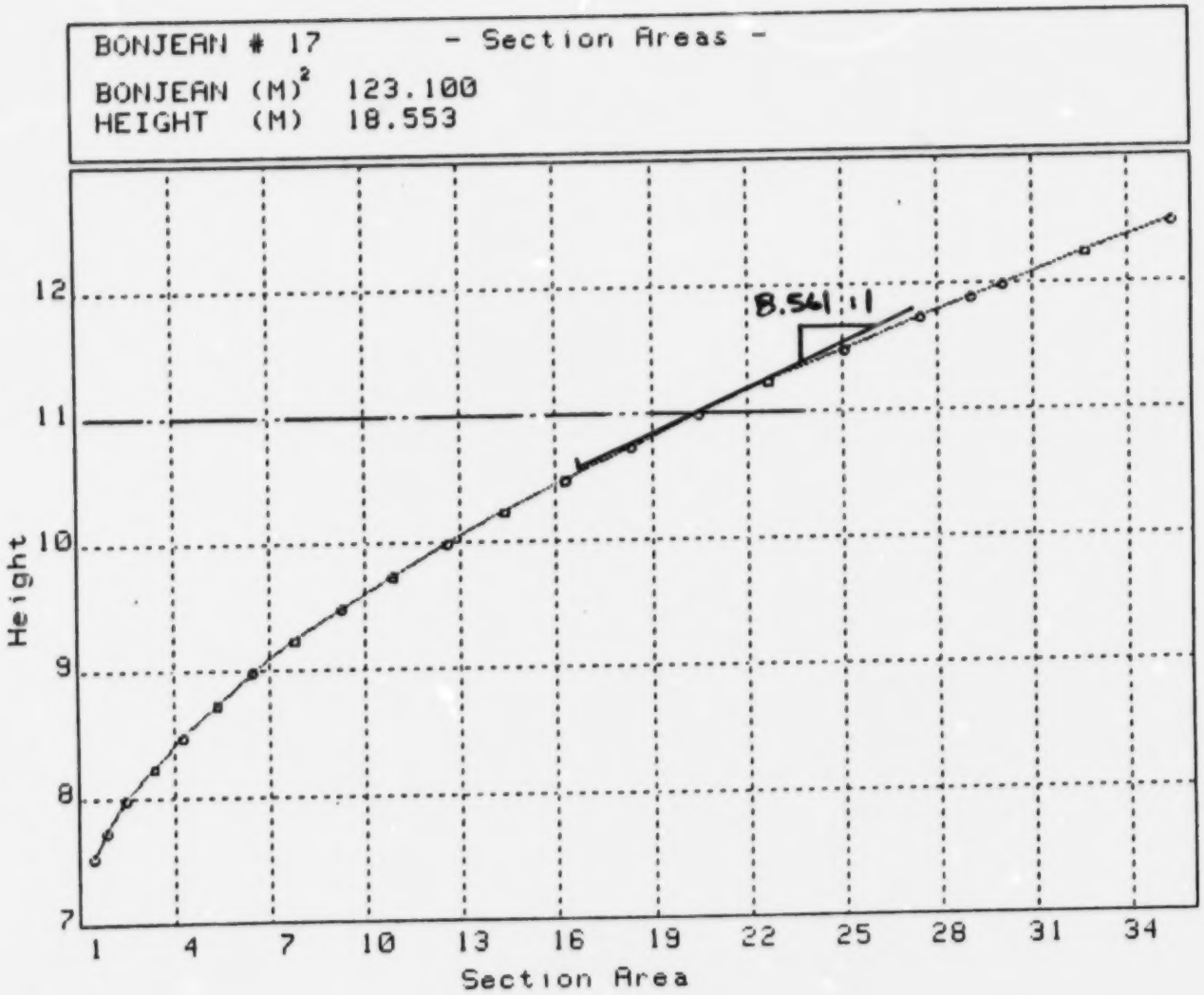
BONJEAN # 17 - Section Areas -
BONJEAN (M)² 123.100
HEIGHT (M) 18.553
8.54 : 1
Height
Section Area
7
8
9
10
11
12
1
4
7
10
13
16
19
22
25
28
31
34

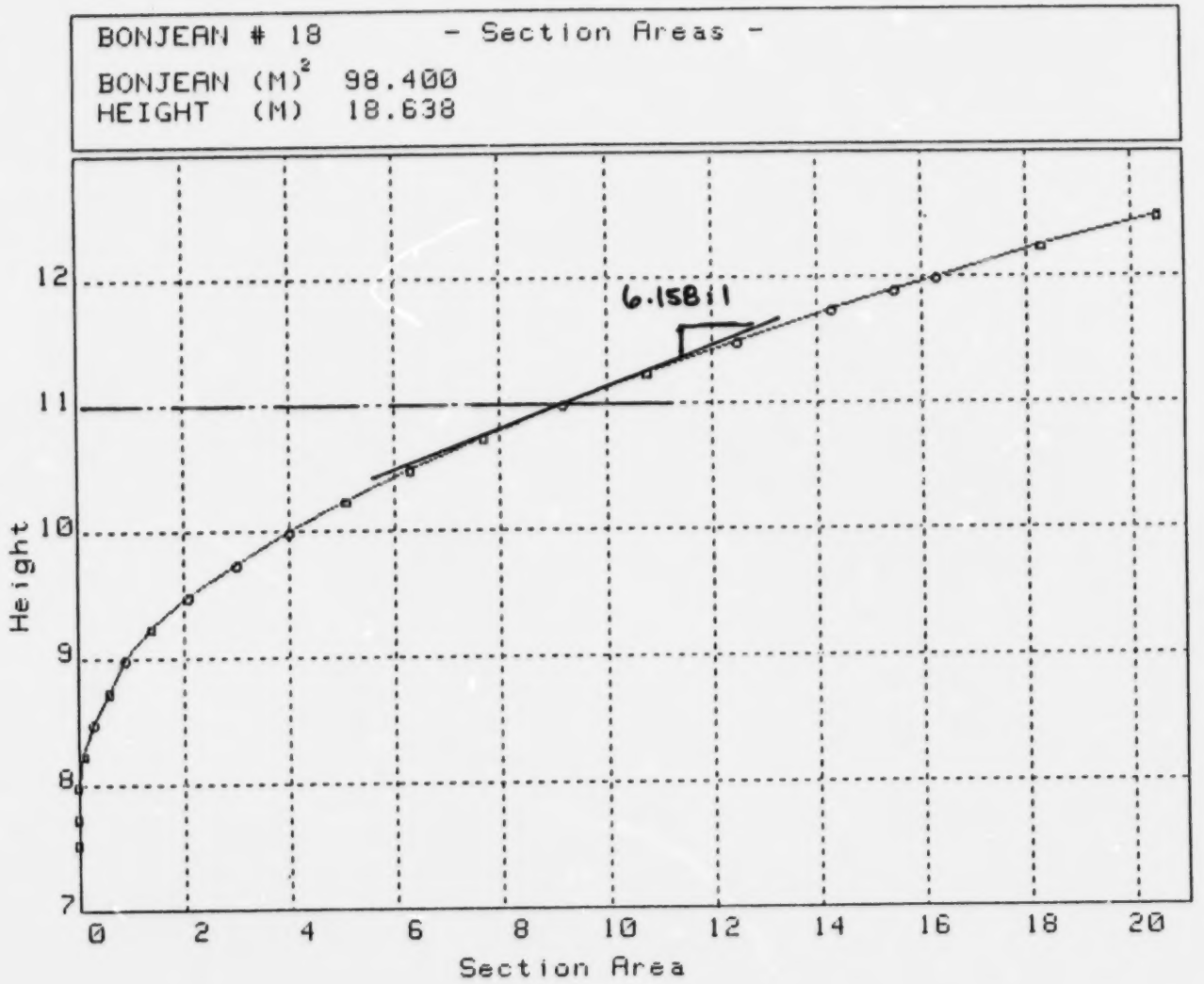
BONJEAN # 18 - Section Areas -
BONJEAN (M)$^2$ 98.400
HEIGHT (M) 18.638
6.158:1
Height
Section Area
7
8
9
10
11
12
0
2
4
6
8
10
12
14
16
18
20

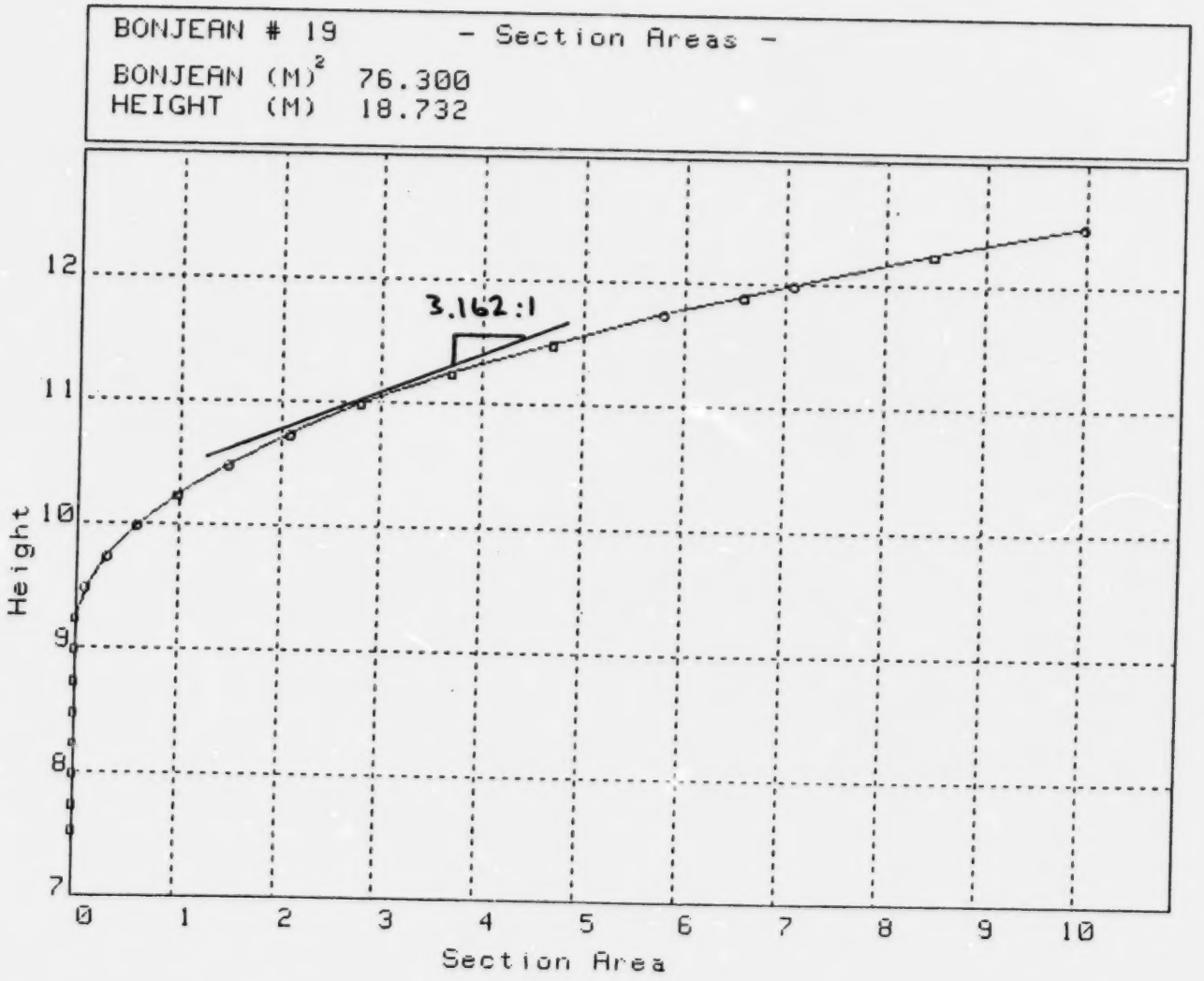
BONJEAN # 19 - Section Areas -
BONJEAN (M)$^2$ 76.300
HEIGHT (M) 18.732
3.162:1
Height
Section Area
12
11
10
9
8
7
0
1
2
3
4
5
6
7
8
9
10

APPENDIX D

## Solution of the Uncoupled Equations of Motion

The uncoupled equations of motion constitute a set of second order differential equations each of the form

$$\ddot{q} + 2\zeta\dot{q} + \omega^2 q = Q \qquad \ldots\ldots(D.1)$$

subject to the initial conditions $q_o$ and $\dot{q}_o$

where $q, \dot{q}, \ddot{q}$ are the generalized displacement, velocity and acceleration respectively

$\omega$ natural frequency of the mode considered

$\zeta$ the modal damping factor as a percent of critical damping

$Q$ generalized load

$q_o, \dot{q}_o$ are the critical displacement and velocity at time $t_o$.

$Q$, $q_o$, and $\dot{q}_o$ are calculated from the structural data using the equations

$$Q = \{\Phi\}^T \{F\}$$

$$q_o = \{\Phi\}^T [M] \{u\} / m_e$$

$$\dot{q}_o = \{\Phi\}^T [M] \{\dot{u}\} / m_e$$

where $\{\Phi\}$ modal displacements of the mode considered

$\{u_o\}$ structure initial displacement at time $t_o$

$\{\dot{u}_o\}$ structure initial velocity at time $t_o$

$\{F\}$ excitation force

$[M]$ structure mass matrix

$m_e$ generalized mass for the mode considered

The excitation force in turn consists of two components - a load vector which is independent of time multiplied by a time dependent amplitude i.e.

$$\{F\} = \{\bar{F}\} A(t)$$

or
$$Q = \{\Phi\}^T \{\bar{F}\} A(t)$$
$$= p A(t)$$

Note that the equivalent load p is independent of time.

An incremental solution of equation (D.1) is performed. A time step H is chosen and it is assumed that the amplitude A varies linearly from the beginning to the end of the time step. Equation (D.1) reduces to .....(D.2)

$$\ddot{q}_i + 2\xi\dot{q}_i + \omega^2 q_i = p\left[A_1(1-\tau) + A_2\tau\right]$$

where $A_1$ and $A_2$ are the force amplitudes at time $t_n$ and $t_n+1$ and $\tau = (t-t_n)/H$

Equation (D.2) has a closed form solution given that q and $\dot{q}$ are known at time $t_n$. The solution for the generalized displacement and velocity at the end of the time step is

$$q_{n+1} = G_1 q_n + G_2 \dot{q}_n + G_3 A_1 + G_4 A_2$$
$$\dot{q}_{n+1} = \dot{G}_1 q_n + \dot{G}_2 \dot{q}_n + \dot{G}_3 A_1 + \dot{G}_4 A_2$$

and the factors $G_i$ and $\dot{G}_i$ are

$$G_1 = e^{\alpha H}\left[\cos\beta H - \frac{\alpha}{\beta}\sin\beta H\right]$$

$$G_2 = e^{\alpha H}\left[\sin\beta H/\beta\right]$$

$$G_3 = \frac{P}{m\omega^2\beta H}\left[e^{\alpha H}\left\{(\alpha H + 1 - 2\zeta^2)\sin\beta H - (1-\zeta^2)^{1/2}(\omega H + 2\zeta)\cos\beta H\right\} + 2\zeta(1-\zeta^2)^{1/2}\right]$$

$$G_4 = \frac{P}{m\omega^2\beta H}\left[e^{\alpha H}\left\{2\zeta(1-\zeta^2)^{1/2}\cos\beta H - (1-2\zeta^2)\sin\beta H\right\} + \beta H - 2\zeta(1-\zeta^2)^{1/2}\right]$$

$$\dot{G}_1 = -\omega(1-\zeta^2)^{1/2} e^{\alpha H}\sin\beta H$$

$$\dot{G}_2 = e^{\alpha H}\left\{\cos\beta H - \frac{\zeta}{(1-\zeta^2)^{1/2}}\sin\beta H\right\}$$

$$\dot{G}_3 = \frac{P}{m\omega^2\beta H}\left[e^{\alpha H}\left\{(\omega^2 H - \alpha)\sin\beta H + \beta\cos\beta H\right\} - \beta\right]$$

$$\dot{G}_4 = \frac{P}{m\omega^2\beta H}\left[\beta - e^{\alpha H}\left\{\beta\cos\beta H - \alpha\sin\beta H\right\}\right]$$

where $\alpha = -\zeta\omega$

$\beta = \omega(1-\zeta^2)^{1/2}$

## APPENDIX E

## Calculation of Quasi-Rigid Body Motion and Moments

### E.1 Equations of Motion

For the rigid body modes the ship can be represented by the following model. The springs represent the restoring forces due to buoyancy. The mass of the beam is assumed to be concentrated at the spring attachment points.

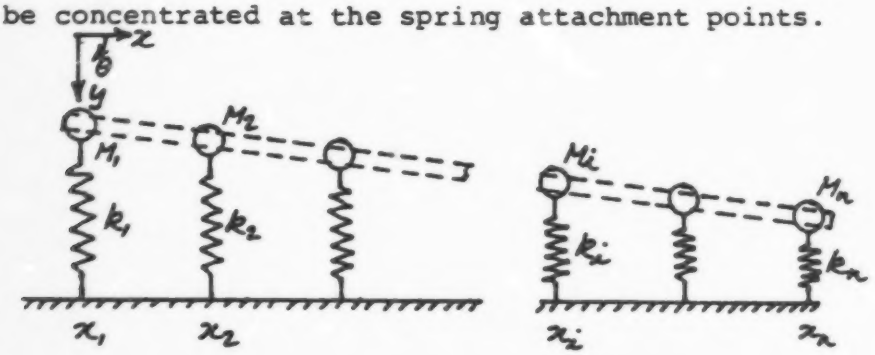


The equations of motion can be set up by substituting appropriately in Lagrange's equation (see, for example, L. Meirovitch, "Elements of Vibration Analysis", McGraw-Hill, 1975):

$$\frac{d}{dt}\left(\frac{\partial T}{\partial \dot{q}}\right) - \frac{\partial T}{\partial q} + \frac{\partial V}{\partial q} = 0 \qquad \text{(E.1.1)}$$

where T = kinetic energy of system

V = potential (strain) energy of the system

q = coordinate

E.1 Equations of Motion (cont'd)

The kinetic energy of a single mass is given by

$$T = \frac{1}{2} M_i (\dot{y} + x_i \dot{\theta})^2$$

and the strain energy of a single mass is given by

$$V = \frac{1}{2} k_i (y + x_i \theta)^2$$

The various terms of Lagrange's equations are

$$\frac{d}{dt}\left(\frac{\partial T}{\partial \dot{y}}\right) = \sum_{i=1}^{n} M_i (\ddot{y} + x_i \ddot{\theta})$$

$$\frac{d}{dt}\left(\frac{\partial T}{\partial \dot{\theta}}\right) = \sum_{i} M_i x_i (\ddot{y} + x_i \ddot{\theta})$$

$$\frac{\partial V}{\partial y} = \sum_{i} k_i (y + x_i \theta)$$

$$\frac{\partial V}{\partial \theta} = \sum_{i} k_i x_i (y + x_i \theta)$$

The substitution of the above in Lagrange's equations leads to the equations of motion:

$$\begin{bmatrix} \Sigma M_i & \Sigma M_i x_i \\ \Sigma M_i x_i & \Sigma M_i x_i^2 \end{bmatrix} \begin{Bmatrix} \ddot{y} \\ \ddot{\theta} \end{Bmatrix} \begin{bmatrix} \Sigma k_i & \Sigma k_i x_i \\ \Sigma k_i x_i & \Sigma k_i x_i^2 \end{bmatrix} \begin{Bmatrix} y \\ \theta \end{Bmatrix} = 0 \qquad \text{(E.1.2)}$$

Assume simple harmonic motion

$$y = \bar{y} \sin \omega t \qquad \ddot{y} = -\omega^2 \bar{y} \sin \omega t$$
$$\theta = \bar{\theta} \sin \omega t \qquad \ddot{\theta} = -\omega^2 \bar{\theta} \sin \omega t \qquad \text{(E.1.3)}$$

Substitution of E.1.3 in E.1.2 yields:

$$\begin{bmatrix} \Sigma k_i - \omega^2 \Sigma M_i & \Sigma k_i x_i - \omega^2 \Sigma M_i x_i \\ \Sigma k_i x_i - \omega^2 \Sigma M_i x_i & \Sigma k_i x_i^2 - \omega^2 \Sigma M_i x_i^2 \end{bmatrix} \begin{Bmatrix} \bar{y} \\ \bar{\theta} \end{Bmatrix} = 0 \qquad \text{(E.1.4)}$$

E.1 Equations of Motion (cont'd)

Let $\Sigma k_i = a \quad \Sigma M_i = d$

$\Sigma k_i x_i = b \quad \Sigma M_i x_i = e$

$\Sigma k_i x_i^2 = c \quad \Sigma M_i x_i^2 = f$

The natural frequencies and modes are obtained by solving the following:

$$\begin{vmatrix} a-\omega^2 d & b-\omega^2 e \\ b-\omega^2 e & c-\omega^2 f \end{vmatrix} = 0 \qquad \text{(E.1.5)}$$

Expansion of E.1.5 leads to a quadratic in $\omega^2$:

$$(df-e^2)\omega^4+(2be-af-cd)\omega^2+ac-b^2=0$$

The natural frequencies are given by the following expression:

$$\omega_1^2, \omega_2^2 = \frac{(af+cd-2be) \mp \sqrt{(2be-af-cd)^2-4(df-e^2)(ac-b^2)}}{2(df-e^2)} \qquad \text{(E.1.6)}$$

and the modes are obtained by substituting $\omega_1$ and $\omega_2$ in E.1.4.

## E.2 Bending Moments for Rigid Modes

Consider vertical undamped motion of mass i.

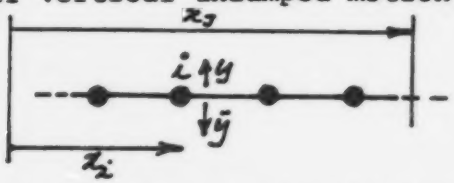


In the sketch above $x_i$ is the horizontal distance from the reference position, and $x_J$ is the position where the bending moment is to be calculated. The dynamic equilibrium of a single mass is shown in the following sketch:

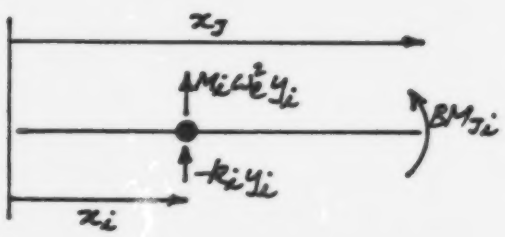


The bending moment at position J, due to the mass, $n_i$, vibrating in mode e is given by

$$BM^e_{Ji} = (M_i\omega^2 y_i - k_i y_i)(x_J - x_i) \qquad \text{(E.2.1)}$$

Now the displacement is given by

$$y_i = \phi_{ei} z_e \qquad \text{(E.2.2)}$$

where $\phi_{ei}$ is the mode shape for position i
i for mode e

and $z_e$ is the modal response

E.2 Bending Moments for Rigid Modes (cont'd)

The substitution of E.2.2 in E.2.1 yields

$$BM^e_{Ji} = (M_i\omega_e^2 - k_i)(x_J - x_i)\phi_{ei}\eta_e$$

The modal bending moment at position J, due to mass, $m_i$, vibrating in mode e is

$$\overline{BM}^e_{Ji} = (M_i\omega_e^2 - k_i)(x_J - x_i)\phi_{ei}$$

The total modal bending moment at position J, vibrating in mode e is given by

$$\overline{BM}^e_J = \sum_{i=1}^{J-1} (M_i\omega_e^2 - k_i)(x_J - x_i)\phi_{ei}$$

The total bending moment is then

$$BM_J = \sum_{e=1}^{N_{modes}} \overline{BM}^e_J \eta_e$$

also $\sigma_J = \dfrac{BM_J}{S_J}$

where $\sigma_J$ = longitudinal bending stress at J

$S_J$ = sectionmodulus at J

M.V.ARCTIC - Natural Frequencies and Mode Shapes
JOBNAME MV1

NODEL CHARACTERISTICS

| MODE | FREQUENCY (HZ) | (R/S) | EQUIVALENT MASS | EQUIVALENT LOAD |
|---|---|---|---|---|
| 1 | 0.000 | 0.000 | 6.946E+07 | -1.000E+00 |
| 2 | 0.108 | 0.679 | 2.384E+07 | 1.000E+00 |
| 3 | 0.134 | 0.843 | 1.088E+07 | -3.818E-01 |

| NODE | X-COOR | STIFFNESS | MASS | MODE 1 | MODE 2 | MODE 3 |
|---|---|---|---|---|---|---|
| 1 | 0.00 | 5.150E+05 | 7.128E+05 | 1.0000 | -0.1745 | 1.0000 |
| 2 | 20.50 | 3.190E+06 | 2.854E+06 | 1.0000 | -0.0407 | 0.8426 |
| 3 | 41.00 | 3.565E+06 | 4.843E+06 | 1.0000 | 0.0930 | 0.6853 |
| 5 | 55.00 | 2.594E+06 | 4.005E+06 | 1.0000 | 0.1844 | 0.5778 |
| 7 | 65.00 | 1.411E+06 | 1.613E+06 | 1.0000 | 0.2496 | 0.5010 |
| 9 | 68.00 | 2.966E+06 | 8.968E+06 | 1.0000 | 0.2692 | 0.4780 |
| 10 | 92.00 | 3.974E+06 | 8.383E+06 | 1.0000 | 0.4258 | 0.2938 |
| 12 | 104.00 | 3.761E+06 | 5.610E+06 | 1.0000 | 0.5041 | 0.2016 |
| 14 | 117.00 | 2.761E+06 | 4.717E+06 | 1.0000 | 0.5889 | 0.1019 |
| 16 | 129.00 | 2.650E+06 | 4.740E+06 | 1.0000 | 0.6672 | 0.0097 |
| 18 | 141.00 | 2.650E+06 | 1.071E+07 | 1.0000 | 0.7455 | -0.0824 |
| 19 | 153.00 | 2.098E+06 | 2.623E+06 | 1.0000 | 0.8238 | -0.1745 |
| 21 | 160.00 | 1.315E+06 | 1.565E+06 | 1.0000 | 0.8695 | -0.2282 |
| 22 | 165.00 | 1.074E+06 | 1.840E+06 | 1.0000 | 0.9021 | -0.2666 |
| 23 | 170.00 | 7.762E+05 | 3.306E+06 | 1.0000 | 0.9347 | -0.3056 |
| 24 | 172.50 | 4.922E+05 | 4.426E+05 | 1.0000 | 0.9511 | -0.3242 |
| 25 | 175.00 | 4.728E+05 | 3.969E+05 | 1.0000 | 0.9674 | -0.3434 |
| 26 | 177.50 | 4.467E+05 | 3.551E+05 | 1.0000 | 0.9837 | -0.3626 |
| 27 | 180.00 | 2.103E+05 | 1.770E+06 | 1.0000 | 1.0000 | -0.3818 |

MODAL FORCE / MOMENT FOR RIGID MODES

| NODE | MODE 1 | MODE 2 | MODE 3 |
|---|---|---|---|
| 1 | 0.000E+00 | 0.000E+00 | 0.000E+00 |
| 2 | -7.128E+05 | -2.098E+06 | 8.370E+06 |
| 3 | -3.567E+06 | -5.761E+06 | 3.680E+07 |
| 5 | -8.410E+06 | -6.527E+06 | 5.739E+07 |
| 7 | -1.241E+07 | -5.695E+06 | 7.063E+07 |
| 9 | -1.403E+07 | -4.947E+06 | 7.500E+07 |
| 10 | -2.300E+07 | -6.504E+06 | 7.083E+07 |
| 12 | -3.138E+07 | -6.722E+06 | 6.175E+07 |
| 14 | -3.699E+07 | -5.812E+06 | 4.870E+07 |
| 16 | -4.171E+07 | -8.264E+05 | 3.592E+07 |
| 18 | -4.645E+07 | 7.888E+06 | 2.306E+07 |
| 19 | -5.716E+07 | -3.864E+06 | 1.511E+07 |
| 21 | -5.979E+07 | -5.592E+06 | 1.019E+07 |
| 22 | -6.135E+07 | -4.247E+06 | 6.439E+06 |
| 23 | -6.319E+07 | -1.885E+06 | 3.003E+06 |
| 24 | -6.650E+07 | -2.451E+06 | 2.486E+06 |
| 25 | -6.694E+07 | -2.332E+06 | 1.624E+06 |
| 26 | -6.734E+07 | -1.514E+06 | 1.000E+06 |
| 27 | -6.769E-07 | 0.000E+00 | 0.000E+00 |

## APPENDIX F

### Validation of DRTRAN, the FESDEC Program for Computing the Response of a Multi Degree of Freedom System to Arbitrary Loading

A simple, but comprehensive, test case was run to establish the accuracy of the program DRTRAN. In the test case the response, damped and undamped, of a cantilever beam to two different force excitations is computed. The first three vibration modes of the cantilever are considered.

The test case used is summarized below. Following this a selected comparison between theoretical and computed results is presented.

#### Description of Test Case

Two different force time-histories are employed, and are described below.

Force Time History #1

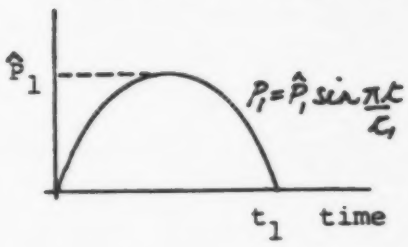


where $\hat{P}_1$ = 100 lbs

$t_1$ = 0.4 secs

Force Time History #2

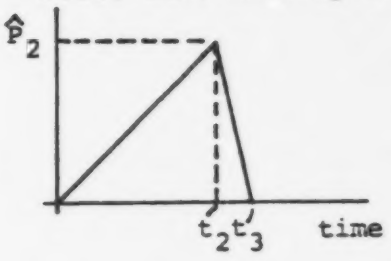


where $\hat{P}_2$ = 200 lbs

$t_2$ = 0.2 secs

$t_3$ = 0.22 secs

The test case structure considered is sketched below.

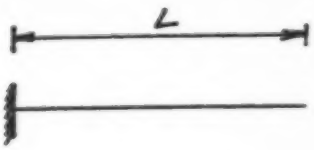


The beam is idealized by ten beam elements, each of equal length. The dynamic properties relevant to this test case are summarized in the table below.

| Mode No. | Natural Frequency (Hz) | Equiv. Mass |
|---|---|---|
| 1 | 0.355 | 25.19 |
| 2 | 2.198 | 26.43 |
| 3 | 6.092 | 28.84 |

The equivalent mass is based on a modal tip amplitude of unity.

Factored versions of the force time histories sketched above are applied to the beam:

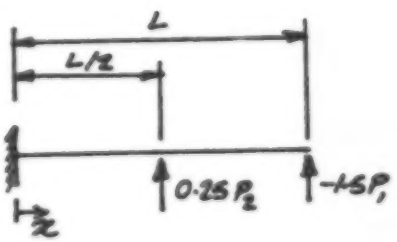

The modal displacements, which are required for the calculation of equivalent loads, are given in the following table:

| Mode | Modal Displacement @ x = L/2 | Modal Displacement @ x = L |
|---|---|---|
| 1 | 0.3389 | 1.0 |
| 2 | -0.7823 | 1.0 |
| 3 | 0.05912 | 1.0 |

Theoretical Solutions

The undamped response of a single degree of freedom system to the force time histories sketched above are available in closed form (for example in J.S. Przemieniecki, "Theory of Matrix Structural Analysis, McGraw-Hill, 1968), and are:

for force time history #1 (i.e. half sine-wave)

displacement

$$\delta = \frac{\hat{P}_1 t_1}{M\omega(\omega^2 t_1^2 - \pi^2)}\left(\omega t_1 \sin\frac{\pi t}{t_1} - \pi \sin\omega t\right) \qquad \text{for } t \leq t_1$$

$$\delta = \frac{-\hat{P}_1 \pi t_1}{M\omega(\omega^2 t_1^2 - \pi^2)}\left[\sin\omega(t - t_1) + \sin\omega t\right] \qquad \text{for } t \geq t_1$$

velocity

$$v = \frac{\hat{P}_1 \pi t_1}{M(\omega^2 t_1^2 - \pi^2)}\left(\cos\frac{\pi t}{t_1} - \cos\omega t\right) \qquad \text{for } t \leq t_1$$

$$v = \frac{-\hat{P}_1 \pi t_1}{M(\omega^2 t_1^2 - \pi^2)}\left[\cos\omega(t - t_1) + \cos\omega t\right] \qquad \text{for } t \geq t_1$$

for force time history #2 (i.e. triangular)

displacement

$$\delta = \frac{\hat{P}_2}{M\omega^2 t_2}\left(t - \frac{\sin\omega t}{\omega}\right) \qquad \text{for } t \leq t_2$$

$$\delta = \frac{\hat{P}_2}{M\omega^2}\left[\left(\frac{1}{t_2} + \frac{1}{t_3 - t_2}\right)\frac{\sin\omega(t-t_2)}{\omega} + \left(1 - \frac{t-t_2}{t_3-t_2}\right) - \frac{\sin\omega t}{\omega t_2}\right] \qquad \text{for } t_2 \leq t \leq t_3$$

$$\delta = \frac{\hat{P}_2}{M\omega^3}\left[\left(\frac{1}{t_2} + \frac{1}{t_3 - t_2}\right)\sin\omega(t-t_2) - \frac{\sin\omega(t-t_3)}{(t_3-t_2)} - \frac{\sin\omega t}{t_2}\right] \qquad \text{for } t_3 \leq t$$

velocity

$$v = \frac{\hat{P}_2}{M\omega^2 t_2}\left(1 - \cos\omega t\right) \qquad \text{for } t \leq t_2$$

$$v = \frac{\hat{P}_2}{M\omega^2}\left[\left(\frac{1}{t_2} + \frac{1}{t_3 - t_2}\right)\frac{\sin\omega(t-t_2)}{\omega} + \left(1 - \frac{t-t_2}{t_3-t_2}\right) - \frac{\sin\omega t}{\omega t_2}\right] \qquad \text{for } t_2 \leq t \leq t_3$$

$$v = \frac{\hat{P}_2}{M\omega^2}\left[\left(\frac{1}{t_2} + \frac{1}{t_3 - t_2}\right)\cos\omega(t-t_2) - \frac{\cos\omega(t-t_3)}{(t_3-t_2)} - \frac{\cos\omega t}{t_2}\right] \qquad \text{for } t_3 \leq t$$

In the equations given above, M is the equivalent mass and $\omega$ is the natural frequency in radians/sec.

The response is calculated using the equations given above. The equivalent loads are calculated by multiplying the applied load by the modal displacement.

Comparison of Theoretical and Computed Solutions

The pages that follow are composed of

(a) input data to program DRTRAN based on test case data given above. This is identified by the heading "TRANSIENT DYNAMICS TEST CASE - CANTILEVER BEAM"

(b) the results of computations performed by DRTRAN, and identified by the heading "RESULTS FOR CASE 7" and

(c) the results based on the theoretical solutions outlined above, and these are identified by the heading "SET #3: TRIANGULAR AND SINUSOIDAL FORCE EXCITATION COMBINED".

In all cases the comparison is seen to be very satisfactory.

for force time history #2 (i.e. triangular)

displacement

$$\delta = \frac{\hat{P}_2}{M\omega^2 t_2}\left(t - \frac{\sin\omega t}{\omega}\right) \qquad \text{for } t \leq t_2$$

$$\delta = \frac{\hat{P}_2}{M\omega^2}\left[\left(\frac{1}{t_2} + \frac{1}{t_3 - t_2}\right)\frac{\sin\omega(t-t_2)}{\omega} + \left(1 - \frac{t-t_2}{t_3-t_2}\right) - \frac{\sin\omega t}{\omega t_2}\right] \qquad \text{for } t_2 \leq t \leq t_3$$

$$\delta = \frac{\hat{P}_2}{M\omega^3}\left[\left(\frac{1}{t_2} + \frac{1}{t_3 - t_2}\right)\sin\omega(t-t_2) - \frac{\sin\omega(t-t_3)}{(t_3-t_2)} - \frac{\sin\omega t}{t_2}\right] \qquad \text{for } t_3 \leq t$$

velocity

$$v = \frac{\hat{P}_2}{M\omega^2 t_2}\left(1 - \cos\omega t\right) \qquad \text{for } t \leq t_2$$

$$v = \frac{\hat{P}_2}{M\omega^2}\left[\left(\frac{1}{t_2} + \frac{1}{t_3 - t_2}\right)\frac{\sin\omega(t-t_2)}{\omega} + \left(1 - \frac{t-t_2}{t_3-t_2}\right) - \frac{\sin\omega t}{\omega t_2}\right] \qquad \text{for } t_2 \leq t \leq t_3$$

$$v = \frac{\hat{P}_2}{M\omega^2}\left[\left(\frac{1}{t_2} + \frac{1}{t_3 - t_2}\right)\cos\omega(t-t_2) - \frac{\cos\omega(t-t_3)}{(t_3-t_2)} - \frac{\cos\omega t}{t_2}\right] \qquad \text{for } t_3 \leq t$$

In the equations given above, M is the equivalent mass and $\omega$ is the natural frequency in radians/sec.

The response is calculated using the equations given above. The equivalent loads are calculated by multiplying the applied load by the modal displacement.

## Comparison of Theoretical and Computed Solutions

The pages that follow are composed of

(a) input data to program DRTRAN based on test case data given above. This is identified by the heading "TRANSIENT DYNAMICS TEST CASE - CANTILEVER BEAM"

(b) the results of computations performed by DRTRAN, and identified by the heading "RESULTS FOR CASE 7" and

(c) the results based on the theoretical solutions outlined above, and these are identified by the heading "SET #3: TRIANGULAR AND SINUSOIDAL FORCE EXCITATION COMBINED".

In all cases the comparison is seen to be very satisfactory.

TRANSIENT DYNAMICS TEST CASE - CANTILEVER BEAM
JOBNAME TDT

| MODE # | MODE TYPE | FREQUENCY (Hz) | FREQUENCY RAD/SEC | EQUIVALENT MASS | DAMPING (%) |
|---|---|---|---|---|---|
| 1 | ELST | 3.5462E-01 | 2.2281E+00 | 2.5195E+01 | 0.00 |
| 2 | ELST | 2.1976E+00 | 1.3806E+01 | 2.6428E+01 | 0.00 |
| 3 | ELST | 6.0916E+00 | 3.8276E+01 | 2.8839E+01 | 0.00 |

RESPONSE TIME DOMAIN

START TIME : 0.00

END TIME : 1.50
INCREMENT : 0.02

FORCE/AMPLITUDE EXCITATION DATA

| TIME | AMPLITUDE CASE 1 | CASE 2 |
|---|---|---|
| 0.00 | 0.000E+00 | 0.000E+00 |
| 0.02 | 1.560E+01 | 2.000E+01 |
| 0.04 | 3.090E+01 | [illegible] |
| [illegible] | [illegible] | [illegible] |
| 0.34 | 4.540E+01 | 0.000E+00 |
| 0.36 | 3.090E+01 | 0.000E+00 |
| 0.38 | 1.560E+01 | 0.000E+00 |
| 0.40 | 0.000E+00 | 0.000E+00 |

FORCE VECTOR #1 : AMPLITUDE CASE 1 - SCALE FACTOR 1.500E+00

| -NODE- | ----FX---- | ----FY---- | ----FZ---- | ----MX---- | ----MY---- | ----MZ---- |
|---|---|---|---|---|---|---|
| 11 | 0.000E+00 | -1.000E+00 | 0.000E+00 | 0.000E+00 | 0.000E+00 | 0.000E+00 |

FORCE VECTOR #2 : AMPLITUDE CASE 2 - SCALE FACTOR 5.000E-01

| -NODE- | ----FX---- | ----FY---- | ----FZ---- | ----MX---- | ----MY---- | ----MZ---- |
|---|---|---|---|---|---|---|
| 6 | 0.000E+00 | 5.000E-01 | 0.000E+00 | 0.000E+00 | 0.000E+00 | 0.000E+00 |

INITIAL CONDITIONS

INITIAL DISPLACEMENTS

| -NODE- | ----DX---- | ----DY---- | ----DZ---- | ----RX---- | ----RY---- | ----RZ---- |
|---|---|---|---|---|---|---|
| ALL | 0.000E+00 | 0.000E+00 | 0.000E+00 | 0.000E+00 | 0.000E+00 | 0.000E+00 |

INITIAL VELOCITIES

| -NODE- | ----VX---- | ----VY---- | ----VZ---- | ----WX---- | ----WY---- | ----WZ---- |
|---|---|---|---|---|---|---|
| ALL | 0.000E+00 | 0.000E+00 | 0.000E+00 | 0.000E+00 | 0.000E+00 | 0.000E+00 |

RESULTS FOR CASE 7

| TIME | DISPLACEMENT MODE 1 | MODE 2 | MODE 3 | VELOCITY MODE 1 | MODE 2 | MODE 3 |
|---|---|---|---|---|---|---|
| 0.00 | 0.000E+00 | 0.000E+00 | 0.000E+00 | 0.000E+00 | 0.000E+00 | 0.000E+00 |
| 0.02 | -5.743E-05 | -6.795E-05 | -5.187E-05 | -8.614E-03 | -1.017E-02 | -7.628E-03 |
| 0.04 | -4.581E-04 | -5.363E-04 | -3.789E-04 | -3.426E-02 | -3.973E-02 | -2.611E-02 |
| 0.06 | -1.537E-03 | -1.768E-03 | -1.096E-03 | -7.623E-02 | -8.583E-02 | -4.458E-02 |
| 0.08 | -3.608E-03 | -4.049E-03 | -2.086E-03 | -1.333E-01 | -1.439E-01 | -5.180E-02 |
| 0.10 | -6.959E-03 | -7.564E-03 | -3.056E-03 | -2.038E-01 | -2.081E-01 | -4.246E-02 |
| 0.12 | -1.184E-02 | -1.237E-02 | -3.696E-03 | -2.858E-01 | -2.717E-01 | -2.017E-02 |
| 0.14 | -1.845E-02 | -1.838E-02 | -3.846E-03 | -3.768E-01 | -3.278E-01 | 4.455E-03 |
| 0.16 | -2.695E-02 | -2.539E-02 | -3.581E-03 | -4.741E-01 | -3.698E-01 | 1.976E-02 |
| 0.18 | -3.744E-02 | -3.304E-02 | -3.162E-03 | -5.749E-01 | -3.921E-01 | 1.942E-02 |
| 0.20 | -4.995E-02 | -4.091E-02 | -2.893E-03 | -6.762E-01 | -3.901E-01 | 6.024E-03 |
| 0.22 | -6.452E-02 | -4.836E-02 | -2.950E-03 | -7.822E-01 | -3.462E-01 | -1.162E-02 |
| 0.24 | -8.125E-02 | -5.447E-02 | -3.304E-03 | -8.904E-01 | -2.596E-01 | -2.132E-02 |
| 0.26 | -1.001E-01 | -5.858E-02 | -3.690E-03 | -9.911E-01 | -1.479E-01 | -1.433E-02 |
| 0.28 | -1.208E-01 | -6.026E-02 | -3.775E-03 | -1.081E+00 | -1.700E-02 | 7.691E-03 |
| 0.30 | -1.432E-01 | -5.918E-02 | -3.349E-03 | -1.158E+00 | 1.256E-01 | 3.453E-02 |
| 0.32 | -1.671E-01 | -5.521E-02 | -2.450E-03 | -1.220E+00 | 2.711E-01 | 5.305E-02 |
| 0.34 | -1.919E-01 | -4.838E-02 | -1.343E-03 | -1.264E+00 | 4.104E-01 | 5.450E-02 |
| 0.36 | -2.175E-01 | -3.890E-02 | -3.828E-04 | -1.290E+00 | 5.343E-01 | 3.936E-02 |
| 0.38 | -2.434E-01 | -2.717E-02 | 1.819E-04 | -1.294E+00 | 6.345E-01 | 1.701E-02 |
| 0.40 | -2.691E-01 | -1.373E-02 | 3.371E-04 | -1.278E+00 | 7.041E-01 | 4.767E-04 |
| 0.42 | -2.944E-01 | 6.971E-04 | 2.517E-04 | -1.250E+00 | 7.291E-01 | -8.597E-03 |
| 0.44 | -3.191E-01 | 1.507E-02 | 2.584E-05 | -1.220E+00 | 6.988E-01 | -1.287E-02 |
| 0.46 | -3.432E-01 | 2.830E-02 | -2.144E-04 | -1.187E+00 | 6.156E-01 | -9.968E-03 |
| 0.48 | -3.666E-01 | 3.938E-02 | -3.351E-04 | -1.152E+00 | 4.857E-01 | -1.500E-03 |
| 0.50 | -3.892E-01 | 4.748E-02 | -2.687E-04 | -1.114E+00 | 3.191E-01 | 7.805E-03 |
| 0.52 | -4.111E-01 | 5.198E-02 | -5.248E-05 | -1.074E+00 | 1.282E-01 | 1.276E-02 |
| 0.54 | -4.322E-01 | 5.254E-02 | 1.931E-04 | -1.032E+00 | -7.234E-02 | 1.059E-02 |
| 0.56 | -4.524E-01 | 4.912E-02 | 3.309E-04 | -9.885E-01 | -2.674E-01 | 2.514E-03 |
| 0.58 | -4.717E-01 | 4.198E-02 | 2.841E-04 | -9.426E-01 | -4.422E-01 | -6.963E-03 |
| 0.60 | -4.901E-01 | 3.166E-02 | 7.878E-05 | -8.948E-01 | -5.835E-01 | -1.256E-02 |
| 0.62 | -5.075E-01 | 1.894E-02 | -1.705E-04 | -8.453E-01 | -6.806E-01 | -1.114E-02 |
| 0.64 | -5.239E-01 | 4.778E-03 | -3.246E-04 | -7.941E-01 | -7.261E-01 | -3.512E-03 |
| 0.66 | -5.393E-01 | -9.742E-03 | -2.976E-04 | -7.413E-01 | -7.166E-01 | 6.078E-03 |
| 0.68 | -5.536E-01 | -2.352E-02 | -1.046E-04 | -6.870E-01 | -6.528E-01 | 1.228E-02 |
| 0.70 | -5.667E-01 | -3.552E-02 | 1.468E-04 | -6.314E-01 | -5.395E-01 | 1.163E-02 |
| 0.72 | -5.788E-01 | -4.483E-02 | 3.163E-04 | -5.745E-01 | -3.853E-01 | 4.488E-03 |
| 0.74 | -5.897E-01 | -5.074E-02 | 3.093E-04 | -5.165E-01 | -2.019E-01 | -5.154E-03 |
| 0.76 | -5.995E-01 | -5.280E-02 | 1.297E-04 | -4.575E-01 | -3.235E-03 | -1.192E-02 |
| 0.78 | -6.080E-01 | -5.087E-02 | -1.222E-04 | -3.975E-01 | 1.957E-01 | -1.203E-02 |
| 0.80 | -6.153E-01 | -4.507E-02 | -3.060E-04 | -3.368E-01 | 3.798E-01 | -5.435E-03 |
| 0.82 | -6.215E-01 | -3.587E-02 | -3.190E-04 | -2.753E-01 | 5.351E-01 | 4.197E-03 |
| 0.84 | -6.264E-01 | -2.394E-02 | -1.541E-04 | -2.134E-01 | 6.499E-01 | 1.149E-02 |
| 0.86 | -6.300E-01 | -1.020E-02 | 9.688E-05 | -1.510E-01 | 7.154E-01 | 1.237E-02 |
| 0.88 | -6.324E-01 | 4.311E-03 | 2.938E-04 | -8.831E-02 | 7.267E-01 | 6.348E-03 |
| 0.90 | -6.335E-01 | 1.850E-02 | 3.267E-04 | -2.545E-02 | 6.829E-01 | -3.214E-03 |
| 0.92 | -6.334E-01 | 3.128E-02 | 1.774E-04 | 3.746E-02 | 5.874E-01 | -1.098E-02 |
| 0.94 | -6.320E-01 | 4.170E-02 | -7.091E-05 | 1.003E-01 | 4.474E-01 | -1.262E-02 |
| 0.96 | -6.294E-01 | 4.895E-02 | -2.797E-04 | 1.629E-01 | 2.734E-01 | -7.221E-03 |
| 0.98 | -6.255E-01 | 5.249E-02 | -3.324E-04 | 2.252E-01 | 7.877E-02 | 2.210E-03 |
| 1.00 | -6.204E-01 | 5.206E-02 | -1.996E-04 | 2.871E-01 | -1.219E-01 | 1.041E-02 |

| | | | | | | |
|---|---|---|---|---|---|---|
| 1.02 | -6.140E-01 | 4.766E-02 | 4.449E-05 | 3.484E-01 | -3.132E-01 | 1.280E-02 |
| 1.04 | -6.065E-01 | 3.969E-02 | 2.638E-04 | 4.090E-01 | -4.809E-01 | 8.049E-03 |
| 1.06 | -5.977E-01 | 2.869E-02 | 3.359E-04 | 4.688E-01 | -6.121E-01 | -1.193E-03 |
| 1.08 | -5.877E-01 | 1.552E-02 | 2.206E-04 | 5.277E-01 | -6.969E-01 | -9.769E-03 |
| 1.10 | -5.766E-01 | 1.165E-03 | -1.776E-05 | 5.855E-01 | -7.289E-01 | -1.209E-02 |
| 1.12 | -5.643E-01 | -1.327E-02 | -2.462E-04 | 6.421E-01 | -7.057E-01 | -8.825E-03 |
| 1.14 | -5.509E-01 | -2.671E-02 | -3.373E-04 | 6.975E-01 | -6.290E-01 | 1.677E-04 |
| 1.16 | -5.364E-01 | -3.811E-02 | -2.402E-04 | 7.515E-01 | -5.046E-01 | 9.067E-03 |
| 1.18 | -5.209E-01 | -4.663E-02 | -9.029E-06 | 8.040E-01 | -3.420E-01 | 1.291E-02 |
| 1.20 | -5.043E-01 | -5.162E-02 | 2.272E-04 | 8.549E-01 | -1.535E-01 | 9.546E-03 |
| 1.22 | -4.867E-01 | -5.270E-02 | 3.366E-04 | 9.041E-01 | 4.671E-02 | 8.584E-04 |
| 1.24 | -4.681E-01 | -4.978E-02 | 2.582E-04 | 9.515E-01 | 2.433E-01 | -8.308E-03 |
| 1.26 | -4.486E-01 | -4.309E-02 | 3.579E-05 | 9.970E-01 | 4.215E-01 | -1.284E-02 |
| 1.28 | -4.283E-01 | -3.313E-02 | -2.066E-04 | 1.041E+00 | 5.678E-01 | -1.021E-02 |
| 1.30 | -4.070E-01 | -2.066E-02 | -3.338E-04 | 1.082E+00 | 6.710E-01 | -1.879E-03 |
| 1.32 | -3.850E-01 | -6.630E-03 | -2.747E-04 | 1.121E+00 | 7.233E-01 | 7.497E-03 |
| 1.34 | -3.622E-01 | 7.905E-03 | -6.232E-05 | 1.158E+00 | 7.209E-01 | 1.269E-02 |
| 1.36 | -3.387E-01 | 2.184E-02 | 1.848E-04 | 1.193E+00 | 6.638E-01 | 1.080E-02 |
| 1.38 | -3.145E-01 | 3.412E-02 | 3.268E-04 | 1.226E+00 | 5.564E-01 | 2.888E-03 |
| 1.40 | -2.897E-01 | 4.382E-02 | 2.893E-04 | 1.256E+00 | 4.069E-01 | -6.638E-03 |
| 1.42 | -2.643E-01 | 5.019E-02 | 8.845E-05 | 1.283E+00 | 2.265E-01 | -1.246E-02 |
| 1.44 | -2.383E-01 | 5.276E-02 | -1.618E-04 | 1.308E+00 | 2.894E-02 | -1.133E-02 |
| 1.46 | -2.120E-01 | 5.133E-02 | -3.218E-04 | 1.331E+00 | -1.708E-01 | -3.878E-03 |
| 1.48 | -1.851E-01 | 4.602E-02 | -3.022E-04 | 1.350E+00 | -3.576E-01 | 5.738E-03 |
| 1.50 | -1.580E-01 | 3.721E-02 | -1.140E-04 | 1.367E+00 | -5.173E-01 | 1.215E-02 |

SET #3 : TRIANGULAR AND SINOSOIDAL FORCE EXCITATION COMBINED

| TIME | DISPLACEMENT MODE 1 | MODE 2 | MODE 3 | VELOCITY MODE 1 | MODE 2 | MODE 3 |
|---|---|---|---|---|---|---|
| 0.00 | 0.000E+00 | 0.000E+00 | 0.000E+00 | 0.000E+00 | 0.000E+00 | 0.000E+00 |
| 0.02 | -5.779E-05 | -6.828E-05 | -5.216E-05 | -8.660E-03 | -1.021E-02 | -7.665E-03 |
| 0.04 | -4.603E-04 | -5.383E-04 | -3.805E-04 | -3.439E-02 | -3.984E-02 | -2.619E-02 |
| 0.06 | -1.543E-03 | -1.773E-03 | -1.100E-03 | -7.647E-02 | -8.601E-02 | -4.467E-02 |
| 0.08 | -3.620E-03 | -4.059E-03 | -2.091E-03 | -1.337E-01 | -1.442E-01 | -5.186E-02 |
| 0.10 | -6.980E-03 | -7.580E-03 | -3.061E-03 | -2.044E-01 | -2.084E-01 | -4.248E-02 |
| 0.12 | -1.187E-02 | -1.239E-02 | -3.702E-03 | -2.865E-01 | -2.721E-01 | -2.018E-02 |
| 0.14 | -1.850E-02 | -1.841E-02 | -3.853E-03 | -3.777E-01 | -3.283E-01 | 4.457E-03 |
| 0.16 | -2.702E-02 | -2.543E-02 | -3.587E-03 | -4.753E-01 | -3.704E-01 | 1.975E-02 |
| 0.18 | -3.754E-02 | -3.310E-02 | -3.169E-03 | -5.763E-01 | -3.926E-01 | 1.942E-02 |
| 0.20 | -5.008E-02 | -4.097E-02 | -2.899E-03 | -6.778E-01 | -3.905E-01 | 6.022E-03 |
| 0.22 | -6.468E-02 | -4.844E-02 | -2.957E-03 | -7.840E-01 | -3.465E-01 | -1.162E-02 |
| 0.24 | -8.145E-02 | -5.455E-02 | -3.310E-03 | -8.924E-01 | -2.598E-01 | -2.132E-02 |
| 0.26 | -1.003E-01 | -5.866E-02 | -3.696E-03 | -9.933E-01 | -1.480E-01 | -1.433E-02 |
| 0.28 | -1.211E-01 | -6.033E-02 | -3.781E-03 | -1.084E+00 | -1.684E-02 | 7.704E-03 |
| 0.30 | -1.436E-01 | -5.926E-02 | -3.355E-03 | -1.161E+00 | 1.259E-01 | 3.456E-02 |
| 0.32 | -1.675E-01 | -5.528E-02 | -2.455E-03 | -1.223E+00 | 2.717E-01 | 5.311E-02 |
| 0.34 | -1.924E-01 | -4.843E-02 | -1.347E-03 | -1.267E+00 | 4.111E-01 | 5.459E-02 |
| 0.36 | -2.180E-01 | -3.894E-02 | -3.843E-04 | -1.292E+00 | 5.351E-01 | 3.943E-02 |
| 0.38 | -2.439E-01 | -2.718E-02 | 1.816E-04 | -1.297E+00 | 6.354E-01 | 1.704E-02 |
| 0.40 | -2.698E-01 | -1.372E-02 | 3.370E-04 | -1.281E+00 | 7.050E-01 | 4.727E-04 |
| 0.42 | -2.951E-01 | 7.172E-04 | 2.515E-04 | -1.253E+00 | 7.300E-01 | -8.597E-03 |
| 0.44 | -3.199E-01 | 1.510E-02 | 2.572E-05 | -1.222E+00 | 6.996E-01 | -1.287E-02 |
| 0.46 | -3.440E-01 | 2.835E-02 | -2.144E-04 | -1.189E+00 | 6.162E-01 | -9.962E-03 |
| 0.48 | -3.674E-01 | 3.944E-02 | -3.349E-04 | -1.154E+00 | 4.861E-01 | -1.495E-03 |
| 0.50 | -3.901E-01 | 4.754E-02 | -2.686E-04 | -1.116E+00 | 3.191E-01 | 7.806E-03 |
| 0.52 | -4.120E-01 | 5.204E-02 | -5.231E-05 | -1.076E+00 | 1.280E-01 | 1.275E-02 |
| 0.54 | -4.331E-01 | 5.260E-02 | 1.931E-04 | -1.034E+00 | -7.290E-02 | 1.058E-02 |
| 0.56 | -4.534E-01 | 4.916E-02 | 3.308E-04 | -9.899E-01 | -2.682E-01 | 2.507E-03 |
| 0.58 | -4.727E-01 | 4.200E-02 | 2.839E-04 | -9.438E-01 | -4.432E-01 | -6.966E-03 |
| 0.60 | -4.911E-01 | 3.166E-02 | 7.858E-05 | -8.959E-01 | -5.846E-01 | -1.255E-02 |
| 0.62 | -5.085E-01 | 1.891E-02 | -1.706E-04 | -8.461E-01 | -6.817E-01 | -1.113E-02 |
| 0.64 | -5.249E-01 | 4.737E-03 | -3.246E-04 | -7.947E-01 | -7.271E-01 | -3.504E-03 |
| 0.66 | -5.403E-01 | -9.800E-03 | -2.974E-04 | -7.417E-01 | -7.174E-01 | 6.082E-03 |
| 0.68 | -5.546E-01 | -2.359E-02 | -1.043E-04 | -6.872E-01 | -6.533E-01 | 1.227E-02 |
| 0.70 | -5.678E-01 | -3.560E-02 | 1.470E-04 | -6.314E-01 | -5.396E-01 | 1.162E-02 |
| 0.72 | -5.798E-01 | -4.491E-02 | 3.163E-04 | -5.743E-01 | -3.851E-01 | 4.478E-03 |
| 0.74 | -5.908E-01 | -5.081E-02 | 3.091E-04 | -5.160E-01 | -2.014E-01 | -5.160E-03 |
| 0.76 | -6.005E-01 | -5.286E-02 | 1.295E-04 | -4.567E-01 | -2.387E-03 | -1.192E-02 |
| 0.78 | -6.090E-01 | -5.090E-02 | -1.224E-04 | -3.965E-01 | 1.968E-01 | -1.203E-02 |
| 0.80 | -6.163E-01 | -4.509E-02 | -3.060E-04 | -3.356E-01 | 3.810E-01 | -5.425E-03 |
| 0.82 | -6.224E-01 | -3.585E-02 | -3.188E-04 | -2.739E-01 | 5.364E-01 | 4.205E-03 |
| 0.84 | -6.273E-01 | -2.390E-02 | -1.538E-04 | -2.117E-01 | 6.511E-01 | 1.149E-02 |
| 0.86 | -6.309E-01 | -1.014E-02 | 9.711E-05 | -1.491E-01 | 7.165E-01 | 1.236E-02 |
| 0.88 | -6.333E-01 | 4.392E-03 | 2.938E-04 | -8.622E-02 | 7.275E-01 | 6.337E-03 |
| 0.90 | -6.343E-01 | 1.859E-02 | 3.265E-04 | -2.314E-02 | 6.834E-01 | -3.223E-03 |
| 0.92 | -6.342E-01 | 3.138E-02 | 1.771E-04 | 3.998E-02 | 5.875E-01 | -1.098E-02 |
| 0.94 | -6.328E-01 | 4.179E-02 | -7.118E-05 | 1.030E-01 | 4.470E-01 | -1.262E-02 |
| 0.96 | -6.301E-01 | 4.904E-02 | -2.797E-04 | 1.659E-01 | 2.727E-01 | -7.209E-03 |
| 0.98 | -6.261E-01 | 5.256E-02 | -3.322E-04 | 2.284E-01 | 7.765E-02 | 2.222E-03 |
| 1.00 | -6.209E-01 | 5.210E-02 | -1.993E-04 | 2.904E-01 | -1.233E-01 | 1.041E-02 |

| | | | | | | |
|---|---|---|---|---|---|---|
| 1.02 | -6.145E-01 | 4.769E-02 | 4.481E-05 | 3.519E-01 | -3.148E-01 | 1.279E-02 |
| 1.04 | -6.069E-01 | 3.967E-02 | 2.639E-04 | 4.127E-01 | -4.825E-01 | 8.036E-03 |
| 1.06 | -5.980E-01 | 2.864E-02 | 3.357E-04 | 4.726E-01 | -6.136E-01 | -1.206E-03 |
| 1.08 | -5.880E-01 | 1.544E-02 | 2.202E-04 | 5.317E-01 | -6.982E-01 | -9.774E-03 |
| 1.10 | -5.767E-01 | 1.063E-03 | -1.815E-05 | 5.896E-01 | -7.299E-01 | -1.289E-02 |
| 1.12 | -5.644E-01 | -1.339E-02 | -2.464E-04 | 6.464E-01 | -7.062E-01 | -8.812E-03 |
| 1.14 | -5.509E-01 | -2.683E-02 | -3.372E-04 | 7.019E-01 | -6.290E-01 | 1.824E-04 |
| 1.16 | -5.363E-01 | -3.823E-02 | -2.398E-04 | 7.560E-01 | -5.041E-01 | 9.075E-03 |
| 1.18 | -5.207E-01 | -4.674E-02 | -8.623E-06 | 8.086E-01 | -3.410E-01 | 1.290E-02 |
| 1.20 | -5.040E-01 | -5.170E-02 | 2.274E-04 | 8.596E-01 | -1.521E-01 | 9.532E-03 |
| 1.22 | -4.863E-01 | -5.274E-02 | 3.365E-04 | 9.088E-01 | 4.840E-02 | 8.421E-04 |
| 1.24 | -4.676E-01 | -4.979E-02 | 2.579E-04 | 9.563E-01 | 2.452E-01 | -8.318E-03 |
| 1.26 | -4.481E-01 | -4.306E-02 | 3.534E-05 | 1.002E+00 | 4.234E-01 | -1.284E-02 |
| 1.28 | -4.276E-01 | -3.307E-02 | -2.069E-04 | 1.045E+00 | 5.696E-01 | -1.019E-02 |
| 1.30 | -4.063E-01 | -2.057E-02 | -3.337E-04 | 1.087E+00 | 6.725E-01 | -1.861E-03 |
| 1.32 | -3.841E-01 | -6.507E-03 | -2.743E-04 | 1.126E+00 | 7.245E-01 | 7.509E-03 |
| 1.34 | -3.612E-01 | 8.046E-03 | -6.184E-05 | 1.163E+00 | 7.215E-01 | 1.269E-02 |
| 1.36 | -3.376E-01 | 2.199E-02 | 1.851E-04 | 1.198E+00 | 6.639E-01 | 1.079E-02 |
| 1.38 | -3.133E-01 | 3.426E-02 | 3.288E-04 | 1.231E+00 | 5.559E-01 | 2.869E-03 |
| 1.40 | -2.884E-01 | 4.394E-02 | 2.890E-04 | 1.260E+00 | 4.058E-01 | -6.652E-03 |
| 1.42 | -2.629E-01 | 5.029E-02 | 8.794E-05 | 1.288E+00 | 2.249E-01 | -1.246E-02 |
| 1.44 | -2.369E-01 | 5.282E-02 | -1.622E-04 | 1.313E+00 | 2.697E-02 | -1.132E-02 |
| 1.46 | -2.104E-01 | 5.135E-02 | -3.218E-04 | 1.335E+00 | -1.730E-01 | -3.858E-03 |
| 1.48 | -1.835E-01 | 4.599E-02 | -3.019E-04 | 1.355E+00 | -3.599E-01 | 5.753E-03 |
| 1.50 | -1.562E-01 | 3.714E-02 | -1.135E-04 | 1.372E+00 | -5.194E-01 | 1.215E-02 |

# A P P E N D I X  G

## Response to Idealized Version of Vertical Force

The typical time history of the force, vertical as well as horizontal, is composed of two parts; first, a gradually increasing force, and second, a series of short duration impulses. The aim of this exercise is to examine the sensitivity of the response, particularly the elastic modes, to the character of the impulsive forces.

A simple approach is taken here in idealizing the applied force. The first part of the force is idealized as a ramp, and the second part as a series of equispaced rectangular impulses. This is illustrated in the sketch below.

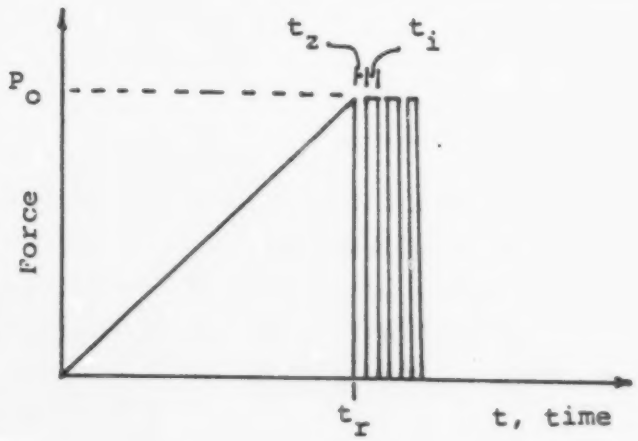


$P_o$ = maximum force
$t_r$ = duration of ramp
$t_z$ = duration of zero force
$t_i$ = duration of rectangular impulse

The magnitude of the impulsive force is assumed to be equal to $P_o$.

The response of a single degree of freedom system to the form of force illustrated below is available in closed form. The undamped response is computed using the Duhamel integral approach which is documented in most engineering vibration texts (for example: J.S. Przemieniecki, Theory of Matrix Structural Analysis, 1968, McGraw-Hill).

The response was computed for the first elastic mode which has a natural frequency of 5.722 rad/sec.

The loading idealized is based on the vertical force load case given in Figure 28 of reference 2. The properties of the ramp assumed are:

$$P_o = 22.6 \text{ MN}$$
$$t_r = 8.6 \text{ secs.}$$

The response was computed for a variety of combinations of durations of rectangular impulse and zero force. A selection of results are given in Figures G1, G2 and G3. The vertical dashed lines indicate the onset of either a rectangular impulse or zero force; lines marked 'P' indicate the onset of an impulse.

In Figure G1 the pulses and the zero forces both have a duration of 0.2 secs., and this is broadly representative of the forces given in reference 2. In Figure G2, the durations of pulse and zero force are 0.3 and 0.1 secs. respectively. The dynamic amplitudes are reduced when compared with the previous case. The amplitude of free vibration response (for times greater than about 13.5 secs.) is clearly dependent on the nature of response at the end of the final

pulse. Figure G3 illustrates the dynamic amplification which can occur when the frequency of pulses (1 Hz) is close to the natural frequency (0.91 Hz).

These results suggest that the response in the region of the impulsive forces and the free vibration response is very sensitive to the nature of the impulsive forces. This sensitivity can be expected to reduce when the natural frequency is very much greater, or less, than the frequency of pulses.

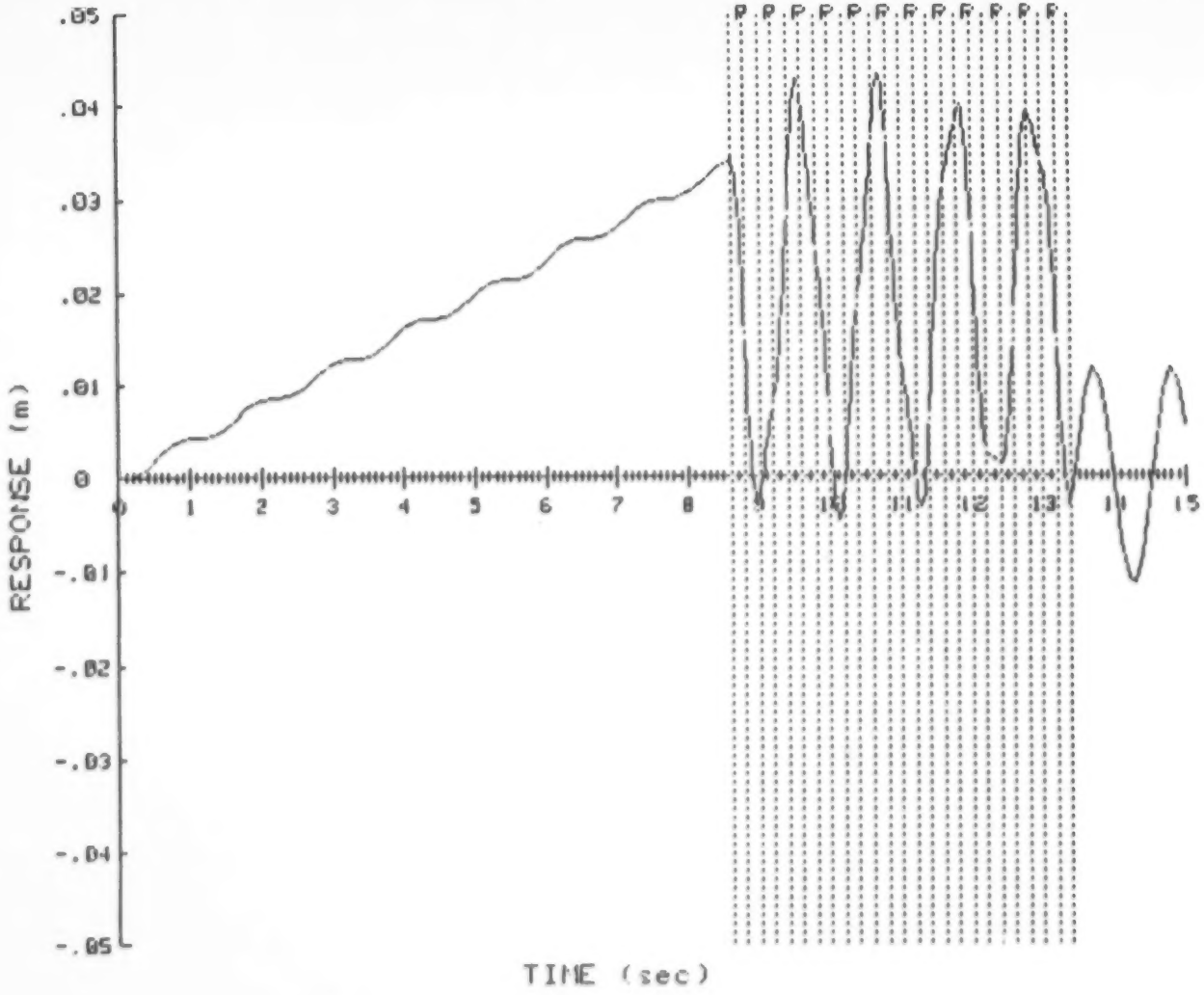
.05
.04
.03
.02
.01
0
-.01
-.02
-.03
-.04
-.05
RESPONSE (m)
0 1 2 3 4 5 6 7 8 9 10 11 12 13 14 15
TIME (sec)

FIGURE C1

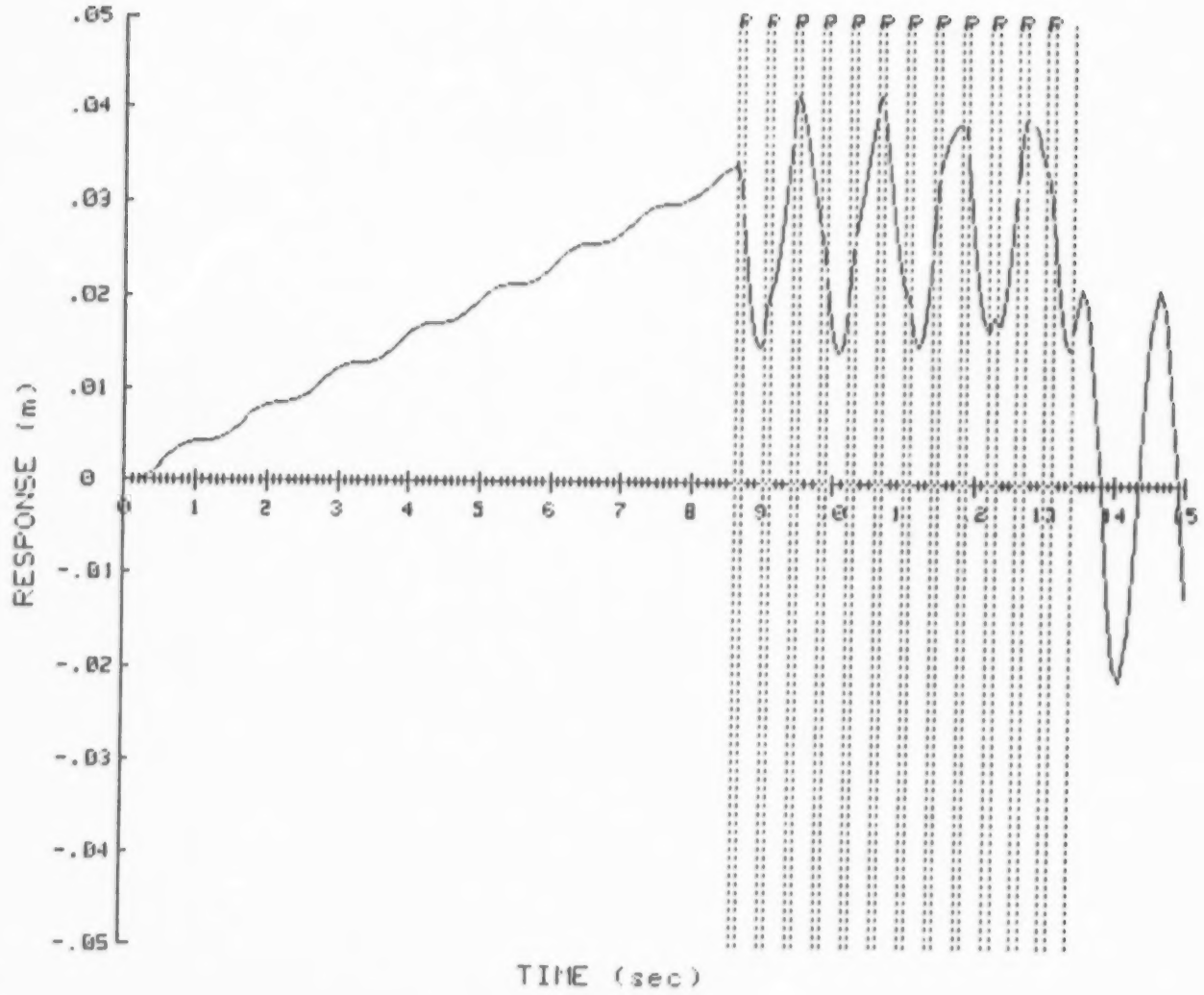


FIGURE G2

A-123

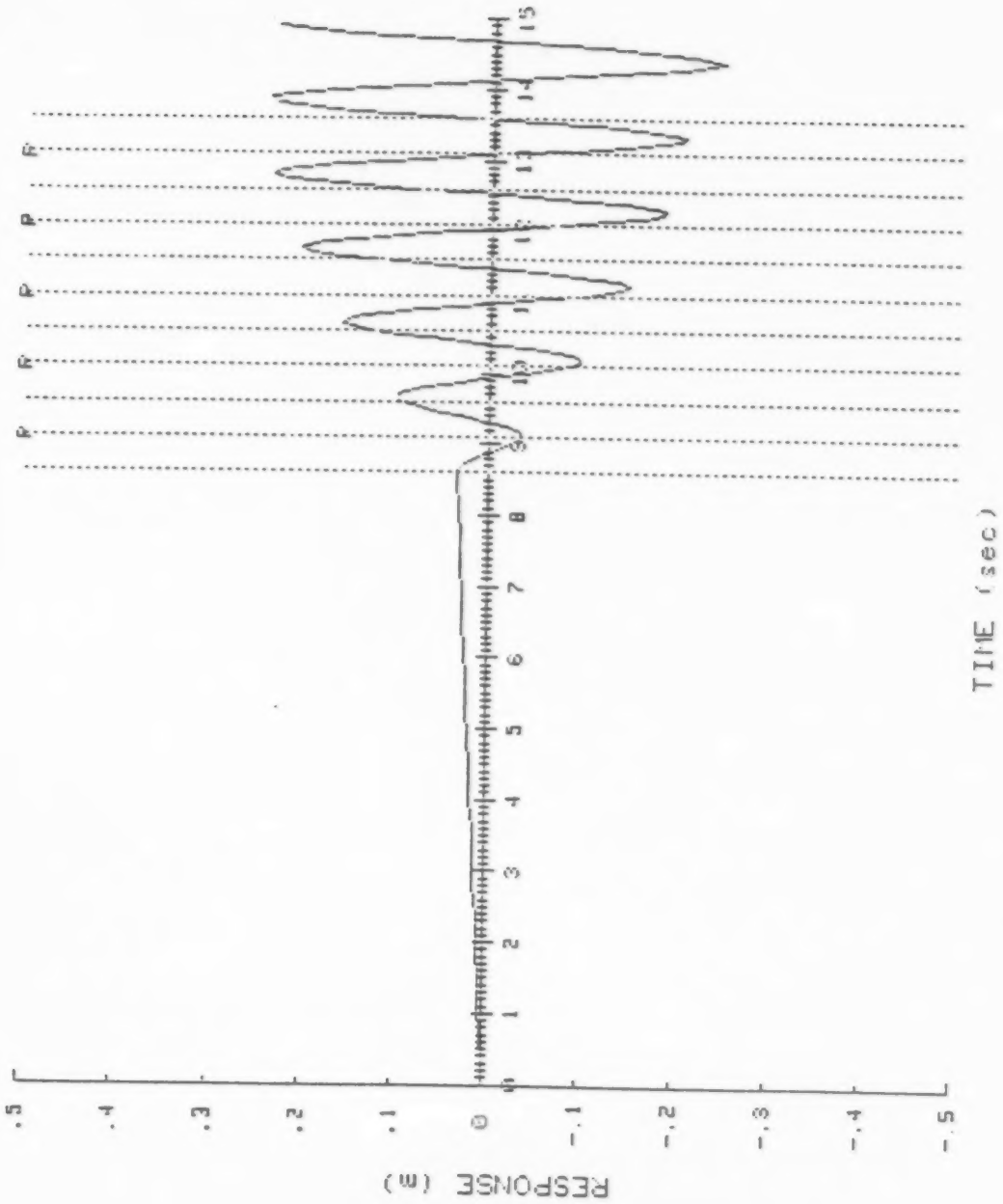


FIGURE G3

# APPENDIX II

## ADDITIONAL CALCULATION DATA OF THE PREDICTION MODEL

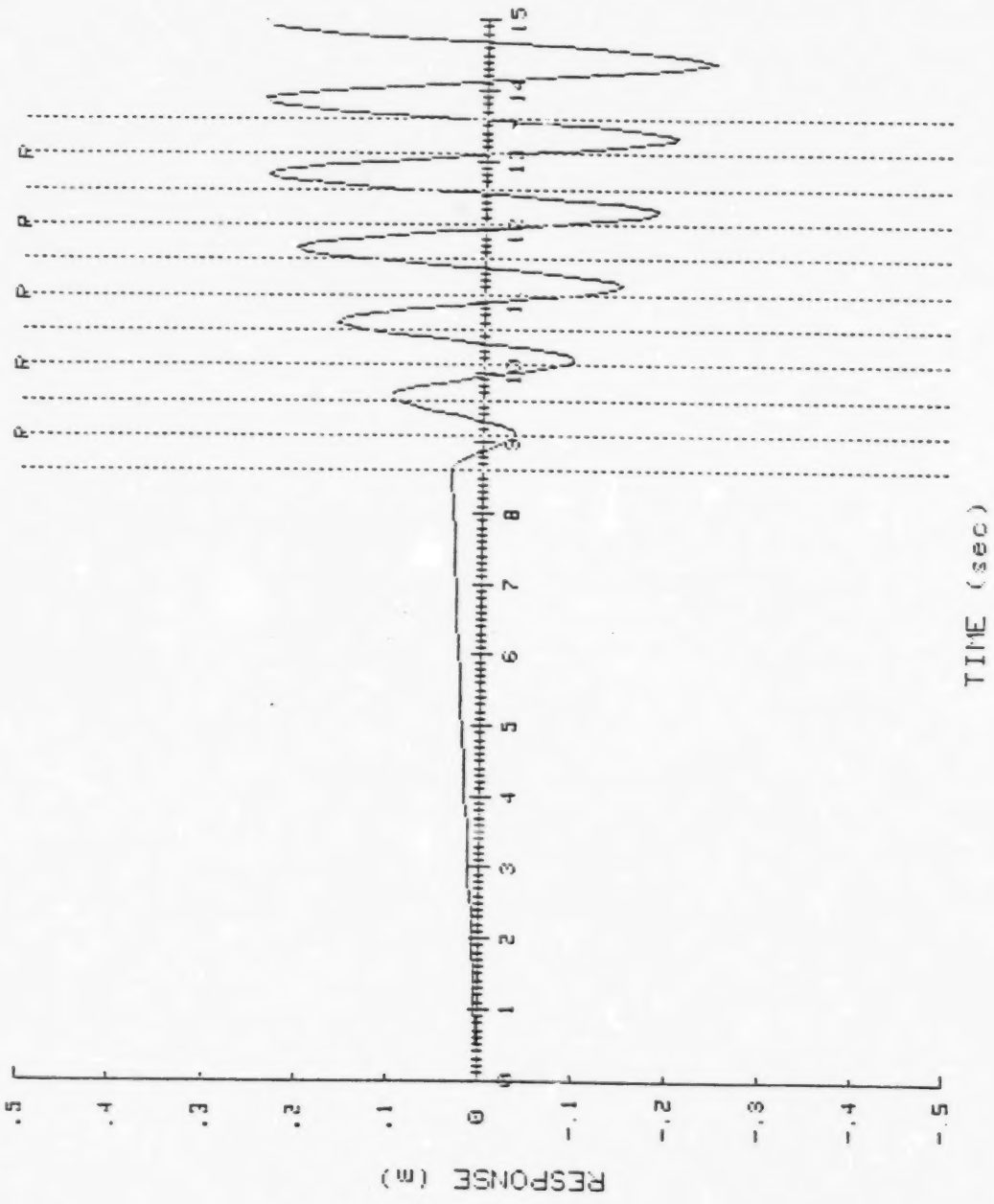
RESPONSE (m)
.5
.4
.3
.2
.1
0
-.1
-.2
-.3
-.4
-.5
TIME (sec)
0
1
2
3
4
5
6
7
8
9
10
11
12
13
14
15
P
P
P
P
P

FIGURE G3

# APPENDIX II

## ADDITIONAL CALCULATION DATA OF THE PREDICTION MODEL

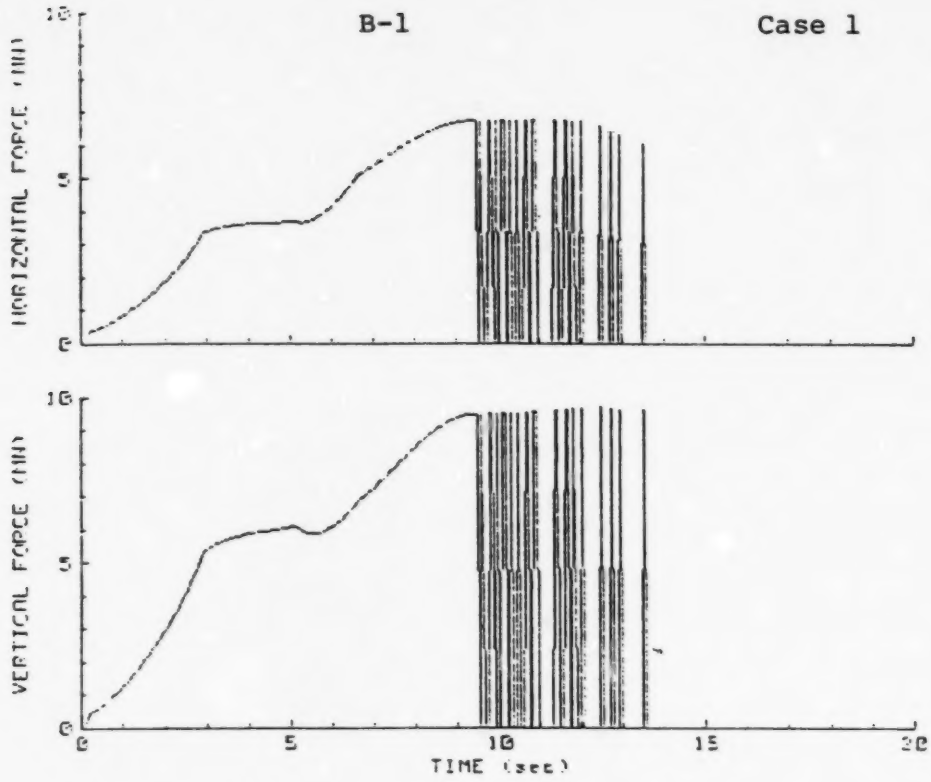


| | |
|---|---|
| INITIAL VELOCITY | 2.00 kn |
| DRAUGHT | 10.00 m |
| ICE FLOE THICKNESS | 10.00 m |
| ICE FREEBOARD | 0.00 m |

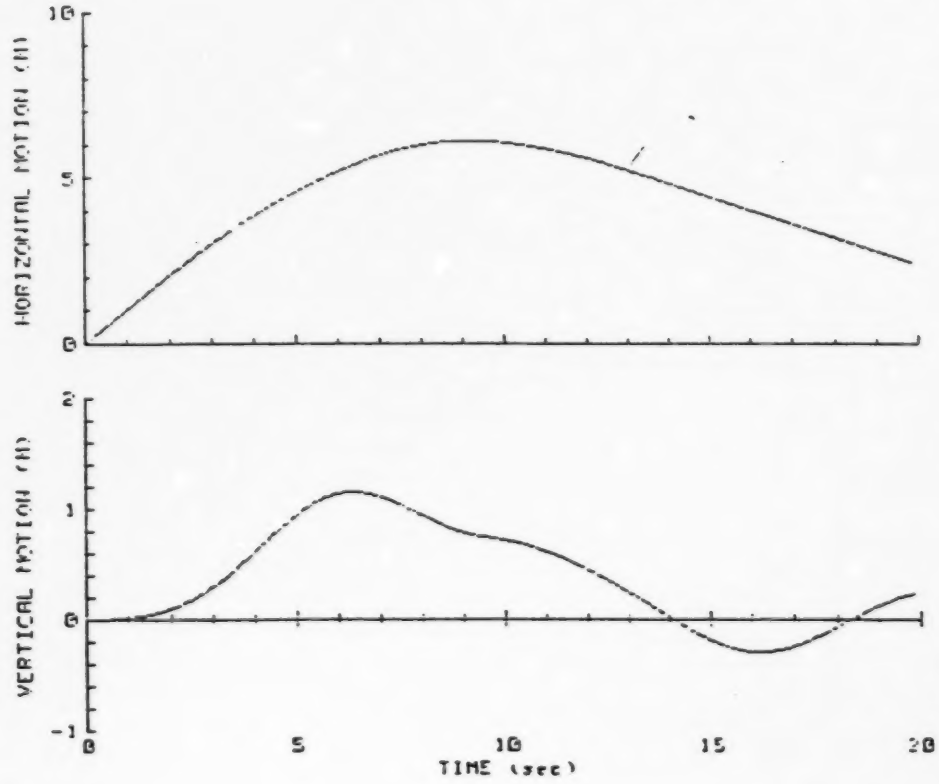

Case 2

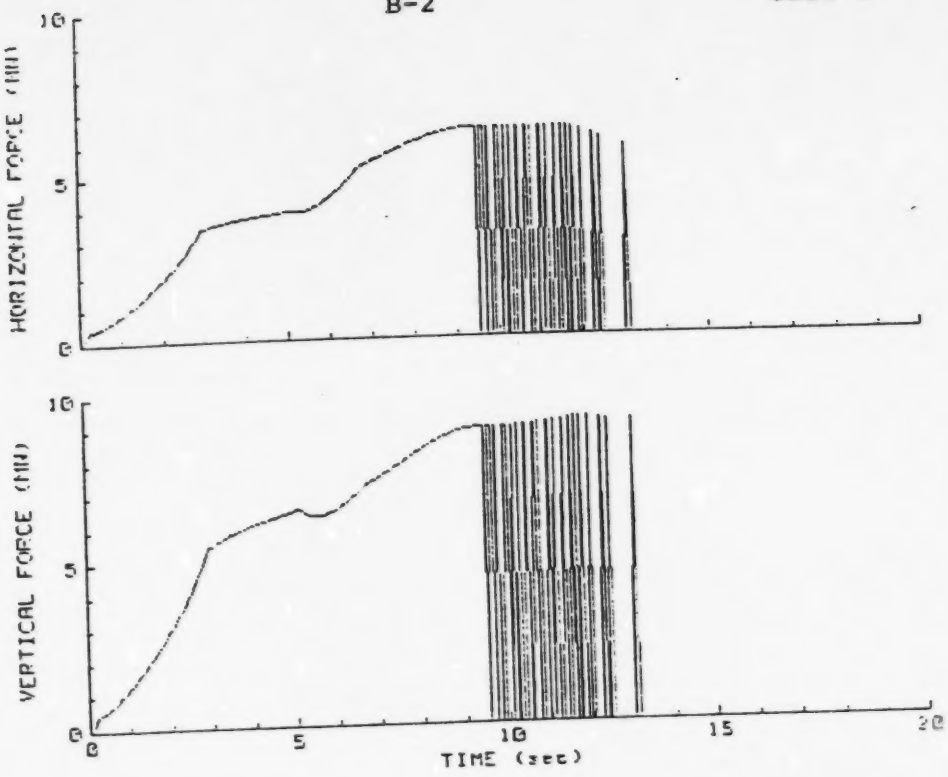


| | |
|---|---|
| INITIAL VELOCITY | 2.00 kn |
| DRAUGHT | 10.00 m |
| ICE FLOE THICKNESS | 10.00 m |
| ICE FREEBOARD | 0.00 m |

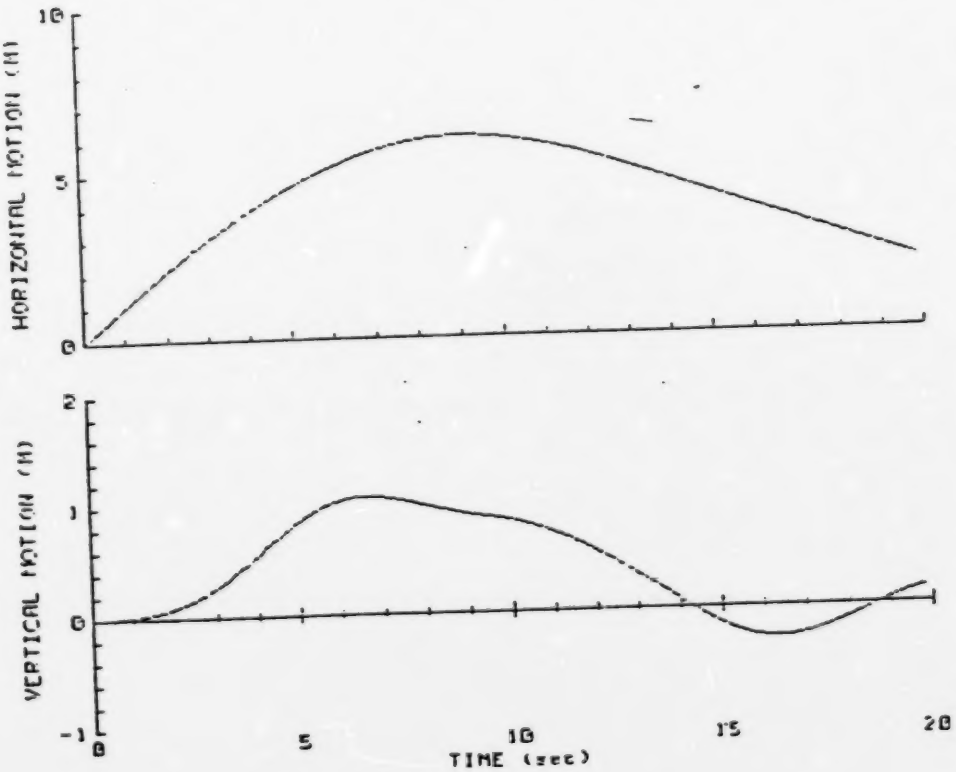

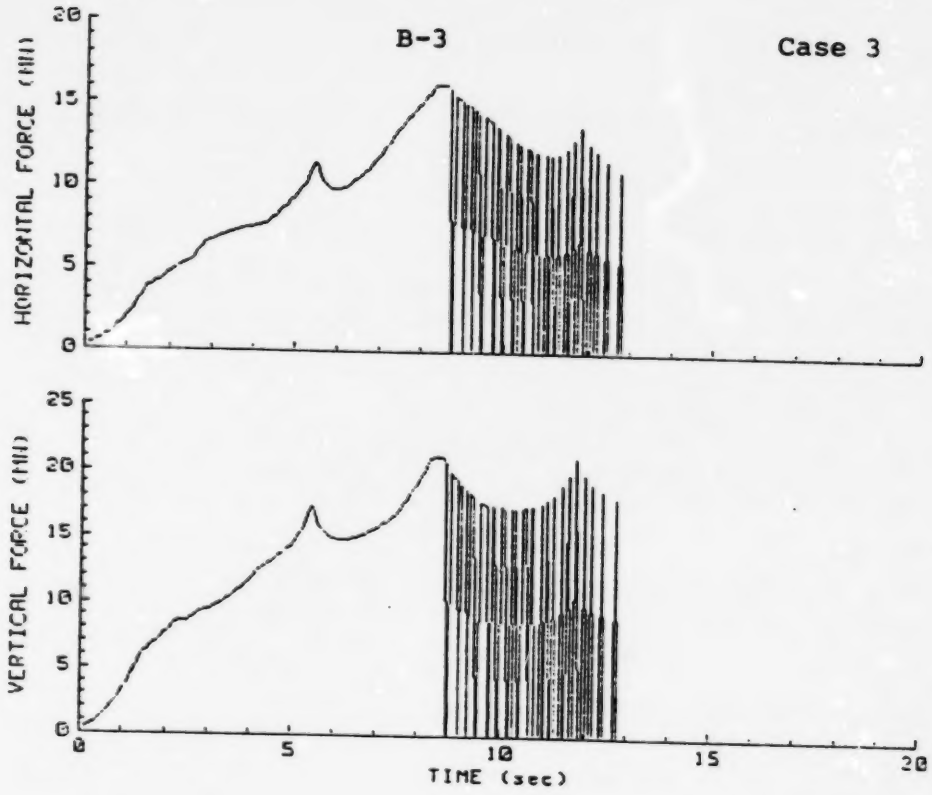


| | |
|---|---|
| INITIAL VELOCITY | 4.00 kn |
| DRAUGHT | 10.00 m |
| ICE FLOE THICKNESS | 10.00 m |
| ICE FREEBOARD | 0.00 m |

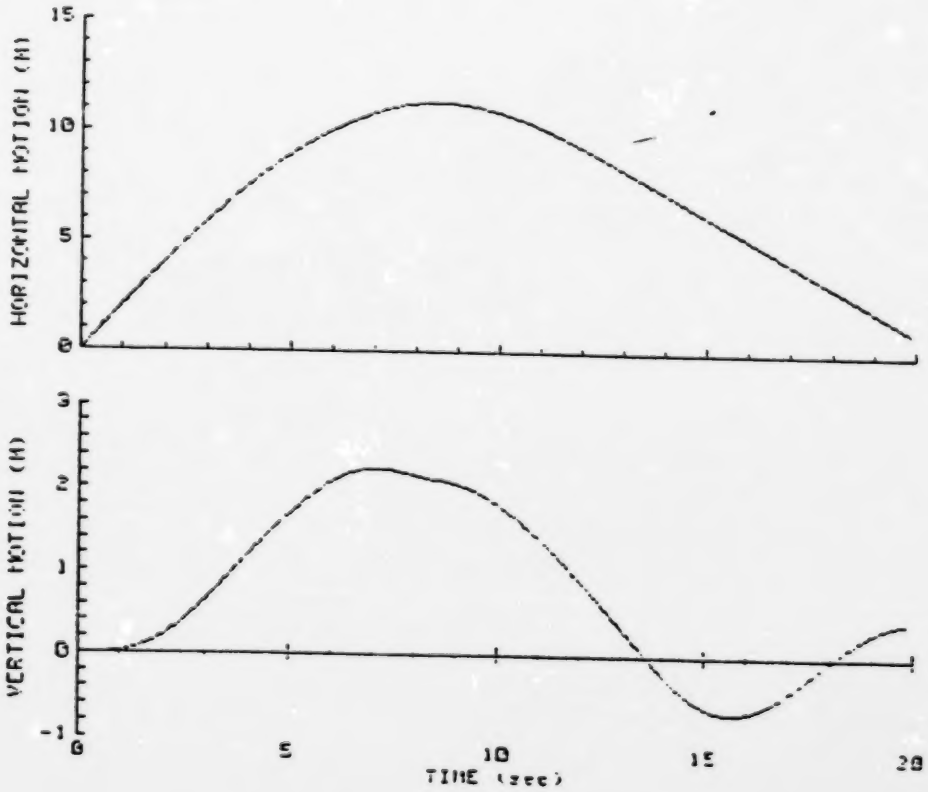

TABLE OF MAXIMUM VALUES FOR CASE 3

| VARIABLE | MAX. VALUE | TIME |
|---|---|---|
| NORMAL DEFLECTION : RIGID MODE #1 | 1.129E+01 | 6.45 |
| NORMAL DEFLECTION : RIGID MODE #2 | 1.900E+00 | 7.25 |
| NORMAL DEFLECTION : RIGID MODE #3 | -9.213E-01 | 6.35 |
| NORMAL DEFLECTION : ELASTIC MODE #1 | 1.904E+00 | 7.25 |
| NORMAL DEFLECTION : ELASTIC MODE #2 | -9.246E-01 | 6.35 |
| NORMAL DEFLECTION : ELASTIC MODE #3 | 5.767E-02 | 8.65 |
| NORMAL DEFLECTION : ELASTIC MODE #5 | -1.449E-02 | 8.50 |
| NORMAL DEFLECTION : ELASTIC MODE #6 | 5.618E-03 | 9.00 |
| NORMAL DEFLECTION : ELASTIC MODE #8 | -1.575E-03 | 8.90 |
| NORMAL DEFLECTION : ELASTIC MODE #9 | 7.949E-04 | 8.50 |
| NORMAL DEFLECTION : ELASTIC MODE #11 | 1.307E-03 | 8.65 |
| NODE #1 : RIGID MOMENT | 0.000E+00 | 0.00 |
| NODE #1 : ELASTIC MOMENT | 0.000E+00 | 0.00 |
| NODE #1 : TOTAL MOMENT | 0.000E+00 | 0.00 |
| NODE #2 : RIGID MOMENT | -1.157E+07 | 6.65 |
| NODE #2 : ELASTIC MOMENT | 3.152E+07 | 9.15 |
| NODE #2 : TOTAL MOMENT | -2.436E+07 | 11.05 |
| NODE #3 : RIGID MOMENT | -4.447E+07 | 6.55 |
| NODE #3 : ELASTIC MOMENT | -7.477E+07 | 11.00 |
| NODE #3 : TOTAL MOMENT | -1.061E+08 | 8.90 |
| NODE #5 : RIGID MOMENT | -6.481E+07 | 6.50 |
| NODE #5 : ELASTIC MOMENT | -1.374E+08 | 11.00 |
| NODE #5 : TOTAL MOMENT | -1.923E+08 | 8.85 |
| NODE #7 : RIGID MOMENT | -7.547E+07 | 6.45 |
| NODE #7 : ELASTIC MOMENT | -1.755E+08 | 8.75 |
| NODE #7 : TOTAL MOMENT | -2.427E+08 | 8.75 |
| NODE #9 : RIGID MOMENT | -7.612E+07 | 6.45 |
| NODE #9 : ELASTIC MOMENT | -1.966E+08 | 8.75 |
| NODE #9 : TOTAL MOMENT | -2.662E+08 | 8.75 |
| NODE #10 : RIGID MOMENT | -7.714E+07 | 6.50 |
| NODE #10 : ELASTIC MOMENT | -3.535E+08 | 8.75 |
| NODE #10 : TOTAL MOMENT | -4.222E+08 | 8.75 |
| NODE #12 : RIGID MOMENT | -6.919E+07 | 6.50 |
| NODE #12 : ELASTIC MOMENT | -4.357E+08 | 8.65 |
| NODE #12 : TOTAL MOMENT | -4.973E+08 | 8.65 |
| NODE #14 : RIGID MOMENT | -5.550E+07 | 6.50 |
| NODE #14 : ELASTIC MOMENT | -4.667E+08 | 8.65 |
| NODE #14 : TOTAL MOMENT | -5.162E+08 | 8.65 |
| NODE #16 : RIGID MOMENT | -3.460E+07 | 6.45 |
| NODE #16 : ELASTIC MOMENT | -4.739E+08 | 8.65 |
| NODE #16 : TOTAL MOMENT | -5.042E+08 | 8.65 |

CASE 3 (cont'd)

| | | | |
|---|---|---|---|
| NODE #18 : | RIGID MOMENT | -8.008E+06 | 5.00 |
| NODE #18 : | ELASTIC MOMENT | -4.916E+08 | 8.65 |
| NODE #18 : | TOTAL MOMENT | -4.960E+08 | 8.65 |
| NODE #19 : | RIGID MOMENT | -2.104E+07 | 8.65 |
| NODE #19 : | ELASTIC MOMENT | -3.851E+08 | 8.65 |
| NODE #19 : | TOTAL MOMENT | -4.062E+08 | 8.65 |
| NODE #21 : | RIGID MOMENT | -1.977E+07 | 8.65 |
| NODE #21 : | ELASTIC MOMENT | -2.866E+08 | 8.65 |
| NODE #21 : | TOTAL MOMENT | -3.050E+08 | 8.65 |
| NODE #22 : | RIGID MOMENT | -1.384E+07 | 8.65 |
| NODE #22 : | ELASTIC MOMENT | -2.020E+08 | 8.65 |
| NODE #22 : | TOTAL MOMENT | -2.148E+08 | 8.65 |
| NODE #23 : | RIGID MOMENT | -6.274E+06 | 8.65 |
| NODE #23 : | ELASTIC MOMENT | -1.138E+08 | 8.65 |
| NODE #23 : | TOTAL MOMENT | -1.196E+08 | 8.65 |
| NODE #24 : | RIGID MOMENT | -6.874E+06 | 8.95 |
| NODE #24 : | ELASTIC MOMENT | -8.093E+07 | 8.65 |
| NODE #24 : | TOTAL MOMENT | -8.733E+07 | 8.65 |
| NODE #25 : | RIGID MOMENT | -6.054E+06 | 7.65 |
| NODE #25 : | ELASTIC MOMENT | -5.068E+07 | 8.65 |
| NODE #25 : | TOTAL MOMENT | -5.634E+07 | 8.65 |
| NODE #26 : | RIGID MOMENT | -3.765E+06 | 7.65 |
| NODE #26 : | ELASTIC MOMENT | -2.346E+07 | 8.65 |
| NODE #26 : | TOTAL MOMENT | -2.700E+07 | 8.65 |
| NODE #27 : | RIGID MOMENT | 0.000E+00 | 0.00 |
| NODE #27 : | ELASTIC MOMENT | 0.000E+00 | 0.00 |
| NODE #27 : | TOTAL MOMENT | 0.000E+00 | 0.00 |

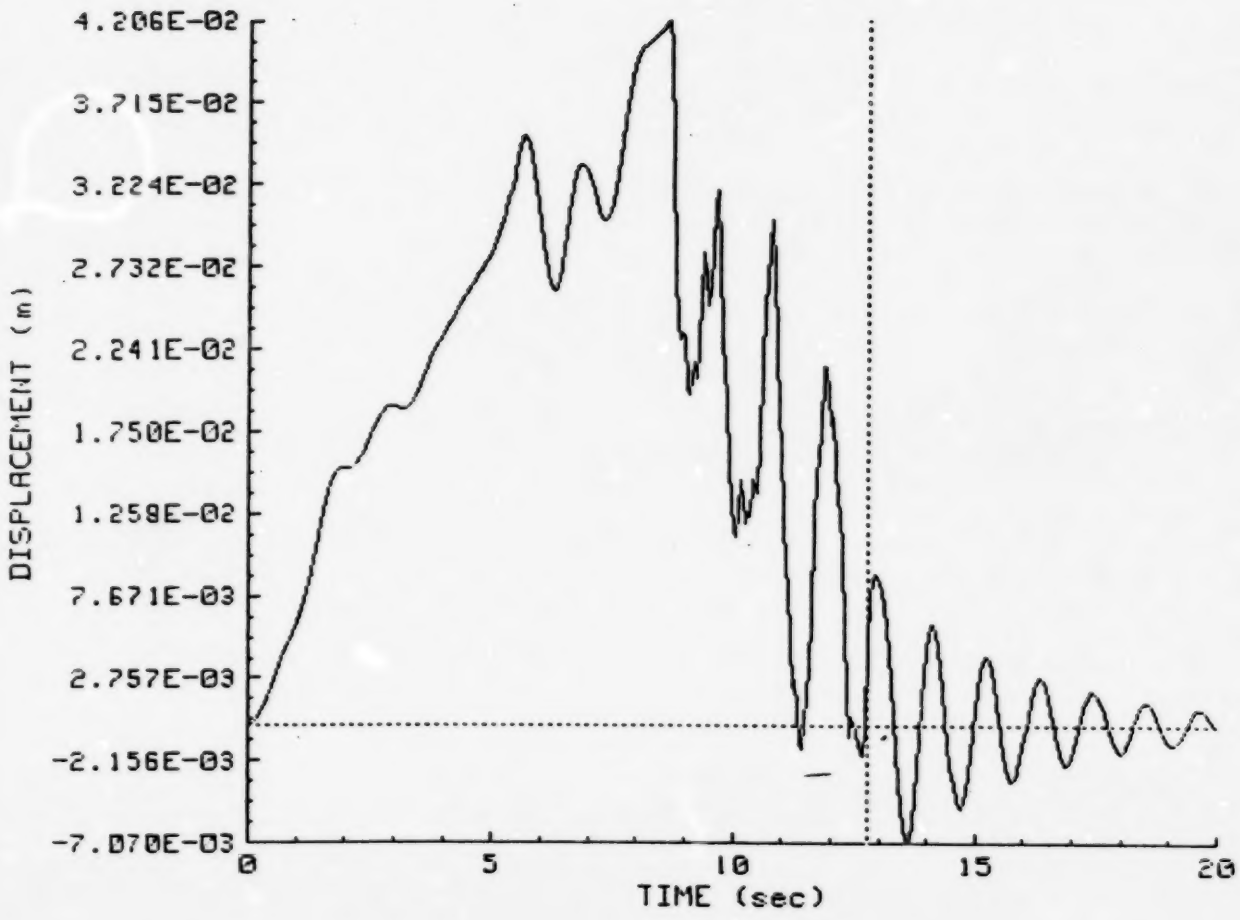


TOTAL VERTICAL ELASTIC DISPLACEMENT AT NODE #27
FOR CASE 3

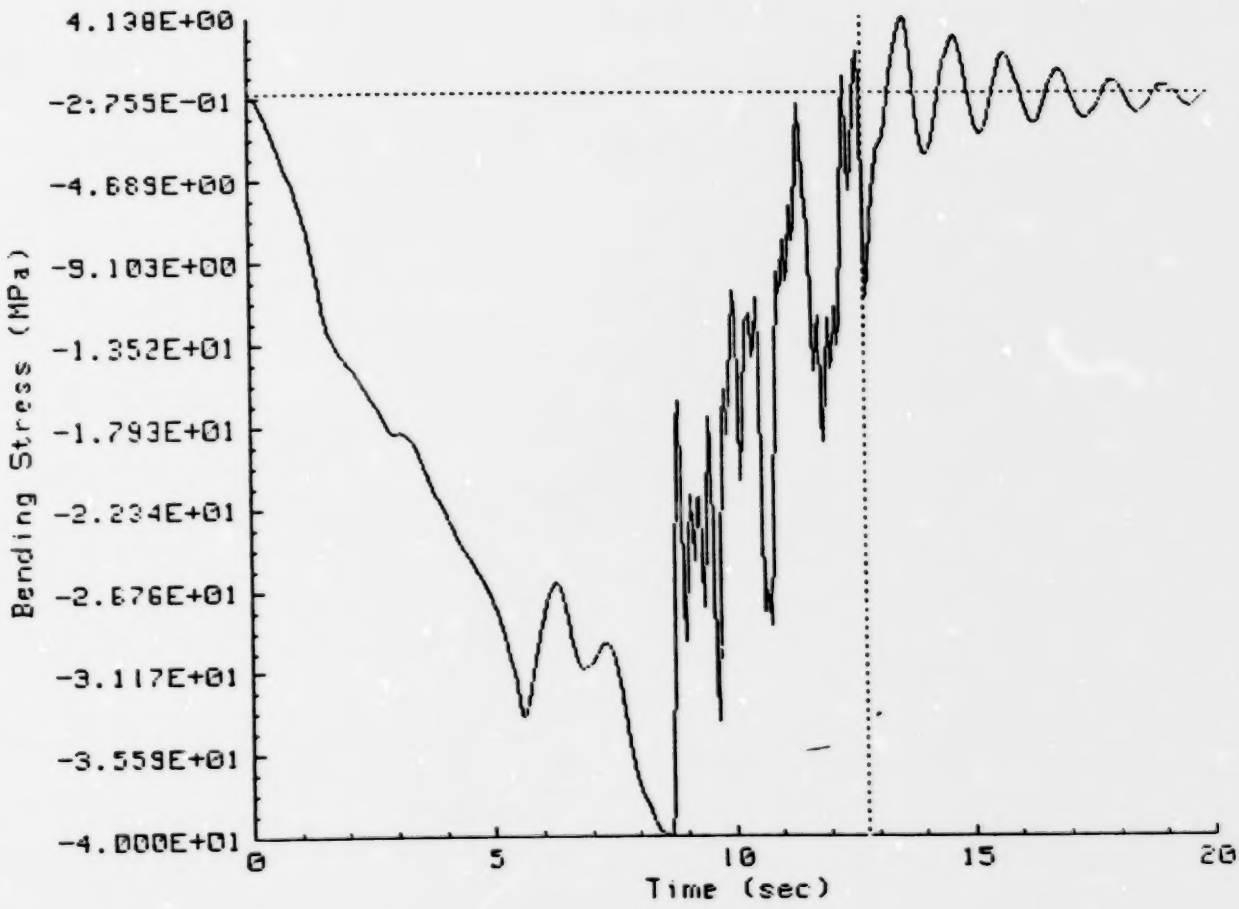


Time History of Total Stresses at Node #18
FOR CASE 3

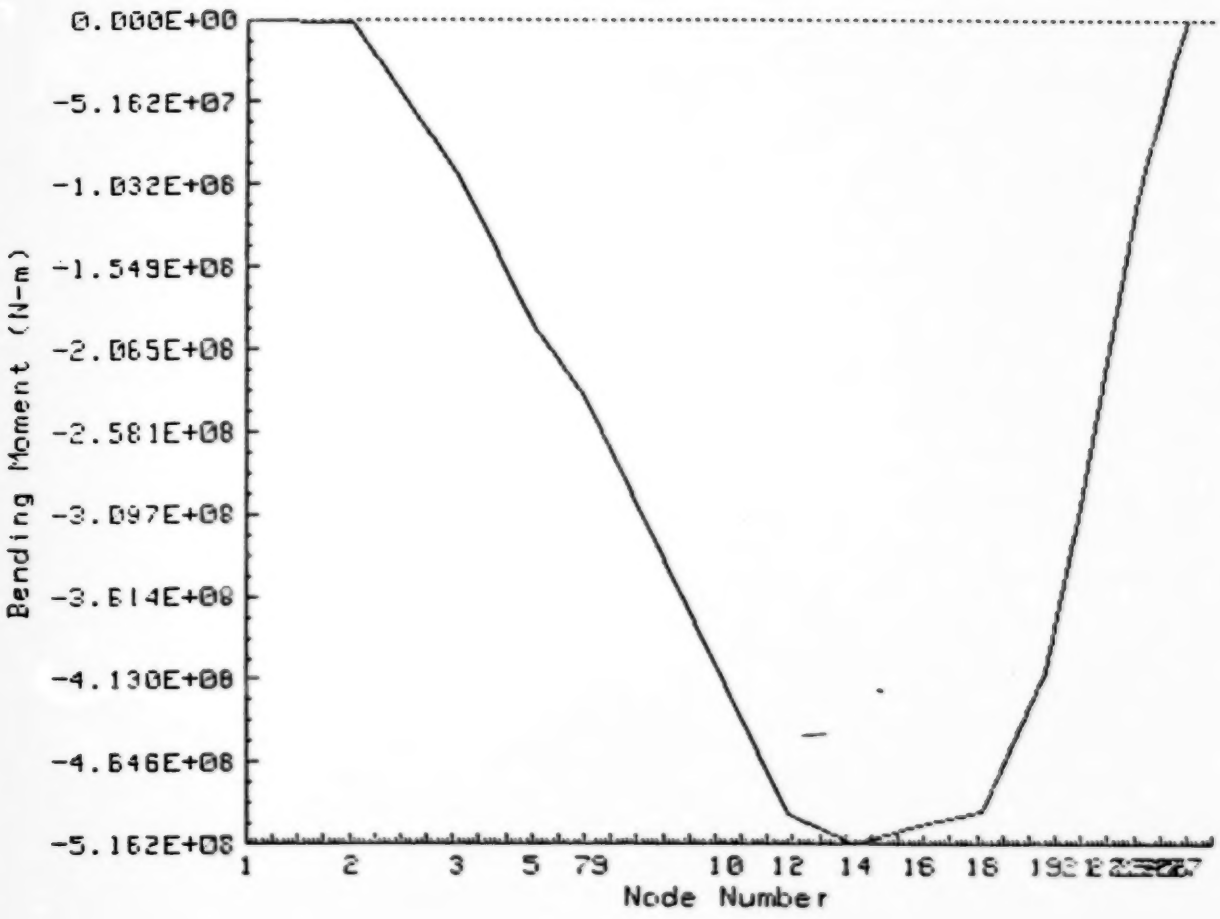


Bending Moment Diagram due to All Modes at Time=8.65 sec
for Case 3

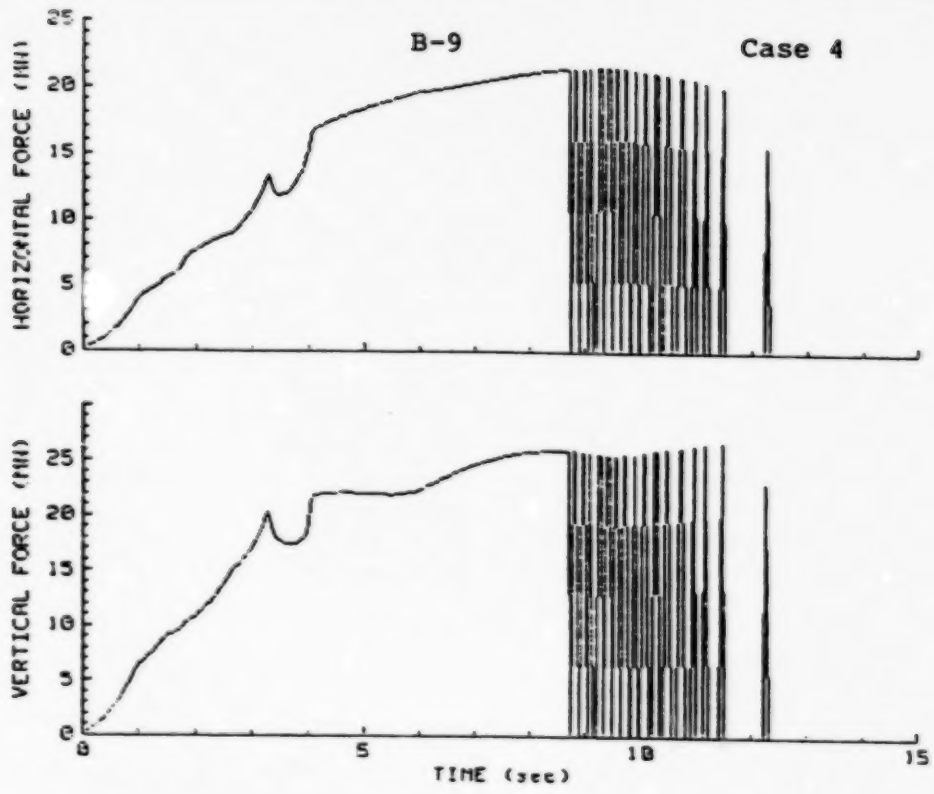


| | |
|---|---|
| INITIAL VELOCITY | 6.00 kn |
| DRAUGHT | 10.00 m |
| ICE FLOE THICKNESS | 10.00 m |
| ICE FREEBOARD | 0.00 m |

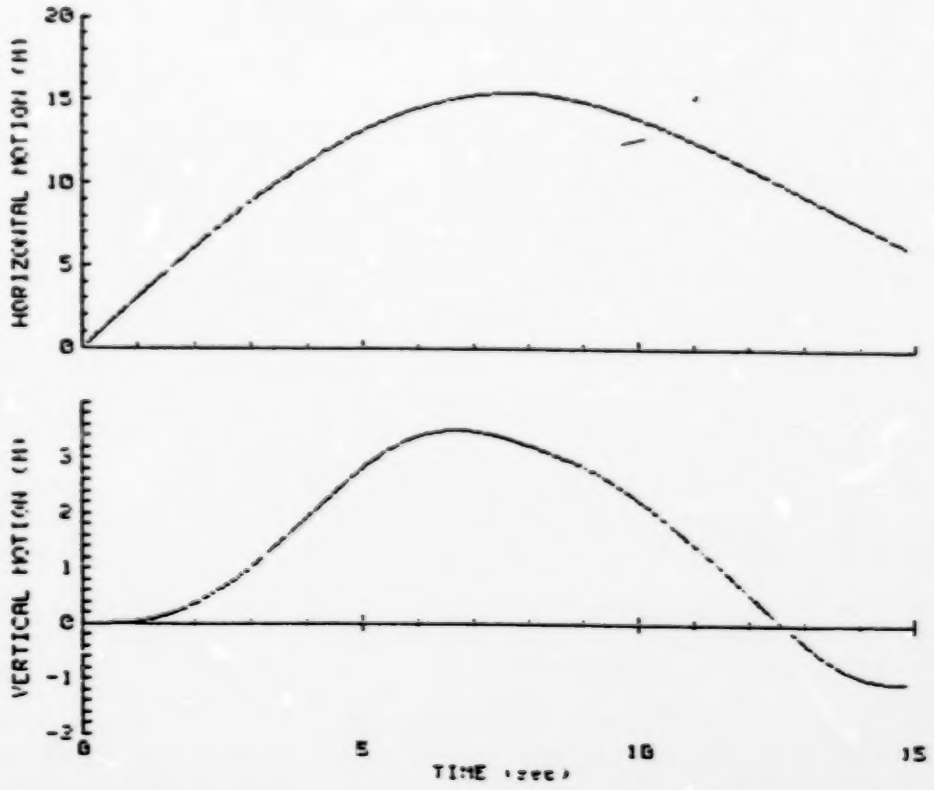

TABLE OF MAXIMUM VALUES FOR CASE 4

| VARIABLE | MAX. VALUE | TIME |
|---|---|---|
| NORMAL DEFLECTION : RIGID MODE #1 | 1.545E+01 | 7.75 |
| NORMAL DEFLECTION : RIGID MODE #2 | 2.961E+00 | 6.90 |
| NORMAL DEFLECTION : RIGID MODE #3 | -1.485E+00 | 5.90 |
| NORMAL DEFLECTION : ELASTIC MODE #1 | 2.966E+00 | 6.90 |
| NORMAL DEFLECTION : ELASTIC MODE #2 | -1.488E+00 | 5.90 |
| NORMAL DEFLECTION : ELASTIC MODE #3 | 7.519E-02 | 7.90 |
| NORMAL DEFLECTION : ELASTIC MODE #5 | -1.757E-02 | 8.55 |
| NORMAL DEFLECTION : ELASTIC MODE #6 | 5.208E-03 | 10.15 |
| NORMAL DEFLECTION : ELASTIC MODE #8 | -1.845E-03 | 10.60 |
| NORMAL DEFLECTION : ELASTIC MODE #9 | 9.135E-04 | 10.75 |
| NORMAL DEFLECTION : ELASTIC MODE #11 | 1.720E-03 | 10.50 |
| NODE #1 : RIGID MOMENT | 0.000E+00 | 0.00 |
| NODE #1 : ELASTIC MOMENT | 0.000E+00 | 0.00 |
| NODE #1 : TOTAL MOMENT | 0.000E+00 | 0.00 |
| NODE #2 : RIGID MOMENT | -1.635E+07 | 6.15 |
| NODE #2 : ELASTIC MOMENT | 4.360E+07 | 10.30 |
| NODE #2 : TOTAL MOMENT | -3.830E+07 | 9.85 |
| NODE #3 : RIGID MOMENT | -7.081E+07 | 6.10 |
| NODE #3 : ELASTIC MOMENT | -1.141E+08 | 9.90 |
| NODE #3 : TOTAL MOMENT | -1.611E+08 | 9.80 |
| NODE #5 : RIGID MOMENT | -1.035E+08 | 6.05 |
| NODE #5 : ELASTIC MOMENT | -2.217E+08 | 9.80 |
| NODE #5 : TOTAL MOMENT | -2.900E+08 | 9.80 |
| NODE #7 : RIGID MOMENT | -1.208E+08 | 6.00 |
| NODE #7 : ELASTIC MOMENT | -2.948E+08 | 9.85 |
| NODE #7 : TOTAL MOMENT | -3.734E+08 | 9.85 |
| NODE #9 : RIGID MOMENT | -1.252E+08 | 6.00 |
| NODE #9 : ELASTIC MOMENT | -3.241E+08 | 9.85 |
| NODE #9 : TOTAL MOMENT | -4.053E+08 | 9.85 |
| NODE #10 : RIGID MOMENT | -1.234E+08 | 6.00 |
| NODE #10 : ELASTIC MOMENT | -4.897E+08 | 9.90 |
| NODE #10 : TOTAL MOMENT | -5.726E+08 | 4.60 |
| NODE #12 : RIGID MOMENT | -1.105E+08 | 6.05 |
| NODE #12 : ELASTIC MOMENT | -5.676E+08 | 7.90 |
| NODE #12 : TOTAL MOMENT | -6.592E+08 | 7.85 |
| NODE #14 : RIGID MOMENT | -8.858E+07 | 6.05 |
| NODE #14 : ELASTIC MOMENT | -6.019E+08 | 7.90 |
| NODE #14 : TOTAL MOMENT | -6.754E+08 | 7.85 |
| NODE #16 : RIGID MOMENT | -5.564E+07 | 5.95 |
| NODE #16 : ELASTIC MOMENT | -6.047E+08 | 7.90 |
| NODE #16 : TOTAL MOMENT | -6.491E+08 | 7.90 |

CASE 4 (cont'd)

| | | |
|---|---|---|
| NODE #18 : RIGID MOMENT | -1.368E+07 | 5.10 |
| NODE #18 : ELASTIC MOMENT | -6.197E+08 | 7.90 |
| NODE #18 : TOTAL MOMENT | -6.245E+08 | 7.90 |
| NODE #19 : RIGID MOMENT | -3.334E+07 | 6.15 |
| NODE #19 : ELASTIC MOMENT | -4.866E+06 | 7.90 |
| NODE #19 : TOTAL MOMENT | -5.151E+08 | 7.90 |
| NODE #21 : RIGID MOMENT | -3.110E+07 | 6.35 |
| NODE #21 : ELASTIC MOMENT | -3.572E+08 | 7.90 |
| NODE #21 : TOTAL MOMENT | -3.848E+08 | 7.90 |
| NODE #22 : RIGID MOMENT | -2.173E+07 | 6.40 |
| NODE #22 : ELASTIC MOMENT | -2.508E+08 | 7.90 |
| NODE #22 : TOTAL MOMENT | -2.703E+08 | 7.90 |
| NODE #23 : RIGID MOMENT | -9.857E+06 | 6.40 |
| NODE #23 : ELASTIC MOMENT | -1.409E+08 | 7.90 |
| NODE #23 : TOTAL MOMENT | -1.497E+08 | 7.90 |
| NODE #24 : RIGID MOMENT | -1.076E+07 | 6.50 |
| NODE #24 : ELASTIC MOMENT | -1.001E+08 | 7.90 |
| NODE #24 : TOTAL MOMENT | -1.099E+08 | 7.90 |
| NODE #25 : RIGID MOMENT | -9.465E+06 | 6.55 |
| NODE #25 : ELASTIC MOMENT | -6.270E+07 | 7.90 |
| NODE #25 : TOTAL MOMENT | -7.140E+07 | 7.90 |
| NODE #26 : RIGID MOMENT | -5.883E+06 | 6.60 |
| NODE #26 : ELASTIC MOMENT | -2.904E+07 | 7.90 |
| NODE #26 : TOTAL MOMENT | -3.448E+07 | 7.90 |
| NODE #27 : RIGID MOMENT | 0.000E+00 | 0.00 |
| NODE #27 : ELASTIC MOMENT | 0.000E+00 | 0.00 |
| NODE #27 : TOTAL MOMENT | 0.000E+00 | 0.00 |

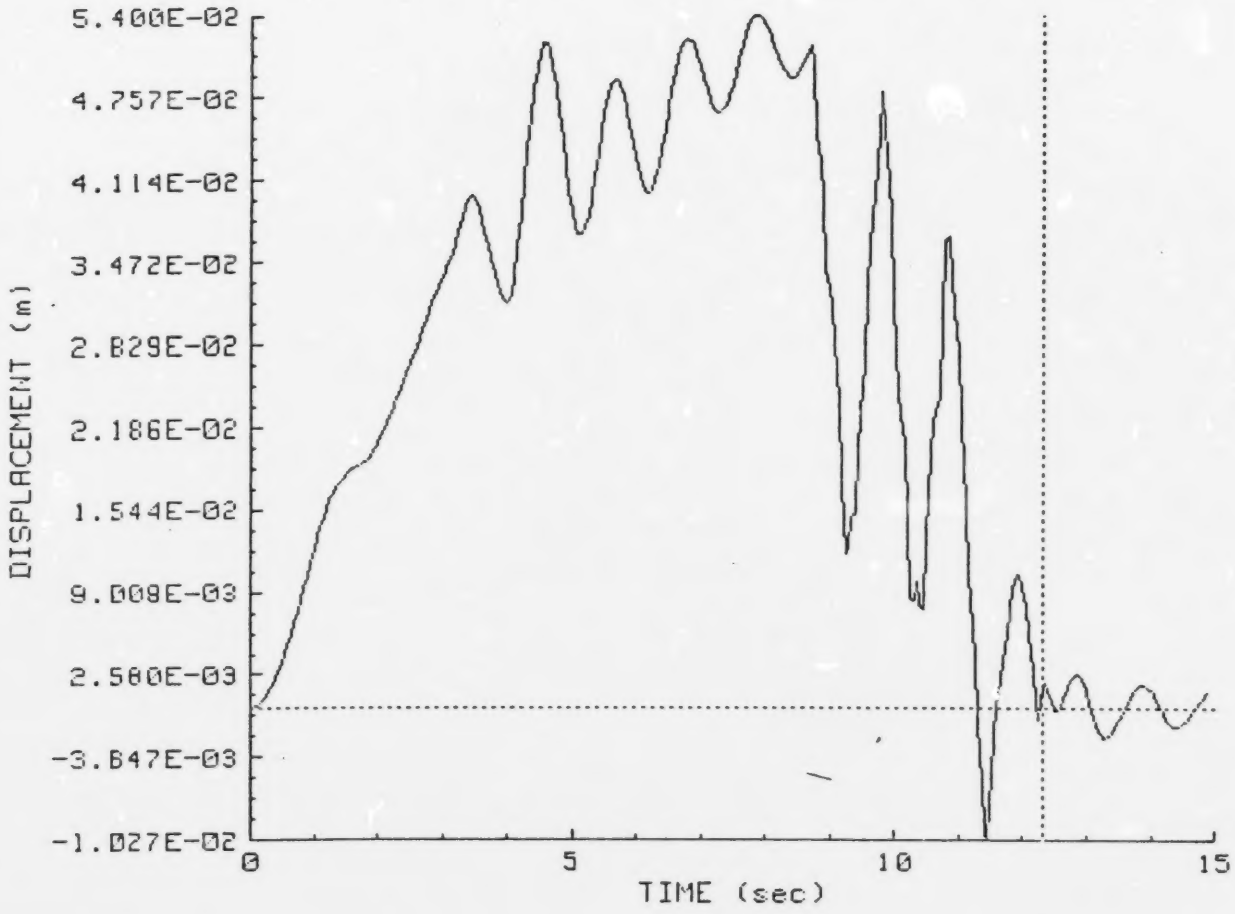


TOTAL VERTICAL ELASTIC DISPLACEMENT AT NODE #27
FOR CASE 4

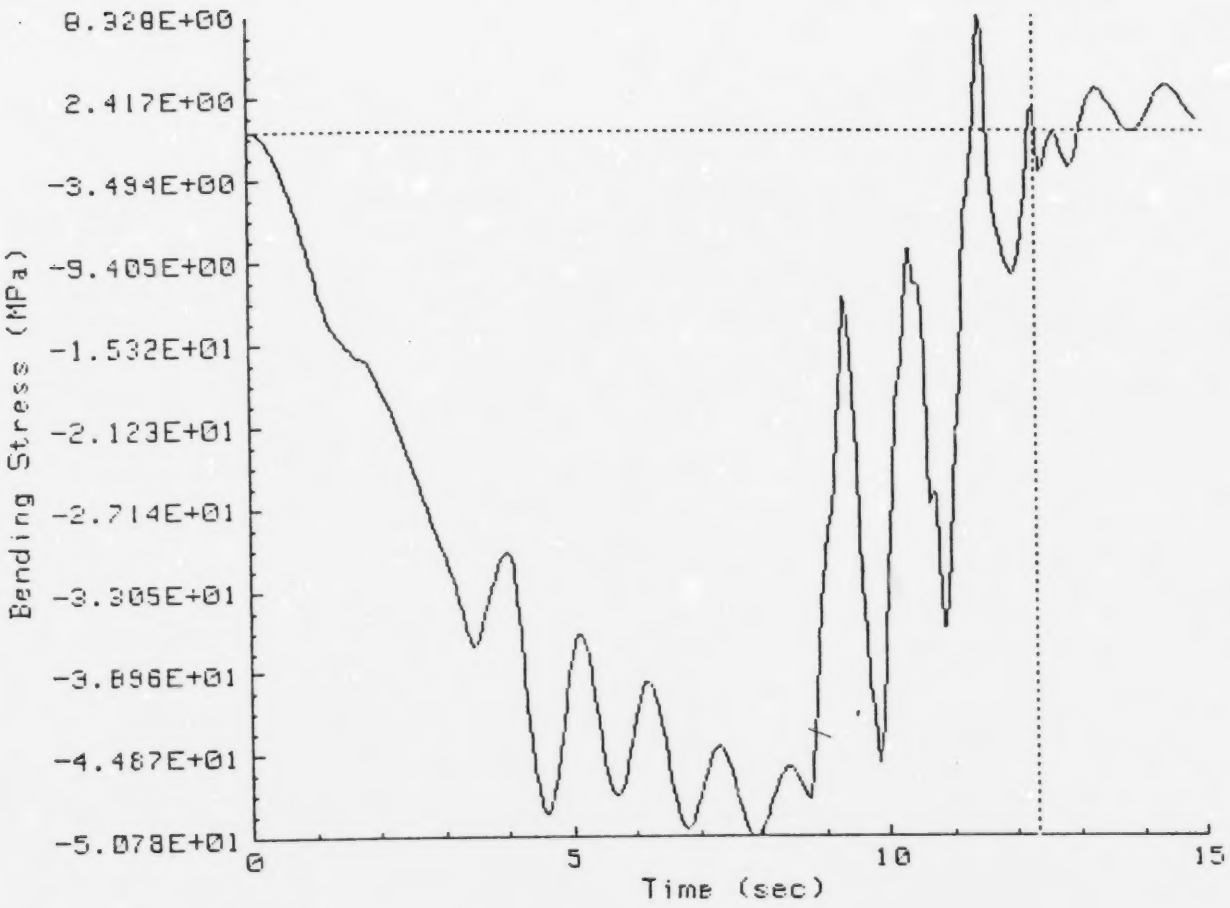


Time History of Total Stresses at Node #14
FOR CASE 4

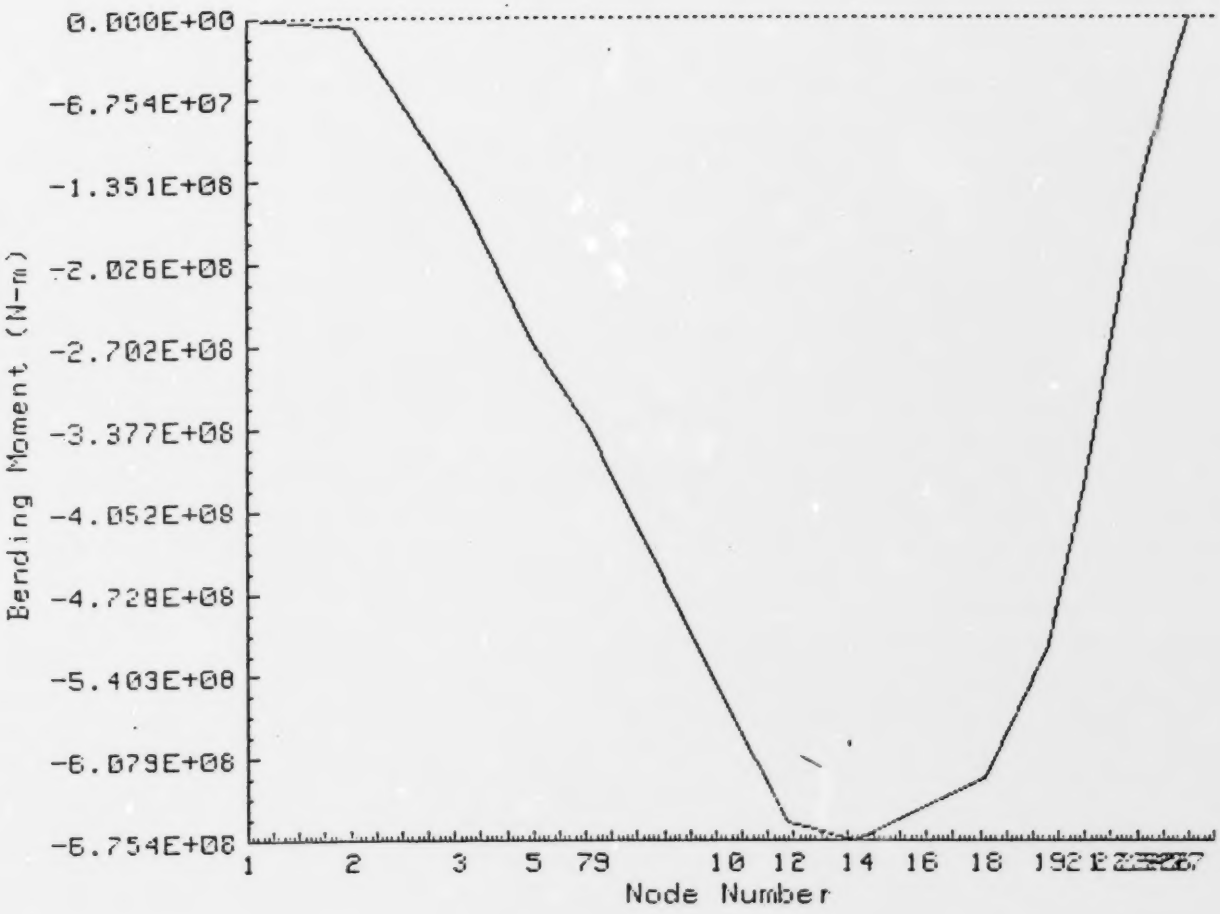


Bending Moment Diagram due to All Modes at Time=7.85 sec

FOR CASE 4

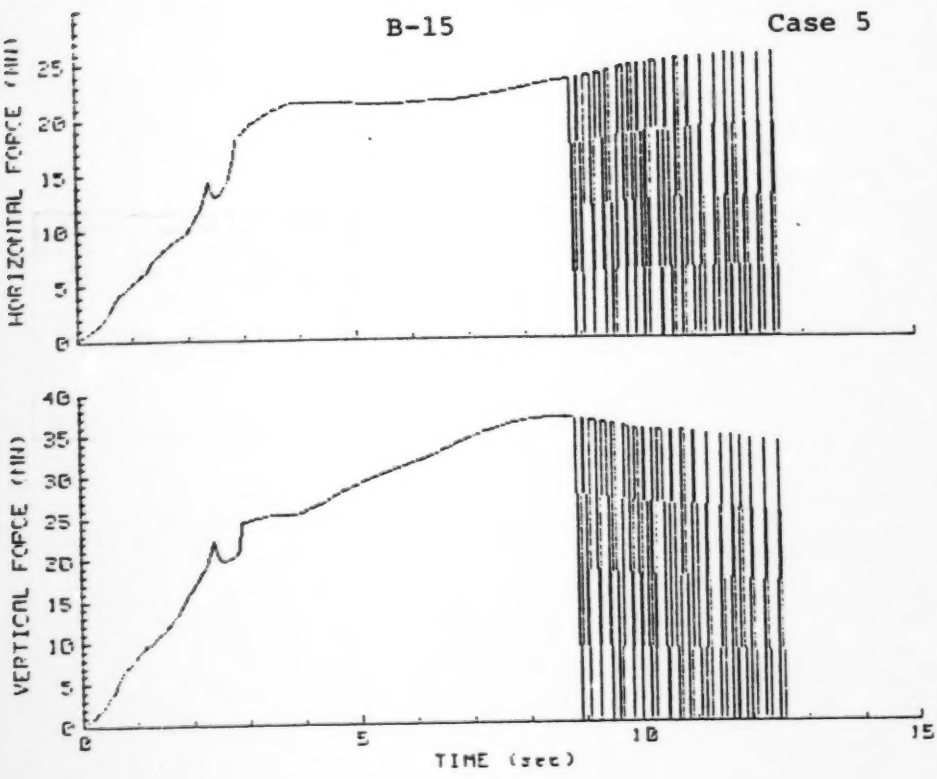


| | |
|---|---|
| INITIAL VELOCITY | 8.00 kn |
| DRAUGHT | 10.00 m |
| ICE FLOE THICKNESS | 10.00 m |
| ICE FREEBOARD | 0.00 m |

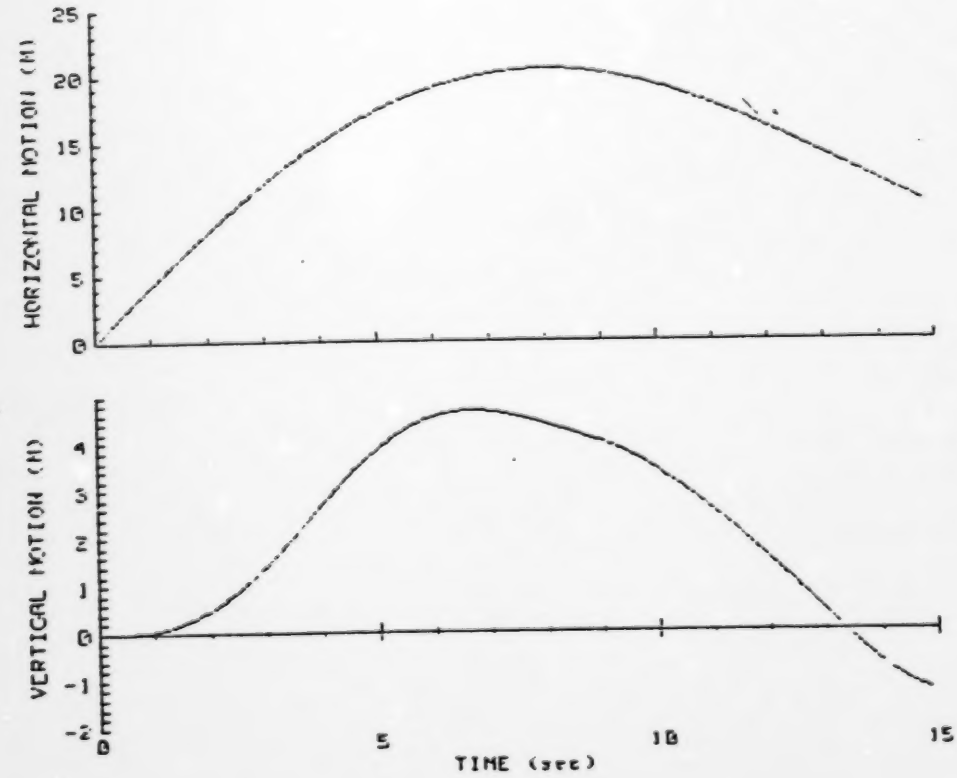

POOR

QUALITY

ORIGINAL